

## INFORMATION TO USERS

This reproduction was made from a copy of a document sent to us for microfilming. While the most advanced technology has been used to photograph and reproduce this document, the quality of the reproduction is heavily dependent upon the quality of the material submitted.

The following explanation of techniques is provided to help clarify markings or notations which may appear on this reproduction.

1. The sign or "target" for pages apparently lacking from the document photographed is "Missing Page(s)". If it was possible to obtain the missing page(s) or section, they are spliced into the film along with adjacent pages. This may have necessitated cutting through an image and duplicating adjacent pages to assure complete continuity.
2. When an image on the film is obliterated with a round black mark, it is an indication of either blurred copy because of movement during exposure, duplicate copy, or copyrighted materials that should not have been filmed. For blurred pages, a good image of the page can be found in the adjacent frame. If copyrighted materials were deleted, a target note will appear listing the pages in the adjacent frame.
3. When a map, drawing or chart, etc., is part of the material being photographed, a definite method of "sectioning" the material has been followed. It is customary to begin filming at the upper left hand corner of a large sheet and to continue from left to right in equal sections with small overlaps. If necessary, sectioning is continued again—beginning below the first row and continuing on until complete.
4. For illustrations that cannot be satisfactorily reproduced by xerographic means, photographic prints can be purchased at additional cost and inserted into your xerographic copy. These prints are available upon request from the Dissertations Customer Services Department.
5. Some pages in any document may have indistinct print. In all cases the best available copy has been filmed.

**University  
Microfilms  
International**

300 N. Zeeb Road  
Ann Arbor, MI 48106



8419116

**Booth, Derek Blake**

GLACIER DYNAMICS AND THE DEVELOPMENT OF GLACIAL LANDFORMS  
IN THE EASTERN PUGET LOWLAND, WASHINGTON

*University of Washington*

Ph.D. 1984

University  
Microfilms  
International 300 N. Zeeb Road, Ann Arbor, MI 48106



PLEASE NOTE:

In all cases this material has been filmed in the best possible way from the available copy. Problems encountered with this document have been identified here with a check mark .

1. Glossy photographs or pages \_\_\_\_\_
2. Colored illustrations, paper or print \_\_\_\_\_
3. Photographs with dark background \_\_\_\_\_
4. Illustrations are poor copy \_\_\_\_\_
5. Pages with black marks, not original copy \_\_\_\_\_
6. Print shows through as there is text on both sides of page \_\_\_\_\_
7. Indistinct, broken or small print on several pages \_\_\_\_\_
8. Print exceeds margin requirements \_\_\_\_\_
9. Tightly bound copy with print lost in spine \_\_\_\_\_
10. Computer printout pages with indistinct print \_\_\_\_\_
11. Page(s) \_\_\_\_\_ lacking when material received, and not available from school or author.
12. Page(s) \_\_\_\_\_ seem to be missing in numbering only as text follows.
13. Two pages numbered \_\_\_\_\_. Text follows.
14. Curling and wrinkled pages \_\_\_\_\_
15. Other \_\_\_\_\_

University  
Microfilms  
International



Glacier Dynamics and the Development of Glacial Landforms  
in the Eastern Puget Lowland, Washington

by

DEREK BLAKE BOOTH

A dissertation submitted in partial fulfillment  
of the requirements for the degree

Doctor of Philosophy

University of Washington

1984

Approved by Brent Haller  
(Chairperson of Supervisory Committee)

Program Authorized  
to Offer Degree Geological Sciences

Date May 25, 1984

### Doctoral Dissertation

In presenting this dissertation in partial fulfillment of the requirements for the Doctoral degree at the University of Washington I agree that the Library shall make its copies freely available for inspection. I further agree that extensive copying of this dissertation is allowable only for scholarly purposes, consistent with "fair use" as prescribed in the U. S. Copyright Law. Requests for copying or reproduction of this dissertation may be referred to University Microfilms, 300 North Zeeb Road, Ann Arbor, Michigan 48106, to whom the author has granted "the right to reproduce and sell (a) copies of the manuscript in microform and/or (b) printed copies of the manuscript made from microform."

Signature Deane Booth

Date May 25, 1984



University of Washington

Abstract

GLACIER DYNAMICS AND THE DEVELOPMENT OF GLACIAL LANDFORMS  
IN THE EASTERN PUGET LOWLAND, WASHINGTON

by Derek Blake Booth

Chairperson of the Supervisory Committee: Professor Bernard Hallet  
Department of Geological Sciences

In the Late Pleistocene, the Puget lobe of the Cordilleran ice sheet covered the Puget lowland in western Washington to an average depth of 1000 m in the Skykomish-Snoqualmie region and abutted against the western front of the Cascade Range.

Reconstructions of the extent, altitude, and mass balance of the Puget lobe lead to an estimate of its sliding velocity and basal water flux. Lobe dimensions are inferred from ice limits and flow-direction indicators. An equilibrium-line altitude of 1220 m is calculated for the maximum of the Vashon advance. Resultant average sliding velocities range up to 600 m/a and average meltwater discharges up to 2500 m<sup>3</sup>/s.

Deeply incised valleys in the eastern lowland reflect considerable erosion primarily by subglacial meltwater. Many of these channels were continuously occupied by water, whereas a broad, submarginal channel carried highly variable discharge as a result of episodic, catastrophic drainage of ice-marginal lakes. The analysis of subglacial water flow is expanded to include the effects of sliding ice, providing a physical model for the development of subglacial

fluvial landforms.

Morainal embankments of glacial, fluvial, and lacustrine sediments fill the mouth of each alpine valley emerging into the east-central lowland. They reflect subglacial sedimentation at and near the grounding line of the Puget lobe adjacent to ice-dammed lakes. Analysis of the physical behavior of ice and water, particularly by detailed reconstruction of the hydraulic potentials, provides geologic insights regarding the location and internal composition of these embankments.

Basal stress conditions control both depositional processes and physical properties of subglacial sediments. Beneath rapidly sliding ice, till, which averages 5-10 m in thickness in the lowland, can accrete only by the accumulation of sediments released by basal meltout. High pore pressures are expected under the glacier except within a few km of the margin, irrespective of subglacial tunnels or till properties. These pore pressures are responsible for low till strength and consequent deformation of subglacial sediments by moving ice, and for overconsolidation values significantly less than the maximum overburden.

## TABLE OF CONTENTS

	Page
List of Figures . . . . .	iv
List of Plates . . . . .	vi
List of Tables . . . . .	vii
List of Maps . . . . .	viii
Acknowledgments . . . . .	ix
Chapter 1: Geology of the Skykomish-Snoqualmie region . . . .	1
Introduction . . . . .	1
Pre-Pleistocene geology . . . . .	6
Pleistocene deposits . . . . .	10
Nonglacial Deposits . . . . .	36
Vashon-age recessional history . . . . .	40
Chapter 2: Mass balance and sliding of the Puget-lobe ice sheet during the Vashon Stade . . . . .	55
Introduction . . . . .	55
Reconstruction of the ice sheet . . . . .	58
Mass balance calculations . . . . .	60
Corroborating evidence . . . . .	66
Sensitivity . . . . .	69
Discussion . . . . .	72
Chapter 3: Landforms of subglacial fluvial erosion . . . . .	75
Introduction . . . . .	75
Origin of channelways . . . . .	84
Predicted behavior of subglacial water flow . . . . .	86

	Page
Geological expression of subglacial fluvial activity . . .	98
Effects of sliding over non-planar topography . . . . .	102
Relative persistence of longitudinal and transverse landforms . . . . .	126
Implications for development of glaciated landscapes . .	132
Chapter 4: Morainal embankments of the eastern Puget Lowland . . . . .	135
Introduction . . . . .	135
Fieldwork and acknowledgments . . . . .	138
Description . . . . .	138
Reconstruction of ice-marginal environments . . . . .	148
Conclusion . . . . .	171
Chapter 5: Basal conditions beneath rapidly sliding ice sheets . . . . .	172
Introduction . . . . .	172
General conditions at the glacier bed . . . . .	172
High excess pore pressures at the glacier bed . . . . .	178
Geological consequences . . . . .	186
Conclusion . . . . .	190
Bibliography . . . . .	192
Appendix: Description of map units . . . . .	210
Pocket Material: Map of the geology of the west half of the Skykomish 1:100,000 quadrangle, Washington . . . . .	back pocket

## LIST OF FIGURES

Number	Page
1.1. Index map showing geographical localities . . . . .	2
1.2. Sources consulted during map preparation . . . . .	5
1.3. Correlation of map units . . . . .	16
1.4. Distribution of recessional outwash deposits . . . . .	42
1.5. Correlation of recessional intervals . . . . .	43
1.6. Puget Lowland localities discussed in text . . . . .	50
2.1. Reconstruction of the Cordilleran ice sheet . . . . .	59
2.2. Altitude-mass balance relationship . . . . .	61
2.3. Velocity measurements on modern glaciers . . . . .	74
3.1. Index map of localities . . . . .	77
3.2. Isolated channelways . . . . .	78
3.3. Multiple channelways . . . . .	79
3.4. Multiple channelways . . . . .	80
3.5. Bedrock hills isolated by multiple channelways . . . . .	82
3.6. Northern segment of submarginal channelway . . . . .	83
3.7. Topography of the Skykomish-Snoqualmie region . . . . .	89
3.8. Ice-surface topography at maximum stage . . . . .	90
3.9. Subglacial hydraulic equipotentials . . . . .	91
3.10. Subglacial water-flow paths . . . . .	92
3.11. Regional subglacial water-flow paths . . . . .	94
3.12. Hydraulic equipotentials beneath sliding ice . . . . .	106
3.13. Dynamic pressure due to sliding over hills . . . . .	114
3.14. Dynamic pressure due to sliding over hemisphere . . . . .	121
3.15. Maximum convergence rate of tools with bed . . . . .	124
3.16. Potential energy dissipation per unit bed area . . . . .	129

Number	Page
4.1. Index map of geographical localities . . . . .	136
4.2. South Fork Tolt embankment . . . . .	140
4.3. Middle-South Forks Snoqualmie embankment . . . . .	143
4.4. Pilchuck-Sultan embankment . . . . .	145
4.5. Subglacial hydraulic equipotentials . . . . .	154
4.6. Possible ice-termini configurations . . . . .	157
4.7. Calligan and Hancock embankments . . . . .	162
4.8. Water-flow paths in an ice-dammed valley . . . . .	164
4.9. Skykomish embankment . . . . .	168
4.10. North Fork Snoqualmie embankment . . . . .	170
5.1. Longitudinal strain rate . . . . .	175
5.2. Water pressure in tunnels . . . . .	185

LIST OF PLATES

Number	Page
I. Southwest view over area of Figure 3.3. . . . .	134

LIST OF MAPS

Number	Page
1. Geology of the west half of the Skykomish River 1:100,000 quadrangle, WA . . . . .	back pocket



### ACKNOWLEDGMENTS

This project could not have been attempted had it not been for the initial encouragement, continued support, and careful reviews of Bernard Hallet. Fred Pessl, Jr., Richard B. Waitt, Jr., and David P. Dethier also offered strong encouragement at critical moments during the inception of this project. Rowland W. Tabor provided both tangible and intangible support from beginning to end; his contribution cannot be overstated. Stephen C. Porter, Charles F. Raymond, and J. Dungan Smith all provided important criticism and review of the concepts presented and the manuscript itself. Financial support was provided by the U. S. Geological Survey, the Department of Geological Sciences Corporation Fund, and Sigma Xi.

**CHAPTER 1**  
**GEOLOGY OF THE SKYKOMISH-SNOQUALMIE REGION**

**INTRODUCTION**

This study of the surficial geology of the western half of the Skykomish River 1:100,000 quadrangle (Figure 1.1) is part of a larger geological investigation of the geology of the Wenatchee 2<sup>0</sup> quadrangle in west-central Washington. This specific area expresses well erosional and depositional processes of ice sheet glaciation, particularly those unique to the ice-marginal areas. Basic geologic data on the distribution and sequence of surficial deposits and the processes that have led to their formation can be used to reconstruct the dynamic behavior of past ice sheets, to elucidate further the Pleistocene history in western Washington, and to inform planners and engineers who must work with these deposits.

This study emphasizes the deposits associated with the most recent invasion of ice from British Columbia, but discusses older units as well. These older units include deposits of earlier glacial advances, local alpine glacial deposits, and bedrock. The bedrock geology of this area is discussed in greater detail by Tabor and others (1982) in a companion map of the Skykomish River quadrangle. Adjacent geological maps include the eastern half of the Skykomish River 1:100,000 quadrangle (Tabor and others, 1982), the Snohomish and Maltby 1:24,000 quadrangles to the west (Minard, 1980, 1981), the Port Townsend 1:100,000 quadrangle to the northwest (Pessl and others, 1983; Whetten and others, 1983), and the Snoqualmie Pass

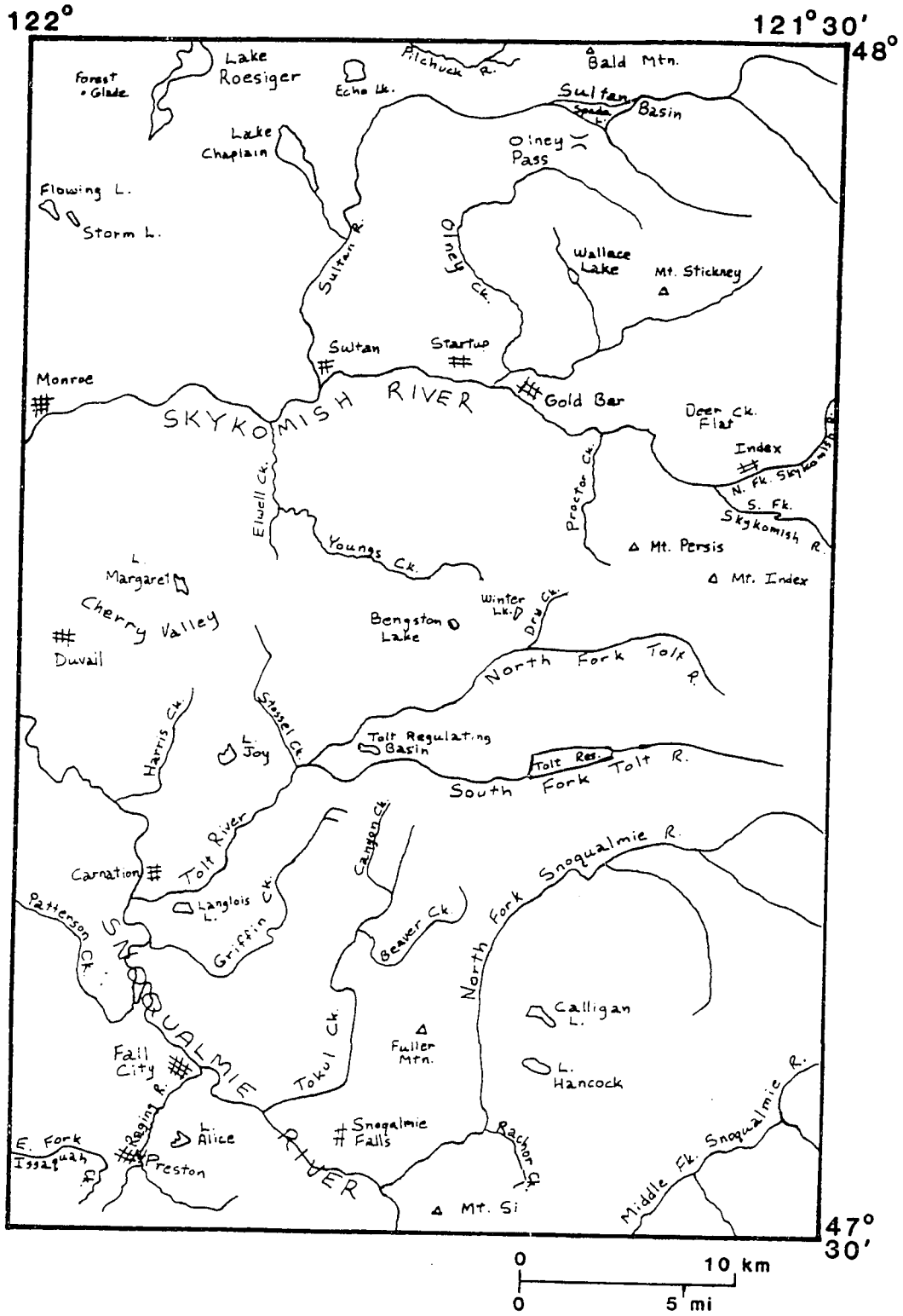


Figure 1.1. Index map showing geographical localities.

1:100,000 quadrangle to the south (Frizzell and others, in press).

#### FIELDWORK AND ACKNOWLEDGMENTS

Field work for this study was accomplished from spring 1981 through fall 1983. Additional field work included a preliminary reconnaissance of the lower Skykomish River valley by R. B. Waitt, Jr. in 1978. S. A. Sandberg, F. Moser, and F. Beall were able field assistants during the summer of 1981.

I would like to acknowledge the discussions and support of R. W. Tabor, R. B. Waitt, Jr., Fred Pessl, Jr., V. A. Frizzell, Jr., J. P. Minard, and D. P. Dethier of the US Geological Survey; Gerald Thorsen of the Washington Department of Natural Resources; Robert Searing of the U. S. Army Corps of Engineers; and consulting geologists W. T. Laprade, Curtis Scott, M. E. Shaffer, and L. R. Lepp. J. C. Yount, E. J. Helley, Fred Pessl, Jr., and R. W. Tabor provided critical review and valuable suggestions on this chapter.

#### PREVIOUS WORK

Willis (1898) first described the Pleistocene stratigraphy and glaciation in the Puget Sound region. Bretz's (1913) reconnaissance emphasized the recessional lake history associated with the last glaciation of the lowland. Cary and Carlston (1937) briefly described a glaciofluvial delta that was built in the upstream direction across the South Fork Skykomish River. They first noted that alpine ice from the Cascades probably did not merge with the large ice sheet occupying the lowland. Mackin (1941) investigated in

detail the character of deposits and drainage along the ice margin abutting the Cascade range front, and reconstructed some of the local details of ice recession and drainage derangement. Maps of various aspects of the surficial geology and covering parts of the study area include: Newcomb (1952) on groundwater resources, Liesch and others (1963) and Livingston (1971) as part of regional geologic compilations, Anderson (1965) and Knoll (1967) with particular emphasis on the recessional glacial history, Williams (1971) on the extent of glaciers in the Middle Fork Snoqualmie River, and Snyder and Wade (1972) on soils of the National Forest lands (Figure 1.2). Thorson (1980, 1981) expanded on the early work of Bretz to delineate a more detailed sequence of local and regional lakes during recession of the last ice sheet. He then used this information to infer amounts and rates of isostatic rebound following deglaciation.

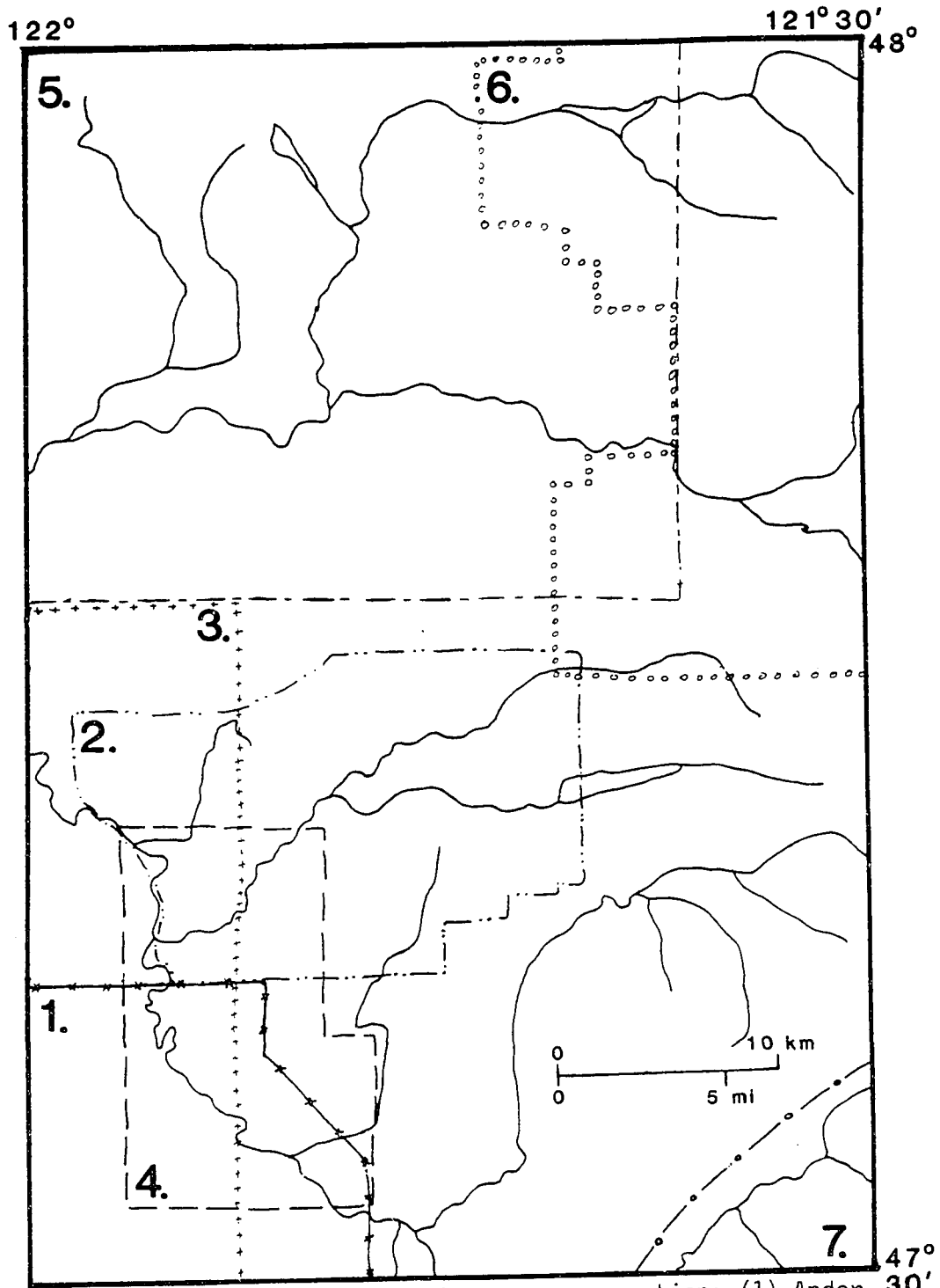


Figure 1.2. Sources consulted during map preparation: (1) Anderson (1965), (2) Knoll (1967), (3) Liesch and others (1963), (4) L. Lepp and J. Walker (written commun., 1982), (5) Newcomb (1952), (6) Snyder and Wade (1972), (7) Williams (1971).

## PRE-PLEISTOCENE GEOLOGY

### HISTORY

Bedrock in the area of this report consists predominantly of Mesozoic marine metasedimentary and metaigneous rocks, overlain by lower and middle Tertiary volcanic and sedimentary rocks, and intruded by middle Tertiary batholiths. The Mesozoic metamorphic rocks underlie much of the terrain west of the Cascade range front, both north and locally south of the Skykomish River. On the basis of lithologic variation and intense deformation, Tabor and others (1982) interpret the Mesozoic rocks to be a melange. By early Tertiary time the melange had been uplifted and eroded; it was subsequently covered by volcanic flows, pyroclastic deposits, and sedimentary rocks. Concurrent in part with this volcanic activity, tonalite and granodiorite intruded the region, forming coalescing batholiths that now underlie the western ridges of the Cascade mountains. Smaller intrusions crop out as isolated bodies scattered up to 6 km (4 mi) west of the roughly NS-trending contact between the main batholiths and country rock.

Folding has warped the volcanic rocks in the western part of the quadrangle into a broad west-plunging syncline. On the northern limb of this fold, erosion has stripped away any overlying volcanic rocks, exposing a wide region of the melange rocks covered discontinuously only by glacial drift. In the northwestern corner of the quadrangle, middle and upper Tertiary fluvial sedimentary rocks are exposed and probably overlie this eroded melange surface.

**BEDROCK**Melange

Mesozoic melange consists of a pervasively sheared matrix of mostly argillite containing outcrop- to mountain-sized phacoids of sandstone, greenstone, amphibolite, metagabbro, meta-andesite, chert, marble, and metatonalite. Towards the east, the melange grades into phyllite, with well-developed foliation commonly parallel to bedding. Landforms in the Wallace Lake/Mount Stickney area that are developed on the phyllite show strong asymmetry and orientation parallel to this foliation. Variability in erosional resistance between components of the melange leads to numerous other instances of structural control of young landforms. A particularly good example is the enormous etched-out block of metagabbro comprising the bulk of Mount Si.

Volcanic and Sedimentary Rocks

Andesite, andesitic breccia and tuff, and minor basalt and rhyolite flows and tuffs overlie much of the melange in the area between the Skykomish and Middle Fork of the Snoqualmie Rivers. Southwest of the Snoqualmie River, more abundant sandstone, siltstone, and conglomerate crop out, along with less common volcanic flows and breccias. The northern volcanic rocks are part of the volcanic rocks of Mount Persis unit (Tabor and others, 1982), dated at about 38 m.yr., and include minor interbeds of volcanic sandstone and siltstone in the upper part of the section, exposed in the wes-



tern portion of the map area. The sedimentary and volcanic rocks to the south correlate with the Puget Group and are about the same age as the Mount Persis unit. The volcanic rocks are generally more resistant to erosion and often form prominent ridges and bluffs, especially well-expressed in the Lake Elsie/ Elwell Creek area 5 km south of Sultan.

#### Intrusive Rocks

The Oligocene Index batholith and the Miocene Snoqualmie batholith constitute the bulk of Tertiary intrusions in this area. Other isolated bodies are present at the head of Youngs Creek, and control the pronounced topographic form of Fuller Mountain northwest of Mount Si. Intrusive rocks north of Spada Lake include the southern portion of the distinctively coarse-grained granodiorite of Bald Mountain of unknown but possibly late Cretaceous or early Tertiary age.

#### Sedimentary Rocks

Lithologies in this unit range from moderately to deeply weathered sandy pebble conglomerate to very-fine-grained sandstone. Coarser beds contain a high percentage of quartzose pebbles; finer beds contain considerable mica and lignite. Deeply weathered exposures usually can be distinguished from old glacial outwash by manganese staining on joint planes, nearly monolithologic conglomerate clasts, and the presence of organic matter. However, isolated exposures can be ambiguous, and have occasionally been identified as early Vashon lake deposits (e.g., Newcomb, 1952). More extensive exposures west of

the map area are considered by Minard (1981) to be Oligocene in age and lithologically similar to the Blakely Formation (Weaver, 1912). To the northwest, similar rocks are described by Danner (1957) as the Riverside Formation and assigned an Oligocene age based on fossils.

## PLEISTOCENE DEPOSITS

### REGIONAL SETTING

The Puget Sound lowland extends as a structural and topographic basin between the Olympic Mountains on the west and the Cascade Range on the east. Less pronounced uplands define its southern boundary, and it extends northward into southern British Columbia to merge with the Fraser Lowland and the Strait of Georgia. The basin's persistence through time is shown by the great thickness of upper Tertiary and Pleistocene sediments that fill it (Glover, 1936; Weaver, 1937; Mullineaux, 1970; Hall and Othberg, 1974). Fault-bounded crustal blocks beneath the sediments may be responsible for the basin (Danes and others, 1965; Stuart, 1961; Gower, 1978, Thorson, 1981).

Glacier ice originating in the mountains of British Columbia has invaded the Puget Lowland at least several times, leaving a discontinuous record of early (?) to late Pleistocene glacial periods (Crandell and others, 1958; Armstrong and others, 1965; Easterbrook and others, 1967). This ice was part of the Cordilleran ice sheet of northwestern North America that advanced into the Lowland, referred to as the "Puget lobe" by many authors since Bretz (1913). The extent of this lobe was limited by the net flux of ice from British Columbia, ablation in the Lowland, and the mountains bordering the Lowland itself.

These mountains were local sources of glaciers as well. Sufficient periodic cooling coupled with the relative proximity of marine moisture generated multiple advances of Olympic and Cascade

alpine glaciers (Crandell and Miller, 1974; Porter, 1976), whose comparatively feeble modern replacements still cling to the slopes of the highest peaks and ridges. During the last glaciation, the Puget lobe, at its maximum stand, probably did not coalesce with alpine ice originating in the Cascades. Speculation on the cause of this lack of synchrony has focused on the shadowing effect of a continental ice sheet on east-trending storm tracks, starving the Cascade glaciers and forcing their retreat.

In the region of this report, postglacial modification has been dominated by the reestablishment of the major drainages from their alpine headwaters into Puget Sound, across the deranged glaciated lowlands. The advances of thick, active ice-sheet lobes forced initial rerouting of these rivers from their preglacial lowland paths into more easterly, south-trending valleys. This diversion often became permanent even after deglaciation, as suggested in this quadrangle by the probable southern diversions of the North Fork of the Snoqualmie River or further south by the present course of the Cedar River (Mackin, 1941). Subsequent fluvial activity has reexcavated valleys filled with glacial and lacustrine sediments and reestablished valley-width floodplains graded with respect to modern river and sea level elevation.

#### SEDIMENTARY PROVENANCES

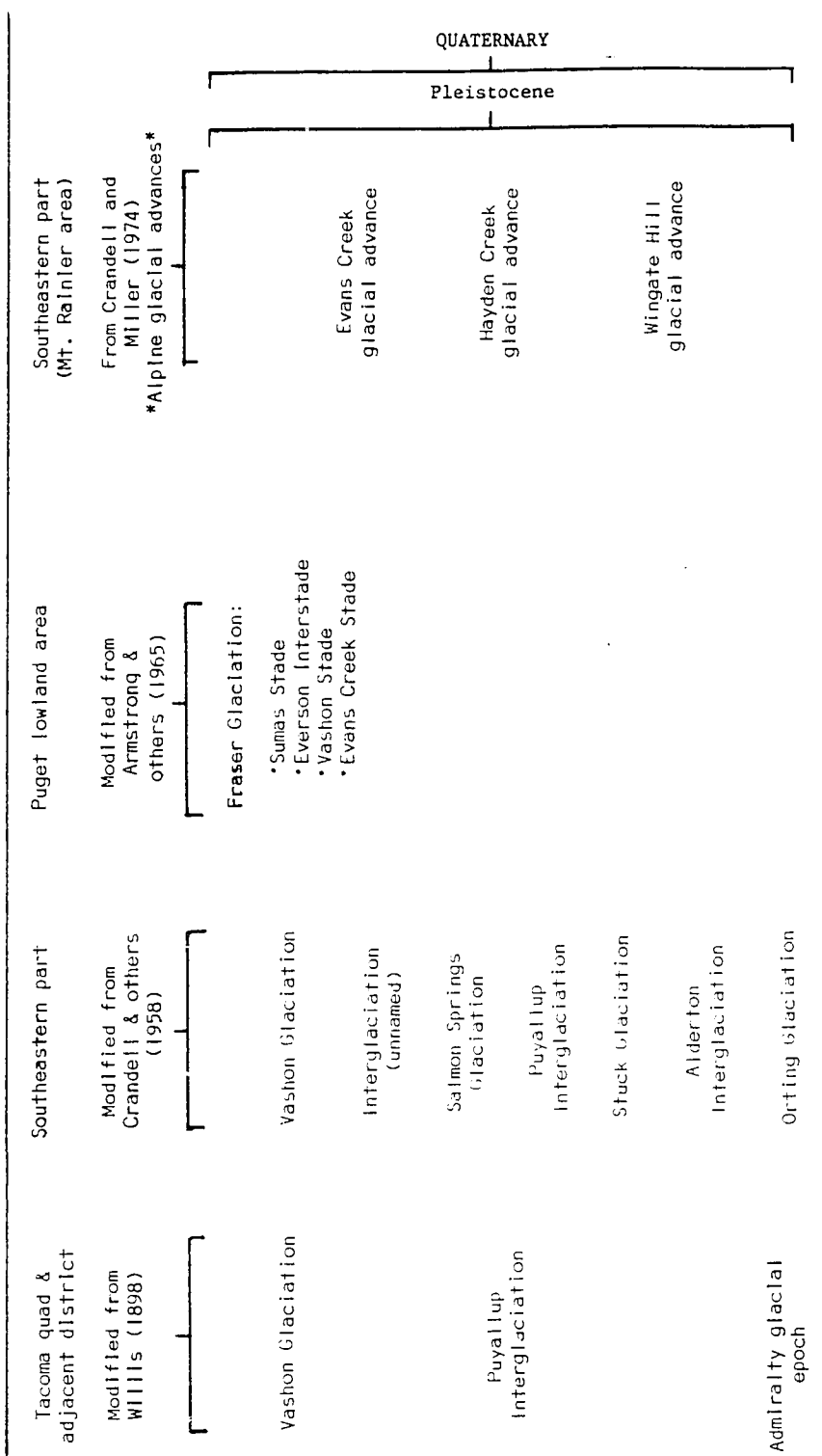
Sediment transported by the Cordilleran ice sheet consists of a wide range of lithologies, as debris was derived both from northern alpine valleys of the Cascades and the mountains of southwestern

British Columbia, Canada. Exotic sediment commonly ranges from 5 to 15 percent. Both Crandell (1963, p. 14) and Dethier and others (1981) report similar percentages of foreign sediment, particularly clasts of high grade metamorphic rocks, incorporated into Puget lobe till southwest and northwest of the study area. The remaining clasts are dominated by local upglacier lithologies. Because of the predominance of tonalite and granodiorite in most of the alpine valleys of this quadrangle, the percentage of clasts of these lithologies is often sufficient to distinguish the source of till deposited within a valley. For example, nearly adjacent exposures of inferred ice sheet and alpine till along the northeastern shore of Calligan Lake contain 15% and 80% of granitic clasts, respectively.

#### REGIONAL STRATIGRAPHY

Previous workers in the Puget Lowland developed a formal Pleistocene stratigraphic nomenclature for both alpine and Cordilleran glacial and non-glacial deposits (Table 1.1). The youngest (Fraser) Glaciation (Armstrong and others, 1965) includes the Evans Creek Stade, during which alpine glaciers in the Cascades reached their maximum extent, and the subsequent Vashon Stade, inferred from the Puget-lobe advance. Limiting dates on the Vashon advance in the Seattle area include a maximum limiting age for the till of this ice lobe of 15,100 +/- 600 <sup>14</sup>C years B.P. (W-1305) (Mullineaux and others 1965), and minimum date of 13,650 +/- 550 <sup>14</sup>C years B.P. (L-346) (Rigg and Gould, 1957). The ages of earlier glaciations are much

Table 1.1. Pleisocene stratigraphy of the Puget Lowland.



more poorly constrained, and have been vigorously debated as well (Stuiver and others, 1978; Easterbrook and others, 1981). Because the current terminology is unsettled, I make no attempt in this report to correlate pre-Vashon ice-sheet deposits with established stratigraphic nomenclature. Such usage in prior local studies has complicated attempts at correlation across the Lowland based on physical parameters, such as weathering characteristics and relative geographic extent, and may require extensive renaming as absolute ages are subsequently obtained.

## DESCRIPTION OF SURFICIAL DEPOSITS (FIGURE 1.3)

Glacial and non-glacial sedimentary deposits of pre-Fraser  
Glaciation age (Pleistocene)

Throughout this quadrangle, only scattered exposures of pre-Fraser deposits exist. Commonly, younger drift is found directly overlying bedrock. This contrasts to the greater prevalence of older deposits preserved in other glaciated terrains also occupied by Late Wisconsin ice sheets (e.g., more central areas of the Puget Lowland and the Great Plains of the mid-continent). There is also little evidence of removal or redeposition of pre-Fraser sediments by the younger ice sheet. Their scarcity in this study area therefore suggests that most have been eroded away in the interglacial interval(s) prior to the most recent Cordilleran ice advance. This conclusion was also reached by Coates and Kirkland (1974) in the Appalachian Plateau, where Late-Glacial deposits of the Laurentide ice sheet also directly overlie bedrock.

## Description and Weathering Characteristics

Older drifts are distinguished by greater weathering than Vashon-age deposits. In outcrop they are generally oxidized the full depth of the exposure (i.e. greater than 1-10 m), either a mottled gray and orange, or a more uniform orange-brown. In less-weathered deposits included in this unit, clasts stand out from the face of an exposure and evidence of clay translocation is visible in the matrix. Weathering rinds are seen on most clasts, and measure 1 to 3 mm on fine-grained volcanics. Granitic clasts are often completely gruss-



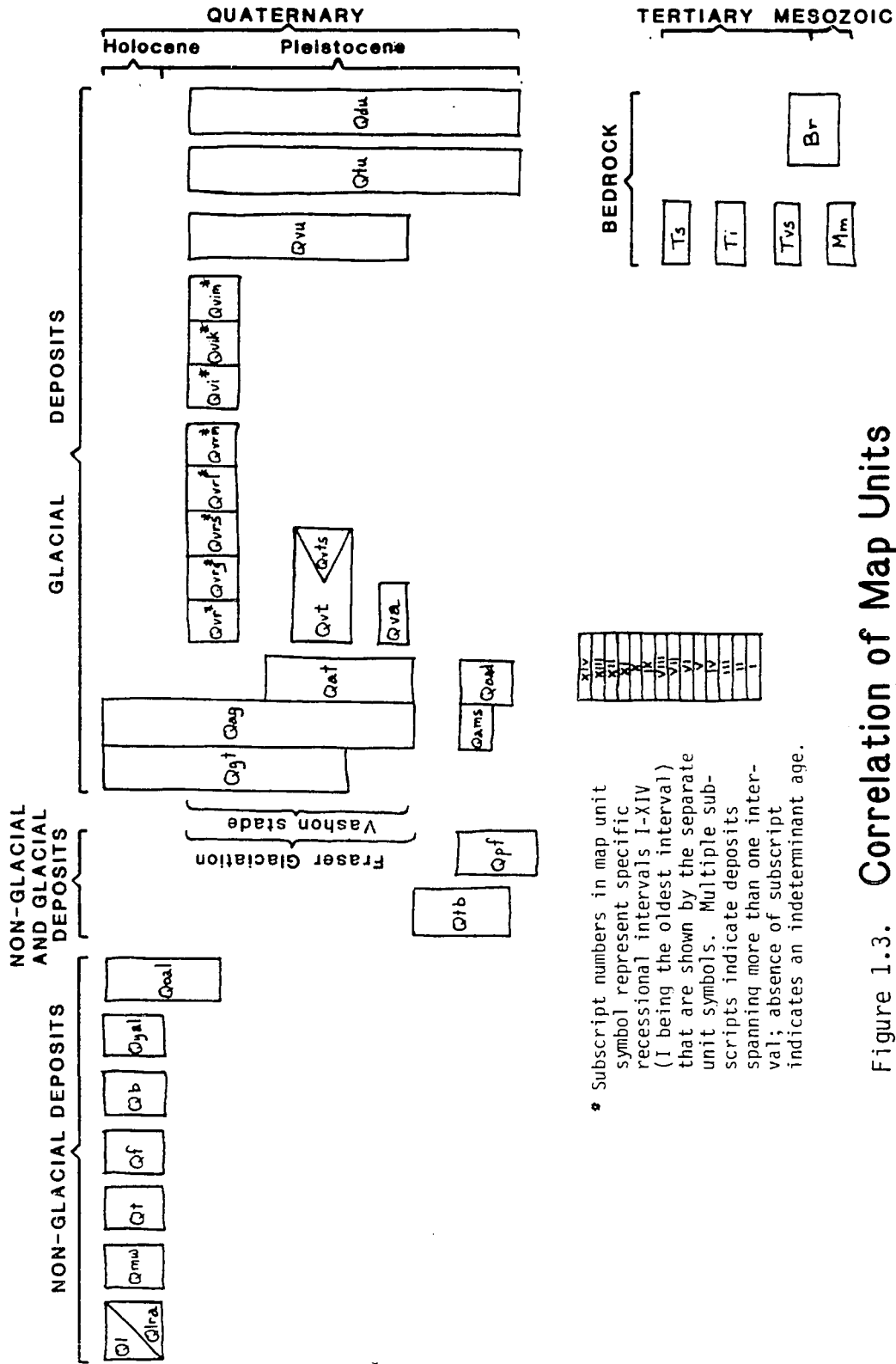


Figure 1.3. Correlation of Map Units

fied, although some show only minimal decomposition.

In more intensely weathered exposures, clasts are generally flush with the surface of the exposure and can be easily cut with a shovel. This degree of weathering often makes lithologic identification of the clasts uncertain. These deposits are largely clay and so are usually quite unstable on steep natural or artificial slopes.

Within these deposits are found both matrix-supported diamictons and bedded clast-supported fluvial gravels and sands. Clast lithologies, where identifiable, usually imply deposition by Puget-lobe ice (of pre-Vashon age). The wide range of weathering intensity observed in these deposits suggests sediment was derived from two or more pre-Fraser glacial and/or interglacial periods, despite likely variations between local weathering environment.

#### Distribution

Older drift is generally found above the maximum altitude of Vashon ice, or beneath Vashon-age deposits where stream incision has exposed it. Above the Vashon ice limit older drift of northern provenance is discontinuously exposed, never more than 50 m (160 ft) above the inferred limit of the younger ice sheet. Older alpine drift occurs both below and well above this level, and is discussed in a later section.

Below the Vashon ice limit, the best and most extensive exposures of pre-Fraser sediments are found in the South Fork and main branch of the Tolt River, where incised meanders and landslide scars expose over 100 m (330 ft) of older drift beneath Vashon deposits.

Although these exposures predominantly display weathered ice-sheet till, locally derived sand, gravel, and minor silt is exposed 1.04 km (0.65 mi) downstream from the Tolt regulating basin, lying above a weathered diamicton and directly below Vashon till. Clast lithologies in this fluvial deposit are consistent with a local source area. Wood in the lower part of this section is 25,600 +/-320 years old (USGS-1625).

#### Transitional Beds

Along the lower reaches of the Skykomish and Snoqualmie Rivers, lacustrine sediments are exposed below Vashon till. In this area and to the west (Minard, 1980, 1981) these deposits rarely exceed 60 m (200 ft) altitude. The sediments are firm gray silty clay and clay with little or no oxidation coloration. They are horizontally laminated except where loading has produced dipping or contorted bedding. The sediments are both impermeable and quite unstable, giving rise to numerous slope failures particularly along the north side of U. S. Highway 2 east of Monroe. These deposits correlate with portions of the Admiralty Clay of Newcomb (1952), and the Pilchuck Clay Member and Lawton Clay Member of the Vashon Drift (Newcomb, 1952; Mullineaux and others, 1965), which have been described as lakebottom sediments deposited in standing water ponded by the advancing Vashon ice sheet. Following Minard (1980, 1981) I map these sediments as transitional beds. They span a period of sedimentation prior to and including the early advance of the Vashon ice sheet. The base of this unit is not

exposed in this area, but the top is clearly marked either by the sand and gravel of the advance outwash or by lodgement till.

#### GLACIAL DEPOSITS

##### Deposits of the Vashon Stade of the Fraser Glaciation of Armstrong and others (1965)

Most Pleistocene deposits exposed in the quadrangle were directly or indirectly derived from the Puget lobe of the Cordilleran Ice Sheet about 15,000-13,500 years ago. The lowermost sediments are lacustrine and fluvial, deposited beyond the edge of the advancing ice. Much of these original deposits were removed by the ice or covered by till, which was subsequently incised and partially covered by meltwater and recessional outwash deposits.

#### Advance Outwash Deposits

##### **Description**

Sand and gravel deposited by proglacial meltwater from the advancing glacier are exposed discontinuously beneath Vashon till. The sand is commonly cross-bedded and tends to grade upward into more gravelly layers. In most exposures the sediments are almost completely unoxidized and, where undisturbed, are almost always compact. The base of this unit is marked by the first appearance of sand above the silt and clay of the transitional beds. This contact may be gradational, representing continuous sedimentation throughout the ice sheet advance. In most exposures the unit is overlain by lodgement till. The contact between outwash and till is locally transitional over as much as a meter, but usually this boundary is rather abrupt

over less than a few centimeters.

The advance outwash is highly variable in thickness and is completely exposed in only a few areas. Maximum observed thickness occurs west of Duvall, on the west side of the Snoqualmie River, where over 100 m (330 ft) of sand and gravel with deltaic foreset beds is exposed between capping lodgement till and river level. A nearby diapir of pebbly silty clay, apparently forced up into the sand from below, suggests the close proximity of the base of the advance outwash. East of Monroe, advance outwash is present only as a discontinuous, contorted stratum between Vashon till and transitional beds, never exceeding a meter in thickness.

### **Engineering Properties**

Where exposed or otherwise inferred to underlie younger deposits, advance outwash is a promising source of relatively shallow groundwater. Newcomb (1952) reports recharge, permeability, and water quality as quite good. However, because this potential aquifer is frequently isolated from contamination by only a thin blanket of till, care must be taken in construction projects not to penetrate this cover. Advance outwash deposits stand on moderate slopes with only minor raveling. They are a good source of clean sand, although their high degree of consolidation and limited extent have apparently discouraged major exploitation in this quadrangle.

## Till

### **Description**

Vashon till is mainly a compact, unoxidized diamicton with a silty sand matrix and with sub- to well-rounded clasts composing approximately 20% of the deposit. The deposit can range from a thin layer of less than a meter thick to several tens of meters thick. In some exposures the till appears to have two distinct facies: the lower is firm and unoxidized with a fine-grained matrix, whereas the upper is looser, sandier, and commonly lightly oxidized. Although in most localities the upper layer is probably weathered till, originally identical to the lower, in some exposures this top layer is more likely melt-out or ablation till consisting of debris released by the melting ice during deglaciation. In these areas it commonly grades into more distinctly water-worked recessional stratified drift, which in turn is found as a discontinuous cover over much of the areas of mapped till.

### **Lithology**

Clasts in Vashon till are dominated by the bedrock lithology present immediately upglacier from it. Observations in many exposures suggest that most clasts in the lodgement till were transported only a few kilometers. There are, however, almost always a few exotic clasts whose presence distinguishes ice-sheet deposits from their alpine counterparts. Till clasts found along the South Fork of the Skykomish River, above the North Fork of the Tolt River upstream of Dry Creek, along the south shore of the Tolt Reservoir,

and near the eastern end of Calligan Lake are exotic to the basins themselves, and so reveal former tongues or bergs of Puget lobe ice that moved up each of these drainages.

### **Weathering**

In most exposures Vashon till is only very slightly weathered. Weathering rinds on fine-grained volcanic clasts are much less than a millimeter thick. Oxidation, if present, extends less than a meter into the deposit, and significant clay translocation is not evident. Only a few granitic clasts are highly decomposed, which can be quite variable even within a single outcrop. Detailed studies of the weathering of Vashon till by Peter Lea (written communication, 1982), Colman and Pierce (1981), and Carson (1970) show mean weathering rind thicknesses from the southern Puget lowland of 0.5 mm or less (on fine grained volcanic clasts), typical oxidation depths of 0.5 m, and no significant alteration of matrix.

### **Distribution and Topographic Expression**

Vashon till mantles most of the rolling uplands above the Skykomish and Snoqualmie River valleys. Recessional deposits are largely confined to channels through this topography and do not obscure it. However, scattered exposures of pre-Vashon deposits and bedrock indicate that Vashon till largely blanketed a pre-existing topography that was not greatly altered by the passage of the ice. Till is significantly thinner on the upglacier side of hills that have at least a few tens of meters of relief than on their downglacier side,

such as around Lake Roesinger, Forest Glade, and Lake Chaplain (all north of the Skykomish River); along the south side of the Skykomish River; and southeast of Cherry Valley. Mullineaux (1970, p. 44-45) and an analysis by Nancy Brown (written communication, 1983) of well data recorded in Liesch and others (1963) show a similar pattern of till deposition to the south and west of this quadrangle.

The till surface is marked by numerous linear depressions and elongate ridges that define consistent ice-flow directions over much of the area. These linear features also align well with striations on bedrock, and, in two localities, with pronounced till fabric. The depressions are generally a few meters deep, approximately 10 m wide, and traverse the countryside for up to several kilometers. They are often poorly drained, and the vegetation that thrives in this boggy environment highlights these features on aerial photographs. Wider depressions are well-expressed by the orientation of Storm and Flowing Lakes, Lake Margaret, and Lake Alice. Elongate ridges may be composed either wholly of till or bedrock, or a mantling of till over bedrock.

Towards the margin of the former ice sheet, patchy till exposures give way to a scattering of rounded pebbles that thins upslope, commonly through a rise in altitude of 30 m (100 ft). Benches, changes in slope, and infrequent moraines also define the most probable ice limit of the Vashon ice sheet.



### **Intra-Till Stratified Sediments**

In some exposures, Vashon till is composed of tough, compact crudely to well-bedded clast-supported deposits with extremely variable proportions of silty matrix. Such deposits commonly lie close to more characteristic lodgement till. The sedimentary materials include sorted sand or gravel interstratified with diamicton, commonly in geographic or stratigraphic locations far from plausible long-term ice margins. They are therefore probably not flowtills associated with subaerial ice-contact environments. I interpret these deposits to be subglacial fluvial sediments, representing either the reworking of recently deposited basal till or the sediment actively transported in subglacial or englacial passageways. Similar material is described and similarly interpreted by Eyles and others (1982) as part of their "lodgement till complex." Examples can be seen in the Monroe-Sultan area on the south side of the Skykomish River, along the lower reaches of Proctor Creek (W. T. Laprade, oral commun., 1982), and along some of the upland channels east of Lake Roy.

### **Engineering Properties**

Vashon till is the "hardpan" of local experience and terminology. It drains poorly, has a low permeability ( $10^{-6}$  cm/s; Olmstead, 1969), is relatively stable on moderate slopes where not immediately underlain by less-competent deposits, and has good undisturbed bearing strength for roads and foundations. Since it is generally thin, however, the ground stability in the proximity of long steep slopes merely capped by till will often be more dependent upon the under-

lying geologic material. Management of the runoff from the nearly impervious till surface then becomes critical in maintaining that stability (Tubbs, 1974).

### Waterlain Ice-Contact Deposits

#### **Depositional Environments**

Continual melting of ice at a glacier's surface, coupled with the flow of new ice and entrained debris out to its edges, provides a steady flux of both sediment and meltwater to the ice margin. The morphology of the sediments deposited in this environment will depend largely on the topography and drainage system adjacent to the ice margin (Flint, 1971). Where an ice tongue extends up a river valley or completely blocks its mouth, sediment will aggrade into that valley, grading from typical ice-contact deposits into a fluvial or lacustrine deposit indistinguishable from those derived from non-ice-contact sources. These multiple deposits are, however, contemporaneous and so are mapped as the same time-stratigraphic unit, or morphosequence (Koteff and Pessl, 1981).

#### **Distribution**

Waterlain ice-contact deposits occur along the maximum or near-maximum position of the former ice sheet, and along the eastern wall of the Snoqualmie River valley where a tongue of ice must have persisted during deglaciation. Additional smaller deposits are present where active ice tongues were stable for long enough for debris to

accumulate. The best example is in the Bengston Lake area north of the North Fork of the Tolt River, where two nested moraines that loop across the upland plain mark the location of a near-maximum recessional stand.

Great embankments of ice-contact deposits fill the mouths of west-draining alpine valleys along the former margin of the Vashon ice sheet. Clast lithologies and occasional foreset beds indicate that these sediments originated outside the local drainage basins and were deposited by ice and water flowing upvalley. Almost all of the major alpine valleys (Sultan, Olney, Wallace, Skykomish, Proctor, South Fork of the Tolt, North Fork of the Snoqualmie, Calligan, and Hancock) are partially or completely blocked by such an embankment. The valley mouth of the North Fork of the Tolt River is also choked by Vashon-age deposits, but here the exposed material is exclusively well-sorted fluvial sand and gravel and so is discussed in the section on recessional history.

### **Sedimentary and Morphological Characteristics**

These deposits show wide variation in both sedimentary character and morphology. They are comprised predominantly of fluvial gravel and sand, commonly with local foreset bedding. However, lenses and thick layers of flowtill and probable lodgement till are also found in many exposures, particularly in the morainal embankments. Till lenses are exposed in the creek cuts of the Hancock and Calligan Lake outlets, and are the primary sediment encountered in test borings

through the embankment just west of Spada Lake (Converse Ward Davis Dixon, unpublished) and north of the Tolt dam (Shannon and Wilson, unpublished). Roadcuts along the eastern, distal slope of the South Fork of the Tolt River embankment, just north of the dam, also expose till up to at least 560 m (1840 ft) altitude. Excavations through the middle of this embankment reveal a thin layer (1-2 m) of distinctly fluvial sediment overlying 50 m (160 ft) of moderately consolidated, crudely bedded, unoxidized, matrix-rich gravel and sandy silt and clay. The deposit is locally clast-supported along sub-horizontal layers. The overall texture is similar to lodgement till exposed throughout the area but includes a greater amount of clay in the matrix. The origin of a similar deposit has been debated by Evenson and others (1977), who infer subaqueous flowtill that moved off the glacier terminus, and Gibbard (1980) who favors subglacial meltout till beneath a floating ice tongue. Further description of glacial sedimentation into lacustrine environments (Eyles and Eyles, 1983) that apply closely to this locality suggest that subglacial meltout is the source of this deposit. A more complete discussion of these embankments is given in Chapter 4.

### **Engineering Properties**

The multiple modes of deposition of these ice-contact sediments yield deposits whose engineering properties vary over short distances. Moderately well-sorted fluvial gravel and sand may be expected where deposited far from former ice margins, and show many of the engineering properties of recessional outwash. Deposits proximal to

the ice-contact surface, however, often show abrupt and unpredictable grain-size variations. Boulders in excess of a meter in diameter are common. Till lenses and larger masses may also be encountered. The two major reservoirs in the area demonstrate the relative impermeability of the morainal embankments behind which they are impounded, but detailed subsurface exploration of each has demonstrated their variability as well (Shannon and Wilson, unpublished; Converse Ward Davis Dixon, unpublished).

#### Recessional Outwash Deposits

##### **Description**

Sediment deposited by meltwater during ice retreat mantles much of the terrain. It ranges in thickness from less than a meter to more than 100 m (330 ft) in large deltas, such as those along the east side of the Snoqualmie valley. Characteristically the sediment is an interbedded mixture of sand and sub-rounded to well-rounded gravel with clasts up to 30 cm in diameter. A light orange oxidation color over otherwise fresh clasts is present through the full depth of exposure. Except where cemented by local iron oxide, the sediments are easily excavated with a shovel. Clast lithologies are characteristic of the Vashon Drift as a whole; although they consist mainly of local types, they generally have an exotic component as well. Fining upward, plausibly reflecting retreat of the ice margin, is uncommon. Neither cross-bedding nor very fine grained sand and silt are as common in these fluvial recessional deposits as they are

in fluvial deposits of the advance outwash.

Maximum and mean grain sizes vary considerably between exposures. Although the largest clasts typically reach 30 cm, extremely coarse boulders (2-3 m diameter) crop out just north of the North Fork of the Tolt River, south of Winter Lake; and along Youngs Creek, 4 km (2.5 mi) above its confluence with Elwell Creek south of Sultan.

Lake sediments deposited during ice recession are generally silt to very fine sand, often thinly laminated. Rare dropstones are present in many exposures. In the North Fork Snoqualmie River valley, lacustrine sedimentary deposits are distinctly coarser than in the other alpine valleys. Medium-grained sand is common here and silt is uncommon, suggesting a rapidly aggrading valley in which deposition kept pace with a rising base level.

### **Distribution**

The greatest volumes of recessional outwash sand and gravel are present as deltas built into a recessional lake formed in the Snoqualmie River valley. The deposits are present at the mouths of streams that drain the uplands to the east, and whose valleys provided routes for meltwater released at the retreating ice margin. The Tolt River valley displays well the downstream transition from a kettled outwash plain through a series of channelized gravels and sands to a corresponding series of deltas built into the Snoqualmie valley. A similar system of deltas just north of Monroe shows the influence of falling lake levels in the Skykomish River valley and the successive activity of several meltwater channels from the north.

### **Marginal Lacustrine Deposits**

The Vashon ice sheet impounded lakes in many of the alpine valleys. The maximum elevation of the resulting lake deposits, commonly well-corellated with elevations of corresponding morainal embankments, and the paucity of ice-rafted pebbles suggest that these embankments dammed the valleys well into the postglacial period. Exposures of Vashon till below lake sediments in the Sultan Basin, the South Fork Skykomish River valley, the South Fork Tolt River valley, and above the northeast shore of Lake Calligan confirm that portions of these lacustrine deposits are recessional. Advancing and receding ice, however, would both have been equally effective in damming these valleys as long as the ice at their mouths was sufficiently thick (Chapter 4).

### **Engineering Properties**

Recessional outwash provides most of the sand and gravel used for construction, which according to Livingston (1971) is the most valuable mineral resource of western Washington. In the Snoqualmie and Skykomish River valleys, most of the large deltas, and many of the smaller ones, are actively mined. Grain sizes commonly range from medium sand to 20 cm cobbles. Fines are rare in the main body of the deltas. Upstream channel deposits, however, can be far more variable in grain size. Many of these channel deposits are merely veneers over subglacially-deposited material, rendering commercial evaluation difficult.

Permeability is high, stability is good, and settlement should be negligible. Areas underlain by thick accumulations of recessional outwash should be well-drained, but because the deposit is commonly underlain by lodgement till or impermeable bedrock, perched groundwater is possible. Shallow wells in recessional outwash are prone to seasonal fluctuations and contamination. Nevertheless, it is an important groundwater source throughout the area (Newcomb, 1952).

In contrast, recessional lacustrine deposits are both weak and impermeable. Poor surface drainage, together with low slope stability and bearing strength, make such areas particularly ill-suited for most types of development.

#### Alpine Drifts and Related Deposits

##### Older Alpine Drift, undifferentiated

Deposits above the limit of Vashon ice on the interfluves between west-draining alpine valleys, particularly south of the North Fork of the Tolt River, were left by Cascade glaciers. They form low-relief surfaces above about 1000 m (3300 ft). Weathering rinds on fine-grained clasts range from 1 to 8 mm thick, and most granitic clasts are decomposed to grus. Oxidation is variable, but it is always more intense than in either ice-sheet or alpine deposits of the last glaciation. Clast lithologies usually specify an alpine source, with granitics common even in those deposits found far west of any granitic bedrock.



### Alpine drift of Mt. Stickney

West of Mt. Stickney, till and stratified drift mantle the bedrock ridges, forming a broad, gently sloping surface with a pronounced morainal crest. The lithology of the drift, 80 to 90% granitic clasts, indicate transport by alpine ice from granite source areas east of Mt. Stickney. This drift is largely above the limit of Puget-lobe ice, although locally above Wallace Lake some has been reworked by the Vashon-age ice sheet. Modern U-shaped alpine valley floors, cut hundreds of meters into the upland surface, were occupied by younger valley glaciers. Thus the glacier responsible for this deposit must have formed as a widespread icecap, covering all but the highest peaks and ridges. Evidence for the extent of this ice north and west of the Cascade front has been completely obscured by younger deposits.

Weathering rinds on fine-grained volcanic clasts on the constructional surface of the deposit measure 1 to 3 mm thick, and granitic clasts show a wide range of decomposition with slightly gussified stones predominating. Sediment exposed and reworked by the Puget lobe is generally less weathered, indicating its long isolation from weathering while deep beneath the original depositional surface.

### Alpine Till

Deposits mapped as alpine till are loose to compact diamictons having angular to subrounded clasts less than 30 cm diameter supported by a silt or sand-rich matrix. Clasts are generally fresh and

unoxidized. Counts of clast lithologies indicate upvalley sources. This unit includes only those few deposits to be sufficiently continuous and well-exposed to map.

#### Alpine Glacial Deposits, undifferentiated

Dense vegetation cover, sporadic exposures, and poor access up most of the alpine valleys here render the identification, subdivision, and delineation of the limits of alpine glacial deposits difficult. The distribution of such deposits, therefore, is inferred primarily from aerial photographs and occasional field exposures. As mapped, they also include significant amounts of colluvium, alluvial fans, recent valley-bottom alluvium, and bedrock. Contacts between this unit and bedrock upslope may be gradational and only approximately located. The weathering characteristics and topographic position of most such deposits are similar to those mapped more specifically as alpine till.

#### Glacial Deposits and Taluses

Some sliderock observed on aerial photographs show ridged, lobate lower boundaries, suggesting either deposition at the base of small glaciers or permanent snowfields, or the presence of active rock glaciers. All are apparently unvegetated, and are found only on north-facing slopes in areas above 1200 m (4000 ft) elevation. Their distinct morphology and lack of extensive vegetation suggest a late Holocene age.

## CORRELATION OF PLEISTOCENE DEPOSITS

### Cordilleran Ice Sheet Advances

Although previous studies in the central Puget Lowland have documented multiple advances of continental glaciers, such evidence is rather sparse in this quadrangle. Older drift, however, is found discontinuously up to 50 m (160 ft) above the maximum elevation of Vashon ice, along much of the ice margin here. The weathering characteristics and relative topographic position are consistent with those deposits reported by Carson (1970) and Peter Lea (oral commun., 1982) in the southwestern and southern Lowland, and so provide additional evidence for a more voluminous pre-Vashon advance. Carson (1970) correlated this maximum ice-sheet advance with the Salmon Springs glaciation of Crandell and others (1958). Correlation of this ice stand with previously named deposits, however, is probably premature and must await additional age data.

### Alpine Glacial Advances

The current stratigraphic framework for alpine deposits on the western slopes of the Cascade range is given by Crandell and Miller (1974). Although speculative, correlation between deposits found near Mount Rainier and those in this quadrangle, 110 km (70 mi) further north, are suggested by certain topographic and weathering characteristics. The degree of weathering and lack of constructional morphology associated with the deposits mapped here as older alpine drift clearly indicate a pre-Evans Creek age. In addition, this unit

includes deposits that more specifically share weathering and morphologic characteristics described by Crandell and Miller (1974, p. 19) for Wingate Hill Drift. Weathering rinds on clasts in the alpine drift of Mount Stickney also indicate a pre-Evans Creek age (Colman and Pierce, 1981). The degree of weathering and loss of constructional morphology, however, is consistently less than in most of the deposits mapped as undifferentiated older drift. These characteristics invite comparison with the Hayden Creek Drift of Crandell and Miller (1974, p. 21-22), and suggest possibilities for future investigation.

Less weathered deposits constitute the remainder of alpine drift found in this area. One deposit in particular, damming a bog 2 km south of Lake Hancock, shows a distinct morainal form, and permits estimation of the equilibrium-line altitude (ELA) of the glacier that formed it. Reconstructing the aerial extent of this glacier by making reasonable assumptions about its gradient and source area, and applying methods of ELA estimation described in Porter (1975) and Pierce (1979), yield an ELA of slightly above 1000 m (3300 ft). Its median altitude is approximately 60 m higher. This compares to within 100 m of values obtained by inspecting Crandell and Miller's map (1974, Plate 1) showing Evans Creek glaciers in the Mount Rainier area, and by calculations performed by Williams (1971) for the Middle Fork Snoqualmie River basin and assigned by him to glaciers of the Evans Creek Stade.

No evidence for the merging of Late-Wisconsin age alpine and

Puget-lobe glaciers was found in this area. The presence of lacustrine sediments in the alpine valleys confirms the retreat of alpine glaciers from their maximum position prior to the Vashon ice sheet's final retreat (Porter, 1976), but sheds no additional light on their relative timing or interaction. Williams (1971) reported deltaic sediments at the upper end of the Vashon-age lake in the Middle Fork Snoqualmie River valley, but field work for this report at this locality disclosed only abundant Holocene alluvial-fan deposits along the steep valley walls.

### **NONGLACIAL DEPOSITS**

#### Older Alluvium

Fluvial gravel and sand above the level of the modern floodplains can be mostly assigned to a recessional interval during the last ice retreat. However, the topographic position of some deposits make this interpretation doubtful. For example, along the upper Raging River south of Preston, terrace remnants stand at 200 m (660 ft) elevation, 10 m (33 ft) above the level of the modern streambanks. Projection of this terrace west down the channel now occupied by the East Fork of Issaquah Creek, a path for recessional meltwaters, indicates that it stands at too low a level to correspond with the Vashon recessional terraces there. Instead, it was probably deposited by the Raging River during or preceding its active incision of the canyon north of Preston. A similar series of three broad terraces along the Skykomish River near Gold Bar cannot be unequivocally assigned to any of the recessional stages in the valley. Indeed,

their surfaces project downstream on reasonable gradients to levels well below those associated with deposits produced during deglaciation. The terraces are numbered on the map from 1 through 3, indicating successively younger intervals of deposition.

#### Younger Alluvium

Recently transported sand and gravel is present along all of the major streams and rivers in the area, generally forming a planar surface devoid of trees. Although the age of these surfaces is inferred from vegetation and morphology to be on the order of years or decades, this unit includes some deposits equivalent in age to mapped older alluvium but lacking any observed topographic demarcation.

#### Bog Deposits

Poorly drained depressions are common throughout much of this area. Identification of bog deposits are based on topography, vegetation characteristic of wet environments, and the presence of standing water. Bogs are also common in valleys occupied in part by flowing streams, and thus may be gradational into younger alluvium. In many such instances, the form and gradient of the channel has been inherited from glacial activity, with the stream passing through both alluvial reaches and nearly standing water. Peat is common in many of these bogs (Rigg, 1958).

#### Alluvial-Fan Deposits

Where tributary streams enter larger valleys having a lower

gradient, some portion of the tributary sediment load is deposited as an alluvial fan at the mouth of the stream. Ephemeral streams on steep sideslopes also transport sediment downslope for varying distances, and this material can coalesce to form an entire hillside of fan deposits. Although truly gradational with sliderock and certain other mass-wastage deposits, fan deposits are distinguished by their characteristic lobate morphology at low hillslope gradients and by the presence of stream channels on steeper slopes.

#### Taluses

Subangular to very angular blocks of local bedrock mantle hillslopes below steep rock cliffs. They are most pronounced above 1000 m (3300 ft) and on north-facing slopes where frost action is most effective. I mapped most deposits from aerial photographs on the basis of surface texture, the absence of vegetation, and topographic position.

#### Mass-wastage deposits (undivided)

On hillslopes of any non-zero gradient, the surface sediment is in sporadic downhill motion by a wide variety of processes dependent on local failures in the soil or underlying rock, expansion and contraction of the surface material, or biological activity. I mapped mass-wastage deposits where sufficiently thick and continuous to obscure both the underlying geologic material and any characteristic topographic features which might serve to identify it.

### Landslide Deposits (Undivided)

I identified landslide deposits largely from characteristic hummocky topography, distinct scarps, or anomalous closed depressions that are not associated with collapse features of ice-contact deposits. They are gradational with areas mapped as mass-wastage deposits but generally involve larger, more coherent blocks of sediment or bedrock. Contacts may include not only the area of the transported geologic material itself but also the slide scarp if its expression is relatively fresh and the material there is potentially unstable as well. Non-horizontal dips in fine-grained sedimentary deposits that are inferred to be undisturbed by glacial action also indicate downslope mass failure by rotation of coherent blocks, particularly if adjacent to areas of active downcutting by streams. Instability is indicated not only by the surface form and presence of discrete scarps and fissures in the ground surface, but also by the character of the vegetation, which commonly includes trees canted irregularly downslope.

### Modified Land

Modified land mapped in this area includes the three major dams in the area, cuts for a powerhouse on the Sultan River, and extensive grading and filling for a power substation northeast of Monroe. Transportation corridors involving the placement of fill on or alongside of Skykomish and Snoqualmie River alluvium are shown only when their width is easily represented at this scale of mapping.



### VASHON-AGE RECESSIONAL HISTORY

As the scoured and channelized topography of the Lowland emerged from beneath the retreating ice sheet, a complex of interconnected meltwater channels and lakes formed. Earlier workers have stressed either the local (Anderson, 1965; Knoll, 1967) or the regional (e.g., Bretz, 1913) character and sequence of these features. The recent study of Thorson (1981), however, provides a far more complete framework of the deglaciation sequence for defining more detailed, localized stratigraphy.

In the study area, the postglacial topography naturally divides the region into three distinct areas: 1) the Snoqualmie valley, 2) the Skykomish valley and its northern tributary valleys, and 3) the upland valleys and channels lying east of the Snoqualmie River. Throughout most of the recessional period, meltwater activity followed a rather simple and consistent pattern. Water draining marginally and submarginally from the north was impounded in a lake occupying the Skykomish valley, and spilled southward first through the broad trough south of Gold Bar, and then through the valley south of Sultan. This water thus entered the upland channel system, combined with additional water derived from the gradually retreating ice margin in this area, and flowed south and southwest into the Snoqualmie valley. The bulk of the ice sheet, blocking the northerly drainage of this valley, impounded a series of lakes that drained into yet other, lower water bodies to the south and west beyond the limits of the quadrangle. Spillways that controlled the altitude of

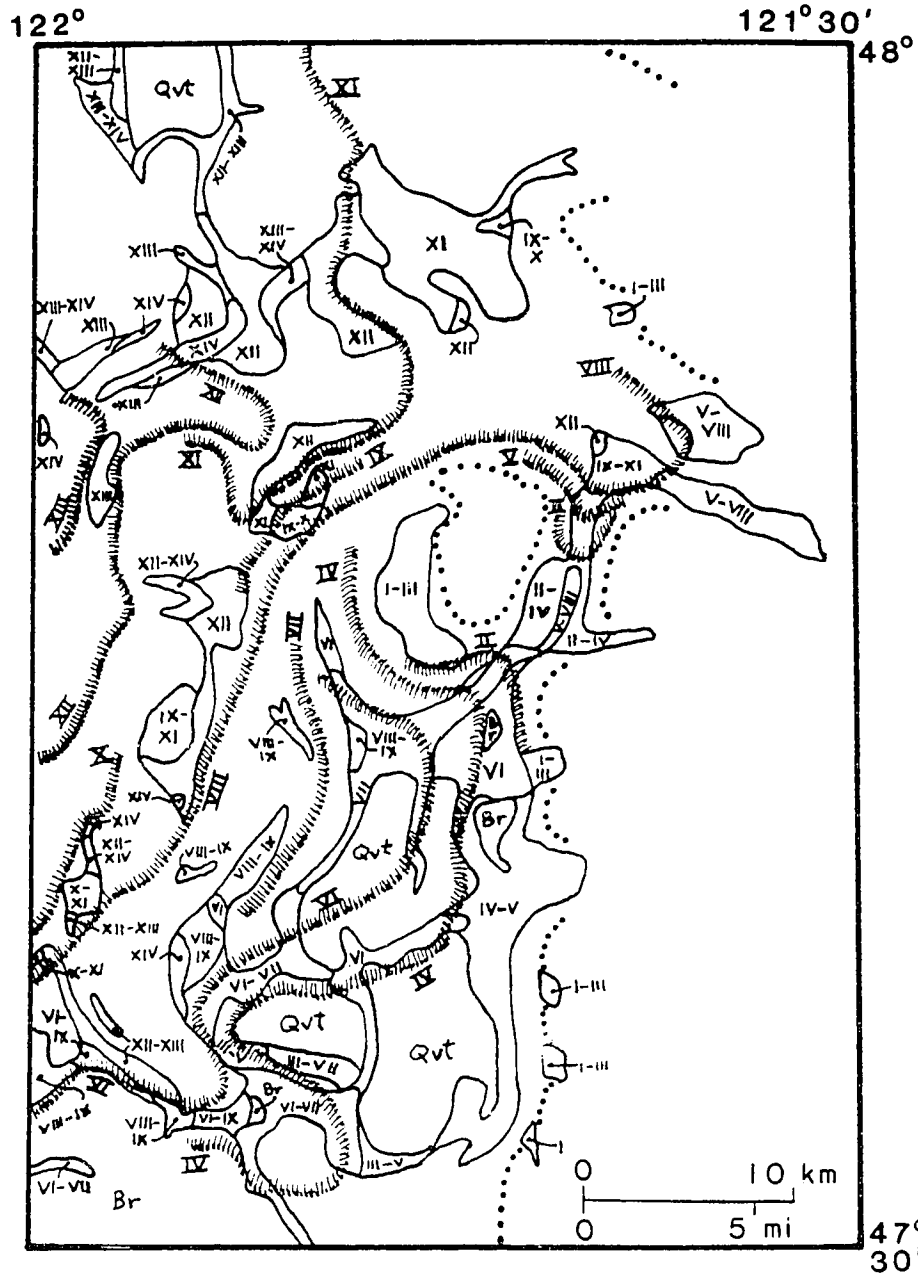
such lakes in both the Snoqualmie and Skykomish River valleys can be identified. Stream deposits, deltas, and lake-bottom sediments associated with these altitudes provide the basis for time-stratigraphic assignment and correlation of the mapped recessional deposits.

To elucidate these relationships, time intervals within the recession are numbered sequentially. Their boundaries are defined either precisely by the opening of a specific spillway or more indefinitely by the position and altitude of particular recessional deposits (Figure 1.4). Because the three major topographic areas are only indirectly connected, events defining a particular time boundary would not simultaneously affect every site of sedimentation throughout the quadrangle. Thus individual recessional deposits and active meltwater routes often include more than one time interval. In the following discussion, Roman numerals in parentheses refer to the time-stratigraphic assignments (I being the oldest), whose relationships can be seen more concisely on the chart of recessional intervals (Figure 1.5). When correlating spatially separated features, we can compensate for the systematic increase in present-day elevations northward due to isostatic rebound since deglaciation by using Thorson's gradient of 0.9 m/km (1979, Figures 17 and 23) along a roughly north-trending transect. This correction appears to be applicable even this close to the edge of the Lowland.

#### Uplands

Early recessional deposits preserved along the ice margin are

Figure 1.4. Distribution and sequence of the recessional outwash deposits of the Vashon Stade of Armstrong and others (1965). Numerals refer to deposits and ice-margin positions of specific recessional intervals from I (oldest) to XIV (youngest). Qvt = Vashon till (Pleistocene); Br = bedrock (Tertiary and Mesozoic)



VII DEPOSITS OF SPECIFIC RECESSIONAL INTERVAL(S)

VII ASSOCIATED ICE MARGIN POSITION (SHADING ON DISTAL EDGE)

..... MAXIMUM ICE LIMIT

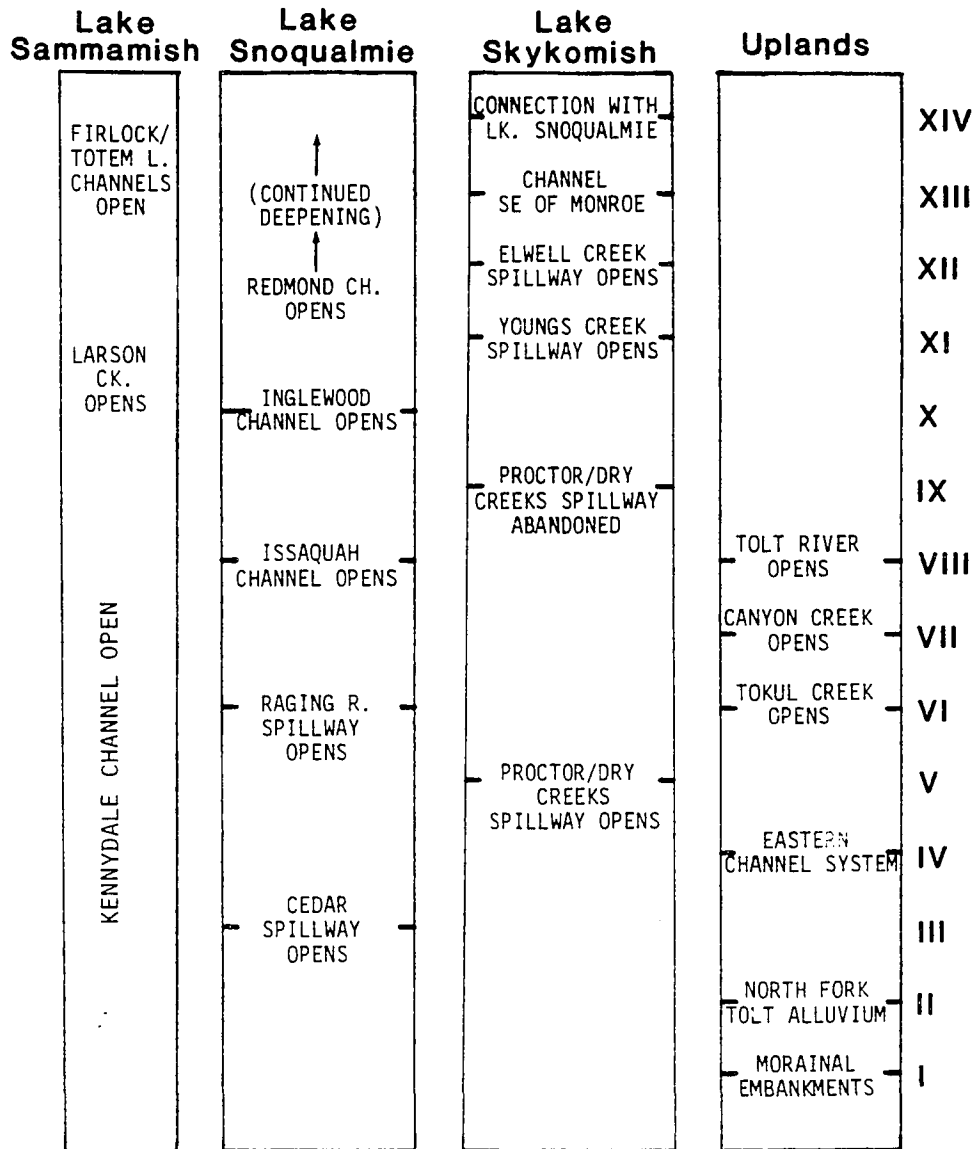


Figure 1.5. Correlation of recessional intervals and spillway activity in the eastern Puget Lowland during the Vashon Stade of Armstrong and others (1965).

limited to moraines and morainal embankments blocking alpine valleys (I-III). Their very variable surface elevations well below their local ice maximum limits, require that they did not form simultaneously (Table 4.1). They must, however, have preceded the deglaciation of all channels further west.

Poor exposure and post-glacial erosion have inhibited interpretation of these embankments. In the Calligan-Hancock area, Mackin (1941) first noted that each valley drains around the south edge of the embankment that blocks it. He suggested the presence of a great ice-marginal river that carried the water from each of the blocked drainages southward, dumping sediments into each valley in turn on their north side and draining off to the south. Yet neither coarse-grained fluvial deposits nor deeply-scoured continuous channels, plausible remnants of such an hypothesized torrent, can be found at or near the level of these embankments.

Such fluvial features, however, are found roughly 200 m (660 ft) below the level of the embankments, on the floor of the upland surface now occupied by the North Fork of the Snoqualmie River. Analysis of the physics of subglacial water flow in this area (Chapter 3) confirms that instead of draining subaerially at the ice margin or across the ice-sheet surface, water would tend to occupy this lower, subglacial position. Subglacial drainage out of the alpine valleys behind each embankment would be favored on the south (downglacier) side of each valley (Chapter 4; Figure 4.8). The deposition rate of embankment sediments should be lowest along this drainage route, and

so post-glacial subaerial drainage will be located here as well. The surface topographies of these embankments generally do not reflect aggradation from the north by river-transported sediments. At Lake Calligan, for example, the high point lies along the central E-W axis of the embankment. Finally, exposures and borings through several of the embankments show that till is common or even dominant relative to fluvial deposits, suggesting that water transport of the sediment was primarily local off the ice surface.

Emergence of subaerial channels in the upland region followed formation of these embankments, as the ice margin began retreating from the mountain front. The highest and easternmost of these channels (IV-V) began as a set of now-beheaded valleys just south of the South Fork Tolt River. They continued south as anastomosing channels in marginal or near-marginal positions and finally built a broad outwash plain, whose base level was fixed by the earliest lake to occupy the Snoqualmie valley (see III, below). The bedrock and till that emerged from beneath the ice in this area is now largely submerged by these deposits.

Further north, an alluvial deposit chokes the valley of Dry Creek and the North Fork Tolt River, with associated lake sediments present further up the North Fork valley (II-IV). The surface elevation of this deposit and isolated position indicate deposition relatively early in the recession, while ice still covered both the Proctor Creek valley just north of it and the lower upland channels to the west. Its continuity with the early outwash surface to the

south (IV-V), discussed above, is ambiguous. Much of the drainage both into and out of this area may have been through subglacial passageways, and therefore diagnostic depositional surfaces are absent.

Continued withdrawal of the ice margin from the upland area allowed the primary routes of meltwater drainage to migrate westward. Although evidence is lacking for any stillstand of the ice margin during this time, the presence of spillways permits assigning discrete intervals within this period. The subaerial emergence of Tokul Creek, Canyon Creek, and the Tolt River define three such intervals (VI, VII, and VIII). Terraces and channels found near Beaver Creek suggest an early connection (VI) between the older "eastern" channels and Tokul Creek. Each of the three main stream channels lies roughly perpendicular to ice-flow indicators and so all were probable marginal or near-marginal streams during their successive activity. Only the Tolt has maintained significant Holocene flow, as it forms the lowest, western-most outlet for a basin otherwise bounded by bedrock divides. Tokul and Canyon Creeks are perched well above this basin and therefore required ice diversion of meltwater for their supply. This is confirmed by the proximity of ice-contact deposits. During their respective occupation by outflow, the basin upstream of the outlet channels aggraded with fluvial sediments to concordant elevations. Their thickness, about 30 m (100 ft), coupled with likely rates of ice retreat required by the less than 1500-year total occupation time of Puget-lobe ice (Rigg



and Gould, 1957; Mullineaux and others, 1965) testify to a remarkably high flux of sediment during this time.

Knoll (1967) proposed an equivalent sequence of recessional stages in the Tolt River area, but he included Griffin Creek as an additional important channel. Griffin Creek, however, has an extremely low gradient at 150 m (500 ft) elevation, 4 km (2.5 mi) downstream of a plausible spillway out of the Tolt basin, and shows no major accumulation of sediment. Since only minor sediment transport could have occurred downstream of this point, significant melt-water occupation of Griffin Creek must have been very short-lived (during VII).

#### Skykomish River Valley

The high bedrock divide just south of the Skykomish River permitted relatively few drainage routes across it. The highest, most easterly, and longest-occupied route is the broad south-trending trough south of Gold Bar, now occupied by Proctor and Dry Creeks (V-VIII). Its location is structurally controlled by a fault-line scarp between resistant Tertiary volcanics and easily eroded Mesozoic argillite-rich melange. This passageway formed the only drainage route for the entire Skykomish valley during most of the Vashon-age glaciation. It would have been equally favorable as a subglacial drainage route, both at ice maximum and for as long during retreat as ice was sufficiently thick to prevent subglacial drainage farther west (e.g., the Elwell Creek valley south of Sultan). All

water at the ice margin and at the glacier bed within several tens of kilometers of the margin, collected from west-flowing alpine valleys and submarginal drainage further north, would thus have been channeled through here. As a subsequent subaerial drainage route, it provided much of the water and sediment for those southern channels closer to the maximum ice margin (V) and for the water and sediment that later entered the Tolt basin (VI-VIII). The top of the Skykomish River morainal embankment and the upper limit of lake sediments found further upstream (V-VIII) are graded to the subaerial elevation of this trough as well (490 m, 1600 ft) (Cary and Carlston, 1937; W. T. Laprade, oral commun., 1982).

Continued ice thinning eventually would have allowed subglacial drainage farther west (IX-X) under a lower hydraulic potential than the now-subaerial Proctor trough. Base level of the Skykomish lake then fell continuously as the ice thinned; therefore, no discrete intermediate intervals can be defined. Once the spillway at Youngs Creek (XI) was exposed south of Sultan, lake level stabilized again and a set of identifiable lacustrine sediments, terraces, and outwash plains graded to 180 m (600 ft) developed. Flow over Olney Pass from water impounded in the Sultan Basin and from an ice margin near Lake Chaplain and Echo Lake contributed in forming the large outwash plain north of Startup. A somewhat perplexing problem is the relatively short distance of ice margin retreat required to open a yet lower path, contrasted with the apparent large volume of sediment graded to the Youngs Creek spillway. The lower spillway, exposed at Elwell

Creek (130 m, 430 ft) (XII), allowed another drop in lake elevation. The location of deposits graded to this base level attest to the ice margin's continued westward retreat out of the Skykomish valley. Final retreat from this valley created a penultimate level of water and deposits (XIII) before the valley merged with the regional lake system, discussed in the next section.

#### Snoqualmie River Valley

Five distinct spillways link the Snoqualmie valley with the rest of the lowland to the south and west (Figure 1.6). Continuous ice retreat impounded a discrete sequence of lakes whose levels were controlled by the currently lowest and most northerly of these spillways, successively exposed from beneath the retreating ice margin. Lake levels are marked particularly well by the elevations of alluvium and deltas deposited during simultaneous drainage from the upland channel system. Because the Snoqualmie valley trends north-south, features distributed along the valley associated with a single late-glacial water plane will now stand at different altitudes, owing to isostatic rebound since the ice retreated. In particular, initially level features will now stand higher to the north since thicker overriding ice ultimately resulted in greater amounts of rebound to the north. To facilitate comparisons, elevations are given with both the present values and their correction required to compensate for rebound relative to Monroe (indicated by "+/"). This arbitrary datum is chosen because the amount of rebound at Monroe is roughly equivalent to that of the entire Skykomish valley and because

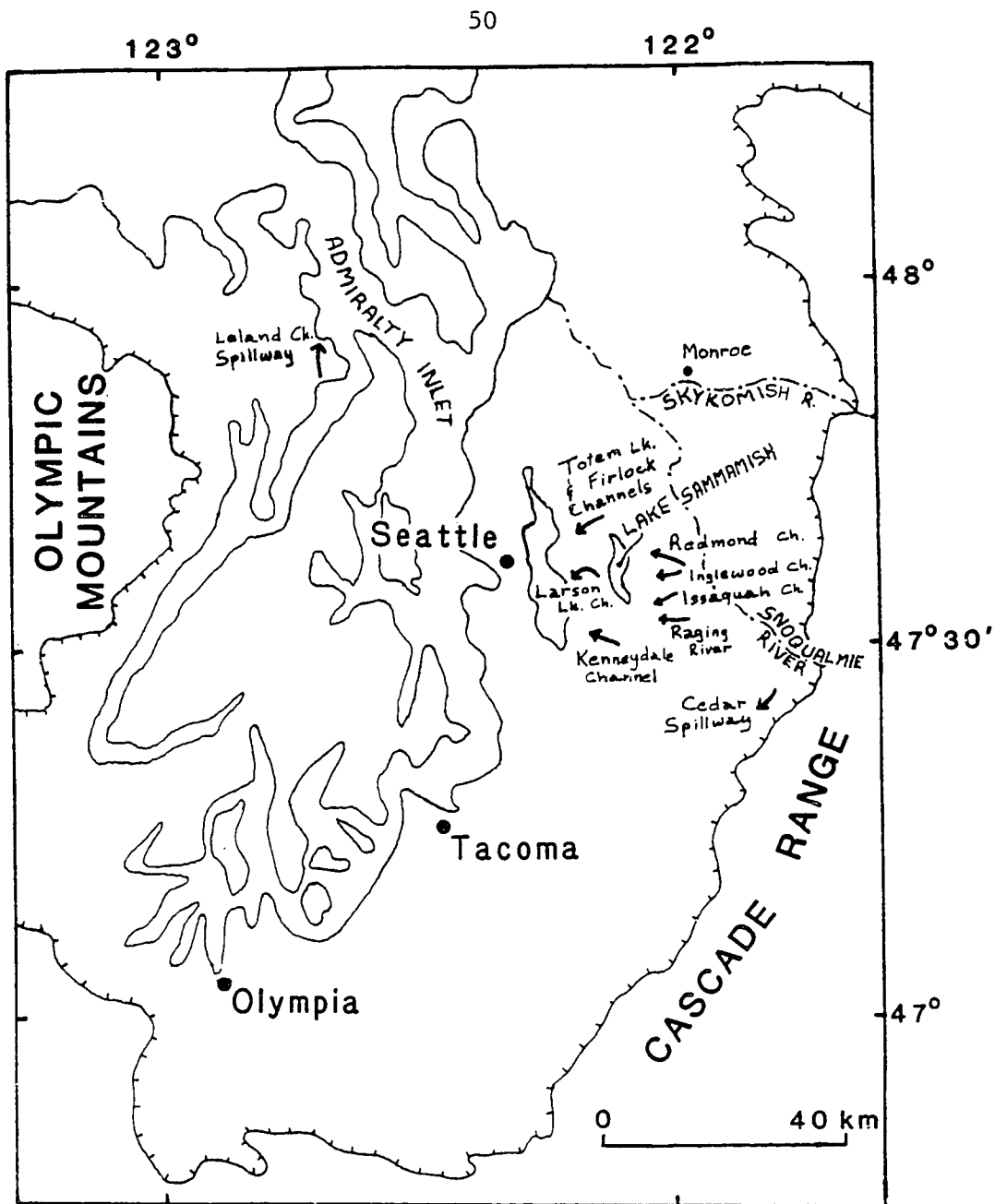


Figure 1.6. Puget Lowland localities discussed in text. Hachured line indicates position of the Puget-lobe ice limit (from Thorson, 1980) during the Vashon Stade of Armstrong and others (1965).

coincidentally it matches the rebound of the last major lake spillway of the entire Puget Sound region (the Leland spillway, discussed below). Estimates of the correction can be made for unspecified features by inspecting Thorson (1979, Plate 1) or, more approximately, by adding 9 m elevation for each 10 km distance (5 ft/mi) south of Monroe.

The broad valley of the Snoqualmie River terminates approximately 8 km (5 mi) south of the map, at the foot of a broad trough (the Cedar spillway) between Rattlesnake Mountain and the Cascade Range front. This trough probably acted as a subglacial meltwater passage. As the ice margin retreated north, it became a subaerial spillway with an elevation of 280/+45 m (920/+150 ft), impounding a proglacial lake between it and the ice (III-V). Both Bretz (1910) and Thorson (1981) called this body Lake Snohomish. Fluvial deposits in the lower North Fork of the Snoqualmie River valley, associated with the upland channel sequence (IV-V), must have in part built into this lake.

Opening of a spillway southwest of Fall City (Anderson, 1965; Curran, 1965) over the divide between the Raging River and the East Fork of Issaquah Creek (158/+36 m, 520/+120 ft) appears to have been roughly synchronous with the opening of Tokul Creek as the primary upland drainage path. Evidence includes the absence of 280-m-level deposits at Tokul Creek or 158-m-level deposits along the lower North Fork of the Snoqualmie River (VI-VII). Drainage to the west was into Glacial Lake Sammamish, the elevation of which was then controlled by

the Kenneydale channel (91/+37 m, 300/+120 ft), located southwest of this quadrangle. The initial diversion of water east of Snoqualmie Falls reflects a nearby ice-margin position, while the multiple levels of the delta at Tokul Creek show active downcutting of the controlling spillway. Voluminous ice-contact fluvial deposits just north, along the east wall of the Snoqualmie valley, show that a tongue of ice extended down the late-glacial precursor of the modern valley both before and during drainage via the Raging River. The low gradient of Griffin Creek at 150 m (500 ft) is easily explained by water and sediment flow from this ice tongue up the modern valley, leaving a gradation from coarse to fine-grained alluvium from the Snoqualmie valley to the large Griffin Creek bogs.

Continued marginal retreat opened in succession two channels northwest of Fall City, which also drained west into Glacial Lake Sammamish. Associated with the Issaquah channel (110/+34 m, 360/+110 ft) are ice contact deposits just north of it, indicating the probable ice margin position at this time; and deposits of the Tolt River delta, including its southern end where fluvial material buried the stagnant tip of the Snoqualmie valley ice tongue (VIII-X). Occupation of the Inglewood channel (107/+31 m, 350/+100 ft) was briefer (X-XI), as only a minor shift of the ice margin position west of the quadrangle exposed a much lower drainage route.

The Redmond channel, 5 km (3 mi) southwest of Carnation, provided the lowest route south of Monroe for drainage to the west. It is therefore the most northerly of the Snoqualmie spillways. The

level of deposits in the main valley indicates that elevation was controlled by the level of Glacial Lake Sammamish, and thus the sequence of spillways identified by Thorson (1980) for that lake are applicable to this valley as well. At first exposure of the Redmond channel, water level in the Snoqualmie valley fell from its Inglewood channel level. Evidence from the deposits north of the Tolt River, at Harris Creek, and from a plausible reconstruction of the ice margin location west of the map area all indicate with excellent agreement that the Larson channel of Glacial Lake Sammamish (76/+33 m, 250/+110 ft), west of this quadrangle, was active at this time (XII-XIII). Consequently, continued retreat of the ice in the map area affected only the location of sedimentation in the lake; lake elevation itself was controlled by the retreat much further west. Lake-bottom silts that form constructional terraces along the sides of the Redmond channel are below the level of this stage (XII-XIII) but above that of the subsequent stage (XIV), necessitating their deposition during this time as well. Although the Redmond channel itself must have deepened as water from the Snoqualmie valley flowed through it, its early recessional existence and exploitation are required by the recessional deposits found within it. Since till caps the surface on either side of the channel and does not appear to drape down into it, the channel was unlikely to be a primary preglacial or subglacial feature. Thus its formation must have been relatively rapid, undoubtedly aided by the easily eroded proglacial outwash present in great thicknesses beneath a relatively thin resis-

tent cover of till.

The next lowest channels draining Glacial Lake Sammamish (Firlock and Totem Lake) allowed for the lake to merge with Lake Bretz (Waite and Thorson, 1983), identified by Thorson (1981) as the last and largest glacial lake to occupy central Puget Sound. Its elevation was fixed by the Leland Creek spillway (68/+0 m, 225/+0 ft) (XIV) on the northeast corner of the Olympic Peninsula, and it persisted until ice margin retreat permitted drainage through the Admiralty Inlet. Deposits within the map area, whose elevations indicate deposition contemporaneous with this stage of recession, include the deltas at Monroe, Stillwater (3 km north of Carnation), and near Griffin Creek (3 km south of Carnation).



**CHAPTER 2**  
**MASS BALANCE AND SLIDING VELOCITY OF THE PUGET-LOBE ICE SHEET**  
**DURING THE VASHON STADE**

**INTRODUCTION**

Most modern glaciers not frozen to their bed are believed to slide, with measured velocities ranging from a few meters to over a kilometer per year. Glaciated landscapes are filled with abundant features, such as striations and streamlined bedforms, indicating that erosion caused by the movement of Pleistocene ice masses has often dominated other geomorphic processes. These effects of glacial sliding can be more properly understood, and perhaps quantified as well, only by evaluating the likely rate of ice motion.

The Puget Lowland provides an excellent opportunity to develop and apply a useful technique for calculating basal sliding rates. Ice invaded the region most recently during the Vashon Stade of the Fraser Glaciation (Armstrong and others, 1965) about 15,000-13,500 years ago (Rigg and Gould, 1957; Mullineaux and others, 1965). The Puget lobe of the Cordilleran ice sheet occupied the broad trough between the Olympic Mountains and Cascade Range, while the adjacent Juan de Fuca lobe extended west, filling the Strait of Juan de Fuca and terminating off the modern northwest Washington coastline. For brevity in this report, these names will also include those portions of the ice sheet in British Columbia that supplied these discrete lobes.

Calculation of the equilibrium mass balance of the ice sheet

forms the basis of this analysis (cf. Pierce, 1979). Net accumulation above any transect across the glacier must be transferred by ice motion through that transect to satisfy the net ablation downglacier from it. This requires a reconstruction of the physical boundaries of the ice mass, topographic contours of its surface, and a relationship between net mass balance and altitude on the ice sheet. An equilibrium-line altitude (ELA) value can then be found that brings the glacier as a whole into balance. The rate of ice flux through any chosen cross section can then be simply calculated. An equivalent relationship between total ablation and altitude on the ice sheet also permits a quantitative estimate of meltwater discharge.

Although this reconstruction contains considerable uncertainties, the inferred order of magnitude of the sliding rate is rather insensitive to them. This is noteworthy, because the geologic significance of calculated horizontal sliding velocities depends less on their precise value than on their magnitude relative to two other velocities intrinsic to any ice sheet. The first such velocity is the average rate of ice flow solely from internal deformation due to viscous creep. The vertically averaged longitudinal velocity for a non-sliding glacier is (Paterson, 1981):

$$\bar{u} = 2A\tau_b^n h / (n+2), \quad (2.1)$$

where  $\bar{u}$  is the ice velocity,  $A$  and  $n$  are flow-law parameters (Glen, 1954),  $h$  is the ice thickness, and  $\tau_b$  the basal shear stress. The

value of  $\tau_b$  for any ice sheet can be calculated from its reconstructed longitudinal profile by

$$\tau_b = \rho g h \cdot \sin \alpha \quad (2.2)$$

where  $\rho$  is the ice density;  $g$ , the acceleration due to gravity; and  $\alpha$ , the surface slope. Analysis of a detailed reconstruction of the Puget lobe below 1300 m altitude by Thorson (1980, Figure 3) yields a value of  $\tau_b$  slightly below 50 kPa (0.5 bars). Values determined from the reconstruction of the southwestern portion of the Cordilleran ice sheet (Figure 2.1) average about 10% less. Using likely maximum values of  $\tau_b = 50$  kPa and  $h = 1500$  m, and flow parameters  $n = 3$  and  $A = 5.3 \times 10^{-15} \text{ s}^{-1} \text{ kPa}^{-3}$  (Paterson, 1981), equations (2.1) and (2.2) give

$$u = 13 \text{ m/a}$$

the maximum longitudinal velocity due solely to viscous creep.

The second intrinsic ice velocity of geologic importance is the rate of vertical flow at the bed due to basal melting. Various geological processes, such as the abrasion of bedrock and the lodgement of clasts on rock surfaces, depend on whether the ratio of horizontal to vertical ice velocity at the bed is close to, or much larger than, unity (Hallet, 1979). Contributions to basal melting include geothermal heat flow, friction from sliding, and flow of subglacial water. Spatially averaged, their combined magnitude is at most a few tenths of a meter per year (Rothlisberger, 1968).

## RECONSTRUCTION OF THE ICE SHEET (FIGURE 2.1)

### ICE LIMITS

Ice limits for the southern boundary of the ice sheet on land are relatively well-constrained by numerous studies. Thorson (1980) and Waitt and Thorson (1983) have most recently compiled data for the Puget lobe and the south boundary of the Juan de Fuca lobe. The now-submerged western boundary of the Juan de Fuca lobe (Clague, 1981) has been inferred (Alley and Chatwin, 1979) to coincide with the edge of the continental shelf southwest of Vancouver Island (U. S. Department of Commerce, National Ocean Survey chart no. 18480). The presence of submerged lobate ridges (e.g., La Perouse Bank) on the outer portion of the continental shelf here is consistent with this interpretation.

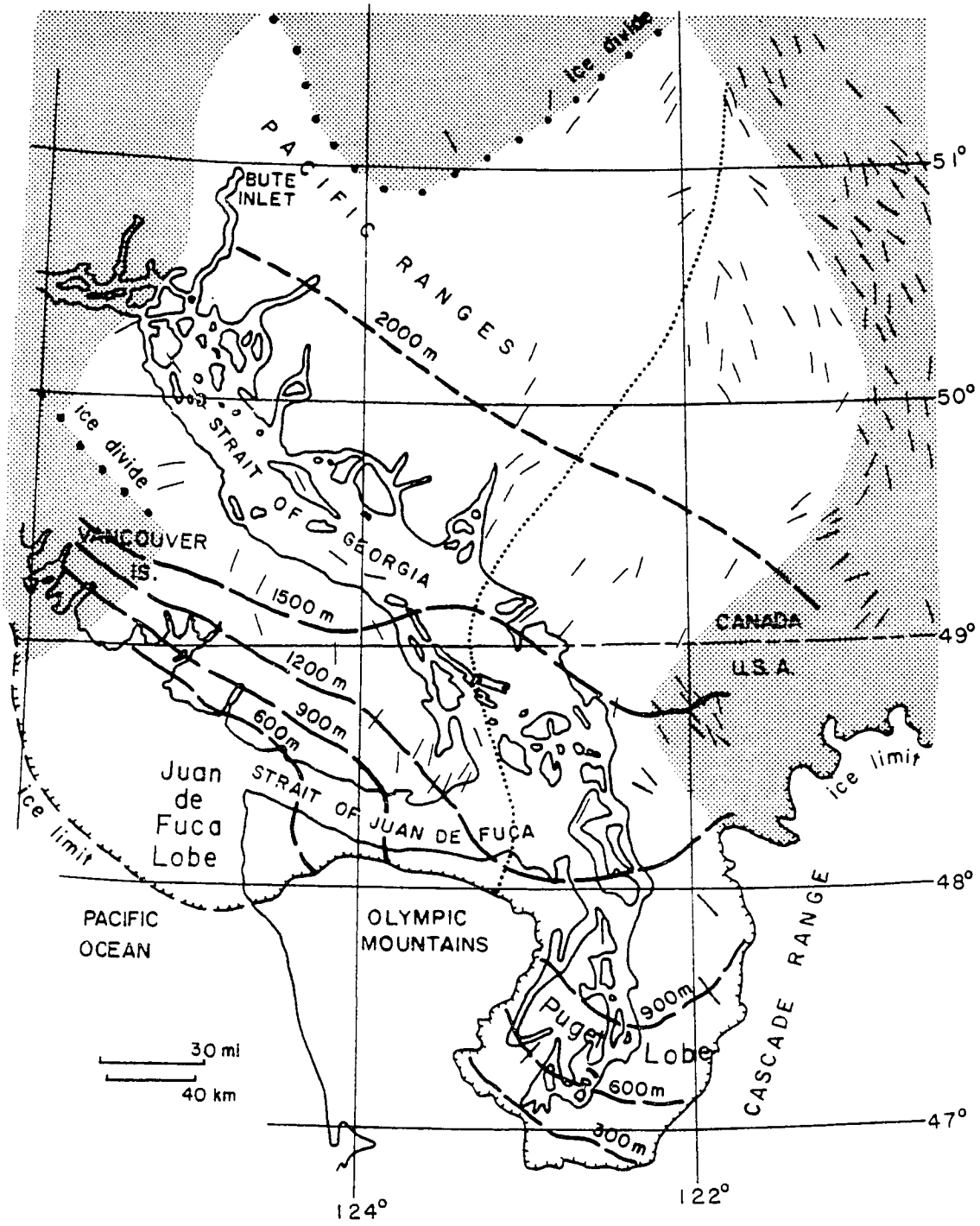
### FLOW BOUNDARIES

Flow-direction indicators, in the form of striations and glacially elongated topography, define a consistent pattern of ice flow throughout the area. Flow boundaries can be drawn between ice of the Puget-Juan de Fuca system and ice to the north, west, and east. Differentiating ice of the Puget and Juan de Fuca lobes from each other is less well constrained by geologic data upglacier from the obvious divergence at the northeast corner of the Olympic Mountains. Consequences of this uncertainty are discussed below.

### TOPOGRAPHIC CONTOURS

Contours on the Puget lobe follow Thorson's reconstruction

Figure 2.1. Reconstruction of a portion of the Cordilleran ice sheet at maximum stage. Short lines indicate local ice-flow direction; hachured line shows southern ice limit. Unshaded ice-covered area includes all ice of the Puget and Juan de Fuca lobes. Ice of these two lobes are separated by the line of fine dots. Sources of data include Geol. Assoc. of Canada (1958), Geol. Survey of Canada (1968), Thorson (1980), Heller (1980), Dethier and others (1981), and F. Pessl, Jr. (written commun. 1983).



(1980), and are relatively well-constrained by ice-margin elevations and abundant ice-flow direction indicators throughout the Lowland. Contours in Canada are largely from the Glacial Map of Canada (1958). Waitt and Thorson (1983) show ice-surface contours in the northern Cascade Range that project into Canada at somewhat higher elevations. The compilation of Figure 2.1 attempts to reconcile these sources, following the basic principles that the ice surface should generally slope in the direction of indicated flow, flow lines should not converge or diverge without commensurate changes in ice thickness or net balance, and averaged basal shear stresses as calculated by equation 2.2 is a slowly varying function.

### **MASS BALANCE CALCULATIONS**

#### **HEIGHT/MASS BALANCE RELATIONSHIP**

Variation in local mass balance are shown in Figure 2.2 as a function of height above or below the equilibrium line. This curve was derived from the averaged values of seven modern maritime glaciers in the Pacific Northwest and Alaska (Meier and others, 1971). The good correlation among these data, representing a variety of local environments, lends some confidence to its application to an obviously larger Pleistocene ice mass. An additional relationship is provided in Figure 2.2 between total ablation and height relative to the ELA, derived from good but limited data from two Norwegian maritime glaciers (IAHS, 1977). These data allow a quantitative estimate of meltwater discharge through transverse cross-sections of the glacier as well as the corresponding values of ice flux.

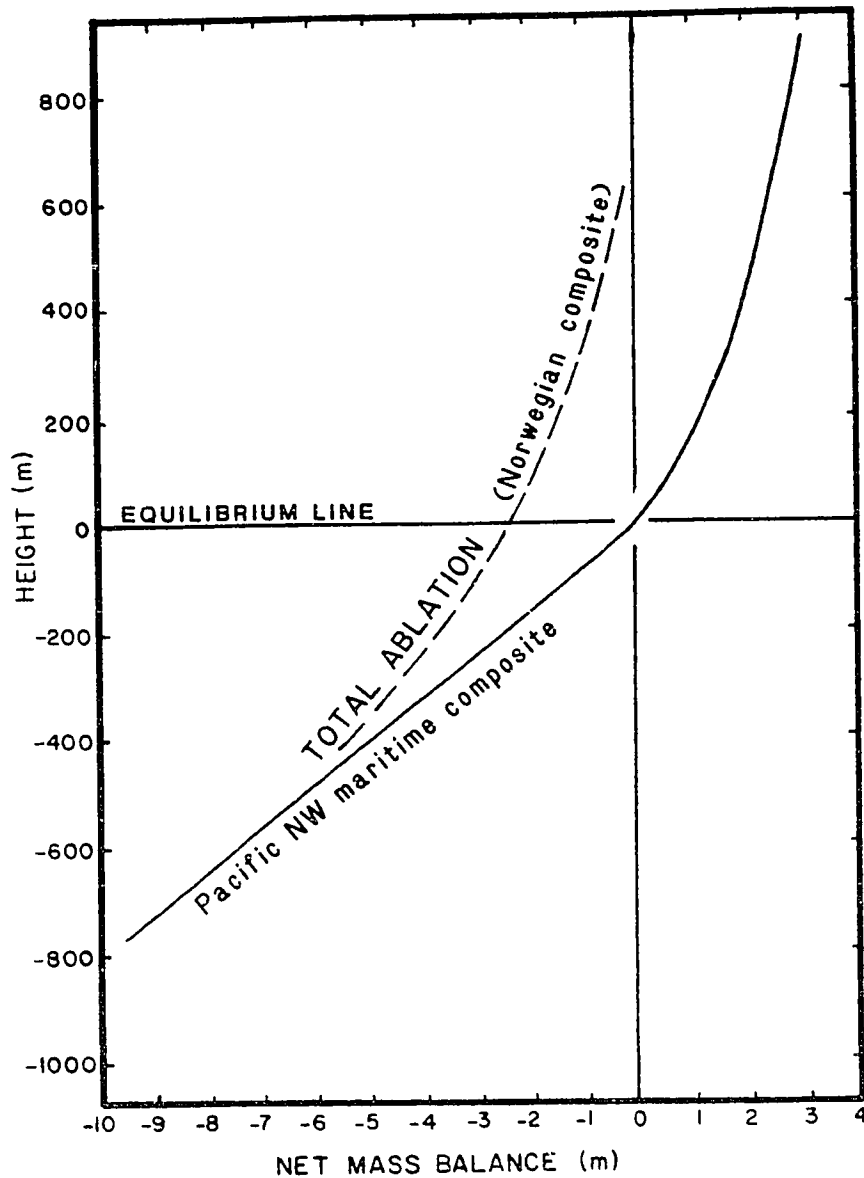


Figure 2.2. Altitude-mass balance relationship for modern maritime glaciers. Altitude is computed relative to the equilibrium line altitude; balance is in cubic meters per square meter of ice surface (per year). Net balance data is from Pacific Northwest glaciers (Meier and others, 1971); total ablation data is from two Norwegian glaciers (Nigardsbreen and Tunsbergdalsbreen) (IAHS, 1977).



## EQUILIBRIUM-LINE ALTITUDE CALCULATIONS

The area of each region of Figure 2.1 that is bounded by contours and flow lines is given in Table 2.1. The altitude of each region was specified for all subsequent calculations by the average of its extreme values. The region above 2000 m was assigned a representative altitude of 2300 m, based on nunatak altitudes (Glacial Map of Canada, 1958) and plausible ice-surface profiles. Total accumulation and ablation rates are calculated for several values of the ELA (Table 2.2). Equilibrium, which should approximate conditions during ice-maximum time, is attained with the ELA equal to ca. 1225 m. The predicted accumulation-area ratio (ca. 0.7) is consistent with modern values reported by Porter (1975).

## SLIDING VELOCITY

On any glacier the ice accumulated above the equilibrium line must be transported into the ablation area. The flux will be greatest at the equilibrium line and decrease through successive downglacier cross sections, as increasing volumes of glacier mass are lost through surface ablation. The inferred pattern of ice flow in the Juan de Fuca lobe (Figure 2.1) is sufficiently complex to introduce large lateral variability in this flux. The Puget lobe, however, has a relatively simple geometry, well-suited to these calculations. Using an ELA of 1225 m (Table 2.2),  $7.1 \times 10^{10}$  m<sup>3</sup>/a of ice must cross the equilibrium line to remain in a balanced state (Table 2.3). The cross sectional area at the equilibrium line is  $1.2 \times 10^8$

Table 2.1. Area of ice lobes, calculated from Figure 2.1 by planimetry.

Altitude interval (m)	Area of Juan de Fuca lobe (km <sup>2</sup> )	Area of Puget lobe (km <sup>2</sup> )
0-300	} 10.1 x 10 <sup>3</sup>	0.8 x 10 <sup>3</sup>
300-600		2.4
600-900	3.2	3.8
900-1200	4.3	6.0
1200-1500	6.5	7.8
1500-2000	23.9	8.6
>2000	27.7	12.4

Table 2.2. Net balance values in  $10^{10} \text{ m}^3\text{a}^{-1}$ . Positive values indicate net accumulation, negative values net ablation. Both lobes are brought into balance by an ELA between 1250 and 1200 m. An ELA value of 1225 m is therefore assumed for all subsequent calculations.

Altitude interval (m)	<u>ELA = 1250 m</u>		<u>ELA = 1200 m</u>		<u>ELA = 1150 m</u>	
	J de F	Puget	J de F	Puget	J de F	Puget
0-300		-1.2		-1.1		-1.0
300-600	-12.9	-2.4	-12.3	-2.2	-11.6	-2.1
600-900	-2.0	-2.4	-1.8	-2.1	-1.6	-1.9
900-1200	-1.1	-1.5	-0.8	-1.1	-0.5	-0.8
1200-1500	0.7	0.8	0.8	0.9	0.9	1.1
1500-2000	5.4	2.0	5.6	2.1	5.9	2.1
>2000	9.5	4.3	9.8	4.4	10.1	4.5
NET BALANCE:	-0.4	-0.4	+1.3	+0.9	+3.2	+1.9

Table 2.3. Ice discharge and velocity through transverse sections of the Puget lobe, ELA = 1225 m. Sections are taken along contour lines shown on Figure 2.1. Ice velocity through these sections will be overwhelmingly by basal sliding (see text).

Contour (m)	Ice width (m)	Average thickness (m)	X-section area (m)	Cumulative mass balance (m <sup>3</sup> /a)	Ice velocity (m/a)
2000	$1.1 \times 10^5$	$1.0 \times 10^3$	$1.1 \times 10^8$	$4.3 \times 10^{10}$	390
1500	1.1	1.1	1.2	6.3	530
1200	1.0	1.2	1.2	7.1	590
900	1.3	0.9	1.2	5.8	480
600	1.1	0.7	0.8	3.4	425
300	1.0	0.4	0.4	1.1	275
TERMINUS	0	0	0	0	0

m<sup>2</sup>, giving an average rate of 590 m/a. As 2% of this can be accounted for by internal deformation of the ice (equation 2.3), the sliding velocity is approximately 580 m/a. Rates of this order would be found downglacier as well, for although flux is decreasing, the cross-sectional area is shrinking also. For example, at the ice-surface altitude of 900 m (about the latitude of Seattle), the rate is still nearly 500 m/a.

#### WATER FLUX

Estimated water production and cumulative downglacier flux are shown in Table 2.4. These values increase from a negligible value, consistent with the dry conditions observed high on modern glaciers (Mayo, in press), to values in excess of the ice flux. Because this water will tend to flow in channels (Shreve, 1972), its geomorphic effects will be more pronounced but more localized than those of the sliding ice, regardless of relative discharges (Chapter 3).

#### CORROBORATING EVIDENCE

##### ESTIMATED EQUILIBRIUM-LINE ALTITUDE

The glacier-wide pattern of ice flow, as expressed by directional indicators, should show marked differences above and below the equilibrium line. Above, flow should diverge from all boundaries, as all points over the ice surface contribute to the net increase in mass. Only locally, such as where an ice tongue projects up an ice-

Table 2.4. Cumulative ice and water discharges through transverse sections of the Puget lobe, ELA = 1225 m. Ice-discharge data from Table 2.3.

Contour (m)	Cumulative ice discharge (m <sup>3</sup> /a)	Cumulative water discharge (m <sup>3</sup> /a)	<u>Water discharge</u> <u>Ice discharge</u>
2000	4.3 x 10 <sup>10</sup>	0.0 x 10 <sup>10</sup>	0
1500	6.3	0.5	1/13
1200	7.1	1.7	1/4
900	5.8	3.0	1/2
600	3.4	5.3	1.5/1
300	1.1	7.6	7/1
TERMINUS	0	8.7	

free alpine valley, can an additional source of heat (i.e., alpine rivers) yield a net loss of mass. Below the equilibrium line, all points on the glacier experience a net loss, and so flow must converge with the ice margins. Lateral ice-surface gradients, expressed by convex downglacier contours, drive this flow. The association of compressive flow with the ablation area (Nye, 1957) also dictates this transverse profile, in order to satisfy mass conservation over a glacier with stable margins. Inspection of Figure 2.1 shows generally convex-down contours and margin-convergent flow directions up to at least 1100 m elevation along the eastern edge of the Puget lobe, and less definitively up to 1200 m.

The longitudinal change in glacier mass, in those portions of an ice sheet with near-parallel lateral boundaries, also reflects the elevation at which net accumulation replaces net ablation. Thorson (1981) showed that the mass of the Puget lobe increases monotonically from the southern ice limit up to the boundary of his investigation, at ice-sheet altitude 1260 m. Cross-section areas of the Puget lobe calculated from Figure 2.1 and the underlying topography also show a maximum between the 1200 and 1500 m contours, implying an ELA within this range (the apparent narrowing near 1500 m reflects the steep southward descent of the Pacific Ranges in this area).

#### ESTIMATED SLIDING VELOCITY

Constraint of the Puget lobe ELA by these geologic data and inferences confirms broadly the more detailed calculations made in

the previous section based on the height/mass balance curve. The advantage of the quantitative approach is that it provides an estimate of sliding velocity as well. The estimated sliding velocity can also be compared with indirect geological data. Near the latitude of Seattle (47°30'), bounding dates on the Vashon-age advance of 15,100  $\pm$  300  $^{14}\text{C}$  yr B.P. (W-1305) (Mullineaux and others, 1965) and 13,650  $\pm$  550  $^{14}\text{C}$  yr B.P. (L-346) (Rigg and Gould, 1957) require that the ice sheet advanced and retreated on average more than 80 km in each direction during the intervening 1500  $\pm$  900 years. Assuming an advance rate half that of the retreat (Weertman, 1964), minimum ice-margin advance rates of 50 to over 200 m/a are required (equal advance and retreat rates increase this value by approximately 1/3). Since ice ablated rapidly at low elevations before even reaching the terminus, the total flux of ice at the equilibrium line must have exceeded significantly this value to sustain the advance.

## SENSITIVITY

### CALCULATIONS OF EQUILIBRIUM-LINE ALTITUDE

#### Ice-Sheet Reconstruction

The boundaries and contours of the Puget lobe below about 1200 m are well-constrained by several geologic studies along the ice sheet margin (Crandell, 1963; Rosengreen, 1965; Carson, 1970; Thorson, 1980; Chapter 1, this report). The flow boundaries of the Puget lobe upglacier of 1200 m were chosen both to be consistent with directional indicators (west and east boundaries) and to yield an ELA



equal to the value that balances the ice sheet as a whole (west boundary).

Although this second assumption ignores the likelihood of temperature or precipitation gradients across the ice sheet, its consequences, within the constraints of indicated flow directions, are not severe. Decreasing the area of the Puget lobe by 20% requires an increase of less than 25 m in the ELA to maintain total net balance. An equivalent increase in area appears implausible from the pattern of directional indicators, and its effect would be equally insignificant. The weak dependence of accumulation on elevation (Figure 2.2; Mayo, in press) also deemphasizes the large uncertainty in ice-surface elevation above 2000 m (e.g., Waitt and Thorson, 1983).

#### Mass Balance Relationship

The relationship between altitude and net mass balance critically determines both the ELA and the mass flux through it. Use of a curve assembled from relatively small glaciers must only approximate the conditions over a continental ice sheet, particularly the consequences of increasing distances between the accumulation area and the source of moisture. The estimates derived from it, however, may still prove satisfactory. As noted previously, the balance curves of these glaciers cluster closely about a single set of values (Meier and others, 1971) despite their variety of geographic locations and ELAs, lending some confidence to the generality of this relationship.

Additional data from the 150 km-long Malaspina-Seward-Hubbard glacier system can address qualitatively the problems of scaling up this mass-balance relationship. Investigations by Marcus and Ragle (1970) on these glaciers show that total precipitation at the ice divide, 150 km from the coastline, is only 15% less than at a point 90 km closer to the ocean. This rather gentle decrease, however, is not monotonic, as the precipitation at a station 138 km from the coast is 46% lower than at the divide. Thus local topography and exposure strongly influence single measurements far beyond the effects of elevation and increasing continentality, which for ocean-facing slopes have opposing influence. A composite curve, representing multiple measurements in a variety of microenvironments, therefore is probably more trustworthy at all scales.

#### SLIDING VELOCITY

Calculated sliding velocities are relatively insensitive to any plausible range in reconstructed ELAs. This can be demonstrated by computing alternative sliding velocities using only a range of assumed ELAs and the height/mass balance relationship for the ablation area only. The latter is likely to be influenced only slightly by the total length of the ice sheet, reducing the inaccuracy of data from smaller modern glaciers. Ice-sheet boundaries and contours are also much better constrained at these lower altitudes. The range of plausible ELAs (1200-1500 m) is constrained by geologic evidence (see above) independent of any assumed mass-balance relationship. For an ELA = 1200 m, the flux through the equilibrium line is  $6.6 \times 10^{10}$

$\text{m}^3/\text{a}$ , giving a sliding velocity of 550 m/a (93% of the value for an ELA = 1225 m). For an ELA = 1500 m, the flux is  $10 \times 10^{10} \text{ m}^3/\text{a}$ , giving a velocity at the equilibrium line of 830 m/a (a 40% increase). Sliding velocities therefore exceed the other characteristic velocities in the glacier, namely the basal melt rate and the internal deformation rate, by one or more orders of magnitude regardless of the estimate used.

## DISCUSSION

### IMPLICATIONS FOR CLIMATIC CHANGE

Predicted high mass flux, expressed as high sliding rates, provides insight into the relatively brief occupancy of the Puget lobe during the Vashon Stade. Since the vast majority of ice accumulated above the equilibrium line merely replaced ice lost below, fluctuations in the ice front at rates of 100 m/a represent only minor perturbations in the total budget of the ice sheet. For example, if the ELA were to move from the hypothesized 1225 m level up to 1250 m, a change of only 3% in the total Fraser-age ELA depression (Porter, 1977), the calculated yearly deficit of  $7.2 \times 10^9 \text{ m}^3$  is equivalent to an averaged retreat rate of 50 m/a. Although this ignores all complexities of an ice sheet's response to non-equilibrium conditions (Nye, 1963) it clearly demonstrates the sensitivity of this body to small climatic changes, and the plausibility of rapid movement of the ice front without equally precipitous climatic changes.

## SURGING OF THE PUGET LOBE

The rapid advance and predicted high sliding velocities of the Puget lobe invite speculation that the ice sheet may have moved erratically, analogous on a vast scale with modern surging valley glaciers (Post, 1969). Although these reconstructed rates are far higher than those reported for most modern non-surging glaciers, they apparently do not require surging behavior. Budd (1975) has classified glaciers as "ordinary", "fast", and "surging", depending on whether they can continuously resupply the volume of ice transported downglacier by sliding. Within this theoretical framework he finds that modern glaciers can be divided empirically into ordinary and surging types by a line of constant energy loss rate (shear stress  $\times$  velocity) over a wide range of surface slopes, velocities, and ice thicknesses. These data, reproduced in Figure 2.3, include the reconstructed value of the Puget lobe at the equilibrium line. They show that in spite of high predicted velocity, this ice sheet lies well in the field of "ordinary" glaciers, having only 2/3 of the energy loss rate necessary to fit the observed characteristics of surging glaciers.

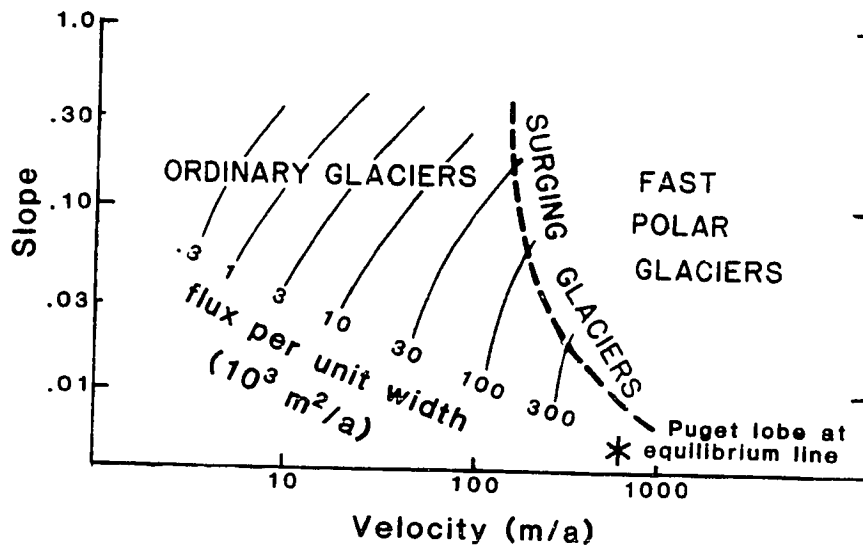


Figure 2.3. Compilation of velocity measurements on modern glaciers, modified from Budd (1975). The division between ordinary and surging glaciers is marked by a line of power per unit bed area (= basal shear stress  $\times$  velocity =  $5.4 \times 10^7$  J/m<sup>2</sup>a). The reconstructed parameters of the Puget lobe yield an energy-dissipation rate that is only 60% of this transition value.

**CHAPTER 3**  
**LANDFORMS OF SUBGLACIAL FLUVIAL EROSION**

**INTRODUCTION**

Along the eastern border of the Puget Lowland, numerous troughs and valleys incise the till and bedrock landscape. Although some appear to result directly from the scouring action of ice or from erosion by subaerial recessional meltwater, other valleys discussed here as "channelways" are inferred instead to reflect erosion by subglacial meltwater. In map view, channelways appear as narrow sinuous to linear valleys occupied by lakes, bogs, or underfit streams. Valley bottoms have low gradients and commonly trivial drainage areas. Their sidewalls are steep, with relief of 10 to greater than 100 m. In addition to bog deposits and modern alluvium, till and recessional outwash deposits are occasionally exposed. They are isolated features in some areas, but generally form either anastomosing or dendritic networks across the landscape.

Channelways are common over much of the marginal zone of the former Puget lobe (Chapter 1). They are generally absent, however, throughout its interior region. Along the eastern margin, these landforms can be followed from approximately the latitude of the reconstructed equilibrium line (Chapter 2) south for over 100 km to where bedrock is completely buried under till and recessional outwash deposits (Crandell, 1963; Frizzell and others, in press). These features are particularly well-developed across bedrock spurs that extend west from the Cascade Range south of the North Fork and South

Fork Stillaguamish Rivers (Granite Falls 15' U.S. Geological Survey topographic quadrangle), south of the Skykomish River (Sultan and Lake Joy 7.5' quadrangles), south of the South Fork Tolt River and west of Lakes Hancock and Calligan (Mount Si 15' quadrangle), and over a 5-km wide area of the Cascade foothills between the Green and White Rivers (Cumberland and Enumclaw 7.5' quadrangles) (Figure 3.1). At the western border of the lowland, exposed bedrock generally terminates more abruptly (Hall and Othberg, 1974). Topographic maps of this region, however, show a few equivalent forms in the marginal zone here as well (particularly the Uncas, Washington, 7.5' quadrangle).

Landforms in these areas share several distinctive characteristics. Where channelized topography is rather poorly developed, single channelways transect bedrock ridges (Figure 3.2). Where this topography is more clearly expressed, multiple channels tend to isolate bedrock hills. These hills are nearly equidimensional in plan view, approximately 100 m high and 4 or 5 times as wide (Figures 3.3 and 3.4). The intervening channels typically vary between 50 and 150 meters in width and are floored with recessional and postglacial deposits. Eskers are also present at two localities, along Stossel Creek 3 km (2 mi) NNE of Lake Joy and 5 km (3 mi) ESE of the town of Granite Falls. These characteristics suggest their similarity to "tunnel valleys" described in central and northern Europe (Schou, 1949; Ehlers, 1981; Grube, 1983) and central North America (Wright, 1973).

Figure 3.1. Index map of localities and specific features discussed or illustrated in text.



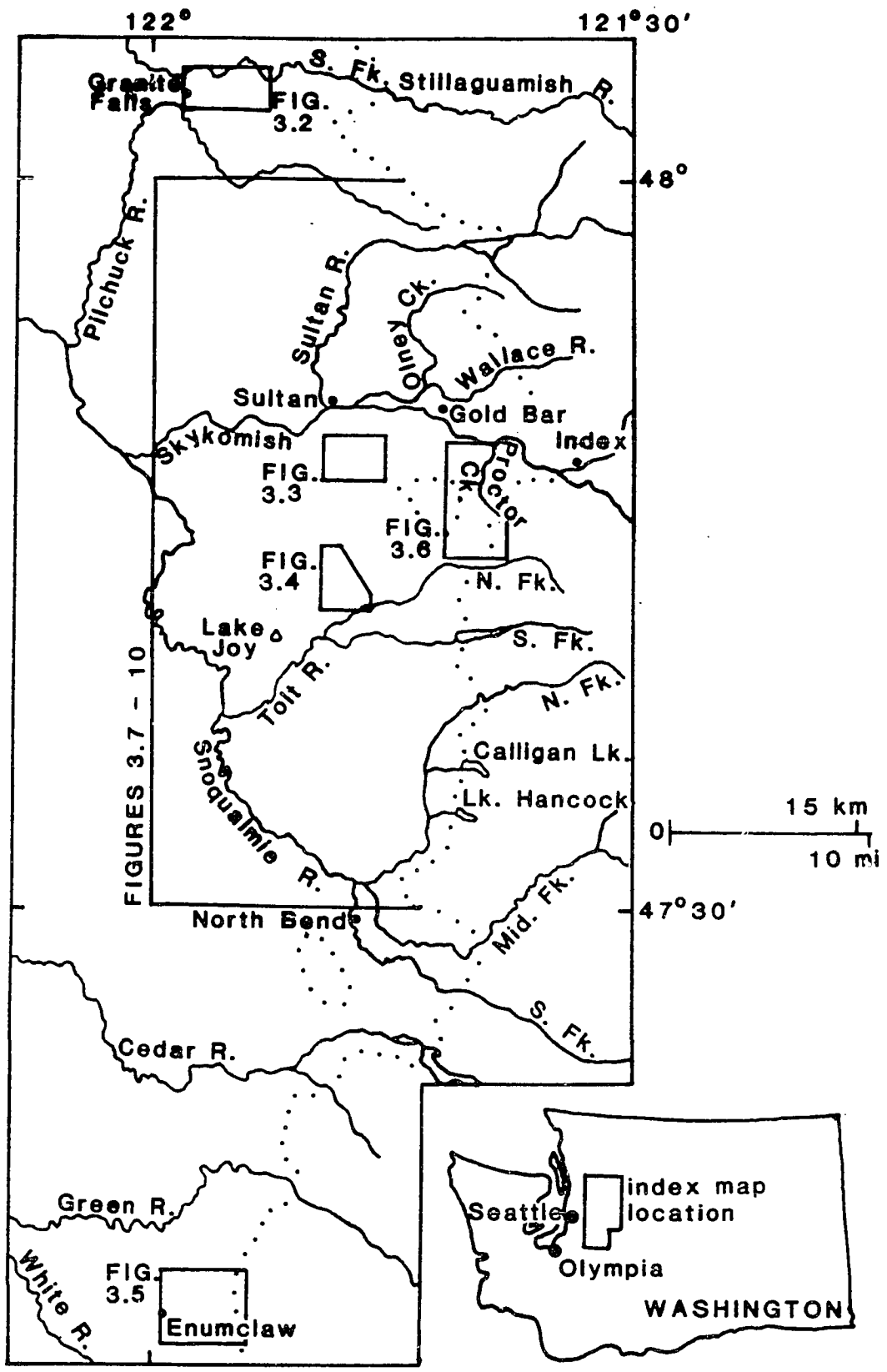
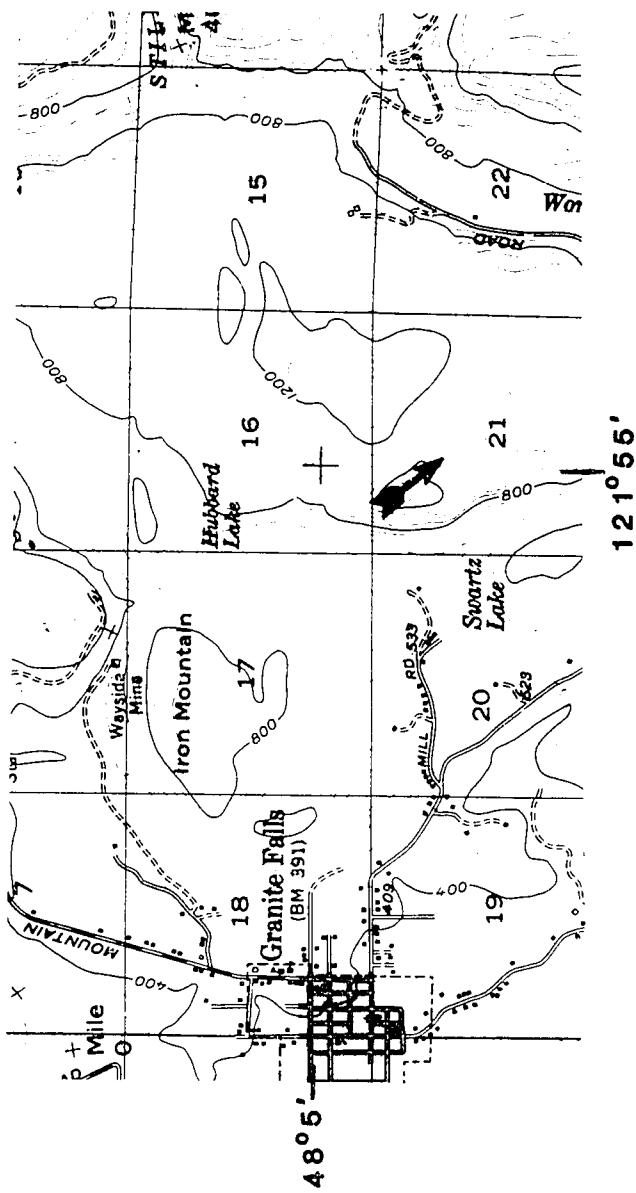


Figure 3.2. Isolated channelways transecting a bedrock ridge. Ice-flow direction shown by arrows; elevation in feet (from Granite Falls 15' topographic map).



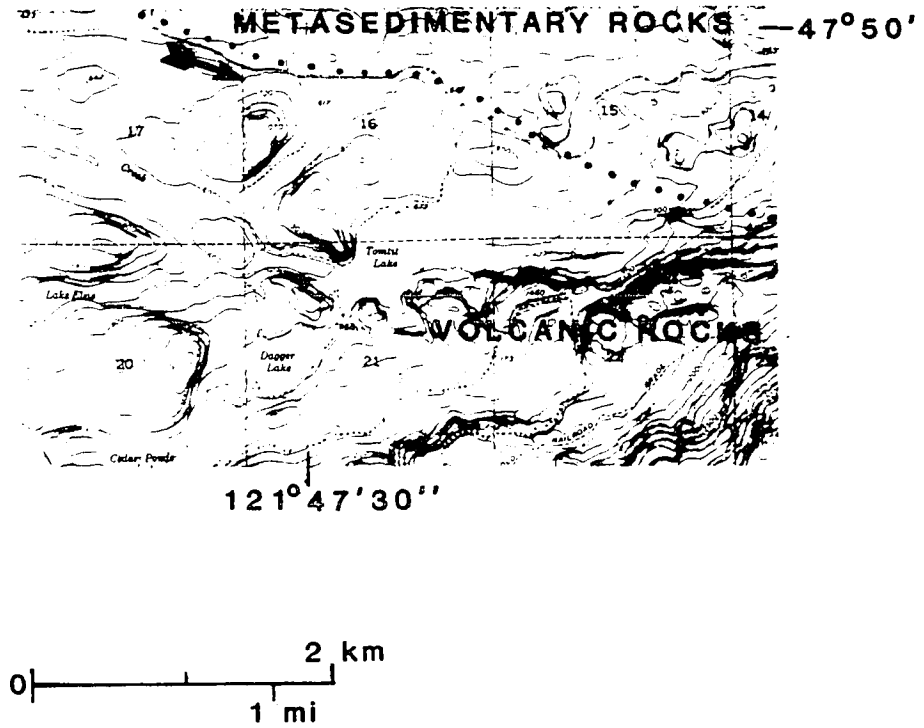


Figure 3.3. Multiple channelways; lithologic contact from Tabor and others (1982). Ice-flow direction shown by arrows; elevation in feet (from Sultan 7.5' topographic map).

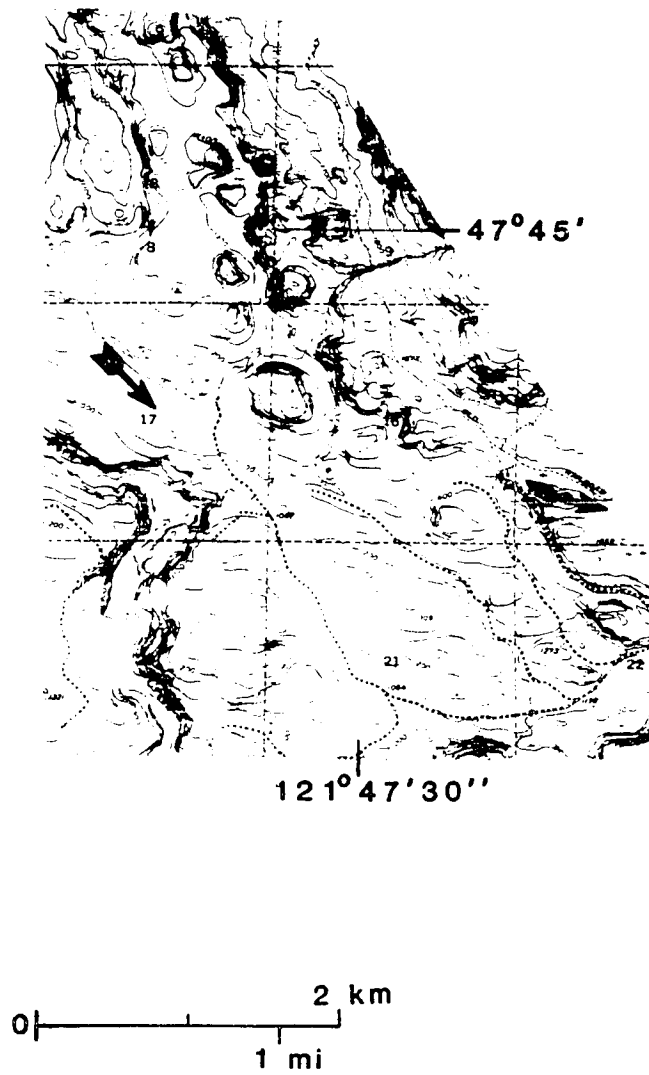


Figure 3.4. Multiple channelways. Ice-flow direction shown by arrows; elevation in feet (from Sultan and Lake Joy 7.5' topographic maps).

Channelized topography is best developed 5 km (3 mi) east and northeast of Enumclaw (Figure 3.5). Here a series of channels, approximately 300 m (1000 ft) altitude below and subparallel to the Vashon-age ice margin, isolate bedrock hills from the main Cascade highlands. The altitudes of these hills decrease gradually (40 m/km) from east to west; conversely, the continuity, depth, and width of the intervening channelways increase along this transect. Just northeast of Enumclaw, these hills are separated by valleys over 1 km wide.

The most extensive channelway system, however, traverses the eastern Puget Lowland margin from the Skykomish River south to the town of North Bend. Holocene erosion by west-flowing alpine rivers has isolated discrete segments of this nearly continuous south-trending valley. The northernmost segment is the broad trough south of Gold Bar, almost 1 km wide and 8 km long, that crosses the major bedrock spur south of the Skykomish River (Figure 3.6). Structural control by a fault-line scarp separating rocks of greatly different erosional resistance (Tabor and others, 1982) may have initiated preglacial drainage in this area. The present form of this broad channel, however, has evolved far beyond the geomorphic effects of subaerial streams, which are limited to minor incision in the north and alluvial-fan deposition in the south (Map 1).

More southerly segments of this near-marginal system invariably lie several hundred meters below the Vashon ice limit. They range from 200 to 500 m wide, but except for the portion now occupied by

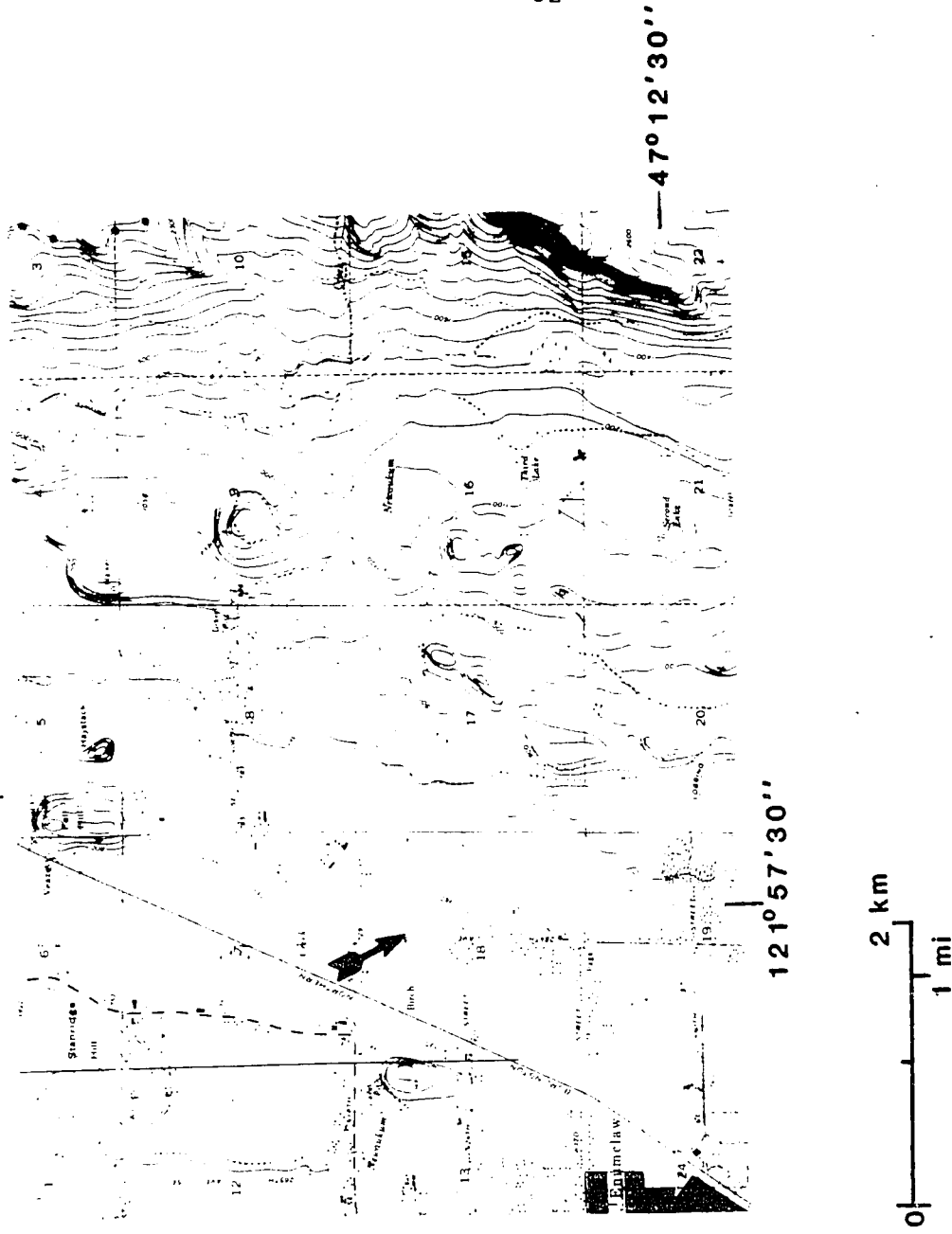
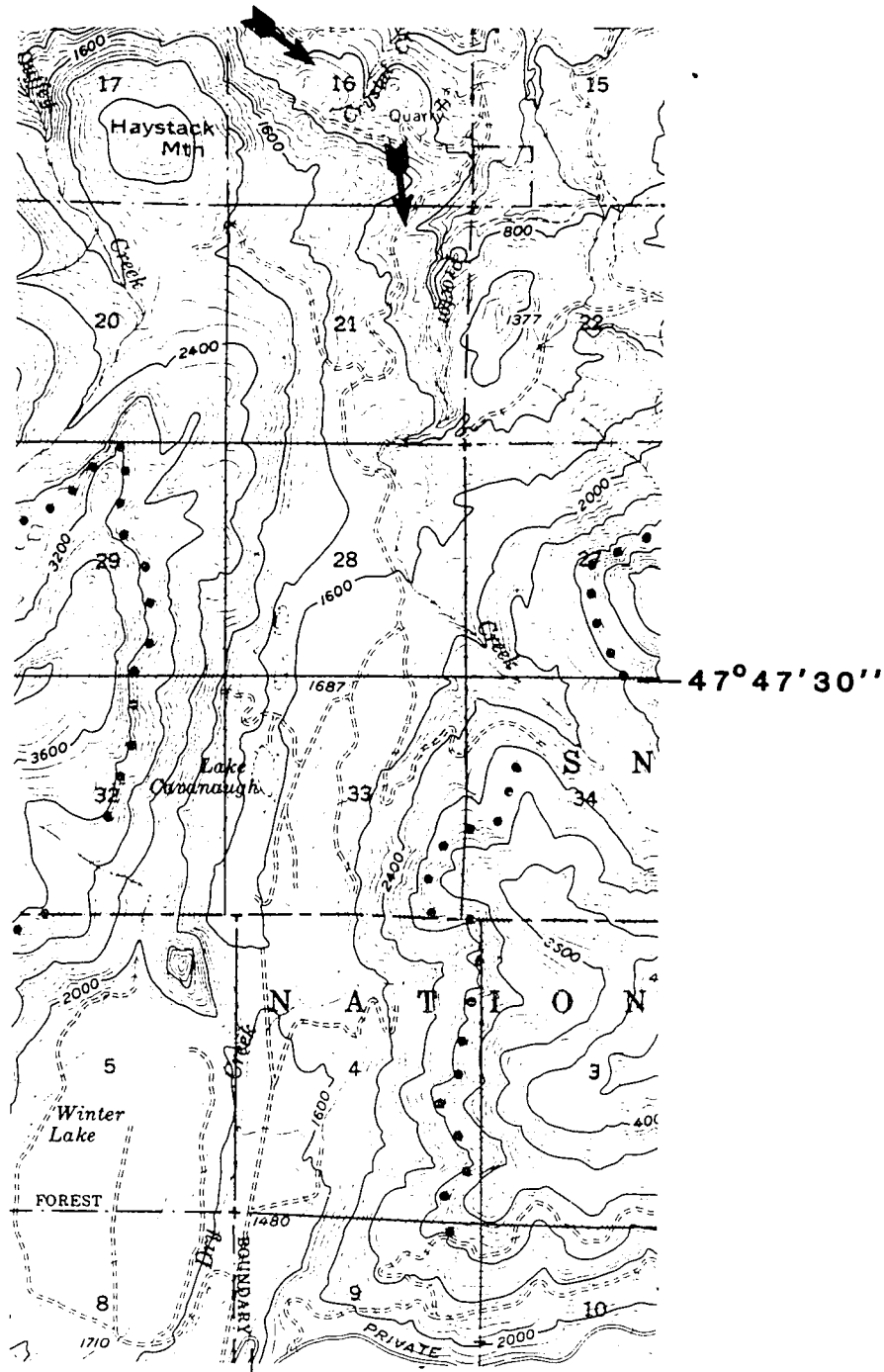


Figure 3.5. Bedrock hills isolated by broad, multiple channelways. Ice-flow direction shown by arrows; elevation in feet (from Enumclaw 7.5' topographic map). Black dots indicate ice-maximum limit during the Vashon Stage of Armstrong and others (1965).

Figure 3.6. Northern segment of the eastern submarginal channel-way system. Ice-flow direction shown by arrows; elevation in feet (from Index 15' topographic map). Black dots indicate ice-maximum limit during the Vashon Stade of Armstrong and others (1965).





the North Fork of the Snoqualmie River, each carries only trivial modern drainage.

### ORIGIN OF CHANNELWAYS

Structural control is rare in the development of this topography. Variation in lithology on the scale of individual features is generally absent. Throughout most of the glaciated Puget lowland where these features are found, the bedrock consists of either extensive gently dipping lava flows and pyroclastic rocks, or metamorphosed graywacke (Tabor and others, 1982). Lithologic changes may not be reflected in the topography at all (e.g., Figure 3.3). Demonstrable fault traces only rarely correspond to channelway locations, and are not likely to be compatible with the numerous sinuous segments.

Although channelways are similar topographically to "overflow channels" and "sluiceways" (Coates and Kirkland, 1974), features attributed primarily to subaerial fluvial erosion, several characteristics are particularly inconsistent with this process (Mannerfelt, 1949; Peel, 1956; Sissons, 1958a, 1958b, 1960, 1963; Derbyshire, 1958, 1961, 1962; Price, 1963; Clapperton, 1971; Pasierbski, 1979; Young, 1980; Ehlers, 1981). They include:

- 1) "humped" or "up-and-down" longitudinal profiles;
- 2) abrupt channel termini without deltas or fans;
- 3) multiple intakes and outflows;
- 4) till, eskers, or other ice-contact sedimentary deposits occasionally exposed in the troughs; and

5) perched topographic position without significant drainage area.

Excavation by sliding ice may have played an active role but appears insufficient for the formation of most channelways. They commonly lie oblique to independent indicators of the ice-flow direction. Their sinuosity is not reflected by any changing orientation of the ice-flow pattern. Because they are characteristically deep, narrow, and steep-walled, they offer higher resistance to ice flow than the unincised topography around them (Weertman, 1979). Therefore deepening of such channels by direct glacier erosion appears unlikely. Finally, the bedrock knobs associated with areas of best-developed channelways are generally non-streamlined, a characteristic that intuitively precludes the dominance of active erosion by ice (Linton, 1963).

Despite the obvious unimportance of subaerial fluvial erosion, many of the morphological features of channelways are suggestive of a fluvial origin. Marginal and proglacial drainage is an appealing and oft-cited explanation for these and similar features (Kendall, 1902; Mackin, 1941; Knoll, 1967). During ice recession some water could have been diverted subaerially through such valleys, but rates of ice retreat (Chapter 1) would allow only trivial occupation times by this means. Only catastrophic drainage from ice-dammed lakes might yield substantial subaerial discharges, but their paths can be predicted and prove to be quite restricted (see below). Erosion by subglacial water, however, is the most plausible mechanism compatible with the observed characteristics and distribution of channelways. The

ubiquity of this water under modern temperate glaciers is unquestioned (e.g., Mathews, 1964; Stenborg, 1968; Englehardt, 1978), and its flux and erosive potential, at least upon its emergence at the snout, is also well-documented. In order to evaluate likely consequences of subglacial fluvial erosion, the physics controlling the flow of this water must first be considered.

### PREDICTED BEHAVIOR OF SUBGLACIAL WATER FLOW

Water flow within or beneath a glacier can be represented by the mathematical formulations developed for groundwater. Water moves from areas of high total hydraulic potential, or total head, to areas of low total head, down the gradient of this potential field (just as a stream flows down the fall line of a hillslope) (Shreve, 1972; Rothlisberger, 1972; Nye, 1976).

Total head at a point has two significant static components independent of ice sliding: 1) the position head, or elevation above a chosen datum; and 2) the pressure head, which for a steady-state water-filled tunnel is nearly equal to the overburden pressure due to the overlying ice (Shreve, 1972). Although Lliboutry (1983) points out that tunnels beneath valley glaciers may be only partially filled with water for much of the year, this phenomenon requires groundwater at about 1° C above the melting point (Lliboutry, 1983, eqn. 20), an unlikely condition beneath an extensive ice sheet (cf. Chapter 5). Since

$$p_i = \rho_{i g h},$$

then by Bernoulli's law, the total head (H) is:

$$H = z + (\rho_i/\rho_{\text{water}})h, \quad (3.1)$$

where  $p_i$  = ice overburden pressure,  
 $\rho_{\text{water}}$  = water density,  
 $\rho_i$  = ice density,  
 $g$  = acceleration due to gravity,  
 $z$  = elevation above datum, and  
 $h$  = the overlying thickness of ice.

Total head will obviously be lowest at the bed of the glacier where  $z = z_b$ , favoring subglacial rather than englacial flow (Shreve, 1972).

We can also predict the gross pattern of water flow rather simply. By differentiating equation 3.1, the total head varies downglacier as

$$\partial H/\partial x = \partial z_b/\partial x + (\rho_i/\rho_w) \cdot \partial (z_s - z_b)/\partial x \quad (3.2)$$

where  $x$  = distance downglacier, and  
 $z_s$  = ice surface elevation =  $z_b + h$ .

If two points on the glacier bed have the same total head,

$$\partial H/\partial x = 0, \text{ and so}$$

$$\partial z_s/\partial x = -0.09 (\partial z_b/\partial x).$$

So long as the bed does not slope upglacier more steeply than eleven times the downglacier ice slope, total head will decrease downglacier and water will follow the ice slope direction, flowing down or up the bed topography with only minor deflection (Shreve, in press).

Using equation 3.2 and maps of bed topography and ice-sheet surface topography, the subglacial equipotentials can be contoured across a region. The area chosen for this analysis corresponds to the mapped area discussed in Chapter 1. No correction is made for

postglacial modification of the bed, as this occurs over a relatively small percentage of the map area and affects neither the overall drainage pattern nor the areas of best-developed and preserved channelways. Isostatic rebound since deglaciation (Thorson, 1980) is also ignored, as the gradient change (approximately  $9 \times 10^{-3}$ ) exerts a negligible effect on the reconstructed patterns. Figure 3.7 is a computer-generated topographic map of this region, bounded on the east by the limit of the Vashon-age ice sheet. Topography was digitized on an Altek digitizer from 15' and 7.5' U. S. Geological Survey topographic maps. Two hundred thousand data points were condensed to a final grid of 120 x 200 uniformly spaced points (representing approximately 300 m lateral spacing).

Figure 3.8 is an equivalent map of the ice sheet at its maximum stand over the region. Its construction was based on geologic evidence of ice limits along the eastern margin (Chapter 1), the assumed parallelism between ice-flow direction indicators (Map 1) and ice surface gradient (Weertman, 1964), and the full Puget-lobe reconstruction by Thorson (1980). From these data the subglacial hydraulic potential field is calculated. The resulting equipotentials, or contour lines of equal total head, represent the effective "topography" of the hypothetical surface down which subglacial water would flow (Figure 3.9). The obvious channelized features are highlighted by Figure 3.10, which traces all major valleys in the potential surface downgradient from where they first enter the map area.

The reconstruction assumes a smooth ice surface, although

Figure 3.7. Ground topography of the Skykomish-Snoqualmie region. Contour interval 100 m (dashed contour = 50 m). Digitized from Monroe 15', Index 15', Mount Si 15', Lake Joy 7.5', Carnation 7.5', Fall City 7.5', and Snoqualmie 7.5' topographic maps. Dark line at eastern border is the Vashon-age ice limit, approximated in each alpine valley.

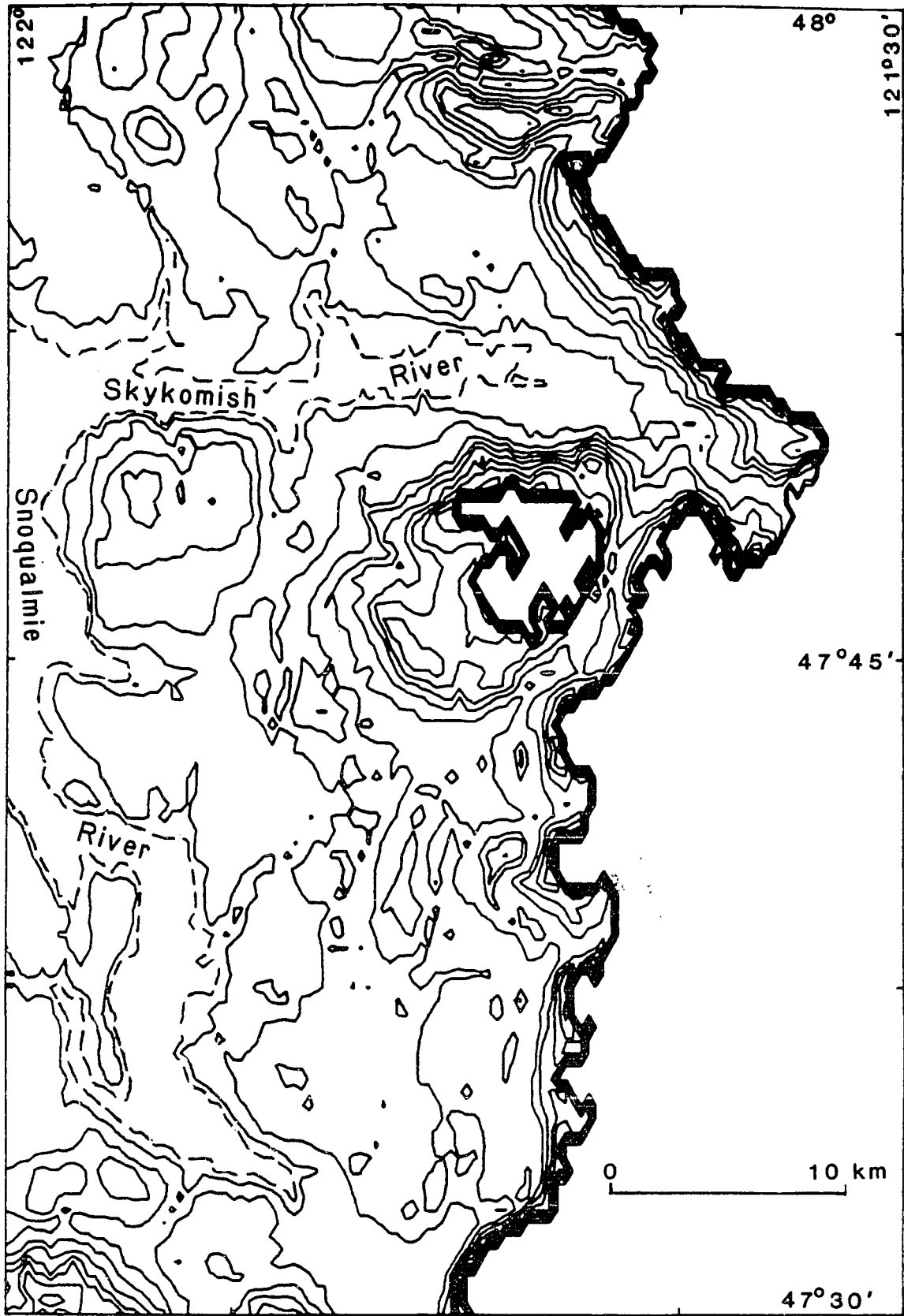




Figure 3.8. Ice-surface topography at maximum stage (contour interval 15 m). Values constrained at western and southern borders by Thorson (1980).

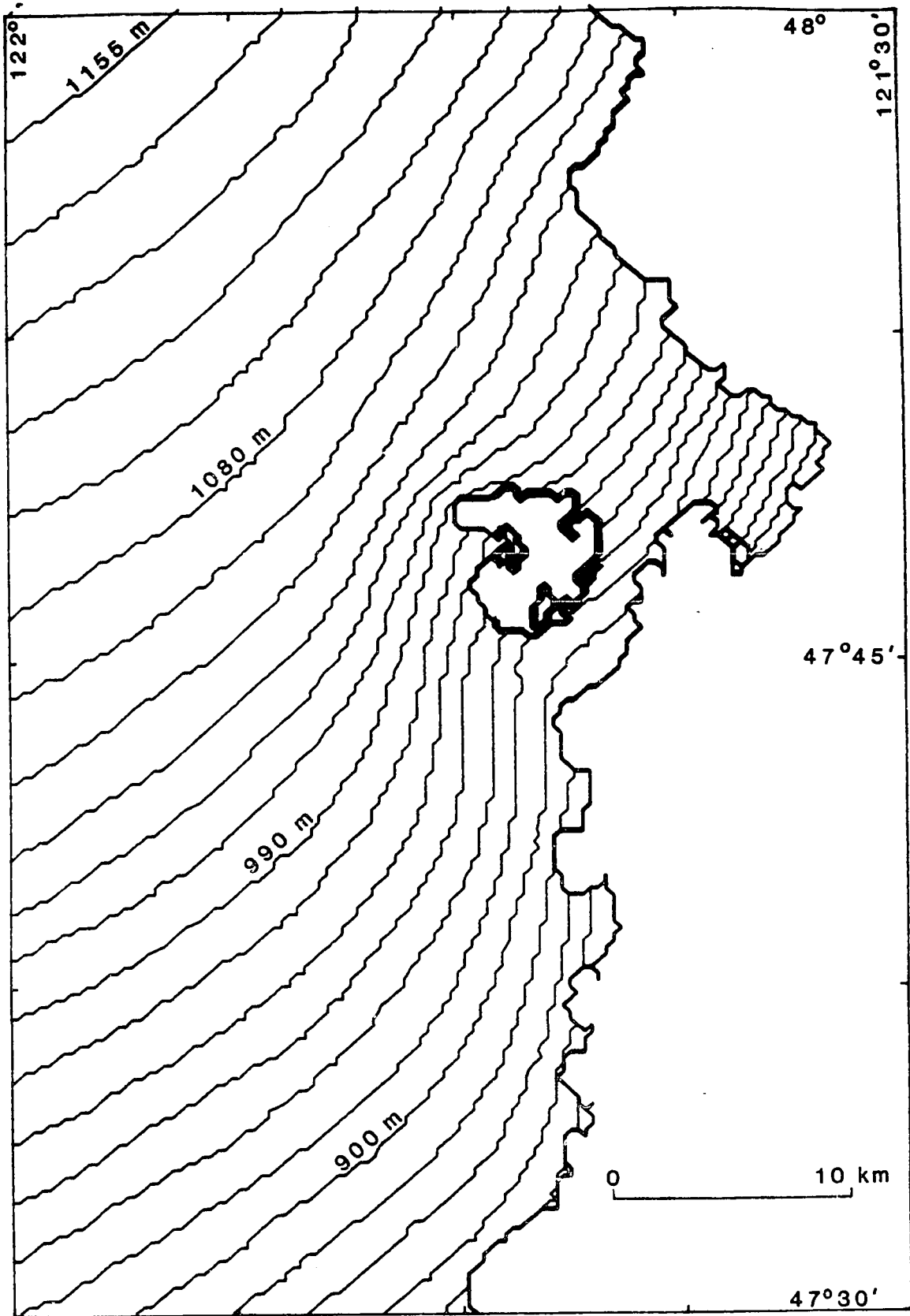


Figure 3.9. Subglacial hydraulic equipotentials at ice-maximum stage (contour interval 15 m). Definition of potential value chosen such that water of a given potential will stand at the equivalent altitude in a borehole or lake (equation 3.1).

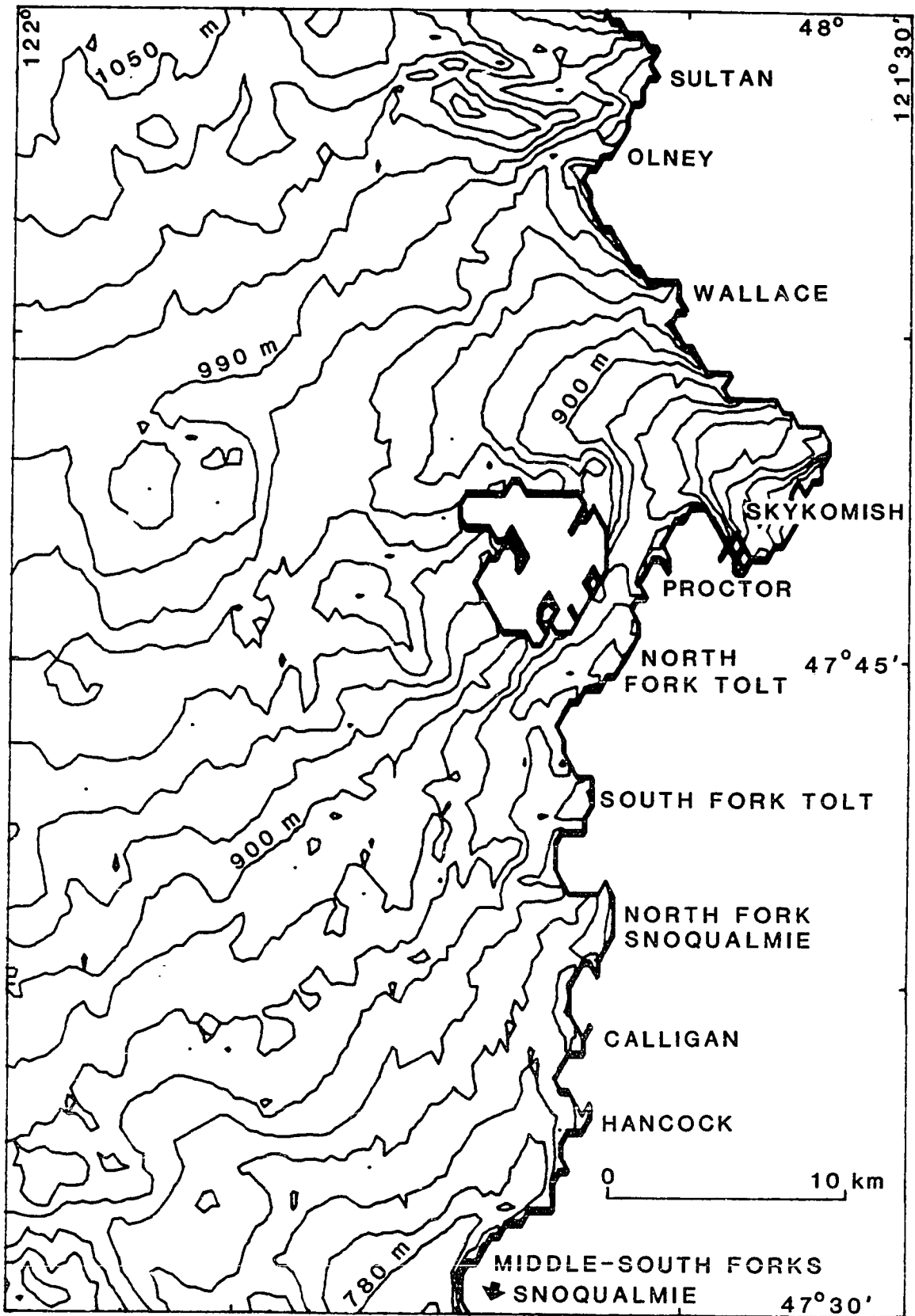
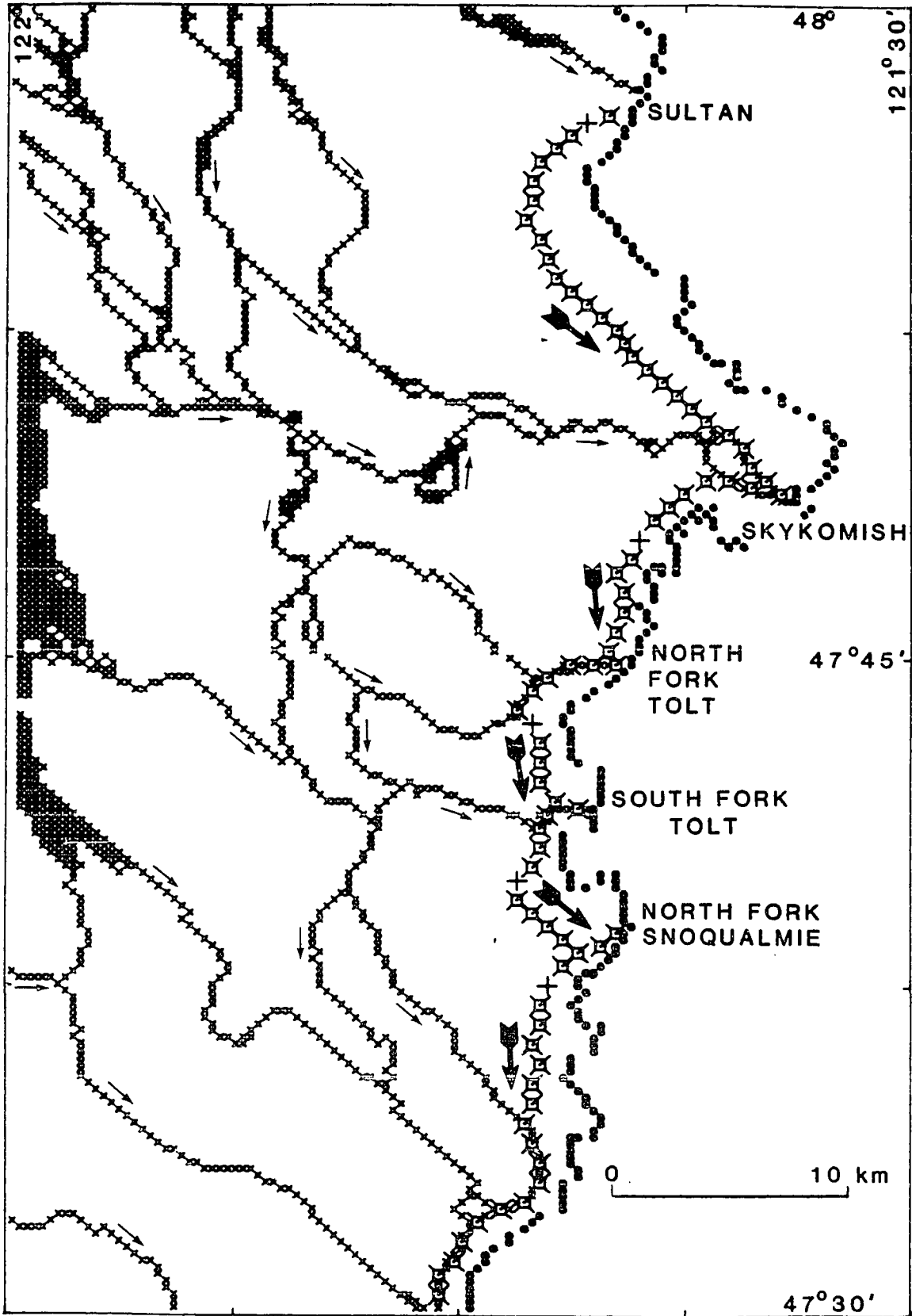


Figure 3.10. Subglacial water-flow paths following the potential surface of Figure 3.9. Steady drainage indicated by crosses; direction of decreasing potential shown by small arrows. The flow path marked by boxed crosses is interrupted by higher-potential saddles, indicated by plus signs. Potentials therefore do not decrease monotonically along this route but instead decrease away from saddles (heavy arrows).

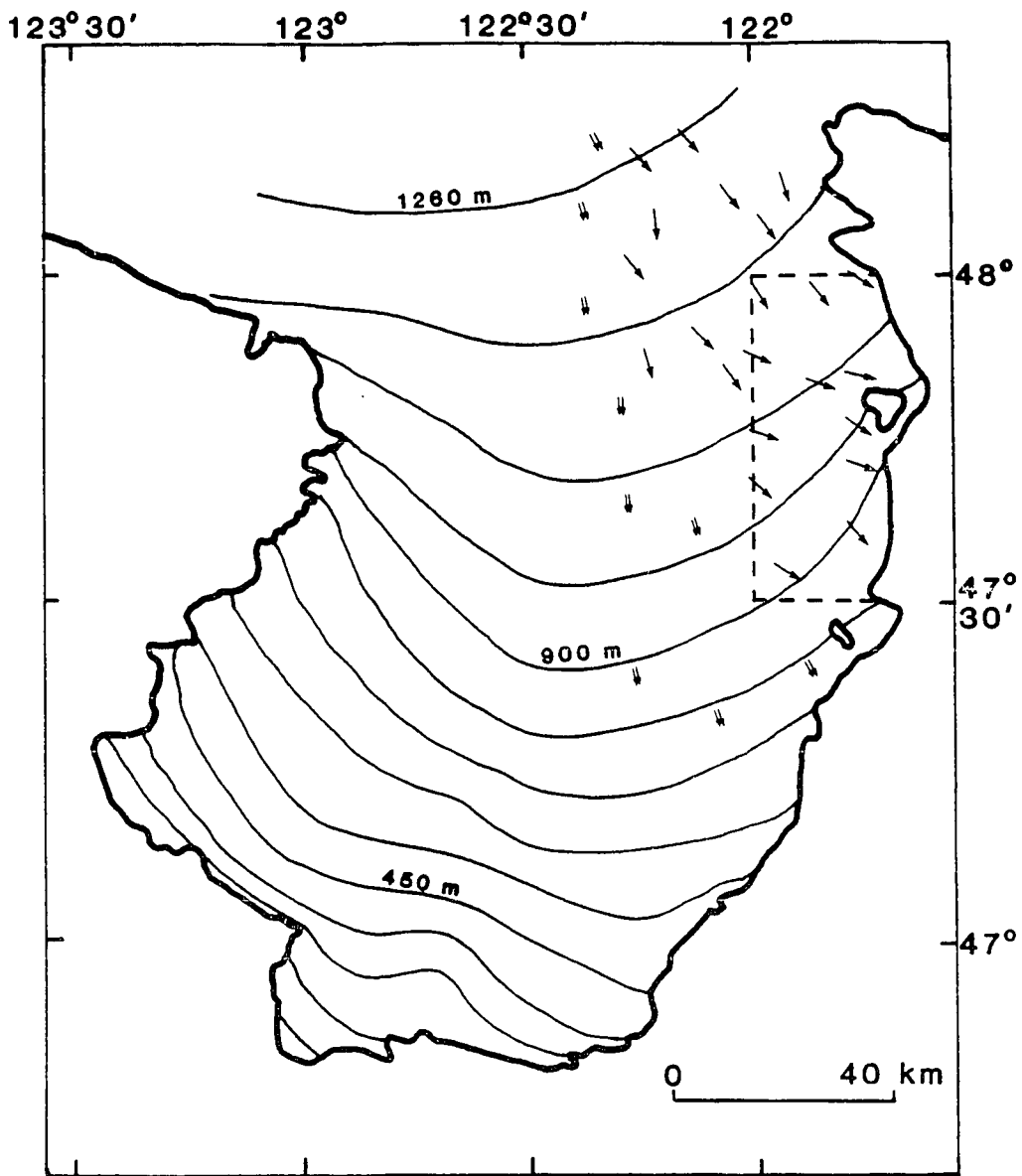


undulations at the bed will cause perturbations in the surface as well (Robin, 1967). The magnitude of these perturbations can be estimated from Hutter (1983, Figs. 4.8-4.9). For glaciers of low slopes ( $< 0.01$ ) and sliding velocities of 100-500 m/a (Chapter 2), rises in the ice surface are virtually in phase with those of the bed. If the bed perturbations are separated by a distance equal to a few times the ice thickness, the corresponding rise at the ice surface will be approximately 1/2 that of the bed. Because ice and bed slopes are in phase the predicted potential gradient that includes this effect will change only in magnitude, not in sign. This effect therefore modifies only the local amplitude of prominences in the potential surface, not the overall pattern.

Figure 3.10 shows two distinct patterns in these reconstructed flow paths that are particularly significant geologically. The first, represented by the "x" symbols in Figure 3.10, are routes of monotonically decreasing gradients. These channels coalesce into a crudely dendritic pattern towards the ice margin. Divergent branches represent areas where the resolution of reconstructed potentials is insufficient to identify a clearly "lower" route. Both branches may have been active simultaneously or at different stages in the evolution of the ice sheet. Although discharges cannot be predicted quantitatively by this reconstruction, the regional trend of subglacial equipotentials (Figure 3.11) suggests that much water entered this area from the west and northwest. Part of this flow went southeast up the Snoqualmie River valley, part was diverted up the

Figure 3.11. Regional subglacial water-flow paths. Puget-lobe limits and surface contours ( 30-m interval) from Thorson (1980). Single arrows show flow paths calculated from ground topography and ice-surface altitude (equation 3.2); small double arrows approximate these paths by the ice-flow direction only. Boxed region is the area of Figures 3.7-3.10.





- ice-surface contours
- ⇄ ice-flow direction
- ↓ decreasing subglacial hydraulic potential

Skykomish River valley to the ice margin, and part continued south over the topographic divide south of Sultan. Several routes are then available for flow across the uplands east of the Snoqualmie River to the marginal zone of the ice sheet. Potential gradients over these routes (expressed by the contour spacing in Figure 3.9) vary considerably, suggesting the likelihood of variable erosive effects as well.

The second distinctive characteristic in the pattern of predicted flow paths, represented by the "X" symbols in Figure 3.10, is a continuous channel in the submarginal zone. This channel does not, however, follow a route of monotonically decreasing potential. Saddles (marked by the symbol "+") interrupt the potential surface with values that decrease north to south. As with subaerial spillways, water would be impounded behind these saddles. Figure 3.9 shows that this water would be diverted to form lakes underneath the ice margin and extending into the alpine valleys immediately north of each saddle (Sultan, Skykomish, North Fork Tolt, South Fork Tolt, and North Fork Snoqualmie). Other subglacial saddles, between the main submarginal channel and the ice margin, would have similarly impounded lakes in the valleys of Olney Creek, Wallace River, Proctor Creek, Calligan Lake, and Lake Hancock. The hydraulic potential of water in each of these lakes, and in water extending beneath the ice to the impounding saddle, would rise as lake level rose from continuous subglacial influx, local melting, and drainage from the Cascades. Once the potential of this water exceeded that of the

saddle, drainage over it would begin. Melting of a tunnel would temporarily remove the component of total potential imparted by the weight of the overlying ice (Nye, 1976). This radical reduction in the potential at the saddle tends to lead to catastrophic lake drainage. This phenomenon, known as a jokulhlaup, has been observed on numerous modern ice-dammed lakes (Stone, 1963; Post and Mayo, 1971). Given these observations and physical considerations (Nye, 1976; Clarke, 1982), the submarginal flow path of Figure 3.10 was probably episodic in nature. It was occupied in its southern reach by more steady flow from the ice sheet interior but primarily experienced discrete, high-discharge events. The mechanics of this drainage and some of its consequences along the margin of the ice sheet are discussed more fully in Chapter 4.

Table 3.1. Parameters of lakes located along the submarginal channelway system of Figure 3.10. Maximum volumes determined at ice-maximum stage, recharge time based on modern measured runoff rates (U. S. Geological Survey, 1983), and discharge calculated from emperical data on drainage of modern ice-dammed lakes (Clague and Mathews, 1973).

Lake	Maximum Volume, km <sup>3</sup>	Recharge time, years	Maximum discharge, m <sup>3</sup> /s
Sultan	31	47	$7 \times 10^4$
Skykomish	120	34	$2 \times 10^5$
North Fork Tolt	3.3	10	$2 \times 10^4$
South Fork Tolt	4.8	27	$2 \times 10^4$
North Fork Snoqualmie	13	29	$4 \times 10^4$

### GEOLOGIC EXPRESSION OF SUBGLACIAL FLUVIAL ACTIVITY

This analysis of subglacial meltwater behavior illuminates many of the observed characteristics of channelized topography. Undulations in the bed topography, now impounding bogs or altogether blocking drainage, are negligible subglacially because of the dominance of ice-surface slope in determining flow directions (Clapperton, 1971; Shreve, 1972; Wright, 1973). Most of these channels effectively parallel the ice-surface gradient. Channel size and drainage area, ill-matched over the modern topography, relate far better given the network of Figure 3.10, particularly through the predicted flow paths draining south from the Skykomish valley.

The best-developed examples of channelized topography should be found where predicted rates of erosion are highest, given the uniform bedrock present here. If bedload mantles the channel bottom, fluvial erosion proceeds most rapidly where boundary shear stress increases along the flow path (Smith, 1970). If instead the sediment supply is limited, erosion will occur whenever clasts are transported over the bed. This bedload flux, and hence rates of fluvial erosion of bedrock, will scale with the basal shear stress (Graf, 1971). Although postglacial deposition has obscured the original subglacial configuration of channelway floors, their erosion regime can be tentatively inferred from their topographic position and form. West and southwest of the Tolt Reservoir, many small channelways begin abruptly at the crest of divides and continue down the downglacier slopes (Map 1). This initiating location corresponds to the point of maximum

shear stress gradient (Shreve, 1972), and suggests that sediments may have mantled the floor of these minor channels. Well-developed channelways, however, completely transect spurs. In spite of low predicted stress gradients, their dimensions indicate high water flux and active bedrock erosion. These conditions are predicted subglacially along the localized flow paths of Figure 3.10 in areas showing particularly steep potential gradients (Figure 3.9), which correlate with high boundary shear stresses. Conditions are particularly favorable in the areas 5 km south of Sultan and 8 km northeast of Lake Joy, which correlate with some of the best expressions of this characteristic and rather bizarre landscape (Figures 3.3 and 3.4).

The reconstructed subglacial drainage pattern also offers insight into the origin of the segmented submarginal channel system. Because this system lies nearly perpendicular to the regional direction of ice flow, ice erosion is particularly ineffective here. Its coincidence with the inferred episodic drainage path of Figure 3.10 points to subglacial water as its primary erosive agent.

The magnitude of discharges along this route can be estimated by Clague and Mathews's (1973) empirical relationship between lake volume and jokulhlaup discharge. This provides a semi-quantitative basis for comparing the glaciofluvial erosion in this area with the observed effects of other catastrophic drainage events. Table 3.1 lists the maximum volume of each impounded lake at ice-maximum stage. Drainage of the largest lake (Lake Skykomish) would probably trigger drainage of lakes in the North and South Forks of the Tolt River

valleys and the North Fork Snoqualmie valley as well. The Clague-Mathews formula (1973),

$$Q_{\max} = 75 (V/10^6)^{0.67}$$

where  $Q_{\max}$  = maximum discharge in m/sec, and  
 $V$  = initial lake volume in  $m^3$ ,

predicts maximum discharges on the order of  $10^5$  m/sec. By way of comparison, this is one to two orders of magnitude less than predictions of Lake Missoula floods (Baker, 1973; Clarke and others, in press), two orders of magnitude greater than reported from Alaskan ice-dammed lakes (Stone, 1963), and five to ten times greater than computed paleodischarges in the Rocky Mountain Trench during deglaciation there (Clague, 1975). Based strictly on modern runoff rates (U. S. Geological Survey, 1983), lakes would refill in 10 to 50 years. Additional drainage from beneath the ice can be calculated approximately from the percentage of the Puget lobe that forms the subglacial "drainage basin" for the Skykomish valley. By inspection of Figure 3.11, approximately a third of the upglacier meltwater would enter this system. From Table 2.4, this flux is of the same order as modern runoff rates and would halve these predicted refill times. Multiple drainage events are therefore probable during the Vashon Stade (Chapter 1), as well as during pre-Vashon glaciations.

Other consequences of impounded and episodically draining water are the great morainal embankments that choke the mouth of each alpine valley at their junction with the lowland. First described by Cary and Carlston (1937) and later studied by Mackin (1941), these features reflect a variety of depositional processes occurring at the

interface of the ice sheet and impounded water. The interrelationship between ice thickness and lake depth controls the sediment, structure, and geographic position of these embankments. These observed characteristics and their dependence on the dynamics of the ice sheet are discussed in Chapter 4.

This static analysis provides a physically based explanation for many of the observed, enigmatic characteristics of channelized topography. Such an approach, however, explicitly ignores all geomorphic consequences of flowing ice. This additional factor not only affects the flow of water but also controls the erosion by ice action directly. The analysis is therefore extended to consider these effects and to assess their relative impact on landform development in glaciated terrane.



**EFFECTS OF SLIDING OVER NON-PLANAR TOPOGRAPHY**

## INFLUENCE ON SUBGLACIAL WATER FLOW

Introduction

Sliding velocities of several hundred meters per year (Chapter 2) over the irregular bed surface will somewhat alter the pattern of predicted subglacial water flow, by affecting the ice pressure at the bed (Weertman, 1957; Lliboutry, 1968; Nye, 1969). This effect was discussed qualitatively by Shreve (1972), and his static analysis can be readily expanded to evaluate quantitatively the significance and consequences of this dynamic component over simple topographic elements. The linear ice flow theory of Nye (1969) and Kamb (1970) is used in the theoretical model. Its inherent inaccuracy, not critical to the problems addressed here (see below), is well-compensated by the theory's simplicity and flexibility.

Consider a simplified representation of the Puget-lobe ice sheet. Ice thickness is 1000 m and surface slope is 0.006 (about latitude  $47^{\circ}30'$ , 90 km north of the terminus), and bed topography is represented by sinusoidal ridges with 100 m amplitude and 1000 m wavelength. Along a longitudinal profile over one such ridge, each component of the total hydraulic potential at the bed surface changes. The change in elevation over one hill (one half wavelength) gives a variation of  $9 \times 10^5$  KPa (9 bars). Over the same downglacier distance, the average ice thickness decreases 3 m, or  $0.3 \times 10^5$  KPa. The maximum pressure difference due to sliding is given by Nye (1969,

eqn. 32, ignoring regelation over this size of obstruction) for 2-dimensional flow over a single sinusoid:

$$p = 4\eta U k_0^2 A, \text{ or} \quad (3.3)$$

$$p = 4 \times 10^5 \text{ kPa,}$$

where  $\eta$  = viscosity =  $3 \times 10^9$  kPa-s (1 bar-year) (Nye, 1970;  
cf. equation 3.9 below)  
 $U$  = ice velocity =  $4 \times 10^2$  m/a (Chapter 2),  
 $k_0$  = wave number of the periodic bedform ( $2\pi$ /wavelength),  
and  $A$  = amplitude of the bedform.

Thus pressure variations over bed irregularities of this scale are largely determined by the static components, but may include a significant dynamic component as well.

### 3-Dimensional Topography

Representing more realistic topography requires a 3-dimensional formulation. Kamb (1970) presented a linear model of sliding which is mathematically equivalent to Nye (1969) but more explicitly developed for 3-dimensional topography. Following Kamb, the bed topography,  $z_0(x,y)$ , is Fourier analyzed:

$$z_0(x,y) = \sum_m \sum_n a_{m,n} \exp(2\pi i(mx/L_1 + ny/L_2)) \quad (3.4)$$

where  $L_1, L_2$  are the length and width of the area of the bed being analyzed, and  $a_{m,n}$  is the coefficient of the  $m,n$  component of the Fourier series.

If the pressure variation across only those features larger than a few meters are considered (i.e. regelation irrelevant around these obstructions) the linear solution to the equations of motion gives:

$$p(x,y) = \sum_n \sum_k 2\eta U \phi |a_{h,k}| \exp(i(hx + ky)) \quad (3.5)$$

where  $p$  = pressure,

$$h = 2 m/L_1,$$

$$k = 2 n/L_2,$$

$$U_p = \text{sliding velocity (due to plastic flow only), and}$$

$$\eta = (h^2 + k^2)^{0.5}.$$

This is subject to two initial assumptions. One is that  $U_x = U_p$  and  $U_y = 0$  on the bed surface. The second is that the normal stress  $\tau_{zz}$  on the horizontal  $x$ - $y$  plane is assumed to equal the normal stress on the tilted bed surface  $z_0(x,y)$ . Both assumptions are strictly true only for infinitesimal roughness  $\partial z_0/\partial x$ , but according to Kamb (1970, p. 686) they yield an acceptable first-order solution for finite bed roughness as well.

#### Basic Configurations

Using this theory, the pressure distribution over any bed geometry with low roughness can be analyzed. The mathematically simplest topography is the sum of single sinusoids in the  $x$  and  $y$  directions, resulting in an "egg-carton" surface. It is represented by setting all  $a_{m,n} = 0$  in equation 3.4 except for  $a_{m_0,1}$  and  $a_{1,n_0}$ , where both  $m_0$  and  $n_0$  are much larger than one and defining

$$L = L_1/m_0 \tag{3.6}$$

$$W = L_2/n_0.$$

$L$  and  $W$  are the dimensions of the actual region of interest and will each include exactly one wavelength of the non-zero Fourier component. Defining

$$h_0 = 2\pi/L,$$

$$k_0 = 2\pi/W,$$

taking the real part of the series (equation 3.4) gives

$$z_0(x,y) = A_x \cos(h_0 x) + A_y \cos(k_0 y). \quad (3.7)$$

If  $L$  and  $W$  are of the same magnitude, equation 3.5 yields

$$p = -2\gamma U_p A_x h_0^2 \sin(h_0 x). \quad (3.8)$$

Only one term (see equation 3.7) appears in the pressure solution, because the value of  $h$  in equation 3.5 when  $a_{h,k} = A_y$  is very much smaller than when  $a(h,k) = A_x$ . This particular topography therefore yields no  $y$ -variation in pressure and is completely analogous to the 2-D case (equation 3.3). As expected, pressure does vary sinusoidally in  $x$ ,  $90^\circ$  out of phase with the bed topography: maximum  $p$  at the midpoint of the upglacier slope, minimum  $p$  similarly on the down-glacier slope. Lateral deflection of water following the total potential gradient over this topography will be caused only by differing elevations in the  $y$  direction.

### **Transverse and Longitudinal Topography**

Varying  $L$  and  $W$  in equation 3.6 while fixing  $m_0 = n_0$  changes the elongation of the topography relative to the ice-flow direction. Figure 3.12 demonstrates the effects of this variation on both the topography and the total pressure distribution under sloped, sliding ice. The patterns of hydraulic potentials over each topography show certain features in common. The hydraulic potential surface is depressed upglacier of the topographic highs. Drainage out of these basins is via the longitudinal channels between hills, with gradients increasing in these channels to maximum values on their lee-side segments. Subglacial water flow is diverted from all points on the

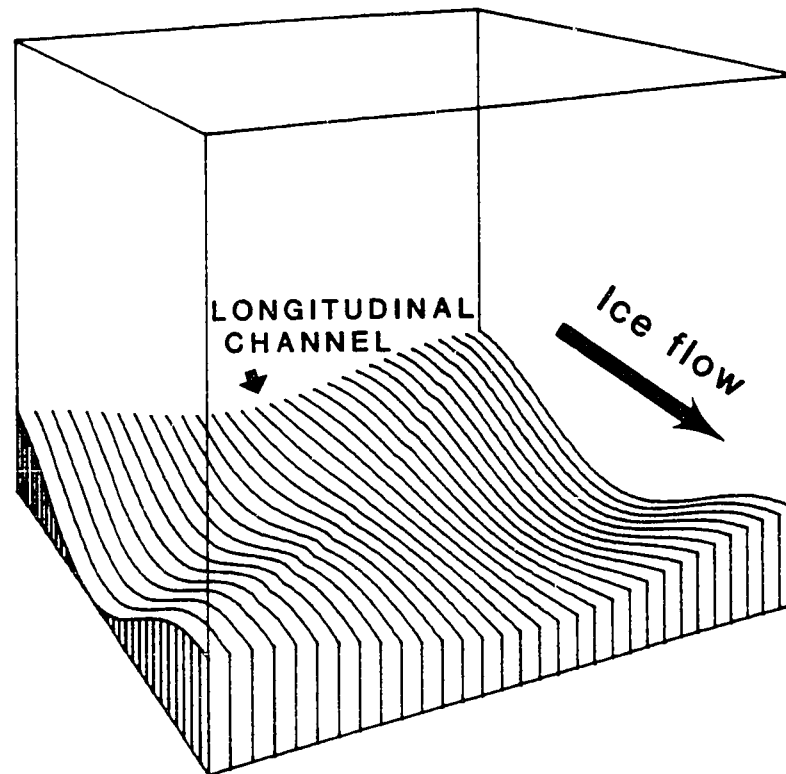


Figure 3.12. Hydraulic equipotentials beneath ice sliding over non-planar topography (ice-flow direction is indicated by long arrow). Bed topography (Figure 3.12a) consists of hills with their apex at the corners of each figure, separated by channels and closed depressions. Total relief = 200 m. Equipotentials (Figures 3.12b-f) mimic the bed topography, but maxima are shifted slightly upglacier of topographic peaks and minima shifted downglacier from depressions. Contour interval arbitrary; using values for ice thickness (1000 m), surface slope (0.006), sliding velocity (400 m/a), and effective viscosity ( $3 \times 10^9$  kPa-s), interval = 25 kPa.

3.12a. Generalized view of bed topography of Figures 3.12b-f. Longitudinal channels are those that extend in the ice-flow direction (transverse channels lie perpendicular to the flow direction).

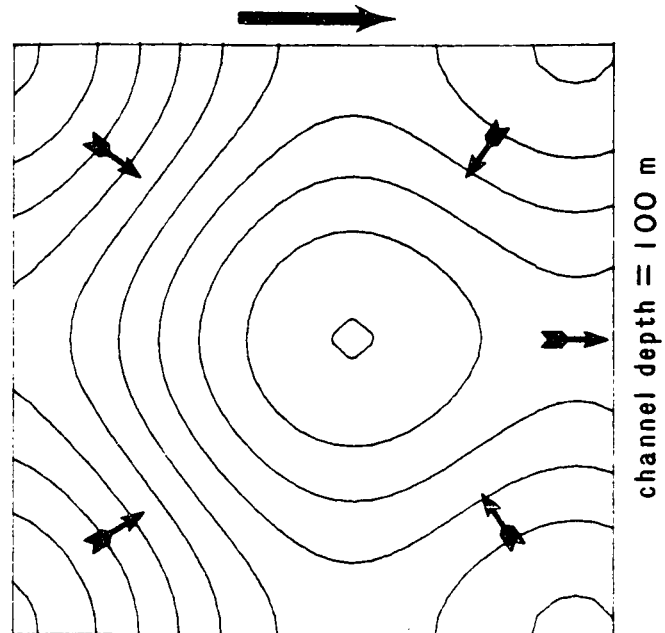


Figure 3.12(cont.)b. Symmetrical hills, spacing = 2000 m;  
channel depths = 100 m.

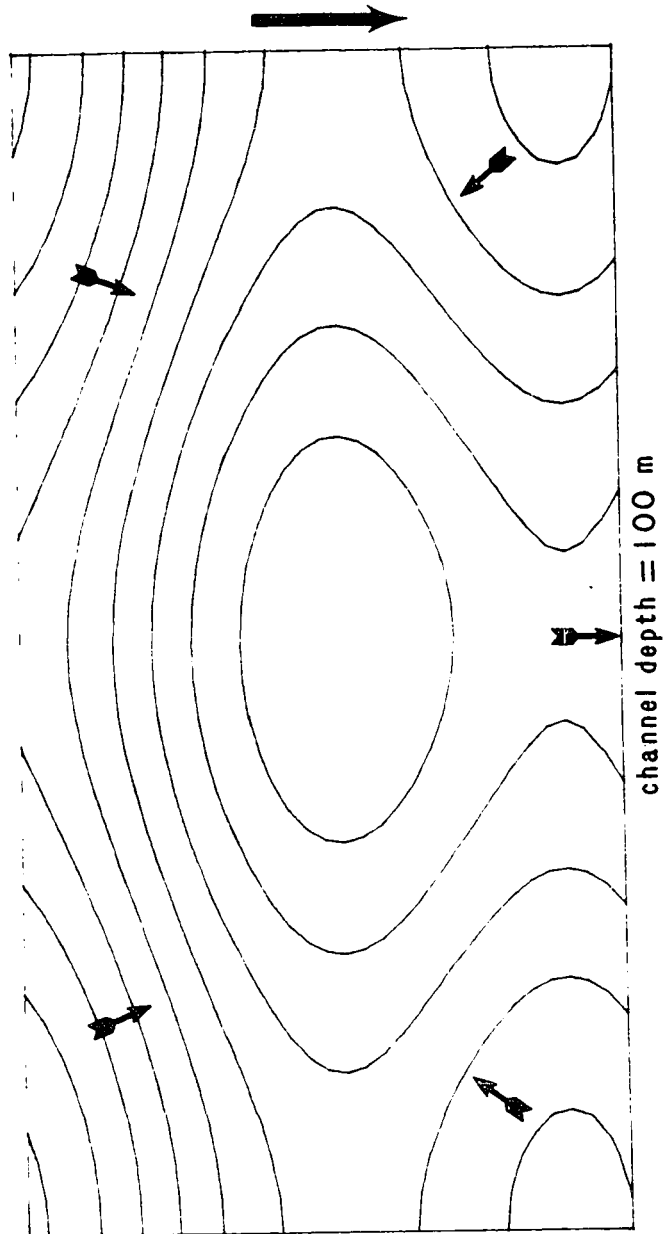


Figure 3.12(cont.)c. Transverse hills: length = 2000 m, width = 4000 m. Channel depths = 100 m.

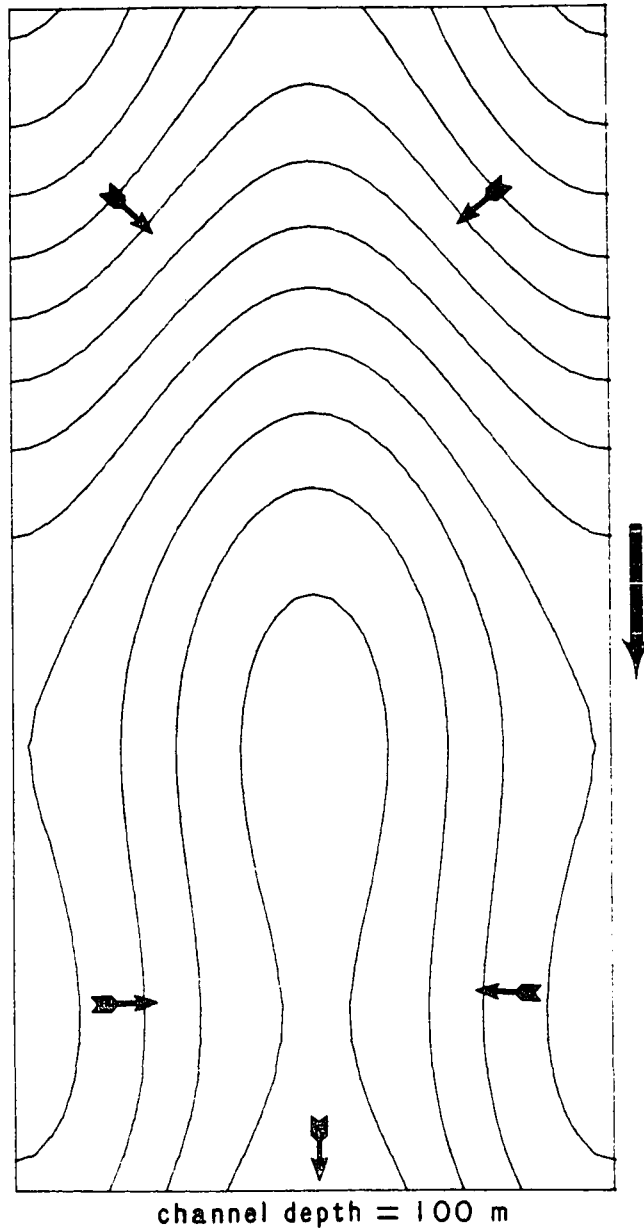


Figure 3.12(cont.)d. Longitudinal hills: length = 4000 m,  
width = 2000 m. Channel depths = 100 m.



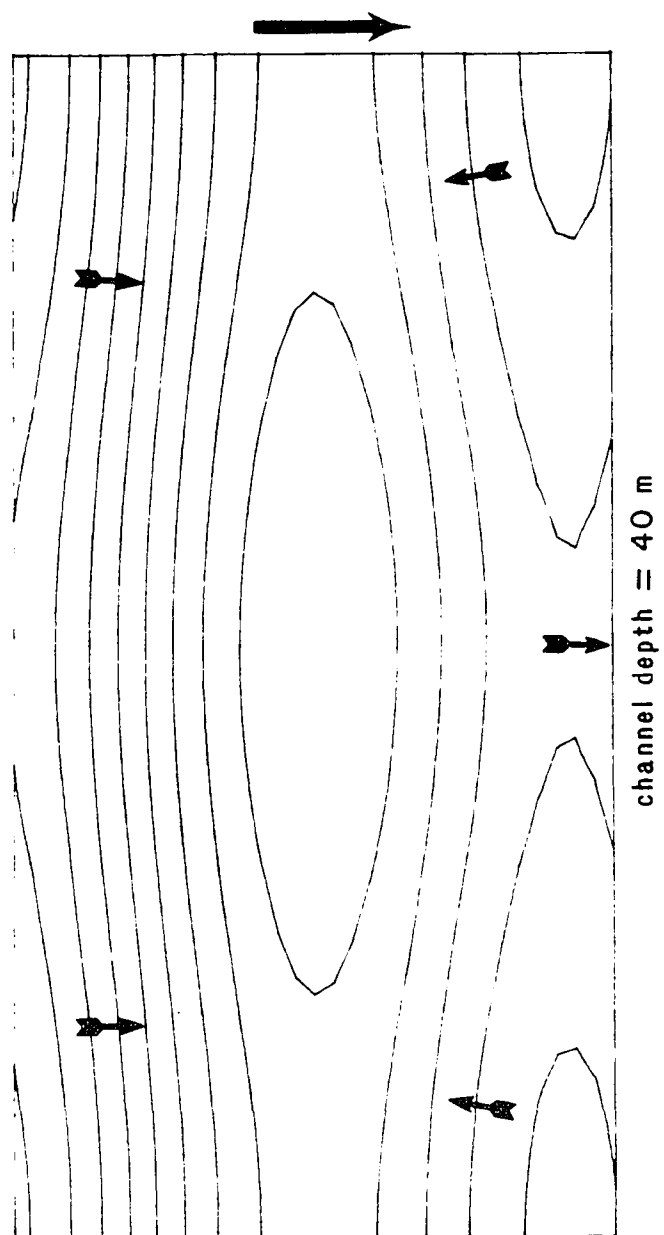


Figure 3.12(cont.)e. Transverse hills: length = 2000 m, width = 4000. Longitudinal channel depth = 40 m; transverse channel depth = 160 m.

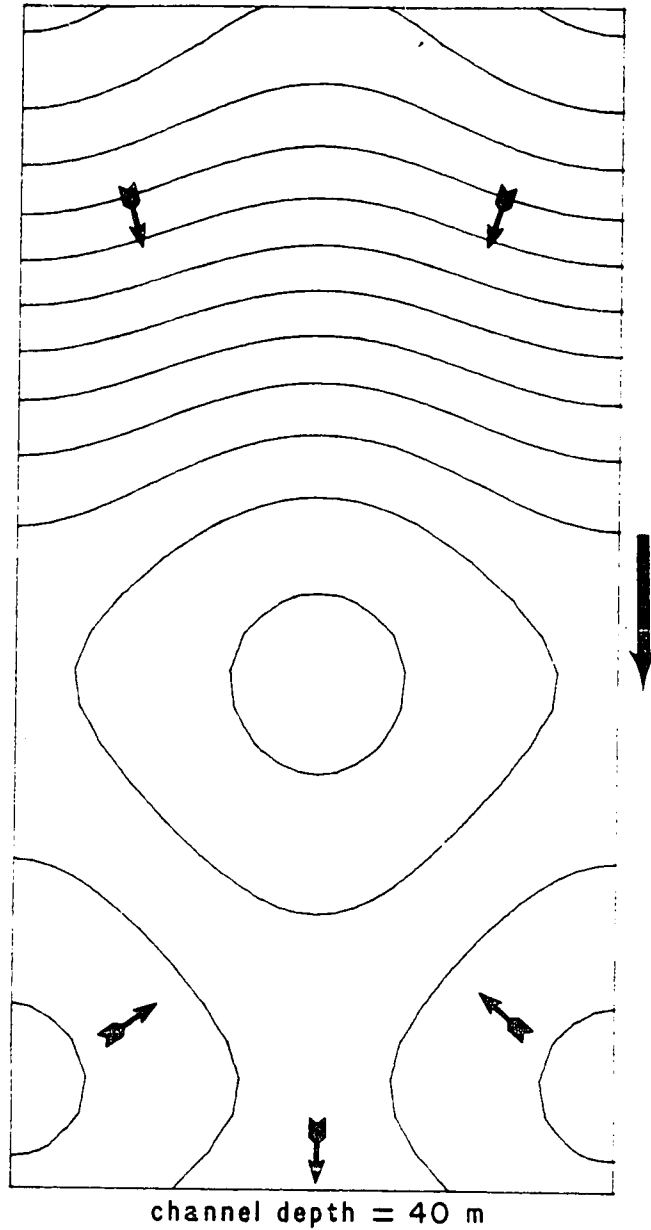


Figure 3.12(cont.)f. Longitudinal hills: length = 4000 m; width = 2000 m. Longitudinal channel depth = 40 m; transverse channel depth = 160 m.

bed surface into these channels.

Several differences are also apparent between potential fields over these bed topographies. Ridges transverse to the ice flow (transverse topography; Figure 3.12c) yield a potential surface having deep, extensive depressions and steep channel gradients. In contrast, longitudinal topography (ridges elongated in the ice-flow direction) generates less extensive upglacier depressions and more gentle gradients in channels (Figure 3.12d; note the absence of closed depressions and the contour spacing relative to Figure 3.12c). This occurs because the dynamic pressure component varies inversely with only the longitudinal wavelength squared ( $h_0^{-2}$  in equation 3.8).

To draw inferences about erosion rates we must assume how shear stress and erosion by bedload transport are coupled. As previous discussed, erosion rate may scale with either shear stress (reflected by the potential gradient) or shear stress gradient. Once bedrock is exposed in the bottom of the channel, erosion will occur at rates proportional to the flux of bedload. This parameter scales with the basal shear stress. Potential gradients are easily compared by inspection of these figures, indicating that fluvial erosion rates of the bedrock topography should be lower over longitudinal than over transverse landforms.

### **Channel Deepening**

Varying the relative amplitudes of the sinusoidal components ( $A_x$  and  $A_y$ ) shows other consequences of topographic changes, specifically the deepening of channels. Figures 3.12e-f differ from 3.12c-d in having a 4:1 (instead of 1:1) ratio between the amplitudes of the x and y components. With increasing channel depth (Figures 3.12c-d), lateral diversion into channels (expressed by contour curvature) increases although the gradient in the lee-side segments (contour spacing) simultaneously decreases. Small channels, inevitably present in preglacial topography, should therefore be exploited and enhanced by subglacial water (cf. Clapperton, 1968; Whillans, 1979), though at steadily decreasing rates.

### Isolated Topographic Elements

#### **Pressure Distribution**

Sliding over isolated hills on an otherwise planar surface can also be modeled to yield insight into both pressure distribution and the accuracy of this theory. A single hill is generated by the product of  $(A \sin(x))$  and  $(A \sin(y))$ , where x and y vary from 0 to  $\pi/2$  and  $A^2 = 100$  m, and is placed on a horizontal surface (Figure 3.13a). This topography is Fourier analyzed, assuming periodic repetition of the bed surface outside the defined region, to give the set of  $a_{m,n}$  coefficients of equation 3.4. Landforms with aspect ratios elongated transverse or parallel to the ice-flow (x) direction can be considered by choosing non-equal values of  $L_1$  and  $L_2$  (Figure 3.13b-c). The dynamic pressure component is then calculated from eqn. 3.5

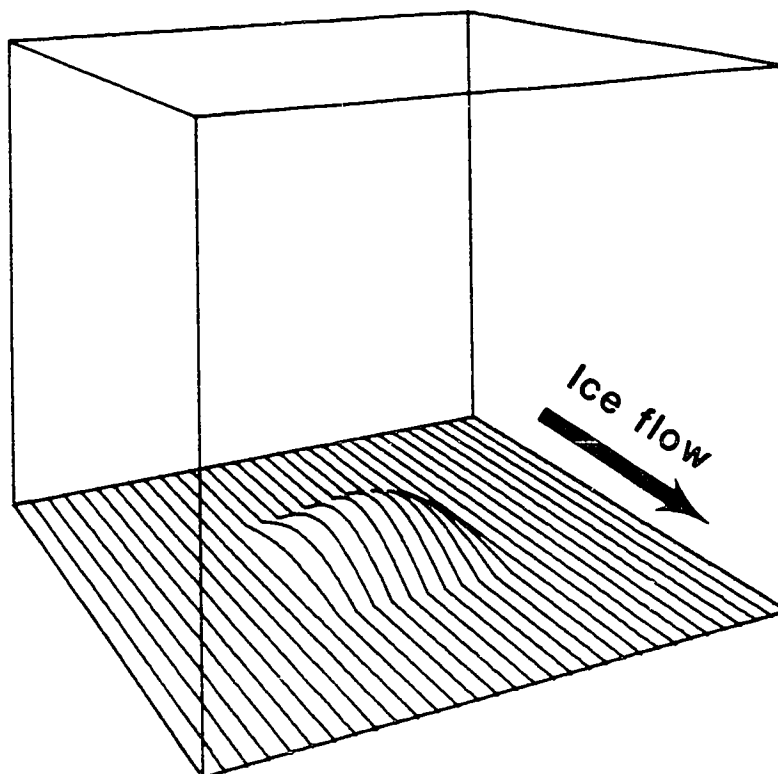


Figure 3.13. Dynamic pressure due to sliding over periodically spaced isolated hills.

3.13a. Generalized view of bed topography of Figures 3.13b-c.

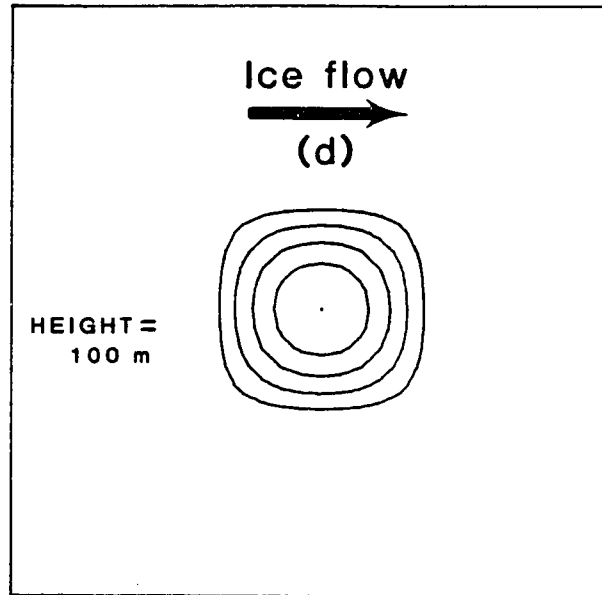


Figure 3.13(cont.)b. Topography of isolated symmetrical hill. Contour interval = 20 m; spacing = 2000 m.

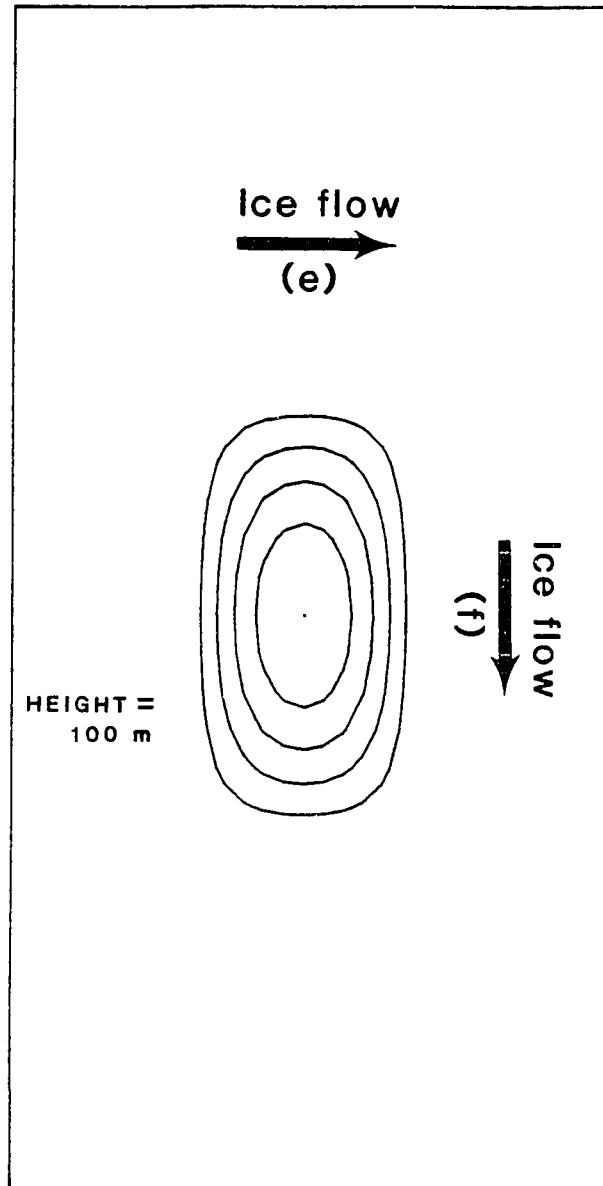


Figure 3.13(cont.)c. Topography of isolated elongated hill. Contour interval = 20 m; spacing = 2000 m in narrowest dimension.

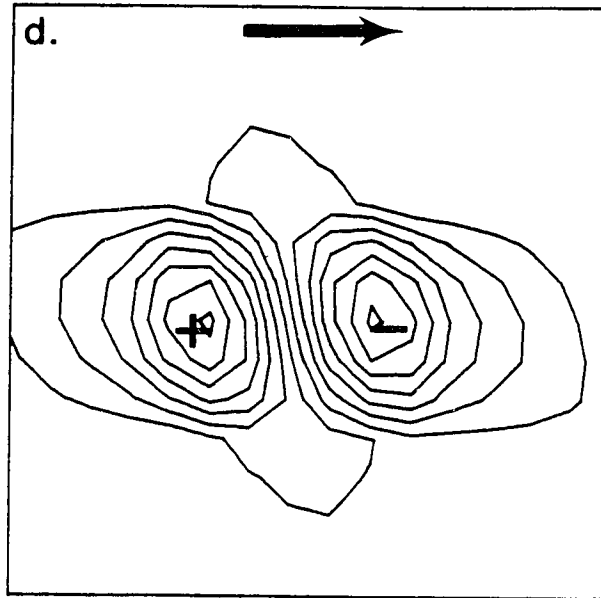


Figure 3.13(cont.)d-f. Contour plots of the pressure component of the subglacial hydraulic potential due to sliding over hills contoured in Figures 3.13b-c. Closed contours up-glacier of the centerline indicate a pressure high; contours downglacier of the centerline indicate a pressure shadow. Asymmetrical patterns are due to numerical errors introduced by non-infinitesimal slopes; they are most extreme over the steepest topography (Figures 3.13b, 3.13d).



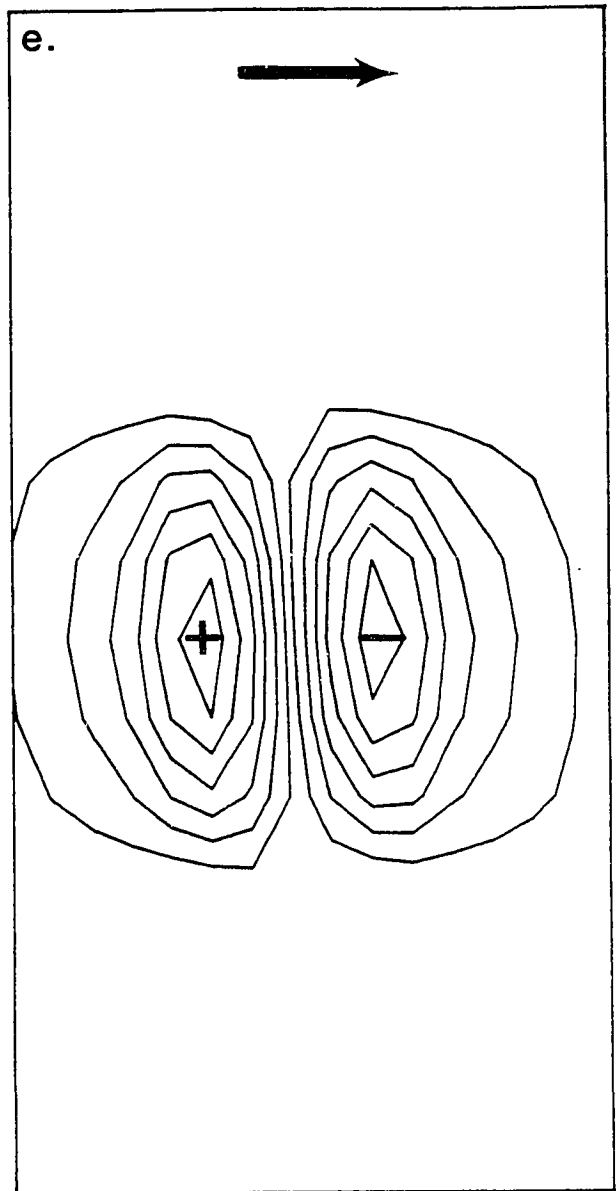


Figure 3.13(cont.)e.

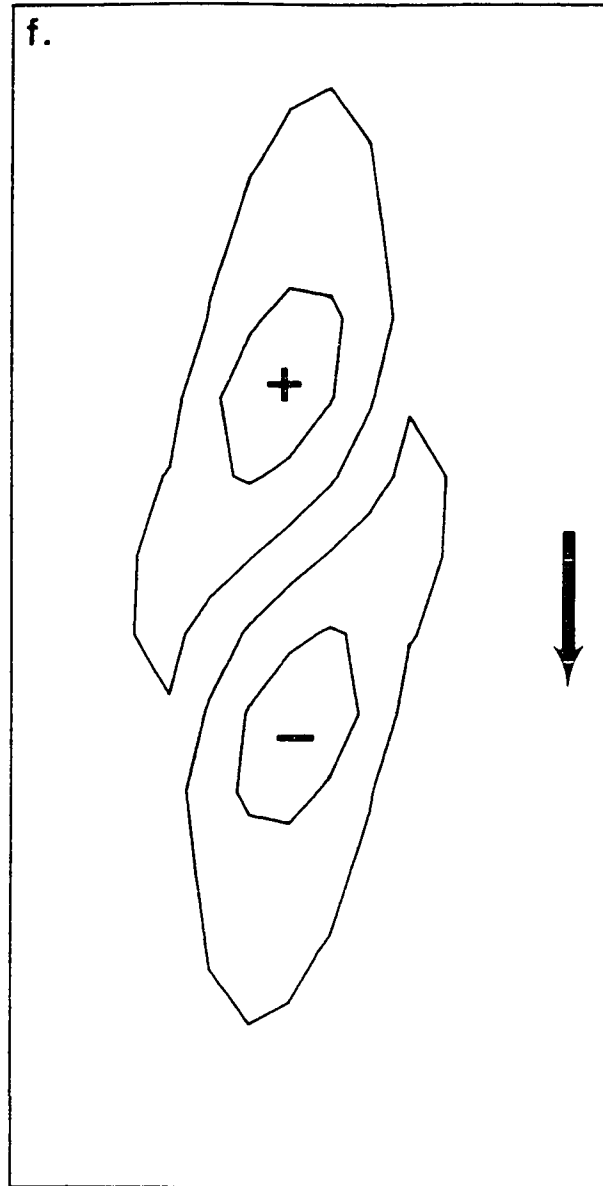


Figure 3.13(cont.)f.

(Figure 3.13d-f). As expected, low-pressure shadows and high side-slope gradients are predicted, consistent with innumerable observations of low-pressure zones behind any obstruction to fluid flow and the distribution of fluviably-scoured features on glaciated bedrock hills (Dahl, 1965; Gray, 1982).

### Comparison with Non-Linear Model

Lliboutry and Ritz's (1978) analysis of non-linear flow around a hemisphere provides an indirect method of checking the numerical results of a linear viscous flow law for ice. This comparison cannot be accomplished by direct matching of equivalent topographies using Kamb's (1970) model, as a hemisphere thoroughly violates the requirement of low surface slopes (such a calculation over this geometry yields predictably meaningless results). Instead, we use the analytic solution for linear flow around a slippery hemisphere (e.g., Happel and Brenner, 1965). To choose a reasonable viscosity, the total drag force over the hemisphere can be set equal in both linear and non-linear cases (Lliboutry and Ritz, 1978):

$$4\pi\eta UR = 8.8\pi R^2(U/BR)^{1/3}, \text{ or}$$

$$\eta = 2.2(R^2/U^2B)^{1/3}, \quad (3.9)$$

where R = hemisphere radius (m),  
 U = ice velocity (m/a),  
 B = flow law constant =  $5.29 \times 10^{-15} \text{ s}^{-1} \text{ kPa}^{-3}$   
 ( $.167 \text{ a}^{-1} \text{ bar}^{-3}$ ) (Paterson, 1981, p. 39).

Using 400 m/a flow over a 100-m hemisphere,  $\eta = 5.0 \times 10^9 \text{ kPa}\cdot\text{s}$  (1.6 bar $\cdot$ a). Calculated pressures around the hemisphere are compared for the two rheologies in Figure 3.14. Their distributions are qualita-

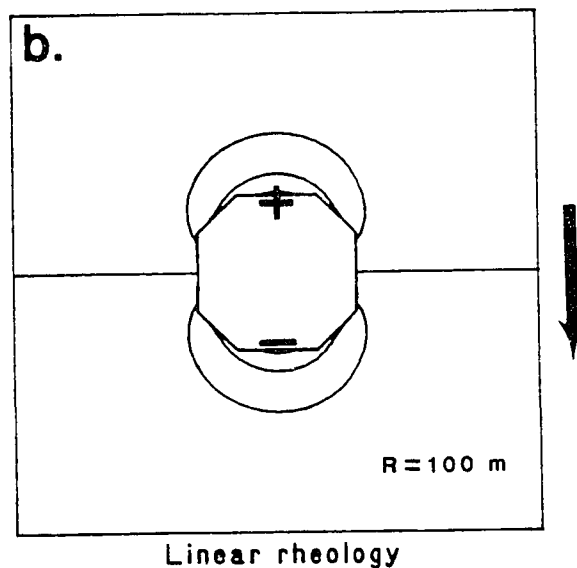
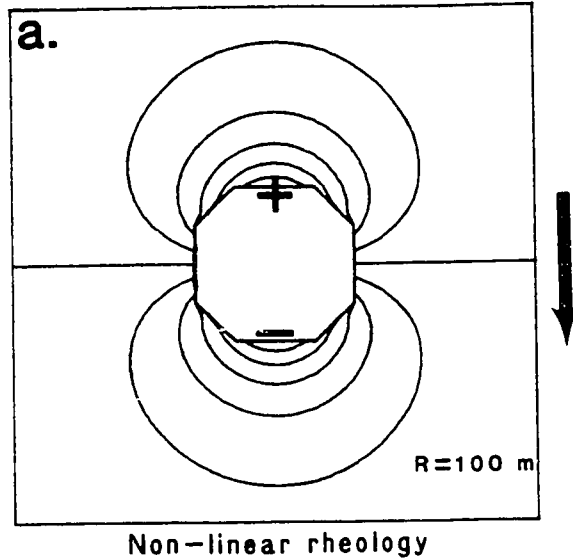


Figure 3.14. Dynamic pressure component due to sliding over an isolated hemisphere of 100-m radius, velocity = 400 m/a (contour interval 20 kPa). (a) models the ice as a power-law fluid with an exponent of 3 (Lliboutry and Ritz, 1978); (b) uses a linear viscous approximation with viscosity =  $5 \times 10^9$  kPa-s. Pressure maxima are on the upglacier surface of the hemisphere, minima on the downglacier surface.

tively very similar, although maximum pressure variations are  $\pm 12$  bars for the non-linear case and only  $\pm 6.4$  bars for the linear case (equivalent values for  $U = 100$  m/a are  $\pm 7.5$  and  $\pm 4.0$  bars). The numerical accuracy of these models is therefore ambiguous, particularly in the case of realistic, non-infinitesimal bed slopes modelled using Nye (1969) or Kamb (1970). The pattern of predicted pressure and, for low bed roughness, its estimated magnitude, nevertheless appear both valid and useful approximations (Nye, 1970).

#### EROSION BY ICE-TRANSPORTED SEDIMENT

Rapid sliding of ice also affects the bed topography directly, by abrasion and plucking. Erosion by combined glacial processes in the Puget Lowland is evident from the abrupt non-structural topographic scarps (Tabor and others, 1982) at the lateral boundaries of the glaciated terrane here, with relief commonly greater than 300 m (cf. Sugden, 1979). Of the two subglacial agents of erosion, only ice action is likely to attenuate bedforms and degrade the entire bed surface, as subglacial water flow only can enhance local relief. Ice erosion is generally considered to result from abrasion and plucking. The controlling parameters of abrasion are far better constrained by theory than those of plucking, although both may be significant components of the total erosion by ice. Yet the abrasion rate should be coupled to the plucking rate, because quarried blocks can subsequently become abrading tools.

Theoretical treatments of abrasion (Boulton, 1974, 1979; Hallet,

1979, 1981) agree that rates are dependent upon several factors. For a given lithology, these include the tool concentration, the velocity of those tools over the bed, and the effective force of contact between tool and bed.

Availability of tools shows a plausible dependence on bedform size. The origin of such tools has been ascribed variously to pre-glacial regolith (Warnke, 1970; Whillans, 1978) and to subglacially plucked debris (Boulton, 1974). The subaerial accumulation rate of regolith at the base of slopes is a function of the slope gradient (Carson and Kirkby, 1972). As the steepest slopes of an elongated hill lie along transects across its narrowest dimension, regolith will be accumulated most rapidly there. Subsequent ice flowing in the direction of steepest bed slopes will therefore carry the greatest amount of sediment over the landform. If ice-erosion rates are limited by the availability of tools, erosion of bedforms of a given amplitude should be inversely related to the longitudinal wavelength of the topography.

Once entrained in ice, the rate at which abrading tools reach the bed depends on the rate of convergence with the bed (Hallet, 1979). Over bedforms 100s to 1000s of meters long, basal melting should be relatively uniform (Rothlisberger, 1968). The pattern of convergence due to longitudinal strain, however, changes significantly over a single bedform and between bedforms of different sizes. Figure 3.15 shows the relative convergence rate of tools over 2-dimensional sinusoids of different wavelengths. Convergence is less

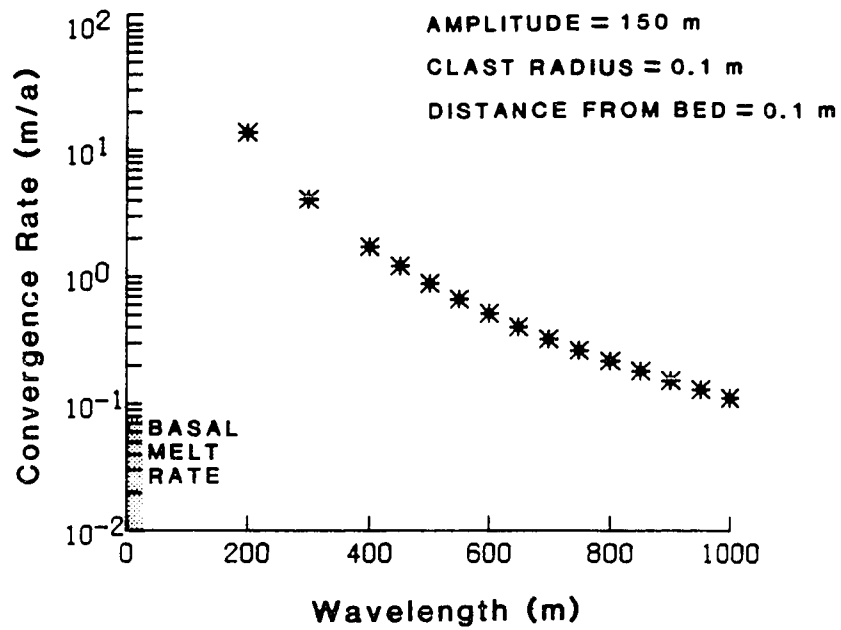


Figure 3.15. Maximum convergence rate of tools with bed as a function of wavelength, calculated from Hallet (1979, eqn. 17). Clast radius = 0.1 m, distance from bed = 0.1 m, velocity = 400 m/a, and amplitude fixed at 150 m for all wavelengths. Basal melting is ignored in these calculations but would become increasingly significant for wavelengths longer than about 1000 m. At short wavelengths the numerical results become increasingly inaccurate due to non-infinitesimal slopes, but the gross functional relationship should still apply (cf. Figure 3.14).

pronounced over long wavelengths and vanishes (but for the component due to basal melting) at the limit of infinite wavelengths.

Predicted variations in the effective contact force depend on the theoretical framework. Using Hallet (1979), effective contact force is primarily determined by convergence rates and so varies along with predicted changes in the tool concentration at the bed. Using the less-plausible theory of Boulton (1974; cf. discussion of Boulton, 1979, P. 38), contact force depends on the total normal stress exerted by the ice on the bed, which will vary only trivially over this scale of bedforms (while tool concentration varies as above). Either model therefore predicts qualitatively equivalent bedform-size dependence, with abrasion rates highest over short-wavelength forms.



## RELATIVE PERSISTENCE OF LONGITUDINAL AND TRANSVERSE LANDFORMS

### Qualitative Factors

The predominance of longitudinal over transverse forms in glaciated landscapes (Linton, 1963; Clayton, 1965) suggests that glacial erosion must generally favor either enhancement of longitudinal features or attenuation of transverse ones. The above discussion qualitatively suggests that ice-erosion rates should be fastest for short-wavelength forms irrespective of their extent in the transverse direction. Although the relief of all bedforms should be reduced by ice abrasion (Hallet, 1979), features of the landscape oriented across the ice-flow direction (transverse landforms) should degrade more rapidly than features of the same size oriented longitudinally.

Where transverse forms persist, the rate of ice erosion must be low relative to the rates of other erosional processes that can accentuate relief in these glaciated landscapes. The theoretical considerations of subglacial hydrology provides a physical explanation for the conditions that preserve or enhance this topography. Initiation requires landscapes where preexisting topography or structural control has developed preglacial landforms (Newell, 1970; Rudberg, 1973; Gordon, 1981) transverse to the ice-flow direction. Lateral margins, where defined by topographic barriers, provide particularly favorable sites, since bedrock ridges that project across the ice flow are more typical here than in the interior region of the ice sheet. The relative dominance of subglacial fluvial erosion over ice erosion, necessary for these landforms to persist, is not con-

stant over the glacier bed. Most generally, water flux increases monotonically downglacier whereas ice flux decreases below the equilibrium line. Conditions for water to dominate glacial erosion thus become increasingly favorable in the ablation zone, particularly where flow is concentrated towards the lateral margins by the convex ice surface. This effect will be greatly enhanced locally by the predicted channelization of water.

#### Rates of Water and Ice Erosion

This relative importance of ice and glaciofluvial erosion can also be estimated. For this large-scale comparison the erosive potentials of both ice and water are characterized by the power of each geomorphic agent per unit area of the bed (Andrews, 1972; Church and Gilbert, 1975; Hallet, 1979, eqn. 2). An estimate can be made of the proportion of energy in the moving fluid that is actually used to comminute bedrock (Boulton's "effective power", 1974, p. 84), and the spatial distribution of that power over the bed can be assessed.

The change in gravitational potential energy per unit time of both ice and water can be calculated from mass-balance data, presented in Table 2.4, as a function of position downglacier by using the relationship:

$$E = (Q \rho) g \Delta h,$$

where E = potential energy loss per year per unit length of the glacier,

Q = volume flux of fluid (ice or water) per year,

$\rho$  = fluid density, and

$\Delta h$  = potential drop per unit length (= (surface slope)•0.5 for ice, (surface slope)•  $\rho_i/\rho_w$  for water).

Dividing by the cross-sectional width then yields the average power per square meter (Figure 3.16). This equation is obtained assuming that the ice moves entirely by basal sliding and that the proportion of the potential energy of water lost as it first drops from the ice surface to the bed (approximately 10% of its total from ice surface to terminus) is negligible.

The proportion of this total fluid power that is actually used to comminute bedrock may influence the relative geomorphic action of these two agents. The order of magnitude of this "efficiency" factor can be estimated, albeit crudely, for both ice and water by calculating the ratio of 1) energy expended in removing bedrock to 2) the total potential energy available in the fluid during the same period.

Measured rates of erosion over glaciated basins in Norway average 0.3 mm/a (Wold, 1983), giving a maximum estimate for the rate due to ice erosion alone. Far more localized data (Lutschg, 1926; Andrews, 1972; Boulton, 1974) suggest a possible range up to one order of magnitude higher. Using typical values for ice flow and basal shear stress (100 m/a and 100 kPa) (Patterson, 1981) and a value for the energy required to comminute quartz and feldspar to a size of 0.01 mm ( $3.3 \times 10^5$  J/kg; Hukki, 1961; consistent with observations of abraded rock and the corresponding coefficient used by

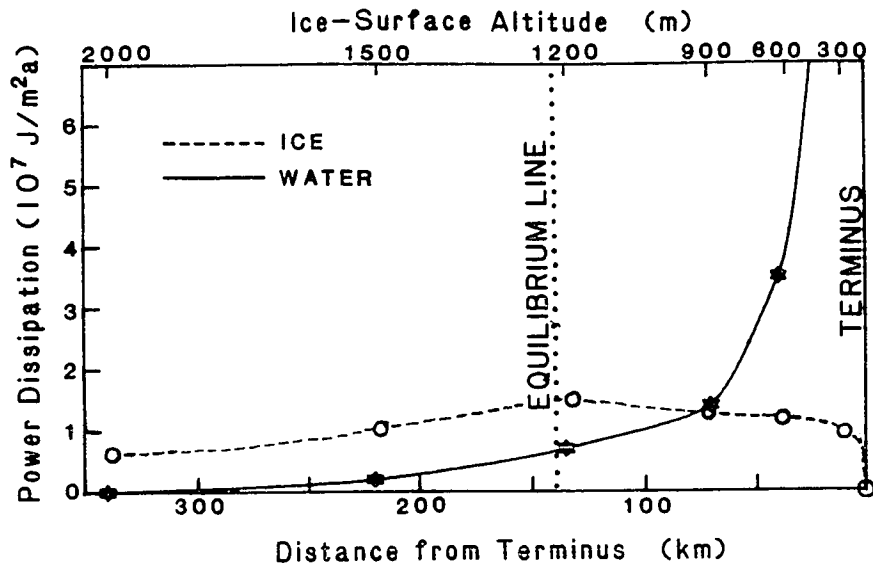


Figure 3.16. Potential energy dissipation per unit bed area per year as a function of longitudinal position. All values spatially averaged (i.e. no channelization assumed). Equilibrium-line position, mass flux data, and ice-surface slopes used in calculations are from Chapter 2.

Metcalf, 1979),

$$\text{efficiency}_{\text{ice}} = 3 \times 10^{-2}.$$

This result is one order of magnitude smaller than calculated by Metcalf (1979), due to his assumption of greater abrasion rates.

Equivalent erosion rates and efficiencies are not readily available for fluvial incision through bedrock. The Late Pleistocene Bonneville flood (Malde, 1968), however, provides an excellent opportunity to infer this information for discharges that are of equivalent magnitude ( $10^5$  m/s) to the jokulhlaups predicted along the submarginal channel system of the Puget lobe. In the Bonneville area,  $1.2 \times 10^9$  m<sup>3</sup> of volcanic rock was removed from a bedrock channel by  $1.2 \times 10^{12}$  m<sup>3</sup> of water falling 120 m. Using a crushing energy ( $1.2 \times 10^3$  J/kg; Hukki, 1961) required to reduce fine-grained rock to sizes of a few tens of millimeters or more (as reported by Malde, 1968),

$$\text{efficiency}_{\text{water}} = 3 \times 10^{-3}.$$

This order-of-magnitude difference in ice and water efficiencies cannot dominate other characteristics of these two erosive agents, particularly their spatial distribution over the glacier bed. For ice, no significant local variations in the flux along any transect is likely except over the most extreme topographies. The power is therefore not at all likely to vary greatly from its average value (Figure 3.16). Channelization of water, however, is indicated by theory (Rothlisberger, 1972; Shreve, 1972), observation (Stenborg, 1968), and geologic inference (Walder and

Hallet, 1979). The width over which its power is expended is therefore only a small fraction of the total width of the glacier, indicating that calculated values of the spatially averaged water power substantially underestimates the local rate of work. The channelway system of the eastern Puget Lowland (Map 1) occupies at most a few percent of the glacier bed. Even if these valleys were occupied simultaneously, the flow concentration in them would still be quite sufficient to dominate the erosive effects of ice flow.

A variety of empirical evidence supports these theoretically based conclusions. These include measured glaciofluvial sediment loads that are nine times the ice load (Hagen and others, 1983) and substantial glaciofluvial incision through bedrock (Sharp, 1947) at rates of millimeters to meters per year (Goldthwait, 1974; Vivian, 1975). Where channelized, subglacial water can become the dominant erosive agent, particularly in the lower reaches of an ice sheet.

### IMPLICATIONS FOR DEVELOPMENT OF GLACIATED LANDSCAPES

Landscapes characteristic of subglacial fluvial erosion will develop and evolve throughout periods of glacial occupation. Such an evolutionary progression has been characterized by Coates and Kirkland (1974) for landforms in the Appalachian Plateau. They observe there a variety of notches, cols, and valleys across drainage divides that suggest progressive enhancement of these forms through repeated episodes of glacial and glaciofluvial activity.

Single channels, given a particularly favorable combination of water flux, occupation time, and bedrock resistance, may become dominant troughs across the landscape. These "through valleys" are sufficiently wide to experience significant ice flow as well as water flow. The trough south of Gold Bar (Figure 3.6) expresses well both the morphology and the geomorphic requirements of such a feature. Exploitation of this valley was by the total drainage of submarginal water from north of the Skykomish River. Diversion into this passage was forced by the west-projecting spur over which it crosses (Figure 3.7) and the margin-ward ice-surface slope in this region (Figure 3.8). Moraines on the northwest wall of the trough and a morainal embankment on its east side (at Proctor Creek) demonstrate that ice has actively occupied and probably eroded this channel as well.

Channelway networks should also evolve through time. Local spatial variations in certain landforms in the Puget Lowland may reflect such a temporal development. Narrow, isolated channels de-

veloped high on bedrock ridges in the uplands east of the Snoqualmie valley contrast distinctly with the well-developed networks present at lower altitudes (e.g., Figure 3.5). These lower topographic positions, generally corresponding to better-developed channelways, should experience longer periods of ice occupancy and thus more extensive subglacial activity. A similar pattern of bedrock degradation just south of Sultan (Figure 3.3) is graphically shown by Plate I. Erosion of such landforms in the path of one or more ice sheets clearly does not result in uniform lowering of the ground surface. Instead, channels are exploited by the localized erosive effects of subglacial meltwater until they transect and behead these spurs. In favorable localities, rates of channel development can far outstrip rates of overall denudation by ice erosion. The resultant channelized topography characterizes those regions dominated by subglacial fluvial erosion in glaciated landscapes.





Plate I. View looking southwest over the area of Figure 3.3. Ice limit lies roughly two-thirds up the main ridge sloping up to the left. Subglacial meltwater channels have dissected this ridge, leaving a characteristic topography of isolated, non-streamlined hills.

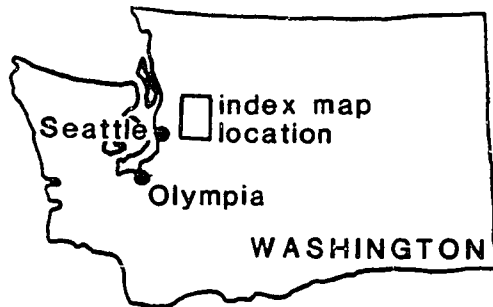
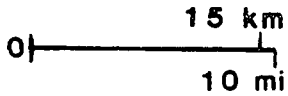
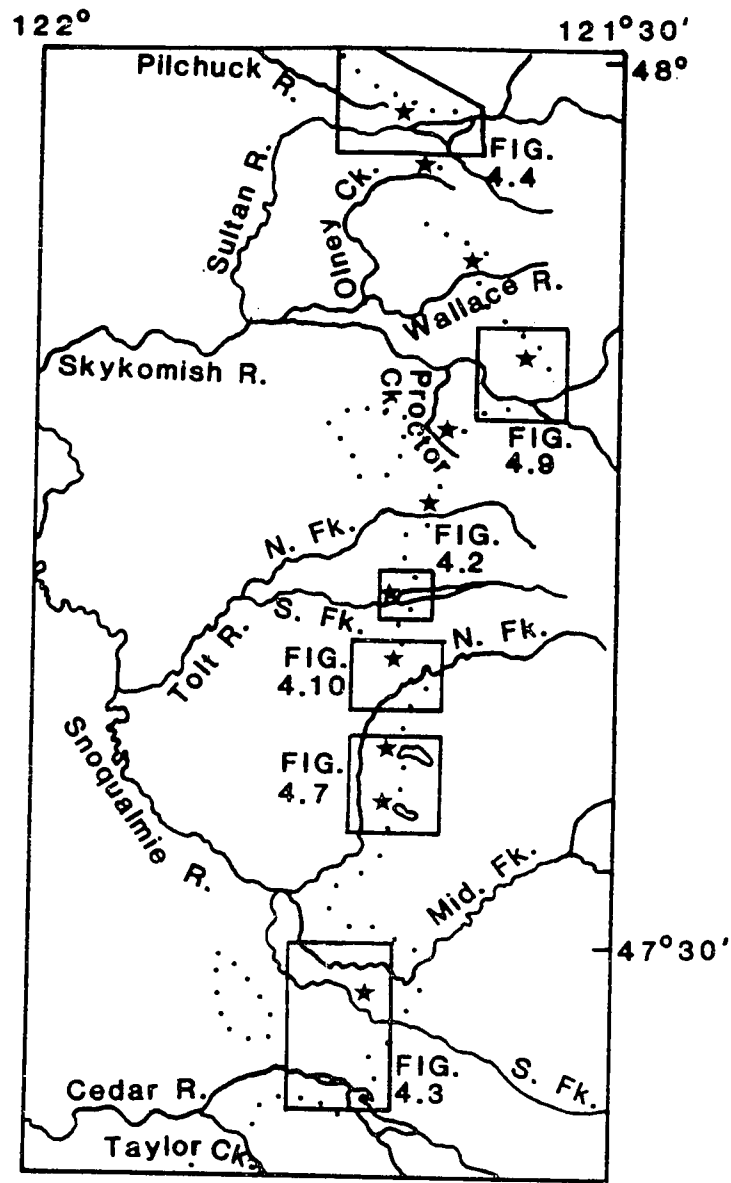
**CHAPTER 4**  
**MORAINAL EMBANKMENTS OF THE EASTERN PUGET LOWLAND**

**INTRODUCTION**

A striking characteristic of the topography along the western slopes of the Cascade Range is the presence of constrictions in river valleys as they pass from their bedrock-walled alpine reaches out into the Puget Lowland. These constrictions are best-developed in western Washington in the Skykomish-Snoqualmie region (Figure 4.1). They do not reflect underlying bedrock topography, but rather are composed of glacial, fluvial, and lacustrine sediment deposited as a distinct embankment. All lie near the outermost margin of the Late-Pleistocene ice sheet that occupied the Puget Lowland most recently about 14,000 years ago (Chapter 1) during the Vashon Stade of the Fraser Glaciation (Armstrong and others, 1965). A slightly earlier advance of alpine glaciers that originated in the Cascade Range is inferred to have climaxed before the time of Vashon maximum (Cary and Carlston, 1937; Williams, 1971; Porter, 1976). Alpine valleys, at least in their lower reaches, were ice-free during much or all of the time that the Puget lobe occupied the Lowland during the Fraser Glaciation.

Eleven valley-constricting deposits can be recognized in this area. They are here referred to as "morainal embankments", following Mackin's (1941) terminology and to avoid genetic implications beyond their glacially related origin. Although a few early workers believed these embankments were deposited by alpine ice flowing down-

Figure 4.1. Index map of geographical localities. Embankments are marked with stars, Vashon-age ice limit with small dots.



valley, most studies of morphology and lithologic provenance have demonstrated that the debris was derived from the Puget lobe (Cary and Carlston, 1937; Mackin, 1941; Knoll, 1967; Williams, 1971; Hirsch, 1972).

Although they have long been recognized, no model has been proposed for formation of these morainal embankments that satisfactorily explains both their ubiquitous location at valley mouths and the variety of sediments encountered within them. Such a model must not merely acknowledge the presence of ice. It must also characterize the physical behavior of ice and depositional processes active wherever the ice margin abutted extensive lakes that filled these ice-dammed alpine valleys (cf. Shaw, 1982). Hypothesized processes of subaqueous deposition adjacent to Pleistocene ice sheets have received considerable recent attention at several other localities found in eastern North America (e.g., Dreimanis, 1982; Eyles and Eyles, 1983). The Puget-Lowland embankments, however, provide a unique opportunity to study these processes in a region where lake geometry, drainage routes, and configuration of the ice sheet can be particularly well-constrained. This example also provides insight into processes of subaqueous glacial deposition that are partially or completely inaccessible in modern glacial environments, but which must be active wherever past or present temperate-ice masses terminate in water.

### **FIELDWORK AND ACKNOWLEDGEMENTS**

The field data for this study were collected as part of a regional mapping project for the U. S. Geological Survey (Booth, 1984; Frizzell and others, 1984). I would like to particularly thank Stephen C. Porter and Fred Pessl, Jr., whose well-intentioned skepticism led me to reconsider fully many of the ideas presented here, and Bernard Hallet, Mark E. Shaffer, Rowland W. Tabor, Richard B. Waitt, Jr., Charles F. Raymond, and Garry K. C. Clarke for invaluable discussions concerning this chapter.

### **DESCRIPTION**

The eleven embankments in this area display widely variable proportions of fluvial and glacial sediment. Three examples, treated in detail, exemplify both their similarities and differences. The South Fork Tolt embankment is composed of thin, discontinuous fluvial deposits covering a rounded ridge of glacially derived sediments. The form of the Middle-South Fork Snoqualmie embankment, by contrast, is dominated by a planar surface of fluvial sand and gravel that extends both upvalley and laterally along the mountain front for many kilometers. The third example, the Pilchuck-Sultan embankment, shares several important characteristics of both. It also serves as a particularly useful example because of good exposure and extensive subsurface study.

## SOUTH FORK TOLT EMBANKMENT

The South Fork Tolt embankment occupies an area of about 2 km<sup>2</sup>, forming a broad north-rising ridge with maximum relief of 150 m (Figure 4.2). Fluvial incision and recent excavations have exposed over 100 m of glacial, glaciolacustrine, and glaciofluvial sediments along the east-west axis of the embankment. These sediments can be subdivided into three primary units. The lowest is an oxidized bouldery diamicton, with 5- to 30-cm-thick layers of compact medium-grained sand. Clast lithologies and degree of weathering indicate probable deposition by an ice sheet of pre-Fraser age. Its base is not exposed; its upper surface lies at an altitude of approximately 500 m (1600 ft).

Overlying this deposit is a massive to crudely bedded diamicton, comprising the bulk of the embankment and defining its surface. Clasts are round to subangular, commonly striated, and of mixed lithology. They range in size from small pebbles to 2 m blocks. No clear fabric is apparent in the clast orientation. The deposit differs from typical Puget-lowland lodgement till in having a lower degree of compaction and a higher silt and clay content in the matrix (cf. Dethier and others, 1981). Throughout this material, subhorizontal pebble-poor zones 5 to 20 cm thick extend laterally for several meters. Larger, discontinuous subhorizontal sand layers extending for 1 to 20 m cluster in (though are not limited to) a 20- to 30-m-thick zone in the middle of this unit. Throughout the entire

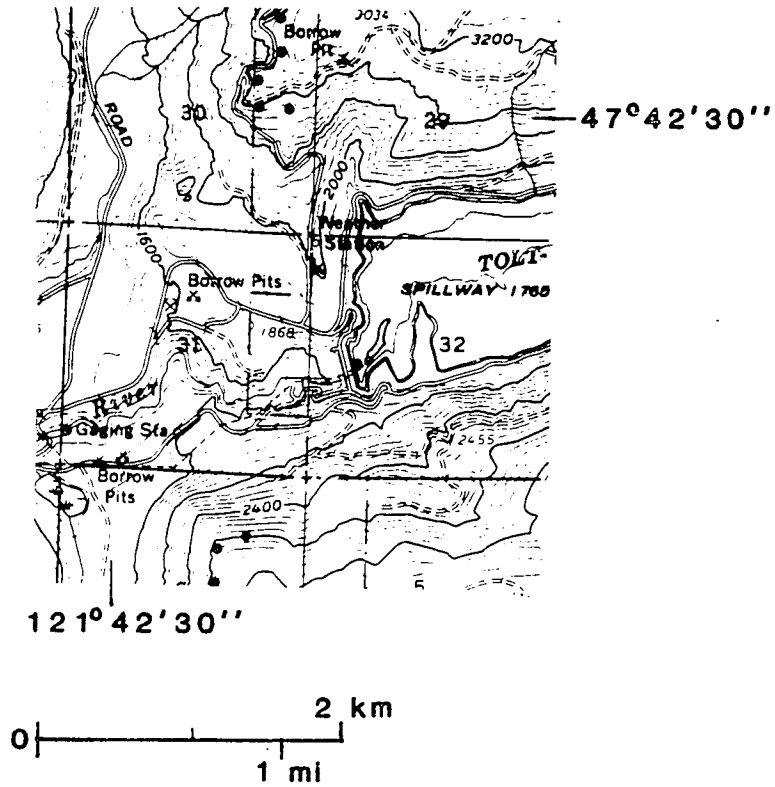


Figure 4.2. South Fork Tolt embankment. Ice-maximum limit shown by black dots; elevation in feet (from Mount Si 15' topographic map).



exposure, horizontal layers with planar contacts preclude any significant deformation of sediment during or following deposition. In one locality near the south dam abutment, silt and clay layers drape and are locally depressed several centimeters by clasts up to 15 cm in diameter.

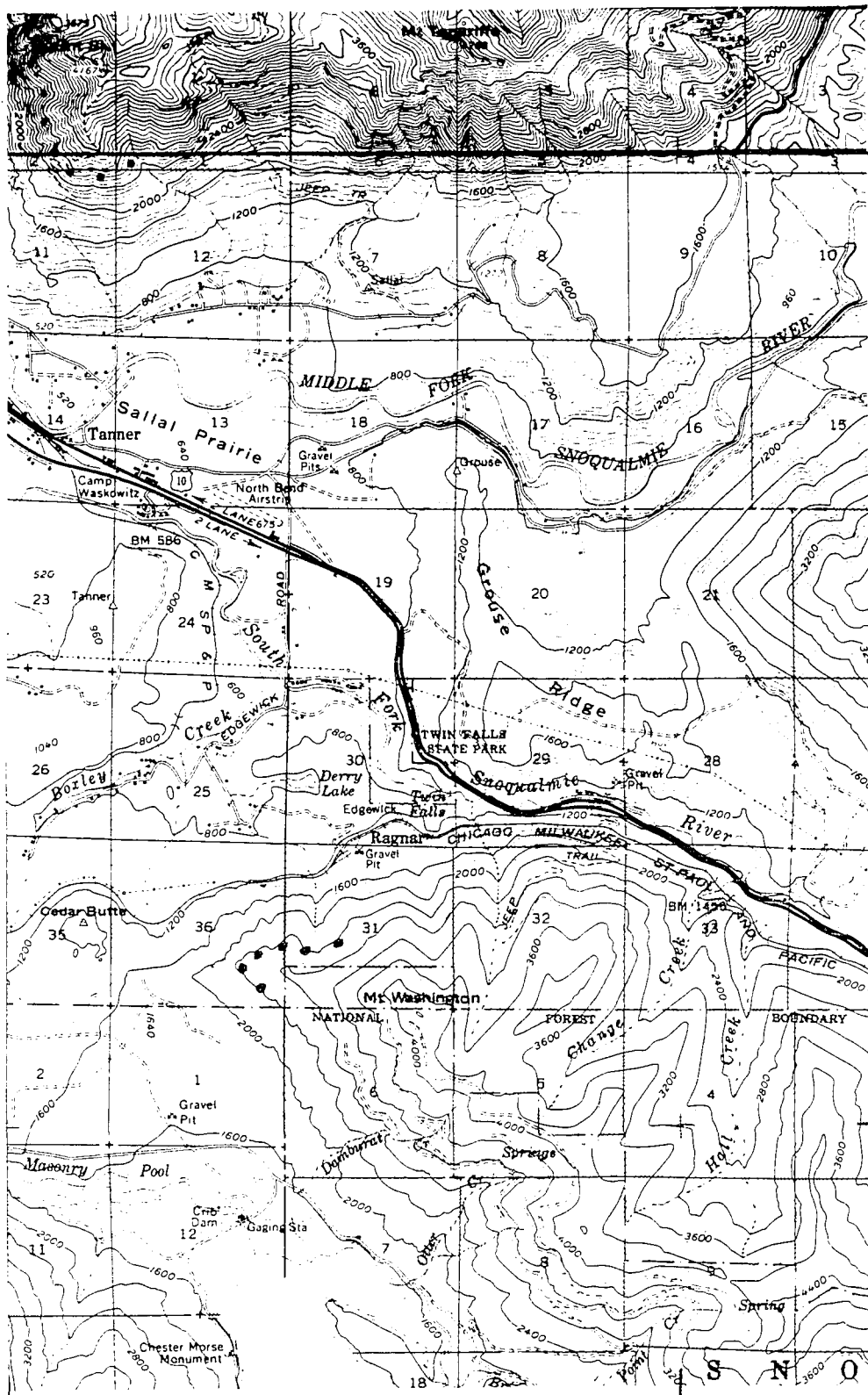
This unit is overlain by a layer of oxidized recessional outwash deposits, generally less than 2 m thick. They drape most of the embankment, and thicken to form a constructional surface only on the lower western (ice-proximal) slopes where they merge with fluvial deposits of the late ice recession in this area (Chapter 1). Sediments comprising the embankment are truncated on its east side, however, suggesting post-glacial erosion of the embankment by the South Fork Tolt River.

## MIDDLE-SOUTH FORK SNOQUALMIE EMBANKMENT

A nearly continuous, flat-surfaced embankment chokes the valley mouths of the Middle and South Forks of the Snoqualmie River (Figure 4.3). It can be traced south for nearly 15 km along the mountain front, blocking the Cedar River valley and terminating at ice-contact sediments at the northeast edge of the Taylor Creek valley (Frizzell and others, 1984). Its surface altitude descends from about 510 m (1670 ft) on the proximal side of the Middle Fork embankment to 500 m (1640 ft) at the South Fork embankment to 475 m (1560 ft) northeast of Taylor Creek (much of this gradient may be due to isostatic rebound; cf. Chapter 1). A classic study by Mackin (1941) of this embankment system characterized it as a set of great fluvial deltas, veneered on their ice-proximal side with till. He believed that they formed at the maximum stand of the Vashon-age ice sheet.

Most of the sediment presently exposed is gravel and sand, subrounded to well-rounded, with better-sorted sand layers and lenses throughout. Median and maximum grain sizes both gradually decrease upvalley, with pebble-poor lacustrine silt deposits predominating beyond about 4 km. The ice-proximal slope of the Middle Fork embankment is characterized by ice-contact topography and moderately to poorly sorted boulder- to cobble-gravel, sand, and silt, and an absence of recognizable lodgement till. A more complex record is revealed at the South Fork embankment, in part perhaps due to more extensive exposure. Exposed on its ice-proximal face just above the highway is a limited area of fine-grained, horizontally bedded sand

Figure 4.3. Middle-South Forks Snoqualmie embankment. Ice-maximum limit shown by black dots; elevation in feet (from Mount Si and Bandera 15' topographic maps).

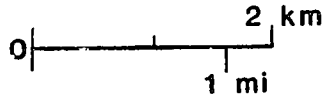


47°  
30'

47°  
25'

121° 45'

121° 40'

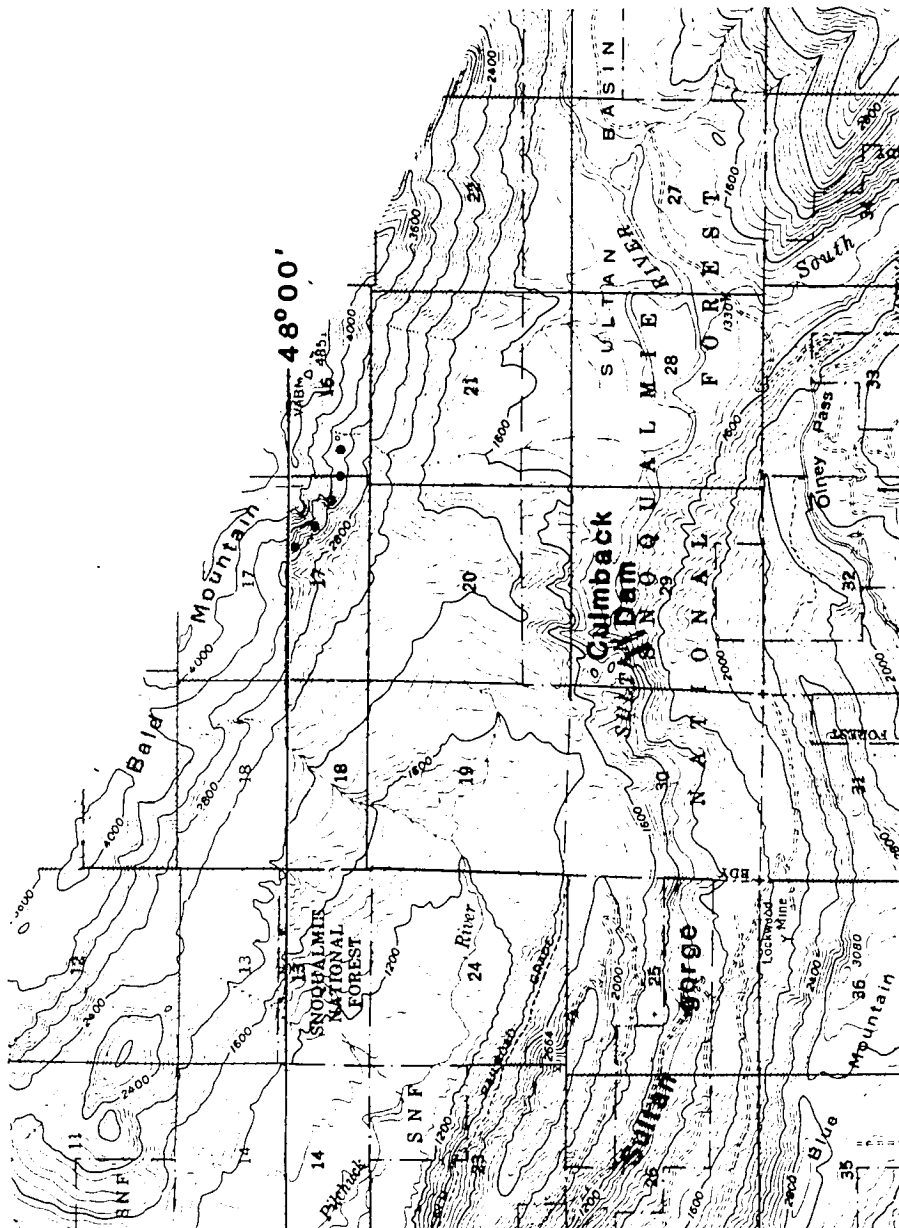


and silt. Wood in these sediments yielded an infinite date (UW-243) (Porter, 1976). Drag folds and faults near the top of the deposit (approximately 300 m, 1000 ft altitude) indicate shearing to the east, presumably by overriding ice (shearing with the same orientation of proglacial fluvial sediments is exposed directly beneath Vashon till 2.6 km northwest of here). Unweathered till, presumably Vashon in age and resting directly on striated bedrock, is only exposed along the river below the older sediment. This till must have been deposited in a valley incised through pre-Vashon debris. The fluvial deposit that forms the upper embankment surface overlies both this till and the older lacustrine sedimentary material, with a thickness of about 200 m in this area.

#### PILCHUCK-SULTAN EMBANKMENT

Deposits comprising the embankment at the head of the Pilchuck River are well-exposed, owing to activity associated with the construction and subsequent raising of adjacent Culmback Dam (Figure 4.4). The lowest sediments, however, are revealed only by multiple drill logs (Converse Ward Davis Dixon, unpublished; Converse Consultants, unpublished). They consist of nearly 200 m of fluvial sand and gravel beneath the present embankment, filling the bottom of the bedrock valley of a pre-Vashon Sultan River. Their upper surface, at an altitude of approximately 420 m (1380 ft), is 30 m above the modern level of the bedrock lip through which the Sultan River now drains into the Sultan gorge. This upper surface may represent a pre-Vashon-age floodplain of the Sultan River, implying that during

Figure 4.4. Pilchuck-Sultan embankment. Ice-maximum limit shown by black dots; elevation in feet (from Index and Silverton 15' topographic maps).



48°00'

121°40'



at least some portion of pre-Vashon time, drainage was also through the Sultan gorge (Mark Shaffer, written commun., 1983).

Overlying these fluvial sediments are 60 to 90 m of pebbly-silty diamicton. The top of this unit lies at about 500 m (1600 ft) altitude in the central and northern portions of the embankment, but is exposed as low as 440 m (1450 ft) near the entrance to the gorge. It is composed primarily of consolidated horizontally bedded silt and very fine-grained sand containing subangular to well-rounded clasts 0.5 to 4 cm in diameter. Portions of this deposit were intermittently exposed at the surface during dam construction (1983). On the south abutment this deposit varies from rather typical Vashon till, massive and stony (clast content roughly 25%), to a poorly sorted deposit containing discontinuous silt layers a 1-2 cm thick and gravel-rich lenses. On the north abutment, clasts consistently comprise less than 5% of this unit. Where present, clasts are subangular to well-rounded, 0.5-4 cm in diameter, and commonly striated. The matrix here consists of fine-grained silt with subhorizontal layers up to 10 cms thick and several meters in lateral extent, defined by faint color changes and slightly coarser texture.

This deposit is covered by bedded gravel and sand that is at least 100 m thick on the northern portion of the embankment. These fluvial sediments form a near-continuous kame terrace that begins at a bedrock notch on the north wall of the Pilchuck valley, continues upvalley as a feature only a few tens of meters wide, and broadens abruptly at the embankment itself. Its gradient is approximately 12



m/km (65 ft/mi).

This embankment has been extensively modified by postglacial erosion. Sand and gravel of the topmost unit are preserved 2 km southeast of the present embankment form on the south side of the Sultan Basin. They are remnants of recessional outwash deposits that extended upvalley (formerly downglacier) from the terrace capping the embankment surface to the subaerial spillway at Olney Pass (Figure 4.4). The underlying diamicton appears to extend at least 3 km upvalley as well on the north side of the Sultan Basin. The present steep east face of the embankment therefore reflects not an abrupt termination of deposition, but incision by the Sultan River in postglacial time. In contrast, the ice-proximal side of the embankment has an even, more gentle slope. It has been only slightly modified by a mantle of rarely terraced outwash deposits and proglacial lacustrine sediments associated with the final withdrawal of the ice.

## RECONSTRUCTION OF ICE-MARGINAL ENVIRONMENTS

### SEDIMENTOLOGICAL EVIDENCE

The origin of deposits similar to those present as the middle layer of both the South Fork Tolt and Pilchuck-Sultan embankments (and perhaps the stratigraphically lowest exposed unit of the South Fork Snoqualmie embankment) has been discussed by many authors, including Dreimanis (1979), Evenson and others (1977), May (1977), Gibbard (1980), and Eyles and Eyles (1983). Common to all hypotheses is the subaqueous nature of the depositional environment, indicated by stratification and high silt and clay percentages. The fall-out of debris released from the base of melting ice, combined with the settling of fine-grained lacustrine sediments, is compatible with virtually all of the characteristics observed here. In particular, variable debris content in the ice coupled with a more uniform accretion rate of fine-grained suspended sediment will yield an irregular appearance of pebble-poor lenses. Currents associated with water flow into or out of the lake beneath the damming ice would result in better-stratified and sorted coarse-grained layers. The consistent absence of flow features rules out significant deposition by subaqueous flowtill (Evenson and others, 1977). The lack of overconsolidation or traction structures near the top of most of these deposits imply that the ice may have only rarely grounded against these sediments (Gibbard, 1980; Eyles and others, 1982; Shaw, 1982).

## ICE-WATER INTERACTION AT THE ICE MARGIN

Although the sedimentological evidence specifies the existence of a lacustrine environment adjacent to the ice sheet, these data alone offer little insight into either the probable character of this glaciolacustrine environment or the configuration of the ice-sheet margin. This acknowledged deficiency in previous studies elsewhere (e.g., Eyles and Eyles, 1983) can be corrected by analyzing the theoretical interaction of ice and water along a glacier margin. From this analysis we can not only define this environment more precisely, but also determine why embankments formed almost exclusively at valley mouths, why they are ubiquitous in this region, and whether they represent climatically induced stillstands of the ice margin.

### Ice Limits

The maximum extent of ice into each alpine valley is not well-expressed by glacial erosion or erratics on their steep sidewalls. However, good data from the adjacent interfluves (Map 1) show that at maximum, ice stood from 100 to over 600 m above the present embankment surface, and in some cases nearly 700 m above the inferred Vashon-age valley floor (Table 4.1). Embankment altitudes bear no systematic relationship to adjacent ice-maximum altitudes, and thus represent neither the position of maximum ice advance (Mackin, 1941; Knoll, 1967) nor a synchronous halt of the ice front during retreat.

Table 4.1. Present-day upper altitude of deposit, inferred glacial-age valley-floor altitude, and reconstructed ice surface altitude for each embankment in this region. Evidence for valley-floor altitude includes the top of bedrock or pre-Fraser material (minimum altitude) and the base of recessional or postglacial deposits (maximum altitude). The best estimate assumes a reasonable concave-up valley profile and is probably accurate in all cases to within 50 m. Reconstructed ice-surface altitudes are from Figure 3.8. The embankment height is the difference between the embankment altitude and the best valley altitude; the ice thickness is the difference between the ice altitude and the embankment altitude. Note the wide variation in this final column, eliminating the possibility that a single ice-sheet stillstand is responsible for these features.

	Embankment altitude (m)	Valley altitude (m)			Embankment height (m)	Maximum ice altitude (m)	Ice thickness (m)
		min	max	best			
Pilchuck- Sultan	680	390	410	390	270	1060	380
Olney	510	370	510	490	20	1050	640
Wallace	800	590	610	590	210	980	180
Skykomish	540	140	160	150	390	860	320
Proctor	760	490	630	580	180	910	150
North Fork Tolt	550	430	460	450	100	880	330
South Fork Tolt	610	500	540	500	90	860	250
North Fork Snoqualmie	600	270	490	390	210	850	250
Calligan Lake	710	550	680	590	120	840	130
Lake Hancock	700	550	660	610	90	830	130
Middle- South Forks Snoqualmie	490	230	360	270	220	780	290

### Marginal Lakes and Subglacial Hydrology

As the Cordilleran ice sheet filled the Puget lowland and advanced to the Cascade Range front, it impounded lakes in the lower reaches of the west-draining alpine valleys (Cary and Carlston, 1937; Mackin, 1941; Knoll, 1967; Williams, 1971; Porter, 1976). Such marginal lakes are commonly observed in modern glacial environments (Stone, 1963; Post and Mayo, 1971). Drainage out of these lakes occurs either via subaerial spillways or beneath the damming ice.

The maximum surface altitude of any such lake equals the maximum hydraulic potential that its drainage route must cross (Nye, 1976). For subaerial drainage, this potential is simply the altitude of the spillway. For subglacial drainage paths the hydraulic potential has two components: the bed elevation of the channel and the pressure of the overlying ice (Chapter 3; Shreve, 1972). They are analogous to the elevation head and pressure head common in groundwater terminology.

The hydraulic potential, or total head, at any point on the glacier bed is expressed as an elevation by equation 3.1, ignoring any dynamic component due to sliding of the ice (chapter 3):

$$H = z_b + (\rho_i/\rho_w)h, \quad (4.1)$$

where  $H$  = the hydraulic potential,  
 $z_b$  = bed elevation,  
 $\rho_i$  = ice density,  
 $\rho_w$  = water density, and  
 $h$  = the thickness of the ice.

$H$  equals the elevation to which water would rise in a borehole that penetrates the glacier to its bed. Any change in  $H$  is primarily

determined by the altitude of the ice surface (Shreve, in press). Equivalent variations in bed altitudes exert an influence only one-eleventh as great.

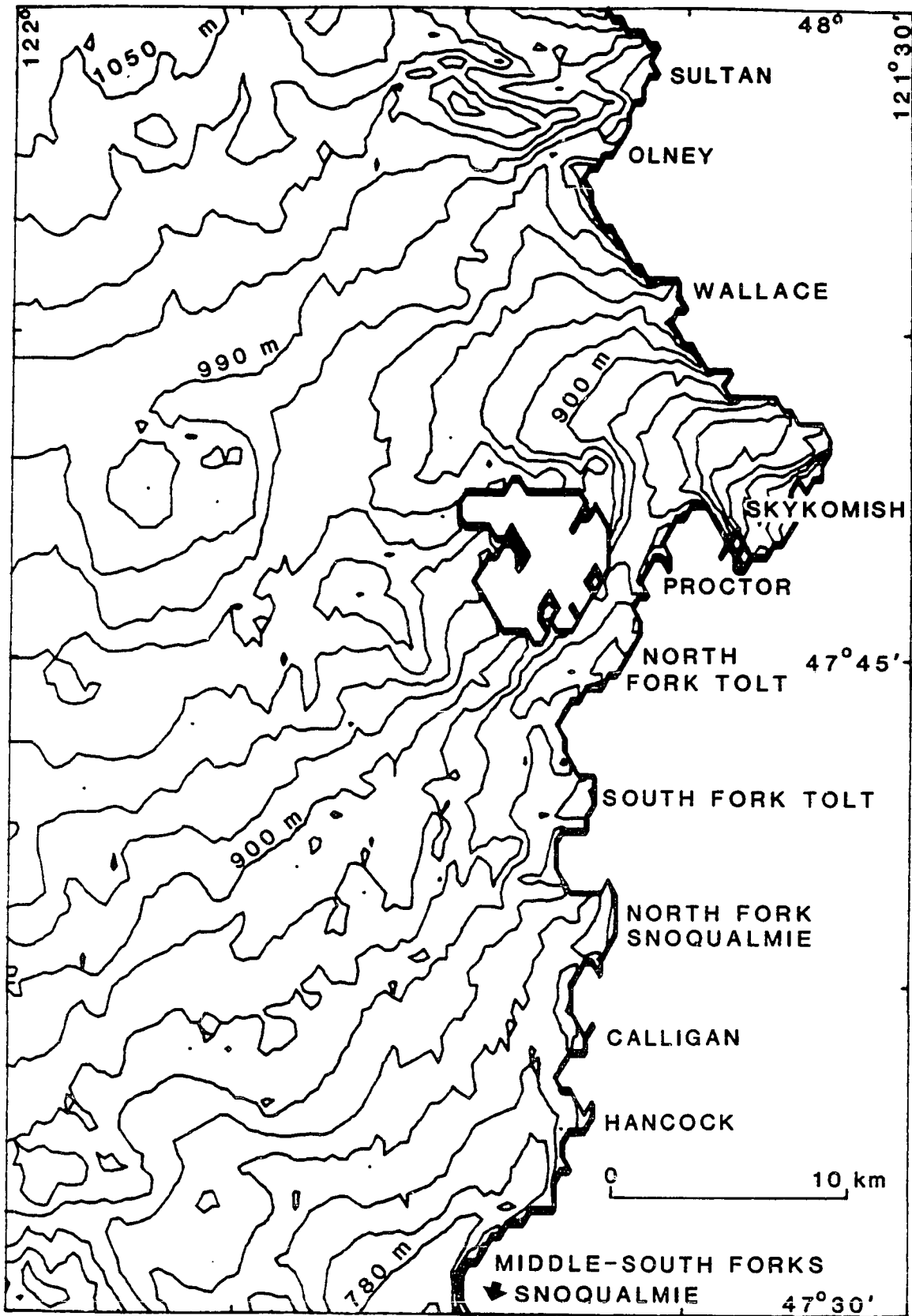
The hydraulic potential beneath ice that extends into alpine valleys thus increases upglacier (in the direction of greater ice-surface altitudes) even though the valley floor descends in this direction. Any potential route of subglacial drainage thus experiences steadily rising hydraulic potentials. As it passes out of the valley into the (ice-covered) lowland, however, water flowing along the glacier bed can turn in a direction of decreasing ice-surface elevation (generally southward in this area) (Figure 4.5). From this point onward, the hydraulic potential decreases monotonically. A maximum value is therefore defined for the potential, which must be exceeded in order to drain the water impounded in the valley. Its location defines the position of an effective spillway for the lake.

Where lake drainage is subglacial and an effective spillway is present some distance upglacier from the snout, some ice between the spillway and margin should begin to float as lake elevation approaches the value of the spillway potential. Such lacustrine ice shelves have been observed in some areas (Nye, 1976; Stone, 1963; Post and Mayo, 1971, lakes no. 6 and 27; Sturm and Benson, unpublished), but are apparently absent or poorly developed in most others (e.g., Holdsworth, 1973; Bindshadler and Rasmussen (1983) note the absence of modern temperate ice shelves in marine environments).

An ice shelf will always tend to advance because its unsupported

Figure 4.5. Subglacial hydraulic equipotentials calculated as described in Chapter 3 (contour interval 15 m).





portion above water level exerts a longitudinal stress greater than the water pressure acting on the submerged ice face (Weertman, 1957; Thomas, 1973). The shelf thickness necessary for appreciable strain rates is observed in Antarctica to be 150-300 m (Robin, 1979; Thomas, 1979). This value was exceeded in most of the major alpine valleys during the Vashon-age ice advance and maximum (Table 4.1).

Water flow into a marginal lake will eventually raise the water surface altitude to equal the spillway potential. If the drainage is subaerial, lake level will stabilize at this point. If drainage is subglacial, a more complex sequence of events first modelled by Nye (1976) typically results in total or near-total drainage of the lake (Clarke, 1982). Subglacial water flow melts a tunnel, whose rate of expansion due to melting initially exceeds its closure rate due to ice deformation. The hydraulic potential along the tunnel thus loses its component from the ice overburden and drops precipitously to equal the bed altitude. Drainage should now proceed catastrophically as a jokulhlaup until lake level falls to the altitude of the highest bed spillway along the drainage route ( $z_b$  in equation 4.1), or until ice finally reseals the tunnel during waning flow. Refilling of the lake begins the process anew. Along the margin of the Puget lobe refill times were a few tens of years (Chapter 3), and so this process probably repeated itself numerous times during the Vashon Stade. Such a cycle is exemplified by numerous modern ice-dammed lakes as well (e.g., Stone, 1963; Post and Mayo, 1971; Mottershead and Collins, 1976).

As alternate, subaerial drainage routes out of the Cascade valleys are absent, each ice-dammed lake in this region would have experienced episodic drainage during some (usually extensive) period of its existence. The absence of incised channels adjacent to each valley at or near the ice-maximum margin also implies a lack of significant marginal drainage (cf. Mackin, 1941). Even at progressively lower ice stands, only in the Sultan River valley would such a path have been uncovered (Olney Pass; see Figure 4.4). The remaining valleys drained subglacially for as long as ice remained at their mouths.

#### A MODEL OF SEDIMENTATION INTO ICE-DAMMED LAKES

##### Processes

The glaciolacustrine environment permits a variety of potential depositional processes to occur (Figure 4.6). These include basal meltout of sediments beneath a floating shelf or bergs, subaqueous flow of till off the glacier snout, fluvial transport of sediments from the glacier directly into a lake, and settlement of suspended lacustrine sediments (variously discussed singly or in combination by Rust and Romanelli, 1975; May, 1977; Evenson and others, 1977; Fecht and Tallman, 1978; Hicock and Dreimanis, 1978; Dreimanis, 1979; Gibbard, 1980; Hillare-Marcel and others, 1981; Orheim and Elverhoi, 1981; Powell, 1981; Dreimanis, 1982; Eyles and Eyles, 1983; Vorren and others, 1983). These processes are not mutually exclusive; most studies have recognized their close association in even single exposures. The rates and predominant sites of sedimentation, however,

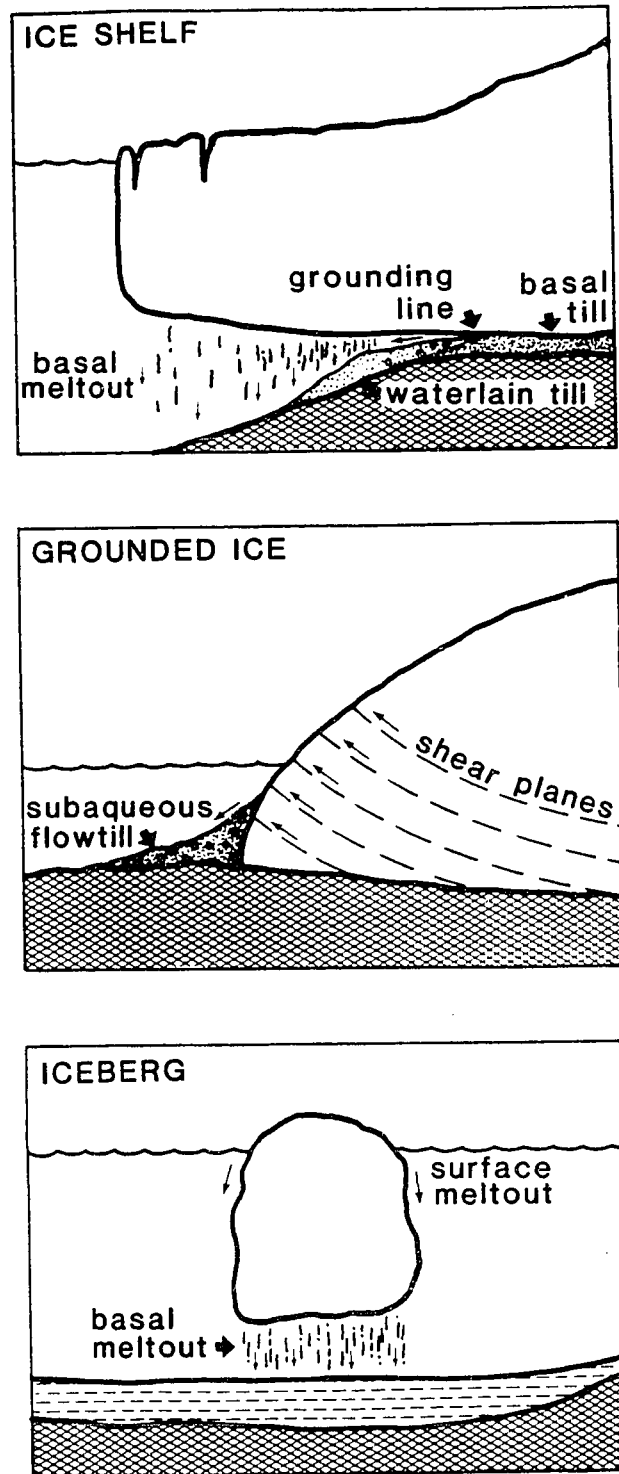


Figure 4.6. Possible ice-termini configurations and depositional processes in glaciolacustrine environments (adapted from Vorren and others, 1983).

may differ for each process.

Sedimentation by most processes will be concentrated at the grounding line (Orheim and Elverhoi, 1981), because the glacier is the primary source of sediment. The load carried by non-glacial streams is generally trivial. Deposition, particularly of coarse particles, will therefore be concentrated adjacent to the ice (Edwards, 1978). Except in the presence of localized fast currents near the ice margin, this should control the distribution of all but the finest sediment as well (Eyles and Eyles, 1983). The resulting deposit should tend to form shoals or ridges immediately beneath the ice at the grounding line. This has been repeatedly observed or inferred beneath modern glaciers and ice shelves (Holdsworth, 1973; Barnett and Holdsworth, 1974; Rust and Romanelli, 1975; Edwards, 1978; Hillaire-Marcel and others, 1981; Carl Benson, oral commun., 1983).

Alternative processes that distribute sediment over a wider area are likely to be ineffective in a confined ice-marginal lake. Because the debris content of ice is highest at its base (Pessl and Frederick, 1981), basal melting will yield the greatest volume of sediment near the grounding line regardless of how far ice ultimately floats or extends into the basin (cf. Anderson and others, 1980). Furthermore, rafting by icebergs is restricted to those months when the lake surface is unfrozen (Holdsworth, 1973). Flowtill released from the leading edge of an extensive ice shelf will be similarly constrained in volume and geographic extent. Any basal melting

occurring during the remainder of the year (Robin, 1979) will continue to release sediments near the grounding line.

Sudden lowering of lake level during a period of episodic drainage would clearly render an ice shelf unstable, and hasten its break-up into bergs (e.g. Post and Mayo, 1971, lake no. 5 photo). Slower refilling of the lake would have a similar, though less-pronounced effect (Holdsworth, 1973; Barnett and Holdsworth, 1974). Such changes in ice configuration upvalley from the grounding line, however, should not significantly affect the general decrease in sedimentation with distance from the grounding line.

#### Location and Stability of the Grounding Line

As the site of maximum subaqueous sedimentation rates, the grounding line controls the pattern of deposition. Formation of a discrete embankment requires that ice terminates against standing water and maintains a relatively stable grounding line for a considerable time (Rust and Romanelli, 1975). A stable grounding line requires, either singly or in combination,

- 1) a long-term climatically determined stillstand of the ice margin, coupled with either a fixed lake level or one that never rises high enough to float a portion of the ice,
- 2) presence of a pre-existing topographic rise or shoal,
- 3) resistance to ice advance by confining topography, or
- 4) a relationship between lake level and ice thickness.

### Ice-Margin Stillstands

In the Puget Lowland, this first alternative appears implausible (Chapter 1; Thorson, 1980). Limiting radiocarbon dates on the Vashon Stade from the central lowland (Rigg and Gould, 1957; Mullineaux and others, 1965) require rapid average advance and retreat rates of about 100 m/a throughout the glaciation. A single stillstand at or near ice maximum (Mackin, 1941) cannot explain the formation of these embankments (Table 4.1). Moreover, evidence in the lowland is utterly lacking for eleven such halts (Map 1).

### Pre-existing Shoals

Given the ubiquitous presence of Vashon-age embankments, pre-existing valley blockades at the arrival of the Vashon ice sheet might be expected from the record of multiple glaciations in the lowland (Armstrong and others, 1965). Older glacial sediments are indeed observed at the core of several of these embankments. This explanation, however, merely displaces back in time the question of why deposition is localized here. It is also inapplicable for those embankments where deep exposures or drill cores reveal no such material.

The effect of shoals may nevertheless become important during the formation of a new embankment. Once sediment begins accumulating, the growth of an incipient embankment will tend to stabilize the grounding line (Post, 1975) and further localize deposition there.

### Topographic Effects

The predominance of embankments at valley mouths empirically demonstrates the importance of the valley-wall configuration. Its most simple consequence is to induce a pause in ice-front advance. As an ice tongue advances into a valley, it must thicken and steepen at the valley entrance to compensate for the added lateral drag (Nye, 1965). The convergent upvalley geometry typical of most valleys amplifies this effect (Mercer, 1961; Funder, 1972). If the valley is perched above the lowland, such as those shown in Figure 4.7, this pause will last even longer while ice thickens at the valley mouth.

### Interrelationship of Water Depth and Ice Thickness

Although the preceding factors can stabilize an ice margin under certain special conditions, they cannot account for deposition of all embankments present here. I propose a model in which ice and water interact in such a way as to form embankments whose characteristics are consistent with those actually observed.

As thickening ice seals subaerial drainage routes out of the basin, rising water complicates these simple factors. Continued deepening of the water, unavoidable in a blocked basin supplied by both runoff and glacier meltwater, must eventually float the snout prior to (or simultaneous with) drainage. The location of the grounding line is then a function of the depth of impounded water and the hydraulic potential at the bed. At the point where these two values are equal, the ice floats. The exact extent and configuration of the



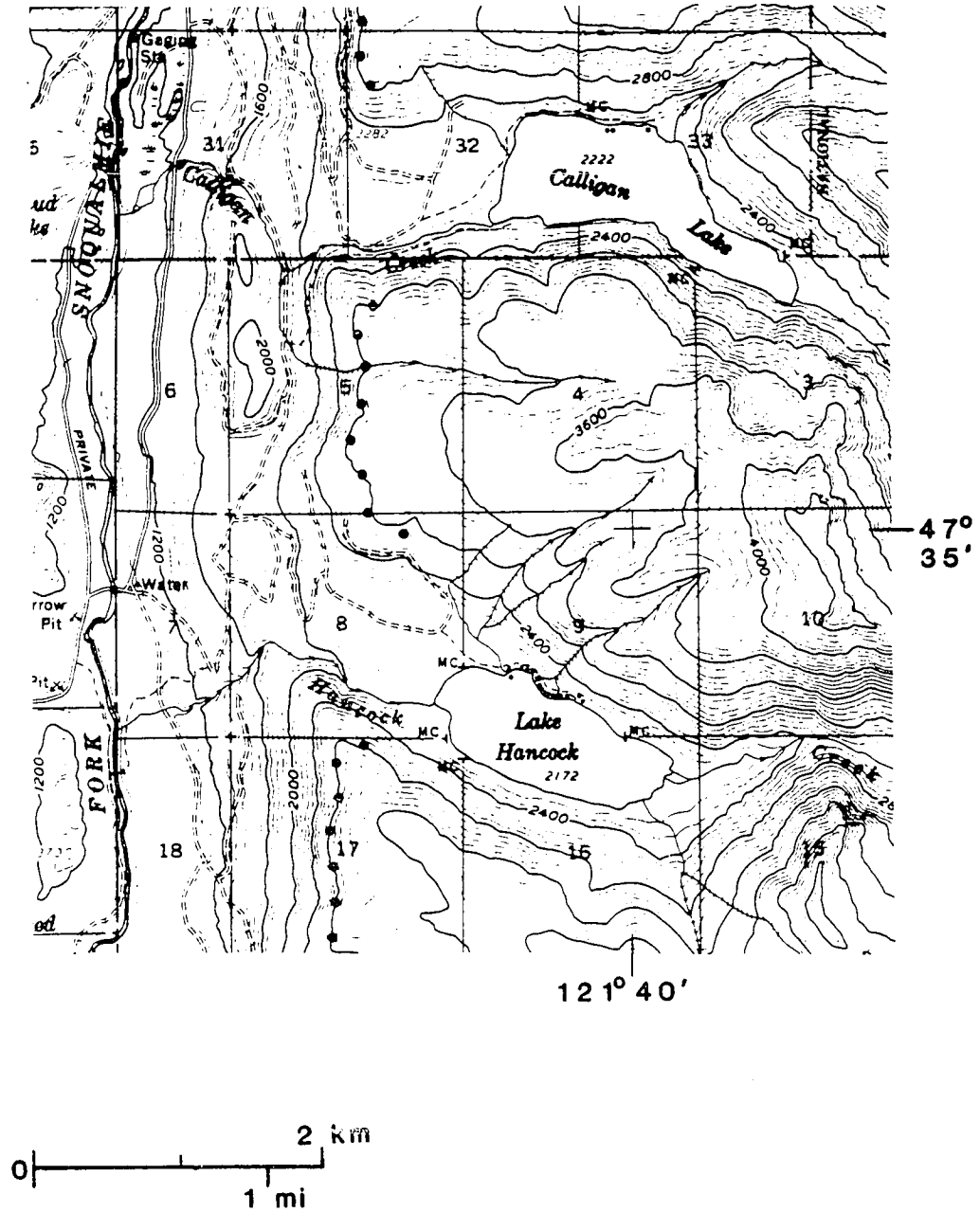


Figure 4.7. Calligan and Hancock embankments. Ice-maximum limit shown by black dots; elevation in feet (from Mount Si 15' topographic map).

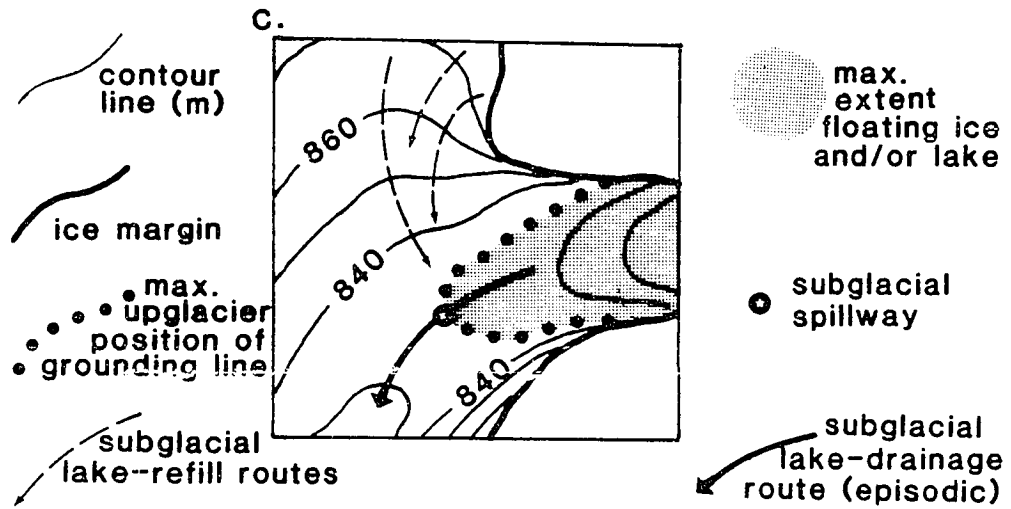
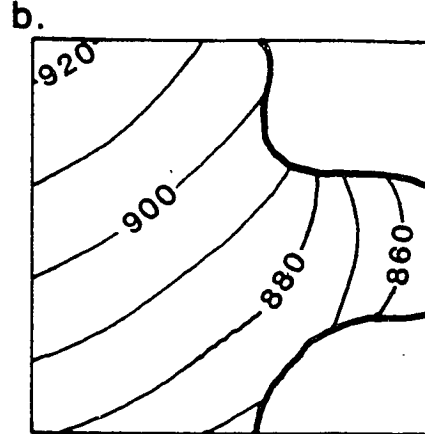
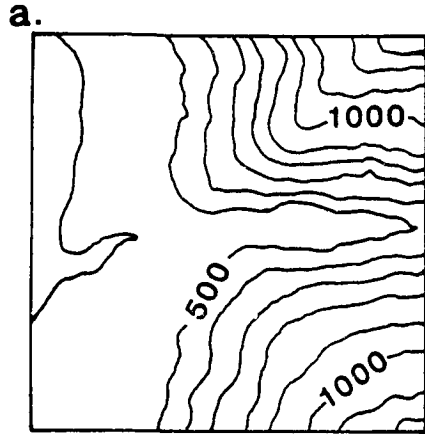
lake ice is irrelevant, for although the ice front will advance as a shelf if it is sufficiently thick (Weertman, 1974; Sanderson, 1979), the location of the grounding line does not depend on the position of the ice front.

Rising water can float ever-increasing thicknesses of ice, causing upglacier migration of the grounding line. As lake level approaches the hydraulic potential of the subglacial spillway and drainage is imminent, the grounding line lies across the ice tongue just downglacier from the spillway (Figure 4.8). Subsequent drainage may allow the grounding line to migrate upvalley some distance, but repeated cycles of deposition during lake filling will tend to stabilize the ice front. This is partially due to the effect both of shoals (Post, 1975) and of the shape of natural reservoirs. Water level rises most slowly, and so grounding-line position changes most gradually, when these lakes are nearly filled to their maximum depth. Thus the grounding line will remain longest at positions closest to that of the spillway, and tend to stabilize at this location through continued sedimentation there.

Lake spillways along this portion of the ice sheet are located in the lowland immediately below the mouth of each valley (Figure 4.8; see also Figure 4.5). This geometry maximizes subaqueous deposition rates at the valley mouths and explains the ubiquitous presence of embankments in this position. These spillway locations for all of the lakes are quite insensitive to changes in the ice thickness. The potential-gradient direction is determined primarily by

Figure 4.8. Reconstruction of subglacial water-flow paths and spillway in a hypothetical ice-dammed valley.

- a. Subglacial bed topography; contour interval 100 m.
- b. Ice-surface topography; contour interval 10 m.
- c. Subglacial hydraulic equipotentials, contour interval 10 m. Grounding line for a given lake level defined by the position of equipotential contour whose value equals the lake-surface altitude. The maximum lake altitude will be determined by the potential of the subglacial spillway. Deposition of embankment sediments occurs in the shaded area, at greatest rates near to the maximum upglacier grounding-line position. Note gradient of the hydraulic potential adjacent to ice margin on the steep sideslopes; extensive marginal drainage not possible in these areas.



the ice-surface slope, and so subglacial spillways will be located near to valley mouths under any appreciable thickness of ice. Deposition during advance, maximum, and retreat stages therefore will be all at the same location.

Only the Sultan River, in draining out the Sultan gorge, has a spillway that is not in the Lowland proper. The embankment in this valley also occupies an atypical position. As predicted by this analysis, the embankment location in the main Pilchuck-Sultan valley is at the point where the subglacial potential there equals the potential of the spillway (located in the Sultan gorge; Figure 4.5).

#### Other Models

This model is similar to that invoked by Hillaire-Marcel and others (1981) for formation of "re-equilibration moraines," localized deposits at ice-water margins during uniform retreat of the eastern Laurentide ice sheet. Their model implicitly assumes sedimentation only during periods when the ice is fully grounded against shallow water, with neither a floating nor an actively calving margin. The processes that actively contribute sediments to this environment, however, will be active at the grounding line regardless of the configuration of the ice farther downglacier. Behavior of the ice during advance and retreat stages will also not radically affect the processes active in the local subaqueous environment. Lake levels will be higher during maximum stands of the ice, but drainage routes and subglacial spillway locations depend only weakly on the absolute

thickness of ice. Thus their model's acknowledged difficulty (p. 212) in explaining massive volumes of sediment, hypothesized to accumulate only during the relatively few years that the ice front actually terminates at a specific locality, is illusory.

Other settings proposed for deposition of fluvial and ice-contact sediment are clearly not applicable to these embankments. Deltaic sedimentation into a proglacial lake, described by Orombelli and Gnaccolini (1978), lack a significant subaqueous component because water depth was controlled by a subaerial spillway at an altitude too low to float the ice. Other generalized ice-contact lacustrine environments are described by Koteff (1974), all with the spillway distinct from the damming ice. The location of deposition in such cases is therefore determined by the position of the ice front itself during temporary stillstands and not by a grounding line that is fixed by the pattern of subglacial hydraulic potentials and resultant subglacial spillways.

## CONTROLS ON EMBANKMENT MORPHOLOGY

The total thickness of waterlain sediments depends primarily on the rate of sedimentation and the length of time that lakes were impounded by ice. This volume of supplied sediment was the limiting factor here, as the theoretical upper limit on sediment accumulation is fixed by the maximum altitude of the ice. In all cases the actual embankment height is significantly below this value (Table 4.1). Neither occupation time nor sediment flux are well-constrained for the Vashon ice advance. Sedimentation rates calculated for mid-continent lakes during deglaciation (about 5 mm/a; Johnson, 1980) are too slow to account for the many tens of meters of sediment that accumulated during a fraction of the 1500-year occupancy of Vashon ice. Observed rates adjacent to modern tidewater glaciers, however, are up to several meters per year (Powell, 1981).

As the ice thinned over and eventually retreated behind the waterlain embankments, deposition of subaqueous till gave way to more fluvially dominated processes. Variability in local environments has led to significant differences in the relative amounts of capping fluvial debris transported and deposited by water flowing subaerially. This material is most prominent on the Middle-South Fork Snoqualmie and Skykomish embankments (Figures 4.3 and 4.9). The uppermost sediment on both are part of extensive recessional outwash deposits well-graded with respect to valley-train deposits or subaerial spillways (Frizzell and others, 1984; Chapter 1, this report). Their sediment was derived from the eastern portion of the retreating

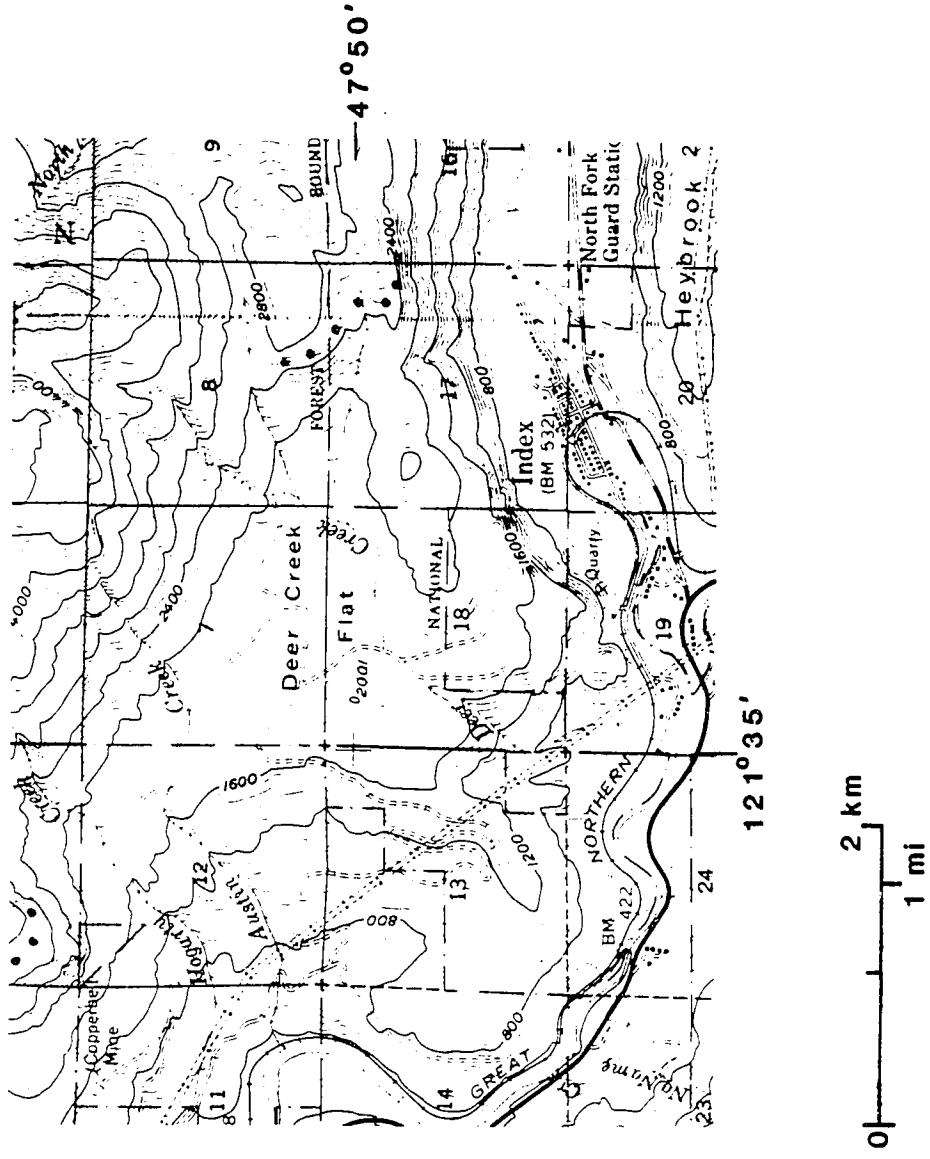


Figure 4.9. Skykomish embankment (Deer Creek Flat). Ice-maximum limit shown by black dots; elevation in feet (from Index 15' topographic map).



ice sheet (Mackin, 1941). These two drainages received a tremendous flux of sediment because each lies immediately upglacier (north) of major bedrock highs that projected west as nunataks during ice maximum. These spurs diverted out to the ice-sheet margin a large percentage of the downglacier-travelling meltwater and entrained sediment collected upglacier. Any subaqueously deposited sediment in these two embankments has been completely covered or eroded during deposition of hundreds of meters of younger fluvial sediment.

Mackin's inferred veneer of till (1941, Fig. 4) on the proximal side of the Snoqualmie embankment may in fact be the remnants of such a core.

Most of the other embankments show more localized covers of recessional outwash. During ice retreat, local marginal drainage and debris brought up at the edge of the active ice (Koteff and Pessl, 1981) would have temporarily supplied sediment to these areas. However, most meltwater was efficiently diverted through the recessional marginal drainage channels off to the south and southwest, away from the smaller embankments (Anderson, 1965; Knoll, 1967; Chapter 1, this report). In some instances this late-recessional meltwater probably truncated ice-proximal portions of those embankments that extended into the lowland (such as the North Fork Snoqualmie embankment, Figure 4.10).

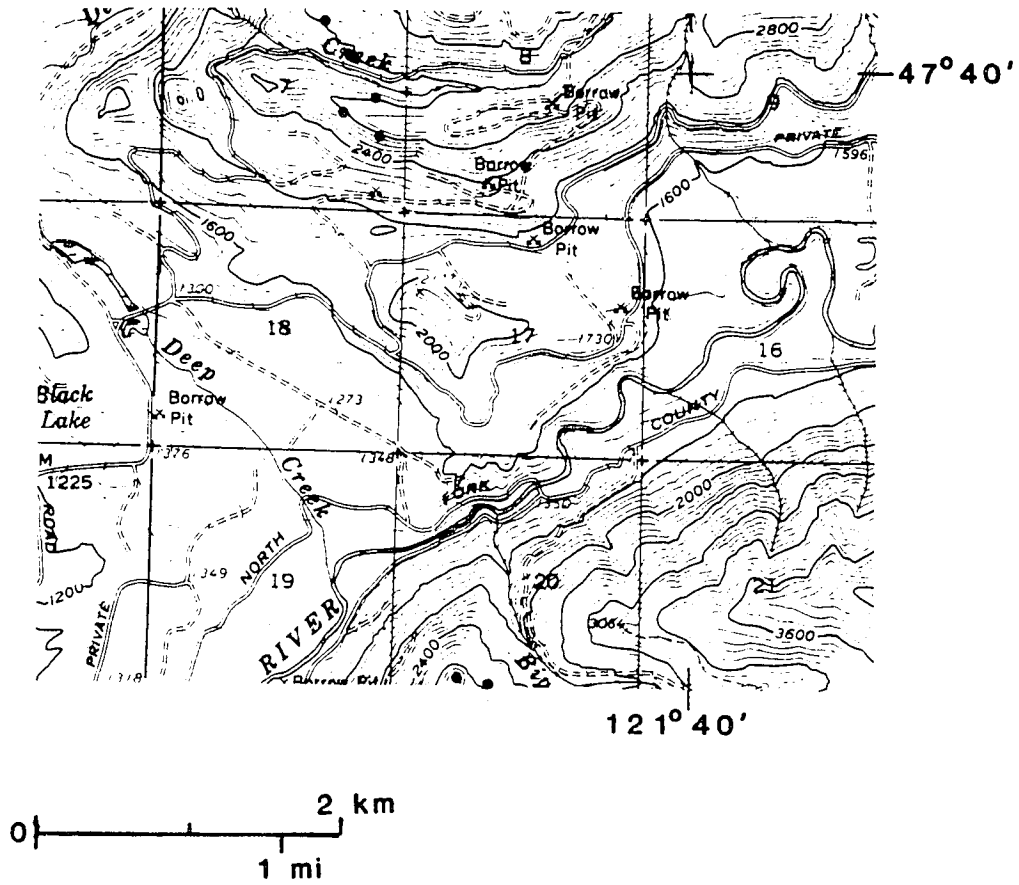


Figure 4.10. North Fork Snoqualmie embankment. Ice-maximum limit shown by black dots; elevation in feet (from Mount Si 15' topographic map).

### CONCLUSION

A set of eleven morainal embankments along the eastern margin of the Puget Lowland provides excellent opportunities to study the processes of glacial sedimentation in ice-dammed lakes. Sedimentary characteristics define a variety of active depositional environments, but only by analyzing the physical behavior of ice and water can deposition of the resulting sediments be understood. Because highest sedimentation rates occur preferentially near the grounding line, the formation of discrete embankments require a stable grounding-line position. This stability is determined by the valley configuration and the interaction of the glacier and lake, not by climatic control of the ice position. The final surface form of each embankment may reflect only late-stage and post-glacial fluvial deposition and not be representative of the variety or duration of processes that have occurred in this environment. Although focused on a particular geographic region, the analysis presented here should be applicable to any locality where modern or Pleistocene glaciers have terminated against ice-dammed water bodies.

**CHAPTER 5**  
**BASAL CONDITIONS BENEATH RAPIDLY SLIDING ICE SHEETS**

**INTRODUCTION**

Basal till is the most ubiquitous of glacial deposits, and yet the physical processes involved in its emplacement are poorly understood. Despite hypothesized categories of till deposition (e.g., Dreimanis, 1976; Lawson, 1981), insufficient effort has been made to characterize the physical conditions carefully at the glacier bed where this deposition occurs. The Puget Lowland of western Washington, occupied by a lobe of the Late-Pleistocene Cordilleran ice sheet, provides an excellent opportunity to better define this environment. Basal till is widespread and well-exposed (Crandell, 1963; Mullineaux, 1970; Chapter 1, this report), sliding velocities can be inferred (Chapter 2), and the presence of basal water is well-documented (Chapter 3). Quantitative reconstruction of the basal environment suggests a simple yet widely applicable model of till deposition with important implications for the characterization of the marginal and interior zones of a glacier, shearing of till, and the overconsolidation of subglacial sediments.

**GENERAL CONDITIONS AT THE GLACIER BED**

**BASAL ICE VELOCITIES**

At the base of a temperate glacier, ice flow has two components that are significant in determining the transport and lodgment of clasts. The first is the sliding velocity, which varies from a few meters to many hundreds of meters per year on modern glaciers

(Paterson, 1981). For the Puget-lobe ice sheet this velocity is calculated to have averaged several hundred meters per year (Chapter 2). The second is the velocity normal to the bed, whose spatial average is due to basal melting primarily from geothermal heating and viscous dissipation from sliding (Rothlisberger, 1968). These rates equal a few centimeters per year, except for high localized values due to regelation melting on stoss surfaces of small-scale bed irregularities.

#### FORCES ON CLASTS ENTRAINED IN BASAL ICE

##### Effective Contact Force on Entrained Clasts

The total normal force applied to clasts in contact with the substrate, but still partly surrounded by ice, can be divided into two distinct components. One is the force resulting from the hydrostatic stress, a consequence of both the fluid nature of ice itself and the availability of pressurized water to fill any ice-free cavity. The static downward force on the upper side of the clast is exactly balanced by an upward force on its lower side, save the buoyant weight of the clast itself. Boulton's (1974) analysis of this physical setting includes the total overburden as a component of the net normal force on a clast. This ignores, however, the nearly hydrostatic condition at the glacier bed (cf. J. Weertman's discussion in Boulton, 1979, p. 38) and results in a physically questionable model.

Vertical ice flow introduces a second, dynamic component that

contributes significantly to the effective contact force between clast and bed. The magnitude of this force scales directly with the vertical flow velocity. For all but the largest (greater than 1 m) clasts this component will greatly exceed the buoyant weight (Hallet, 1979).

#### Till Deposition beneath Rapidly Sliding Ice

By most definitions, lodgment till is deposited when clasts become stationary because their frictional drag against the bed (e.g., Lawson's (1981) "tractional impairment") exceeds the force urging the clast forward. In his analysis of isolated clasts on a rock substrate, Hallet (1979, 1981) showed clast motion ceases only if the forward ice velocity is of the same order or smaller than the normal ice velocity (because friction coefficients are of order 0.5-0.9). Where ice is sliding many times faster than it melts at the base, bare rock surfaces should be swept clean and no lodgment should occur.

Continued meltout of entrained debris, however, will lead to the accumulation of unconsolidated sediments in a growing layer at the base of the ice (Nobles and Weertman, 1971). Compressive longitudinal strain of the glacier in its ablation zone should not significantly reduce this downward transport except very close to the terminus (Figure 5.1). As accumulation proceeds individual clasts are no longer completely surrounded by ice, thereby reducing the dynamic force inducing downglacier motion and rendering the model of Hallet (1979) inapplicable. An indeterminate portion of this layer

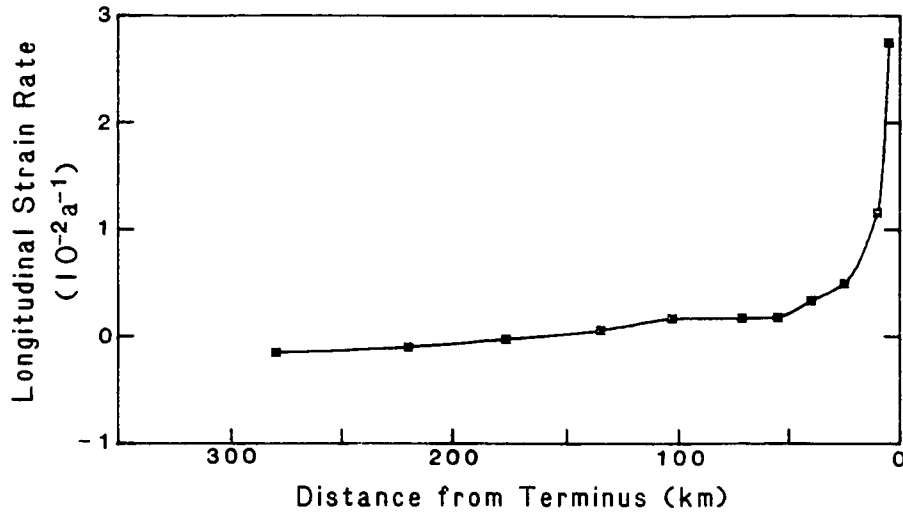


Figure 5.1. Longitudinal strain rate as a function of position, based on the velocity reconstruction of Chapter 2. The basal one meter of ice would thicken at a rate approaching that of melting at its base only within a few kilometers of the terminus.

of accumulating sediments may still be effectively coupled to or sheared by the sliding glacier (Boulton, 1979, Fig. 7), depending on the presence of pore ice and the frictional strength of the substrate (cf. Dreimanis's (1976) "deformation till"). However, widespread examples of undeformed till in central North America (Kemmis, 1981) and the presence of undisrupted layers of well-sorted granular sediment exposed within lodgment till (Eyles and others, 1982; Chapter 1, this study) demonstrate that the deformation of buried sediments commonly is localized and ceases while still beneath active ice. "Lodgement" still implies frictional resistance (strength) in excess of the tractional force (shearing), but this process is not restricted to the upper surface of the glacier bed and is the only physically plausible means of till deposition beneath rapidly sliding ice.

Although accumulation of basal sediments depends only on basal melting of debris-laden ice, the rate of till deposition may be influenced by certain parameters not explicitly addressed by this model. Numerous authors have related continent-scale patterns of erosion and deposition to the basal thermal regime, with varying degrees of success (Boulton and others, 1977; Sugden, 1978; Gordon, 1979; Moran and others, 1980). As the depositional process discussed here is obviously applicable to warm-based glaciers, it should be relevant to the interior of ice sheets even if they have a cold-based margin (Hooke, 1977).

A second parameter that must influence deposition rates is the



net supply of sediment, reflected in the entrainment of sediment and the debris concentration of the ice. Measured debris contents of temperate ice (e.g., compilation of available data (15 examples) by Essl and Frederick, 1981) are equivalent to a layer of ice-free sediment on the order of 0.1 to 1 m thick. Continuous replenishment of this debris by erosion and entrainment is required because observed till deposits are typically much thicker than a fraction of a meter. Numerous studies (e.g., Shilts, 1973; Dreimanis, 1976; Whillans, 1978) have emphasized the short (a few km) transport distances of this sediment. Till deposits will therefore reflect the local supply, as the volume of far-travelled sediment is insufficient to obscure local variations. Thin or absent till deposits can indicate conditions not conducive to the entrainment and transport of sediment rather than an unfavorable depositional environment.

#### Effective Normal Stresses

Effective normal stresses in subglacial sediments, as inferred by measured overconsolidation (Aario, 1971; Boulton, 1976; Mickelson and others, 1979; Laprade, 1983), are generally low relative to the total ice overburden. This condition has significant implications for the behavior of the substrate. Shear strength,  $S$ , is typically modeled as

$$S = C + (\sigma_n') \tan \phi,$$

where  $C$  = cohesion,

$\sigma_n'$  = effective normal stress = overburden - pore pressure,  
and  $\phi$  = angle of internal friction.

Shearing of sediments should occur wherever the basal shear stress applied by the glacier (approximately 100 kPa) exceeds  $S$ . Such deformation has been theorized (Boulton and Jones, 1979), observed (Boulton, 1979) down to a depth of about a meter, and inferred from geologic evidence (MacClintock and Dreimanis, 1964; Ramsden and Westgate, 1971; Boulton and others, 1974; Kruger, 1979; Stone and Koteff, 1979). Because the intrinsic sediment properties ( $C$  and  $\phi$ ) vary over a limited range ( $C \approx 0$  and  $\tan \phi = 0.5 \pm 0.1$ ), these low strengths must reflect effective normal stresses that are only a small fraction of the maximum total overburden (up to ca. 10 MPa for thick ice sheets).

#### HIGH EXCESS PORE PRESSURES AT THE GLACIER BED

Low effective normal stress under thick ice obviously requires high pore water pressure in the subglacial sediments. Boulton and others (1974) and Boulton and Jones (1979) both recognized and addressed this necessity analytically. Their models, however, combine into a single, complex equation the effects of meltwater production, overburden, and substrate permeability. They implicitly assume that all water flows through the subglacial sediments to the terminus without assessing the effect of drainage through subglacial tunnels and channels. They are further limited by requiring constant overburden loads and water-production rates and hence cannot treat situations involving transient loading (Mathews and Mackay, 1960).

The analysis can be simplified and rendered more flexible by using general solutions for the generation of pore pressures in

excess of hydrostatic (Bredehoeft and Hanshaw, 1968; Hanshaw and Bredehoeft, 1968). They approach a variety of geologic problems by utilizing the mathematical analogy between the flow of groundwater and the conduction of heat, for which a wide array of analytical solutions are available (Carslaw and Jaeger, 1959). The thermal properties of a conducting medium, conductivity and heat capacity, are analogous to the hydraulic properties of the aquifer, namely its permeability ( $k$ , defined as the proportionality factor between discharge and gradient in Darcy's Law) and its specific storage ( $S_s$ ). This value is defined as the volume of water expelled per unit volume of soil per unit change in effective stress, and depends on the elastic properties of both soil and water. Solutions to the appropriate heat-conduction problem (e.g., Carslaw and Jaeger, 1959) are then directly applicable to groundwater flow and the generation of excess pore pressure. Two sources of excess pore pressure, transient loading and steady-state meltwater production into a low-permeability layer, are potentially important in glacial environments.

#### TRANSIENT EXCESS PORE PRESSURES

Rapid loading of saturated sediments generates excess pore pressures that initially approach the overburden pressure and then dissipate through time. The dissipation of this pore pressure as a function of time is solved by assuming a single till layer of thickness  $z$  (where  $z \ll$  lateral extent) overlying an aquifer that

drains perfectly (e.g., till over proglacial sand and gravel). The load is applied instantaneously at time  $t = 0$ . At the upper till surface, excess pore pressures that nearly equal the applied load are maintained for:

$$t > z^2 S_s / 9k_t \quad (\text{Bredehoeft and Hanshaw, 1968, Fig. 2}).$$

An example demonstrates the rapid dissipation of high pore pressures in all but thick sedimentary layers of very low permeability. Using values of  $k_t$  ( $1 \times 10^{-8}$  m sec $^{-1}$ ) for the silty till most commonly found in the Puget Lowland (Olmstead, 1969), plausible values for  $S_s$  ( $1 \times 10^{-4}$  m $^{-1}$ ) (Domenico and Mifflin, 1965), and a typical till thickness of 5 m (Mullineaux, 1970),

$$t > 8 \text{ hours.} \quad (5.2)$$

Variability in soil properties may introduce an uncertainty of one or two orders of magnitude, but dissipation times will still be less than about a month. The sensitivity of the dissipation time to variations in the drainage-path length ( $z$ ), however, can have more significant consequences. Where the underlying aquifer offers additional flow resistance from discontinuities or gaps, the effective length of this path greatly increases. Puget-Lowland till, for example, is found overlying not only proglacial sand and gravel but also lacustrine silt and clay or bedrock (Chapter 1). Similar variability is likely throughout other glaciated areas. These situations, though localized, could easily lower drainage rates of pressurized pore water by over an order of magnitude.

The width of the zone affected by transient loading will

scale with the velocity of the advancing ice edge as well as by the properties of the substrate. For the Puget-lobe ice sheet this effect is short-lived (equation 5.2), and so sliding rates of a few hundred meters per year (Chapter 2) would affect only a narrow zone. Under surging glaciers, or wherever drainage is impeded, a far wider marginal area should experience low effective normal stresses from transient loading.

## STEADY-STATE EXCESS PORE PRESSURES

### Basic Analysis

Beneath the interior of a glacier, advance or retreat of the margin does not rapidly change the overburden load. In this region, elevated pore pressures can only result from the rapid steady-state production of basal meltwater. The rate of melting expected beneath an extensive temperate ice sheet can be shown to generate very high pore pressures in subglacial sediments. At the bed, water enters the till layer at a rate  $q_0$  (flux per unit area) and drains into a continuous sub-till layer of high (but finite) permeability  $k_s$ . It assumes that meltwater enters this sub-till layer along its entire length ( $x$ , where  $x = 0$  is the terminus and  $x = L$  is the length of the ice sheet). At the terminus of the glacier, the pore pressure is assumed to equal zero. The total (horizontal) flux per unit width through this layer is therefore the product of  $q_0$  and  $L-x$ , and the flux per unit area is  $q_0(L-x)/d$ , where  $d$  is the thickness of the sub-till layer. By integrating Darcy's Law ( $q = k \cdot dH/dx$ ), and applying

the boundary condition at  $x = 0$ ,

$$(q_0/dk_s)(Lx-x^2/2) = H.$$

Using values of each parameter appropriate to the Puget lobe (Olmstead, 1969, with permeabilities variable within an order of magnitude; Rothlisberger, 1968; Mullineaux, 1970; Thorson, 1980; Chapter 1; Chapter 2) of  $k_s = 1 \times 10^{-4}$  m/sec,  $d = 5$  m,  $L = 300$  km, and  $q_0 = 5$  cm/a, calculated values of  $H$  greatly exceed the overburden pressure for all  $x > 0$ . This result indicates that beneath such ice sheets much of the drainage of both surface and basal meltwater must be via subglacial tunnels. Reducing  $q_0$  to the rate due to geothermal heating alone does not significantly alter this conclusion. Only by reducing the total length of the ice sheet ( $L$ ) by an order of magnitude or more can the total basal-meltwater flux be accommodated by subglacial percolation. Beneath such limited glaciers, a complex representation of sediment permeabilities (e.g., Boulton and others, 1974) may be potentially useful.

#### Effect of Subglacial Tunnels

Subglacial drainage must therefore include alternate flow paths such as channels at the glacier bed (Stenborg, 1968; Shreve, 1972; Walder and Hallet, 1979). If these channel pressures are low relative to the overburden, they will effectively reduce predicted pore pressures in subglacial sediments. Lliboutry (1983) argues that such channels beneath valley glaciers will not be completely filled with water throughout most of the year. He argues that sensible heat may be supplied by entering groundwater together with heat released

through viscous dissipation melts open a tunnel more rapidly than ice flows in to replace it. Where these conditions are met, channels will remain unfilled and at atmospheric (i.e. zero) pressure. They would provide an efficient low-resistance alternative to drainage routes through subglacial sediments to the glacier margin.

Beneath a thick ice sheet, however, this effect is severely attenuated. Figure 5.2, calculated from Lliboutry (1983, equation 20), shows the pressure reduction in tunnels (relative to their static pressure) beneath 1000-m and 500-m thick ice for a range of water discharges and groundwater temperatures. The pressure reduction due solely to viscous dissipation of potential energy in the flowing water is represented by the curve  $T = 0$ . Sensible heat from groundwater leads to a significant reduction in the tunnel pressure only in those tunnels carrying low discharges only. Under no plausible circumstances beneath thick, extensive ice sheets, where groundwater should be well-buffered to a fraction of a degree of the freezing point, are tunnels substantially depressurized relative to the surrounding substrate. The calculation for 500-m thick ice yields the same fundamental conclusion.

Within a few kms of the margin of an ice sheet, tunnels may drain and remain open following the melt season (Mathews, 1964; Lliboutry, 1983). Their pressurization is therefore a transient and cyclic phenomenon with a recurrence interval of approximately nine months. Each change in the tunnel pressure propagates through the surrounding sediment with a transient effect that decays through

time. The time required to establish steady-state pressures can be calculated by analogy to the temperature change in an infinite cylinder (as a function of time and radius) with a central conduit fixed at temperature = 0 (Carslaw and Jeager, 1959, p. 207, eqn. 15). Using till properties of  $k = 1 \times 10^{-8}$  m/sec and  $S_s = 1 \times 10^{-4}$  m<sup>-1</sup>, steady-state conditions at a distance equal to four tunnel radii are reached after only a few hours. Thus wherever tunnels are depressurized relative to the overburden for a major portion of the year, migration of groundwater to them should rapidly lower pore pressures in the full thickness of subglacial sediments. The reduction in tunnel pressure, illustrated for relatively thick ice in Figure 5.2, becomes progressively more pronounced beneath thinner ice. Combining the Gauckler-Manning formula (Clarke, 1982, eqn. 5) with Shreve's equation for the pressure reduction in tunnels (1972, eqn. 2), yields:

$$p = -3.7(0.56Q/(dh/dx)^{0.5})^{.076}, \quad (5.4)$$

where  $Q$  = discharge through tunnel, and  
 $dh/dx$  = ice-surface slope.

For plausible maximum values of the discharge near the terminus (up to  $10^4$  m<sup>3</sup>/sec; Chapter 2), tunnel pressures will be 60-70 kPa lower than the overburden.

## GEOLOGICAL CONSEQUENCES

### CHARACTERIZATION OF INTERIOR AND MARGINAL ZONES

The rate and mechanism of till deposition will vary as the controlling physical parameters change at the glacier bed. Such



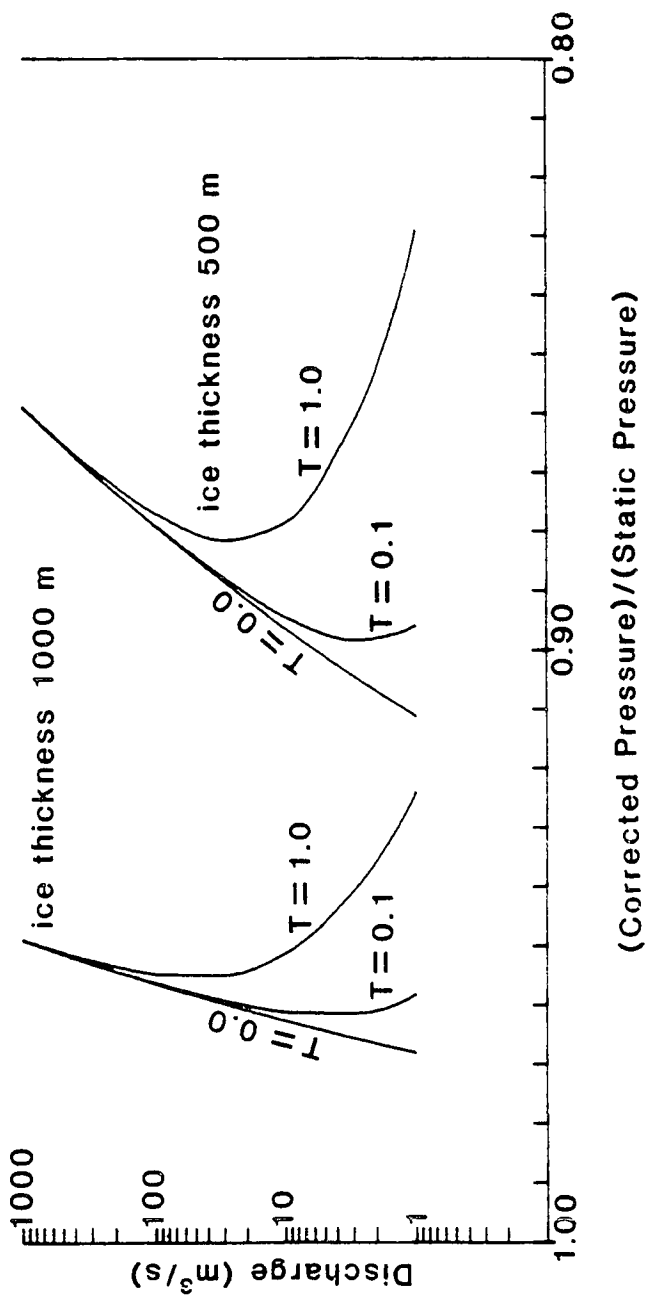


Figure 5.2. Water pressure in tunnels. The static pressure assumes that (water pressure) = (ice pressure), whereas the corrected pressure accounts for the effects of viscous dissipation and water temperature above freezing (0C) (Lliboutry, 1983, eqn. 20).

One thousand m<sup>3</sup>/s exceeds the predicted average discharge of the Puget lobe at the equilibrium line (Chapter 2) and could be carried by a single tunnel of approximately 10-m radius (Clarke, 1982, eqn. 5).

changes can occur spatially, under different parts of the glacier at a given moment, or temporally, in particular as the glacier progresses through advancing and retreating stages. An intuitive division has often been suggested between the "interior" and "margin" (e.g., Smalley and Unwin, 1968; Mickelson and others, 1979). An actual length scale can be calculated, however, over which parameters controlling lodgment should vary. This can lead to a more useful and precise definition of the marginal region of a glacier.

Within the interior zone, water derived from basal melting alone is ample to produce pore pressures approaching the overburden load. Because required melt rates are only a small fraction of those expected for sliding temperate glaciers, pore pressures should closely approximate the total normal stress for a wide range of sliding rates, substrate permeabilities, and basal position relative to channels and tunnels. Thus, effective normal stresses and till strengths are both expected to be uniformly low.

Towards the glacier margins this situation changes. Total normal stress, equal to the overburden, decreases as the glacier thins. The pore pressure in the substrate, however, becomes a complex function of not only total distance to the ice margin but also the nature and proximity of the local drainage routes. Reduced distance to the margin also introduces more significant spatial variability in pore pressure due to local differences in the thickness and permeability of the subglacial sediments. Within a few kms of the margin, pressures in subglacial tunnels will drop substan-

tially below the overburden pressure. Elevated pore pressures in subglacial sediments should therefore dissipate rapidly.

These various factors probably result in an overall reduction in pore pressure towards the ice margin, superposed on an unpredictable variability reflecting the proximity of subglacial channels and the distribution, thickness, and hydraulic properties of subglacial sediments. The total normal stress, in contrast, reduces monotonically beneath the thinning ice. Changes in effective normal stress (= total normal stress - pore pressure) and till strength should therefore be unpredictable as well, despite some overconsolidation data suggesting a more regular pattern (Harrison, 1958; cf. Boulton, 1976). Although the theoretical maximum of this parameter decreases to zero at the position of the ice-maximum terminus, the actual values typically follow no simple function of either ice thickness or distance from the edge of the glacier (Aartio, 1971; Boulton, 1976; Laprade, 1983).

The transition from consistently low effective normal stresses to a more variable and unpredictable regime defines a physically significant boundary between the interior and marginal zones of a glacier. The approximate distance of this boundary from the ice edge is suggested by the distance at which tunnel pressure diverges significantly from the overburden increasing the effective normal stress at the bed. By this proposed definition, the marginal zone of the glacier is on the order of 5-10 km. This represents less than 3% of the total length of the Puget lobe and the ice mass that fed it

from the mountains of British Columbia.

Within the marginal zone effective normal stresses are likely to vary and perhaps locally approach a significant fraction of the total overburden load. Till strength will follow suit, potentially forming the nuclei hypothesized by Boulton (1979) and Menzies (1979) for drumlin initiation. Upglacier of this marginal region the relatively small rate of meltwater production required for low effective stresses should swamp other sources of variability, leaving the bulk of the glacially-covered terrane under nearly uniform conditions. The consequences of this uniformity should include the low strength of till, its homogeneity over hundreds of square kilometers (Karrow, 1976), and the potential for widespread shearing and redistribution of subglacial sediment.

#### BASAL CONDITIONS DURING ADVANCE AND RETREAT

Deposition of till during a particular portion of the advance/retreat cycle has been inferred by many authors at particular localities (e.g., Goldthwait, 1958, 1974; Mickelson, 1973; Whillans, 1978). These inferences have been hampered by the lack of any systematic characterization of basal conditions, whose temporal variation may influence the rate or mechanism of till deposition. Any such variation is predicted (by equation 5.4) only for the marginal area. The process of till accretion in the interior region by basal meltout is dominated by the effects of low effective stresses and the obvious insensitivity of sliding velocities, shear

stresses, and overburden loads to short-term motion of the ice terminus.

Within the marginal zone, several characteristics of the advance stage relative to retreat can be expected. Sliding velocities at the margin will obviously be higher. Proglacial sediments that are not preconsolidated will be more available for incorporation or redistribution by the ice. Rapid overriding of this material may also result in a zone of temporarily elevated pore pressures near to the advancing ice edge (Mathews and Mackay, 1960). The permeability of these overridden sediments, however, should be highest during advance, as they will not yet have been blanketed by basal till. The ice front should be steeper (Barnham, 1974), resulting in greater total normal stress at any given distance from the edge of the ice.

These variables in combination do not exert an entirely consistent effect on predicted processes of till deposition and deformation. Lower effective stresses should result during advance from transient loading by the ice. Large-scale shearing in the sediments (Clayton and Moran, 1974) is most likely during this time, given higher pore pressures (which may be further aided by drainage-impeding permafrost), higher shear stresses, and a relatively unconfined substrate. Higher effective stresses, however, may also result during advance from both thicker ice and drainage unimpeded by a layer of low-permeability till (relevant only close to the margin; cf. equation 5.4). These differences therefore do not imply that stages of glaciation should universally correlate with particular

characteristics of till or processes of till deposition. They instead emphasize that in the marginal zone, generally unpredictable local variability in sediment properties and drainage characteristics should dominate large-scale changes in sliding velocity and basal stresses.

The non-uniform basal conditions probable in the marginal zone will retreat along with the edge of a wasting glacier. They will eventually affect every portion of the till surface now exposed for geological investigation. Observed characteristics of till, such as rarely reported patterns of increasing overconsolidation values in subglacial sediments (Harrison, 1958; Kazi and Knill, 1969) and size sorting (Humlum, 1981), may therefore reflect only the variable conditions of the ice-marginal zone.

### CONCLUSION

Basal melting beneath temperate ice sheets will generate subglacial pore pressures that approach the overburden load over nearly all of the glacier bed. Drainage is occluded almost exclusively by virtue of the horizontal distance glacially-derived groundwater must travel to reach the edge of the ice. Low-pressure tunnels provide an alternative drainage route, but are expected only within a few kms of the terminus. In the interior, tunnel pressure will approach the ice overburden. Spatial variability in the hydraulic properties of subglacial sediments and the existence of subglacial channels will significantly affect pore pressures only within a few kms of the ice margin.

The inferred geologic consequences of this predicted distribution of pore pressure varies between interior and marginal zones. In the interior, pore pressures should uniformly approach the overburden stress. Till, accumulated by the meltout of basal sediments, will have low strength and therefore be susceptible to transport and deformation. Homogeneity (Karrow, 1976) and clast alignment (e.g., MacClintock and Dreimanis, 1964) are both likely consequences of these conditions.

In the marginal zone, variable hydraulic conditions are expected from the local changes in substrate properties and the presence of tunnels. Effective stresses may reach a substantial fraction of the overburden (300-400 kPa), to be recorded as overconsolidation values in now-exposed subglacial sediments. The retreat of this zone should imprint the effect of these more variable conditions on sediments that accumulated under the relatively uniform conditions characteristic of the glacier's interior.

## BIBLIOGRAPHY

- Aario, R., 1971, Consolidation of Finnish sediments by loading ice sheets: Bull. Geol. Soc. Fin., v. 43, p. 55-65.
- Alley, N. F., and Chatwin, S. C., 1979, Late Pleistocene history and geomorphology, southwestern Vancouver Island, British Columbia: Can. J. Earth Sci., v. 16, p. 1645-1657.
- Anderson, C. A., 1965, Surficial geology of the Fall City area, Washington: University of Washington, Department of Geological Sciences, M.S. thesis, 70 p.
- Anderson, J. B., Kurtz, D. D., Domack, E. W., and Balshaw, K. M., 1980, Glacial and glacial marine sediments of the Antarctic continental shelf: J. Geol., v. 88, p. 399-414.
- Andrews, J. T., 1972, Glacier power, mass balance, velocities and erosion potential: Z. Geomorph. N. F., Suppl. Bd. 13, p. 1-17.
- Armstrong, J. E., Crandell, D. R., Easterbrook, D. J., and Noble, J. B., 1965, Late Pleistocene stratigraphy and chronology in southwestern British Columbia and northwestern Washington: Geol. Soc. Am. Bulletin, v. 76, p. 321-330.
- Baker, V. R., 1973, Paleohydrology and sedimentology of Lake Missoula flooding in eastern Washington: Geol. Soc. Am. Spec. Paper 144, 79 p.
- Barnett, D. M., and Holdsworth, G., 1974, Origin, morphology, and chronology of sublacustrine moraines, Generator Lake, Baffin Island, Northwest Territories, Canada: Can. J. Earth Sci., v. 11, p. 380-408.
- Barnham, P. H., 1975, Glacitectonic structures: a general discussion with particular reference to the contorted drift of Norfolk: in Wright, H. E., Jr., and Moseley, F., eds., Ice ages ancient and modern: Proc. of 21<sup>st</sup> Inter-University Geol. Congr., State University of New York, Binghamton, 1974, p. 69-91.
- Bindschadler, R. A., and Rasmussen, L. A., 1983, Finite-difference model predictions of the drastic retreat of Columbia Glacier, Alaska: U. S. Geological Survey Professional Paper 1258-D, 17 p.
- Boulton, G. S., 1974, Processes and patterns of glacial erosion: in Coates, D. R., ed., Glacial geomorphology: State University of New York, Binghamton, p. 41-87.



- 1975, Processes and patterns of subglacial sedimentation: a theoretical approach: in Wright, H. E., Jr., and Moseley, F., eds., Ice ages ancient and modern: Proc. of 21st Inter-University Geol. Congr., State University of New York, Binghamton, 1974, p. 7-42.
- 1976, The development of geotechnical properties in glacial tills: in Legget, R. F., ed., Glacial tills, an interdisciplinary study: Ottawa, Royal Soc. of Canada, p. 292-303.
- 1979, Processes of glacial erosion of different substrata: J. Glac., v. 23, p. 15-38.
- Boulton, G. S., Dent, D. L., and Morris, E. M., 1974, Subglacial shearing and crushing, and the role of water pressure in tills from southeast Iceland: Geogr. Ann., v. 56A, p. 135-145.
- Boulton, G. S., and Jones, A. S., 1979, Stability of temperate ice caps and ice sheets resting on beds of deformable sediment: J. Glac., v. 24, p. 29-44.
- Boulton, G. S., Jones, A. S., Clayton, F. M., and Kenning, M. J., 1977, A British ice-sheet model and patterns of glacial erosion and deposition in Britain: in Shotton, F. W., ed., British Quaternary studies, recent advances: Oxford, Clarendon Press, p. 231-246.
- Bredehoeft, J. D., and Hanshaw, B. B., 1968, On the maintenance of anomalous fluid pressure: I. Thick sedimentary sequences: Geol. Soc. Am. Bulletin, v. 79, p. 1097-1106.
- Bretz, J. H., 1910, Glacial lakes of Puget Sound: J. Geol., v. 18, p. 448-458.
- 1913, Glaciation of the Puget Sound region: Washington Geological Survey Bulletin no. 8, 244 p.
- Budd, W. F., 1975, A first simple model for periodically self-surging glaciers: J. Glac., v. 14, p. 3-21.
- Carslaw, H. S., and Jaeger, J. C., 1959, Conduction of heat in solids: Oxford, Clarendon Press, second ed., 510 p.
- Carson, M. A., and Kirkby, M. J., 1972, Hillslope form and process: Cambridge University Press, 475 p.
- Carson, R. J., III, 1970, Quaternary geology of the south-central Olympic Peninsula, Washington: University of Washington, Department of Geological Sciences, Ph.D. dissertation, 67 p.

- Cary, A. S., and Carlston, C. W., 1937, Notes on Vashon stage glaciation of the South Fork of the Skykomish River valley, Washington: Northwest Science, v. 11, p. 61-62.
- Church, M., and Gilbert, R., 1975, Proglacial fluvial and lacustrine environments: in Jopling, A. V., and McDonald, B. C., eds, Glaciofluvial and Glaciolacustrine Environments, Soc. Econ. Paleo. Min. Spec. Pub. no. 23, p. 22-100.
- Clague, J. J., 1975, Sedimentology and paleohydrology of late Wisconsinan outwash, Rocky Mountain trench, Southeastern British Columbia: in Jopling, A. V., and McDonald, B. C., eds., Glaciofluvial and Glaciolacustrine Environments, Soc. Econ. Paleo. Min. Spec. Pub. no. 23, p. 223-237.
- 1981, Late Quaternary geology and geochronology of British Columbia, part 2: Geological Survey of Canada, paper 80-35, 41 p.
- Clague, J. J., and Mathews, W. H., 1973, The magnitude of jokulhlaups: J. Glac., v. 12, 501-504.
- Clapperton, C. M., 1968, Channels formed by the superimposition of glacial meltwater streams, with special reference to the East Cheviot Hills, Northeast England: Geogr. Ann., v. 50A, p. 207-220.
- 1971, The pattern of deglaciation in part of Northumberland: Trans. Inst. Brit. Geogr., v. 53, p. 67-78.
- Clarke, G. K. C., 1982, Glacier outburst floods from "Hazard Lake", Yukon Territory, and the problem of flood magnitude prediction: J. Glac., v. 28, p. 3-21.
- Clarke, G. K. C., Mathews, W. H., and Pack, R. T., in press, Outburst floods from Glacial Lake Missoula: Quat. Res.
- Clayton, K. M., 1965, Glacial erosion in the Finger Lakes region (New York State, U. S. A.): Z. Geomorph. N. F., v. 9, p. 50-62.
- Coates, D. R., and Kirkland, J. T., 1974, Application of glacial models for large-scale terrain derangements: in Mahoney, W. C., ed., Quaternary environments: Proceedings of a symposium, York University Monograph no. 5, p. 99-136.
- Colman, S. M., and Pierce, K. L., 1981, Weathering rinds on andesitic and basaltic stones as a Quaternary age indicator, western United States: U. S. Geological Survey Professional Paper 1210, 56 p.

- Converse Ward Davis Dixon, unpublished, Final geotechnical investigation, raising of Culmback Dam, Sultan River project, stage II: report for Public Utility District No. 1 of Snohomish County, Washington, 1979.
- Crandell, D. R., 1963, Surficial geology and geomorphology of the Lake Tapps quadrangle, Washington: U. S. Geological Survey Professional Paper 388A, 84 p.
- 1969, Surficial geology of Mount Rainier National Park, Washington: U. S. Geological Survey Bulletin 1288, 41 p.
- Crandell, D. R., and Miller, R. D., 1974, Quaternary stratigraphy and extent of glaciation in the Mount Rainier region, Washington: U. S. Geological Survey Professional Paper 847, 59 p.
- Crandell, D. R., Mullineaux, D. R., and Waldron, H. H., 1958, Pleistocene sequence in the southeastern part of the Puget Sound lowland, Washington: Am. J. Sci., v. 256, p. 384-397.
- Curran, T. A., 1965, Surficial geology of the Issaquah area, Washington: University of Washington, Department of Geological Sciences, M.S. thesis, 57 p.
- Dahl, R., 1965, Plastically sculptured detail forms on rock surfaces in northern Nordland, Norway: Geogr. Ann., v. 47A, p. 83-140.
- Danes, Z. F., Bonno, M. M., Brau, E., Gilham, W. D., Hoffman, T. F., Johansen, D., Jones, M. H., Malfait, B., Masten, J., and Teague, G. O., 1965, Geophysical investigation of the southern Puget Sound area, Washington: J. Geophys. Res., v. 70, p. 5573-5580.
- Danner, W. R., 1957, A stratigraphic reconnaissance in the northwestern Cascade mountains and San Juan islands of Washington state: University of Washington, Department of Geological Sciences, Ph.D. dissertation, 562 p.
- Derbyshire, E., 1958, The identification and classification of glacial drainage channels from aerial photographs: Geogr. Ann., v. 40, p. 188-195.
- 1961, Subglacial col gullies and the deglaciation of the North-east Cheviots: Trans. Inst. Brit. Geogr. v. 29, p. 31-46.
- 1962, Fluvio-glacial erosion near Knob Lake, central Quebec-Labrador, Canada: Geol. Soc. Am. Bulletin, v. 73, p. 1111-1126.

- Dethier, D. P., Safioles, S. A., and Pevear, D. R., 1981, Composition of till from the Clear Lake quadrangle, Skagit and Snohomish Counties, Washington: U. S. Geological Survey Open-File Report 81-517, 55 p.
- Domenico, P. A., and Mifflin, M. D., 1965, Water from low-permeability sediments and land subsidence: *Water Resources Res.*, v. 1, p. 563-576.
- Dreimanis, A., 1976: Tills: their origin and properties: in Legget, R. F., ed., *Glacial tills, an interdisciplinary study*: Ottawa, Royal Soc. of Canada, p. 11-49.
- 1979, The problem of waterlain tills: in Schluchter, C., ed., *Moraines and varves*: Rotterdam, A. Balkema, p. 167-177.
- 1982, Two origins of the stratified Catfish Creek till at Plum Point, Ontario, Canada: *Boreas*, v. 11, p. 173-180.
- Easterbrook, D. J., Briggs, N. D., Westgate, J. A., and Gorton, M. P., 1981, Age of the Salmon Springs Glaciation in Washington: *Geology*, v. 9, p. 87-93.
- Easterbrook, D. J., Crandell, D. R., and Leopold, E. B., 1967, Pre-Olympia Pleistocene stratigraphy and chronology in the central Puget Lowland, Washington: *Geol. Soc. Am. Bulletin*, v. 78, p. 13-20.
- Edwards, M. B., 1978, Glacial environments: in Reading, H. G., ed., *Sedimentary environments and facies*: Blackwell, Oxford, p. 416-438.
- Ehlers, J., 1981, Some aspects of glacial erosion and deposition in northern Germany: *Annals of Glaciology*, v. 2, p. 143-146.
- Englehardt, H., 1978, Water in glaciers: observations and theory of the behavior of water levels in boreholes: *Z. Gletsch. u. Glaz.*, v. 14, p. 35-60.
- Evenson, E. B., Dreimanis, A., and Newsome, J. W., 1977, Subaquatic flow tills: a new interpretation for the genesis of some laminated till deposits: *Boreas*, v. 6, p. 115-133.
- Eyles, C. H., and Eyles, N., 1983, Sedimentation in a large lake: a reinterpretation of the Late Pleistocene stratigraphy at Scarborough Bluffs, Ontario, Canada: *Geology*, v. 11, p. 146-152.
- Eyles, N., Sladen, J. A., and Gilroy, S., 1982, A depositional model for stratigraphic complexes and facies superimposition in lodgement tills: *Boreas*, v. 11, p. 317-333.

- Fecht, K. R., and Tallman, A. M., 1978, Bergmounds along the western margin of the channeled scablands, south-central Washington: Abstr. with Progr., 1978 Annual Meeting, Geol. Soc. Am., v. 10(7), p. 400.
- Flint, R. F., 1971, Glacial and Quaternary geology: New York, John Wiley and Sons, 892 p.
- Frizzell, V. A., Jr., Tabor, R. W., Booth, D. B., and Waitt, R. B., Jr., in press, Preliminary geologic map of the Snoqualmie 1:100,000 quadrangle, Washington: U. S. Geological Survey Open-File Report.
- Funder, S., 1972, Deglaciation of the Scoresby Sundfjord region, northeast Greenland: in Price, R. J., and Sugden, D. E., eds., Polar geomorphology: Inst. Brit. Geogr. Spec. Pub. no. 4, p. 33-42.
- Geological Assoc. of Canada, 1958, Glacial map of Canada: scale 1:3,801,600.
- Geological Survey of Canada, 1968, Glacial map of Canada: Map 1253A, scale 1:5,000,000.
- Gibbard, P., 1980, The origin of stratified Catfish Creek till by basal melting: Boreas, v. 9, p. 71-85.
- Glen, J. W., 1954, The stability of ice-dammed lakes and other water-filled holes in glaciers: J. Glac., v. 2, p. 316-318.
- Glover, S. L., 1936, Hammer Bluff formation of western Washington (abs.): Pan-American Geologist, v. 65, p. 77-78.
- Goldthwait, R. P., 1958, Wisconsin age forests in western Ohio, 1: age and glacial events: Ohio J. Sci., v. 58, p. 209-230.
- 1974, Rates of deformation of glacial features in Glacier Bay, Alaska: in Coates, D. R., ed., Glacial geomorphology: State University of New York, Binghamton, p. 163-185.
- Gordon, J. E., 1979, Reconstructed Pleistocene ice-sheet temperatures and glacial erosion in northern Scotland: J. Glac., v. 22, p. 331-344.
- 1981, Ice-scoured topography and its relationship to bedrock structure and ice movement in parts of northern Scotland and west Greenland: Geogr. Ann., v. 63A, p. 55-66.

- Gower, H. D., 1978, Tectonic map of the Puget Sound region, Washington, showing location of faults, principle folds, and large-scale Quaternary deformation: U. S. Geological Survey Open-File Map 78-426.
- Graf, W. H., 1971, Hydraulics of sediment transport: New York, McGraw-Hill, 513 p.
- Gray, J. M., 1982, Unweathered, glaciated bedrock on an exposed lake bed in Wales: *J. Glac.*, v. 28, p. 483-497.
- Grube, F., 1983, Tunnel valleys: in Ehlers, J., ed., *Glacial deposits in north-west Europe*: Rotterdam, A. Balkema, p. 257-258.
- Hagen, J. O., Wold, B., Liestol, O., Ostrem, G., and Sollid, J. L., 1983, Subglacial processes at Bondusbreen glacier, Norway: preliminary results: *Annals of Glaciology*, v. 4, p. 91-98.
- Hall, J. B., and Othberg, K. L., 1974, Thickness of unconsolidated sediments, Puget Lowland, Washington: Department of Natural Resources, Geologic Map GM-12.
- Hallet, B., 1979, A theoretical model of glacial abrasion: *J. Glac.*, v. 23, p. 39-50.
- 1981, Glacial abrasion and sliding: their dependence on the debris concentration in basal ice: *Annals of Glaciology*, v. 2, p.23-28.
- Hanshaw, B. B., and Bredehoeft, J. D., 1968, On the maintenance of anomalous fluid pressure: II. Source layer at depth: *Geol. Soc. Am. Bulletin*, v. 79, p. 1107-1122.
- Happel, J., and Brenner, H., 1973, *Low Reynolds number hydrodynamics*: Leiden, Noordhoff Intl. Publ., 553 p.
- Harrison, W., 1958, Marginal zones of vanished glaciers reconstructed from the preconsolidation-pressure values of overridden silt: *J. Geol.*, v. 66, p. 72-95.
- Heller, P. L., 1980, Multiple ice-flow directions during the Fraser Glaciation in the lower Skagit River drainage, North Cascade Range, Washington: *Arc. Alp. Res.*, v. 12, p. 299-308.
- Hicock, S. R., and Dreimanis, A., 1978, Late Wisconsin marine subaqueous flow tills, Victoria, British Columbia: *Abstr. with Progr.*, 1978 Annual Meeting, *Geol. Soc. Am.*, v. 10(7), p. 421.

- Hillaire-Marcel, C., Occhietti, S., and Vincent, J. S., 1981, Sakami moraine, Quebec: a 500 km-long moraine without climatic control: *Geology*, v. 9, p. 210-214.
- Hirsch, R. M., 1975, Glacial geology and geomorphology of the upper Cedar River watershed, Cascade Range, Washington: University of Washington, Department of Geological Sciences, M.S. thesis, 48 p.
- Holdsworth, G., 1973, Ice calving into the proglacial Generator Lake, Baffin Island, Northwest Territories, Canada: *J. Glac.*, v. 12, p. 235-250.
- Hooke, R. LeB., 1977, Basal temperatures in polar ice sheets: a qualitative review: *Quat. Res.*, v. 7, p. 1-13.
- Hukki, R. T., 1961, Proposal for a Solomonic settlement between the theories of von Rittinger, Kick, and Bond: *Trans. AIME*, v. 220, p. 403-408.
- Humlum, O., 1981, Observations of debris in the basal transport zone of Myrdalsjokull, Iceland: *Annals of Glaciology*, v. 2, p. 71-77.
- Hutter, K., 1983, *Theoretical glaciology*: Dordrecht, Holland, D. Reidel, 510 p.
- International Association of Hydrological Sciences, 1977, *Fluctuations of glaciers*: v. 3, International Commission on Snow and Ice, Paris, IAHS-UNESCO, 269 p.
- Johnson, T. C., 1980, Late-Glacial and postglacial sedimentation in Lake Superior based on seismic-reflection profiles: *Quat. Res.*, v. 13, p. 380-391.
- Kamb, B., 1970, Sliding motion of glaciers: theory and observation: *Rev. of Geophys. and Space Sci.*, v. 8, p. 673-728.
- Karrow, P. F., 1976, The texture, mineralogy, and petrography of North American tills: in Legget, R. F., *Glacial till, an interdisciplinary study*: Ottawa, Royal Soc. of Canada, p. 83-98.
- Kazi, A., and Knill, J. L., 1969, The sedimentation and geotechnical properties of the Cromer till between Happisburgh and Cromer, Norfolk: *Q. J. Eng. Geol.*, v. 2, p. 63-86.
- Kemmis, T. J., 1981, Importance of the regelation process to certain properties of basal tills deposited by the Laurentide ice sheet in Iowa and Illinois, U. S. A.: *Annals of Glaciology*, v. 2, p. 147-152.
- Kendall, P. F., 1902, A system of glacier lakes in the Cleveland Hills: *Quart. J. Geol. Soc.*, v. 58, p. 471-571.

- Knoll, K. M., 1967, Surficial geology of the Tolt River area, Washington: University of Washington, Department of Geological Sciences, M.S. thesis, 91 p.
- Koteff, C., 1974, The morphologic sequence concept and deglaciation of southern New England: in Coates, D. R., ed., Glacial geomorphology: State University of New York, Binghamton, p. 121-144.
- Koteff, C., and Pessl, F., Jr., 1981, Systematic ice retreat in New England: U. S. Geological Survey Professional Paper 1179, 20 p.
- Kruger, J., 1979, Structures and textures in till indicating subglacial deposition: *Boreas*, v. 8, p. 323-340.
- Laprade, W. T., 1982, Geologic implications to pre-consolidated pressure values, Lawton Clay, Seattle, Washington: Proc. of 19th annual Eng. Geol. and Soils Eng. Symp., Idaho State Univ., Pocatello, p. 303-321.
- Lawson, D. E., 1981, Sedimentological characteristics and classification of depositional processes in the glacial environment: U. S. Army, CRREL Report 81-27.
- Leisch, B. A., Price, C. E., and Walters, K. L., 1963, Geology and ground water resources of northwestern King County, Washington: Washington State Water Supply Bulletin no. 20, 241 p.
- Linton, D. L., 1963, The forms of glacial erosion: *Trans. Inst. Brit. Geogr.*, v. 33, p. 1-28.
- Livingston, V. E., 1971, Geology and mineral resources of King County, Washington: Washington Division of Mines and Geology Bulletin no. 63, 200 p.
- Lliboutry, L., 1968, General theory of subglacial cavitation and sliding of temperate glaciers: *J. Glac.*, v. 7, p. 21-58.
- 1983, Modification to the theory of intraglacial waterways for the case of subglacial ones: *J. Glac.*, v. 29, p. 216-226.
- Lliboutry, L., and Ritz, C., 1978, Ecoulement permanent d'un fluide visqueux non lineaire (corps de Glen) autour d'une sphere parfaitement lisse: *Ann. Geophys.*, t. 34, fasc. 2, p. 133-146.
- Lutschg, O., 1926, *Über Niederschlag und Abfluss in Hochgebirge Sonderdarstellung des Mattmark gebietes*: Zurich, 500 p.
- MacClintock, P., and Dreimanis, A., 1964, Reorientation of till fabric by overriding glacier in the St. Lawrence Valley: *Am. J. Sci.*, v. 262, p. 133-142.



- Mackin, J. H., 1941, Glacial geology of the Snoqualmie-Cedar area, Washington: *J. Geol.*, v. 49, p. 449-481.
- Malde, H. E., 1968, The catastrophic Late Pleistocene Bonneville flood in the Snake River Plain, Idaho: U. S. Geological Survey Professional Paper 596, 52 p.
- Mannerfelt, C. M., 1949, Marginal drainage channels as indicators of the gradients of Quaternary ice caps: *Geogr. Ann.*, v. 31, p. 194-199.
- Marcus, M. G., and Ragle, R. H., 1970, Snow accumulation in the Icefield Ranges, St. Elias Mountains, Yukon: *Arc. Alp. Res.*, v. 2, p. 277-292.
- Mathews, W. H., 1964, Water pressure under a glacier: *J. Glac.*, v. 5, p. 235-240.
- 1974, Surface profile of the Laurentide ice sheet in its marginal areas: *J. Glac.*, v. 13, p. 37-43.
- Mathews, W. H., and Mackay, J. R., 1960, Deformation of soils by glacier ice and the influence of pore pressure and permafrost: *Trans. Roy. Soc. Canada*, v. 54, ser. 3, p. 27-39.
- May, R. W., 1977, Facies model for sedimentation in the glacio-lacustrine environment: *Boreas*, v. 6, p. 175-180.
- Mayo, L. R., in press, 25 years of mass balance and runoff research in the U. S. A.: *Geogr. Ann.*
- Meier, M. F., Tangborn, W. V., Mayo, L. R., and Post, A., 1971, Combined ice and water balances of Gulkana and Wolverine Glaciers, Alaska, and South Cascade Glacier, Washington, 1965 and 1966 hydrologic years: U. S. Geological Survey Professional Paper 715A, 23 p.
- Menzies, J., 1979, The mechanics of drumlin formation with particular reference to the change in pore-water content of the till: *J. Glac.*, v. 22, p. 373-384.
- Mercer, J. H., 1961, The response of fjord glaciers to changes in the firn limit: *J. Glac.*, v. 3, p. 850-858.
- Metcalf, R. C., 1979, Energy dissipation during subglacial abrasion at Nisqually Glacier, Washington, U. S. A.: *J. Glac.*, v. 23, p. 233-246.

- Mickelson, D. M., 1973, Nature and rate of basal till deposition in a stagnating ice mass, Burroughs Glacier, Alaska: *Arc. Alp. Res.*, v. 5, p. 17-27.
- Mickelson, D. M., Acomb, L. J., and Edil, T. B., 1979, The origin of preconsolidated and normally consolidated tills in eastern Wisconsin, U. S. A.: in Schluchter, C., ed., *Moraines and varves*, Rotterdam, A. Balkema, p. 179-187.
- Minard, J. P., 1980, Geology of the Maltby quadrangle, Washington: U. S. Geological Survey Open-File Map 80-2013, scale 1:24,000.
- 1981, Geology of the Snohomish quadrangle, Washington: U. S. Geological Survey Open-File Map 81-100, scale 1:24,000.
- Moran, S.R., Clayton, L., Hooke, R. LeB., Fenton, M. M., and Andriashek, L. D., 1980, Glacier-bed landforms of the prairie region of North America: *J. Glac.*, v. 25, p. 457-476.
- Mottershead, D. N., and Collin, R. L., 1976, A study of glacier-dammed lakes over 75 years--Brimkjelen, southern Norway: *J. Glac.*, v. 17, p. 491-505.
- Mullineaux, D. R., 1970, Geology of the Renton, Auburn, and Black Diamond quadrangles, King County, Washington: U. S. Geological Survey Professional Paper 672, 92 p.
- Mullineaux, D. R., Waldron, H. H., and Rubin, M., 1965, Stratigraphy and chronology of late interglacial and early Vashon glacial time in the Seattle area, Washington: U. S. Geological Survey Bulletin 1194-0, 10 p.
- Newcomb, R. C., 1952, Groundwater resources of Snohomish County, Washington: U. S. Geological Survey Water Supply Paper 1135, 133 p.
- Newell, W. L., 1970, Factors influencing the grain of the topography along the Willoughby Arch in northeastern Vermont: *Geogr. Ann.*, v. 52A, p. 103-112.
- Nobles, L. H., and Weertman, J., 1971, Influence of irregularities of the bed of an ice sheet on deposition rate of till: in Goldthwait, R. P., ed, *Till, a symposium*: Ohio State University Press, p. 117-126.
- Nye, J. F., 1957, The distribution of stress and velocity in glaciers and ice-sheets: *Proc. Roy. Soc. Lon., Ser. A*, v. 239, p. 113-133.

- 1963, The response of a glacier to changes in the rate of nourishment and wastage: Proc. Roy. Soc. Lon., Ser. A, v. 275, p. 87-112.
- 1965, The flow of a glacier in a channel of rectangular, elliptic or parabolic cross-section: J. Glac., v. 5, p. 661-690.
- 1969, A calculation on the sliding of ice over a wavy surface using a Newtonian viscous approximation: Proc. Roy. Soc. Lon., ser. A, v. 311, p. 445-467.
- 1970, Glacier sliding without cavitation in a linear viscous approximation: Proc. Roy. Soc. Lon., ser. A, v. 315, p. 381-403.
- 1976, Water flow in glaciers: jokulhlaups, tunnels and veins: J. Glac., v. 17, p. 181-207.
- Olmstead, T. L., 1969, Geotechnical aspects and engineering properties of glacial till in the Puget Lowland, Washington: in Proc. 7th Annual Eng. Geol. and Soils Eng. Symp., Moscow, Idaho, p. 223-233.
- Orheim, O., and Elverhoi, A., 1981, Model for submarine glacial deposition: Annals of Glaciology, v. 2, p. 123-128.
- Orombelli, G., and Gnaccolini, M., 1978, Sedimentation in proglacial lakes: a Würmian example from the Italian Alps: Z. Geomorph. N. F., v. 22, p. 417-425.
- Pasierbski, M., 1979, Remarks on the genesis of subglacial channels in northern Poland: Eiszeitalter u. Gegenwart, v. 29, p. 189-200.
- Paterson, W. S. B., 1981, The physics of glaciers: Oxford, Pergamon Press, 380 p.
- Peel, R. F., 1956, The profile of glacial drainage channels: Geogr. Journ., v. 122, p. 483-487.
- Pessl, F., Jr., Dethier, D. P., and Minard, J. P., 1983, Surficial geologic map of the Port Townsend quadrangle, Washington: U. S. Geological Survey Miscellaneous Investigation Map 1198, scale 1:100,000.
- Pessl, F., Jr., and Frederick, J. E., 1981, Sediment source for melt-water deposits: Annals of Glaciology, v. 2, p. 92-96.
- Pierce, K. L., 1979, History and Dynamics of glaciation in the northern Yellowstone National Park area: U. S. Geological Survey Professional Paper 729F, 90 p.

- Porter, S. C., 1975, Equilibrium-line altitudes of late Quaternary glaciers in the southern Alps, New Zealand: *Quat. Res.*, v. 5, p. 27-47.
- 1976, Pleistocene glaciation in the southern part of the North Cascade Range, Washington: *Geol. Soc. Am. Bulletin*, v. 87, p. 61-75.
- 1977, Present and past glaciation threshold in the Cascade Range, Washington U. S. A.: topographic and climatic controls, and paleoclimatic implications: *J. Glac.*, v. 18, p. 101-116.
- Post, A. S., 1969, Distribution of Surging glaciers in western North America: *J. Glac.*, v. 8, p. 229-240.
- 1975, Preliminary hydrography and historic terminal changes of Columbia Glacier, Alaska: U. S. Geological Survey Hydrologic Investigations Atlas 559, 3 sheets.
- Post, A. S., and Mayo, L. R., 1971, Glacier dammed lakes and outburst floods in Alaska: U. S. Geological Survey Hydrologic Investigations Atlas 455, 10 p.
- Powell, R. D., 1981, A model for sedimentation by tidewater glaciers: *Annals of Glaciology*, v. 2, p. 129-134.
- Price, R. J., 1963, A glacial meltwater drainage system in Peeblesshire, Scotland: *Scott. Geogr. Mag.*, v. 79, p. 133-141.
- Ramsden, J., and Westgate, J. A., 1971, Evidence for reorientation of a till fabric in the Edmondton area, Alberta: in Goldthwait, R. P., ed., *Till, a symposium*: Ohio State University Press, p. 335-344.
- Rigg, G. B., 1958, Peat resources of Washington: Washington Division of Mines and Geology Bulletin 44, p. 69-95.
- Rigg, G. B., and Gould, H. R., 1957, Age of Glacier Peak eruption and chronology of postglacial peat deposits in Washington and surrounding areas: *Am. J. Sci.*, v. 255, p. 341-363.
- Robin, G. de Q., 1967, Surface topography of ice sheets: *Nature*, v. 215, p. 1029-1032.
- 1976, Is the basal ice of a temperate glacier at the pressure melting point?: *J. Glac.*, v. 16, p. 183-196.
- 1979, Formation, flow, and disintegration of ice shelves: *J. Glac.*, v. 24, p. 259-271.

- Rosengreen, T. E., 1965, Surficial geology of the Maple Valley and Hobart quadrangles, Washington: University of Washington, Department of Geological Sciences, M.S. thesis, 71 p.
- Rothlisberger, H., 1968, Erosive processes which are likely to accentuate or reduce the bottom relief of valley glaciers: *Int. Assoc. Sci. Hydrol.*, v. 79, p. 87-97.
- 1972, Water pressure in intra- and subglacial channels: *J. Glac.*, v. 11, p. 177-203.
- Rudberg, S., 1973, Glacial erosion forms of medium size--a discussion based on 4 Swedish case studies: *Z. Geomorph. N. F., Suppl. Bd.* 17, p. 33-48.
- Rust, B. R., and Romanelli, R., 1975, Late Quaternary subaqueous outwash deposits near Ottawa, Canada: in Jopling, A. V., and McDonald, B. C., eds., *Glaciofluvial and glaciolacustrine sedimentation: Soc. Econ. Paleo. Min. Spec. Publ. no. 23*, p. 177-192.
- Sanderson, T. J. O., 1979, Equilibrium profile of ice shelves: *J. Glac.*, v. 22, p. 435-460.
- Schou, A., 1949, The landscapes: v. 1 of Nielsen, N., ed., *Atlas of Denmark: Copenhagen, H. Hagerup*, 32 p.
- Shannon and Wilson, unpublished, Foundation investigation of the Tolt River regulating basin: Geotechnical report for the City of Seattle Engineering Department, 31 p., 1959.
- Sharp, R. P., 1947, The Wolf Creek glacier, St. Elias Range, Yukon Territory: *Geogr. Rev.*, v. 37, p. 26-52.
- Shaw, J., 1982, Meltout till in the Edmondton area, Alberta, Canada: *Can. J. Earth Sci.*, v. 19, p. 1548-1569.
- Shilts, W. W., 1973, Glacial dispersal of rocks, minerals, and trace elements in Wisconsinan till, southeastern Quebec, Canada: *Geol. Soc. Am. Mem.*, 136, p. 189-219.
- Shreve, R. L., 1972, Movement of water in glaciers: *J. Glac.*, v. 11, p. 205-214.
- in press, Esker characteristics in terms of glacier physics, Katahdin esker system, Maine: *Geol. Soc. Am. Bulletin*.
- Sissons, J. B., 1958a, Subglacial stream erosion in southern Northumberland: *Scott. Geogr. Mag.*, v. 74, p. 163-174.

- 1958b, Supposed ice-dammed lakes in Britain with particular reference to the Eddleston valley, southern Scotland: Geogr. Ann., v. 40, p. 159-187.
- 1960, Some aspects of glacial drainage channels in Britain (Pt. I): Scott. Geogr. Mag., v. 76, p. 131-146.
- 1963, The glacial drainage system around Carlops, Peeblesshire: Trans. Inst. Brit. Geogr., v. 32, p. 95-111.
- Smith, J. D., 1970, Stability of a sand bed subjected to a shear flow of low Froude number: J. Geophys. Res., v. 75, p. 5928-5940.
- Snyder, R. V., and Wade, J. M., 1972, Soil resource inventory, Snoqualmie National Forest, Skykomish, North Bend and White River ranger districts: U. S. Forest Service.
- Stenborg, T., 1968, Glacier drainage connected with ice structures: Geogr. Ann., v. 50A, p. 25-53.
- Stone, B. D., and Koteff, C., 1979, A Late Wisconsinan ice readvance near Manchester, N. H.: Am. J. Sci., v. 279, p. 590-601.
- Stone, K. H., 1963, Alaskan ice-dammed lakes: Assoc. of American Geogr., Annals, v. 53, p. 332-349.
- Stuart, D. J., 1961, Gravity study of crustal structure in western Washington: U. S. Geological Survey Professional Paper 424C, p. 273-276.
- Stuiver, M., Heusser, C. J., and Yang, I. C., 1978, North American glacial history back to 75,000 years b.p.: Science, v. 200, p. 16-21.
- Sturm, M., and Benson, C. S., unpublished, Report on Strandline Lake flooding hazard: Report prepared for Chugach Electric, Anchorage, 28 p., 1982.
- Sugden, D. E., 1978, Glacial erosion by the Laurentide ice sheet: J. Glac., v. 20, p. 367-391.
- 1979, Ice sheet erosion--a result of maximum conditions?: J. Glac., v. 23, p. 402-404.
- Tabor, R. W., Frizzell, V. A., Jr., Booth, D. B., Whetten, J. T., Waitt, R. B., Jr., and Zartman, R. E., 1982, Preliminary geologic map of the Skykomish River 1:100,000 quadrangle, Washington: U. S. Geological Survey Open-File Map 82-747, scale 1:100,000.

- Thomas, R. H., 1973, The creep of ice shelves: theory: *J. Glac.*, v. 12, p. 45-53.
- 1979, The dynamics of marine ice sheets: *J. Glac.*, v. 24, p. 167-177.
- Thorson, R. M., 1979, Isostatic effects of the last glaciation in the Puget Lowland, Washington: University of Washington, Department of Geological Sciences, Ph.D. dissertation, 154 p.
- 1980, Ice sheet glaciation of the Puget Lowland, Washington, during the Vashon Stade: *Quat. Res.*, v. 13, p. 303-321.
- 1981, Isostatic effects of the last glaciation in the Puget Lowland, Washington: U. S. Geological Survey Open-File Report 81-370, 100 p.
- Tubbs, D. W., 1974, Landslides in Seattle: Washington Department of Natural Resources Information Circular no. 52, 15 p.
- U. S. Geological Survey, 1983, U. S. Geological Survey water resources data, Washington, water year 1981: v. 1, 337 p.
- Vivian, R., 1975, Les glaciers du Alpes occidentales: Imprimerie Allier, 513 p.
- Vorren, T. O., Hald, M., Edvardsen, M., and Lind-Hansen, O. W., 1983, Glacigenic sediments and sedimentary environments of continental shelves: general principles with a case study from the Norwegian shelf: in Ehlers, J., ed., *Glacial deposits in north-west Europe*: Rotterdam, A. Balkema, p. 61-73.
- Waitt, R. B., Jr., and Thorson, R. M., 1983, The Cordilleran ice sheet in Washington, Idaho, and Montana: in Porter, S. C., and Wright, H. E., Jr, eds., *Late-Quaternary environments of the United States*: University of Minnesota Press, v. 1, p. 53-70.
- Walder, J., and Hallet, B., 1979, Geometry of former subglacial water channels and cavities: *J. Glac.*, v. 23, p. 335-346.
- Warnke, D. A., 1970, Glacial erosion, ice rafting and glacial-marine sediments: Antarctica and the southern ocean: *Am. J. Sci.*, v. 269, p. 276-294.
- Weaver, C. E., 1912, A preliminary report on the Tertiary paleontology of western Washington: Washington Geological Survey Bulletin no. 15, 80 p.

- 1937, Tertiary stratigraphy of western Washington and northwestern Oregon: Washington University, Seattle, Publications in Geology, v. 4, 266 p.
- Weertman, J., 1957, On the sliding of glaciers: J. Glac., v. 3, p. 33-38.
- 1957, Deformation of floating ice shelves: J. Glac., v. 3, p. 38-42.
- 1964, Rate of growth or shrinkage of non-equilibrium ice sheets: J. Glac., v. 5, p. 145-158.
- 1964, The theory of glacier sliding: J. Glac., v. 5, p. 287-303.
- 1974, Stability of the junction of an ice sheet and an ice shelf: J. Glac., v. 13, p. 3-11.
- 1979, The unsolved general glacier sliding problem: J. Glac., v. 23, p. 97-115.
- Whetten, J. T., Carroll, P. I., Gower, H. D., Brown, E. H., and Pessl, F., Jr., 1983, Bedrock geologic map of the Port Townsend quadrangle, Washington: U. S. Geological Survey Miscellaneous Investigations Map 1198, scale 1:100,000.
- Whillans, I. M., 1978, Erosion by continental ice sheets: J. Geol., v. 86, p. 516-524.
- 1979, Erosion of grooves by subglacial meltwater streams: J. Glac., v. 23, p. 424-425.
- White, W. A., 1972, Deep erosion by continental ice sheets: Geol. Soc. Am. Bulletin, v. 83, p. 1037-1056.
- Williams, V. S., 1971, Glacial geology of the drainage basin of the Middle Fork of the Snoqualmie River: University of Washington, Department of Geological Sciences, M.S. thesis, 45 p.
- Willis, B., 1898, Drift phenomenon of Puget Sound: Geol. Soc. Am. Bulletin, v. 9, p. 111-162.
- Wold, B., 1983, Materialtransportundersøkelser i norske breelver 1981: Norges vassdrags-og elektrisitetsvesen, Hydrologisk avdeling, Rapport 1-83, 39 p.
- Wright, H. E., Jr., 1973, Tunnel valleys, glacial surges, and subglacial hydrology of the Superior lobe, Minnesota: Geol. Soc. Am. Mem., v. 136, p. 251-276.



Young, J. A. T., 1980, The fluvioglacial landforms of mid-Strathdearn, Inverness-shire: *Scott. J. Geol.*, v. 16, p. 209-220.

**APPENDIX**  
**DESCRIPTION OF MAP UNITS**

**NON-GLACIAL DEPOSITS**

- m1** MODIFIED LAND (HOLOCENE)--Gravel or diamicton as fill, or extensively graded natural deposits
- LANDSLIDE DEPOSITS, UNDIVIDED (HOLOCENE)--Divided into:
- Q1** Landslide deposits--Diamicton of angular clasts of bedrock and surficial deposits derived from upslope. Many with no letter symbol, only arrows denoting downslope direction of movement
- Q1ra** Rock avalanche deposits--Huge angular boulders on or at the base of steep slopes
- Qm** MASS-WASTAGE DEPOSITS (HOLOCENE)--Colluvium, soil, or landslide debris with indistinct morphology, mapped where sufficiently continuous and thick to obscure underlying material. Deposit is gradational with units Qf and Q1
- Qt** TALUSES (HOLOCENE)--Non-sorted angular boulder gravel to boulder diamicton. At lower altitudes gradational with Qf. At higher altitudes includes small rock avalanche deposits as well as some Holocene moraines, rock glaciers, and protalus rampart deposits that lack characteristic morphology. Generally unvegetated
- Qf** ALLUVIAL FAN DEPOSITS (HOLOCENE)--Poorly sorted cobble to boulder gravel, deposited as either a discrete lobe at the intersection of a steep stream with a valley floor of lower

gradient or as a broad apron of coalescing fluvial material on steep sideslopes

- Qb** BOG DEPOSITS (HOLOCENE)--Peat and alluvium. Poorly drained and intermittently wet annually. Grades into unit Qya1
- Qya1** YOUNGER ALLUVIUM (HOLOCENE)-- Moderately sorted cobble-gravel to pebbly sand along rivers and streams. Generally unvegetated; gradational with both Qf and Qb
- Qoa1** OLDER ALLUVIUM (HOLOCENE AND PLEISTOCENE)--Similar material to unit Qya1, but standing above modern floodplain level and generally separated from it by a distinct topographic scarp. In the Skykomish River valley, terrace sequence is indicated by subscripts, from 1 (oldest) to 3 (youngest)

### GLACIAL DEPOSITS

ALPINE DRIFTS AND RELATED DEPOSITS (HOLOCENE AND PLEISTOCENE)--  
Divided into:

- Qgt** GLACIAL DEPOSITS AND TALUSES--Similar material to unit Qt but showing distinct lobate form indicating deposition at terminus of small glacier or permanent snowfield, or an active rock glacier. Generally unvegetated
- Qag** ALPINE GLACIAL DEPOSITS--Ranges from till in uplands and upvalley to gravelly outwash on broad valley floors. On valley sides includes areas veneered with drift but also showing bedrock, alluvial fans, colluvium, or taluses.

On valley floors may also include small fans, bogs, and modern stream alluvium. Areas of thin, sparse drift with sporadic bedrock exposures generally included in this unit as well. In the headward reaches of alpine streams, grades into unit Qgt

- Qat** ALPINE TILL--Fresh diamicton of locally derived lithologies, similar to most till mapped as part of unit Qag
- Qams** ALPINE DRIFT OF MT. STICKNEY--Till and stratified drift forming a broad morainal ridge extending northwest from Mt. Stickney
- Qoad** OLDER ALPINE DRIFT, UNDIVIDED--Moderately to strongly weathered diamicton. The lithologic composition of this deposit indicates transport by alpine ice

DEPOSITS OF VASHON STADE OF FRASER GLACIATION OF ARMSTRONG AND OTHERS (1965) (PLEISTOCENE)--Divided into:

- Qvr\*** RECESSIONAL OUTWASH DEPOSITS--Stratified sand and gravel, moderately to well-sorted, and well-bedded silty sand to silty clay.

Roman numeral subscripts indicate specific depositional intervals, with I being the oldest. Multiple subscripts indicate deposits spanning more than one interval; the absence of subscripts indicates an indeterminate age. This deposit represents predominantly outwash plain and valley-train environments in the lowland areas that may, locally, be divided into:

- Qvrs\*** Sand-dominated recessional outwash deposits
- Qvrg\*** Gravel-dominated recessional outwash deposits
- Qvr1\*** Fine-grained deposits of ice-dammed lakes associated with specific recessional intervals
- Qvrm\*** Deposits associated with marginal lakes dammed by ice or debris in the major west-draining alpine valleys
- Where units Qvr and Qvt are mapped together, topographic form of composite unit is controlled by the underlying till, but is blanketed with near-continuous fluvial sedimentary material. This composite unit is gradational with units Qvr and Qvt
- Qvi\*** WATERLAIN ICE-CONTACT DEPOSITS--Deposits are often similar in texture to unit Qvr, but show structure or morphology that indicate(s) deposition in close proximity to active or stagnant ice. Numerical subscripts follow same conventions as for the recessional outwash deposits units. Locally divided into:
- Qvik\*** Kame and kettle deposits--Underlie areas with characteristic topographic form indicative of deposition around or above stagnant ice
- Qvim\*** Moraines and morainal embankment deposits--Includes high percentage of loose to compact diamicton beneath and interstratified with fluvial materials, deposited at or near active ice margins

**Qvt** TILL--Mainly compact diamicton with subangular to rounded clasts, glacially transported and deposited. In ice-marginal areas or where covered by a thin layer of recessional outwash, contact with units Qvi or Qvr is gradational.

In certain areas where both till and bedrock are mapped together, overall topographic form of unit is controlled by bedrock, with exposures of both materials present. Composite unit includes areas with colluvium of angular clasts and uniform lithology in close proximity to till, with or without corresponding bedrock exposures.

Also, locally includes:

**Qvts** Intra-till stratified sedimentary deposits--Minor deposits of inferred subglacial fluvial origin interbedded with till

**Qva** ADVANCE OUTWASH DEPOSITS--Well-bedded gravelly sand to fine-grained sand, generally firm and unoxidized; deposited by proglacial streams

**Qvu** DRIFT, UNDIVIDED

#### **NON-GLACIAL AND GLACIAL DEPOSITS**

**Qtb** TRANSITIONAL BEDS (PLEISTOCENE)--Pre-Vashon and early-Vashon age deposits of laminated clayey silt to clay; occasional dropstones present. Grades upward into unit Qva

**Qpf** GLACIAL AND NON-GLACIAL SEDIMENTARY DEPOSITS OF PRE-FRASER  
GLACIATION AGE (PLEISTOCENE)--

Deeply weathered stratified sand and gravel, or clay-rich diamicton. Strong in-place weathering is indicated by oxidation, gussification, rind development, and clay-mineral development throughout the depth of exposure. Consists of deposits with a wide age range (pre-dating the Fraser glaciation)

**Qtu** TILL, UNDIVIDED (PLEISTOCENE)--Compact diamicton for which weathering and stratigraphic position are insufficient to assign to either unit Qvt or Qpf. On the western edge of the map, may include small areas of non-glacial sediments

**Qdu** GLACIAL DRIFT, UNDIVIDED

**BEDROCK**

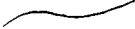
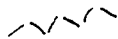

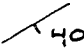
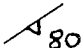




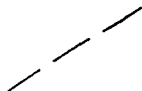
**Ts** SEDIMENTARY ROCKS (TERTIARY)--Moderate to deeply weathered sandy pebble-conglomerate to fine-grained sandstone. Quartzose pebbles common in coarser-grained deposits; mica common in finer-grained sands

**Ti** INTRUSIVE ROCKS (TERTIARY)--Mostly biotite-hornblende and hornblende-biotite granodiorite and tonalite, but locally includes quartz diorite, quartz monzonite, and granite




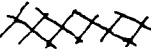
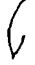

**Tvs** VOLCANIC AND SEDIMENTARY ROCKS (TERTIARY)--Mostly andesite and andesitic breccias and tuffs with minor basalt, dacite, and rhyolite. Southwest of the Snoqualmie River, sandstone, siltstone, and conglomerate predominate

**br** BEDROCK, UNDIVIDED (TERTIARY AND MESOZOIC)

**Mm** MELANGE (MESOZOIC)--Argillite, phyllite, graywacke, chert, greenstone, marble, amphibolite, metatonalite, and metagabbro; pervasively sheared and disrupted. Sheared argillite commonly forms a matrix for blocks that are composed of the other lithologies, whose dimensions may range from one to thousands of meters

- |   |   |
|---|---|
|    | Contact   |
|   | Contact (gradational)   |
|  | High angle fault--bar and ball on downthrown side   |
|  | Strike and dip of bedding   |
|  | Strike and dip of foliation in metamorphic rocks  |
|  | Strike and dip of bedding in glacial outwash deposits   |
|  | Till fabric--symbol aligned with consistent horizontal trend of the long axis of pebbles                            |
|  | Striation--direction of motion indicated by arrow head  |
|  | Flow of glacial meltwater inferred from surface morphology  |
|  | Ice-flow indicator--elongated hills, valleys, and closed depressions inferred to show direction of basal ice motion |



-  Approximate limit of Puget-lobe ice sheet
-  Crest of moraine associated with Puget-lobe ice sheet
-  Crest of moraine associated with alpine glaciers
-  Channelway
-  Direction of landslide motion
-  Spillway controlling altitude of impounded meltwater (number corresponds to recessional interval)

## VITA

Derek Blake Booth

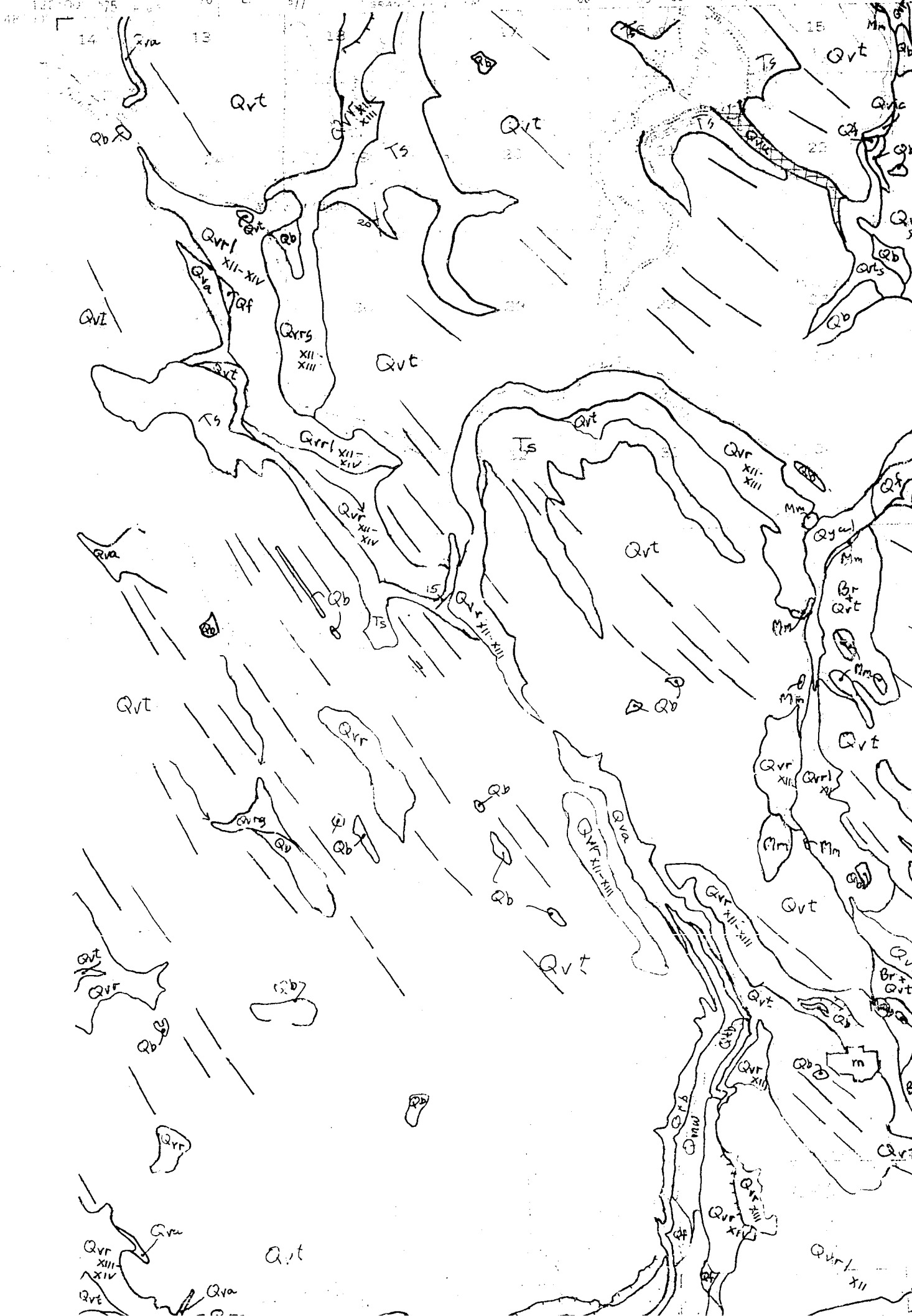
Born April 7, 1953

### Education:

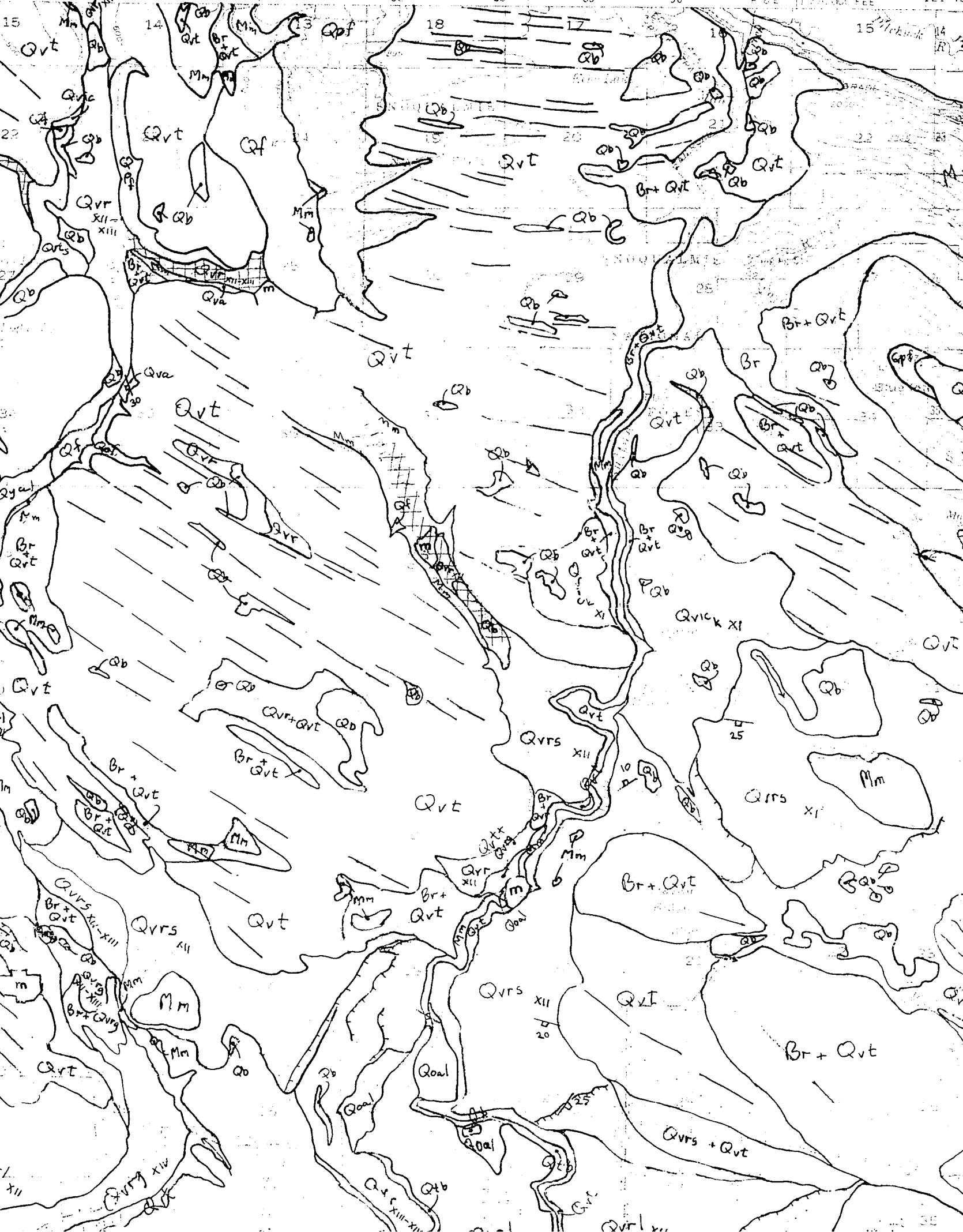
Hampshire College, Amherst, Mass.	B.A. (Literature)	June 1974
Univ. of California, Berkeley, Ca.	B.A. (Geology)	March 1978
Stanford University, Stanford, Ca.	M.S. (Geology)	June 1980
Univ. of Washington, Seattle, Wa.	Ph.D. (Geology)	June 1984

Title of dissertation: "Glacier Dynamics and the  
Development of Glacial Landforms in the Eastern Puget  
Lowland, Washington"











13  
INOCUALMIE  
NATIONAL  
FOREST



Qv

Fi

Mm

Qvicm

Qvicm

Qvmm

Qvmm

Br+Qvt

Br+Qvicm

Qvmm

Br+Qvmm

Mm

Mm

Qvic k

Br+Qvt

Qvt

Qvicm

Qvrs

Qvmm

70

70

60

70

Br+Qvt

Qvrs

Br+Qvt+

Qvrs

Qv

Qams

Br+Qvt

Qvt

Qvt

Qvt

Qvt

Qvt

Qvt

Qvt

Qvt

Qvt

Qvt

Qvt

Qvt

Qvicm

Qf

Qf

Qf

Qf

Qf

Qf

Qvrs xi

Qvrs xii

Qvrs xiii

Br+Qvt +  
Qvr

Br+Qvt +  
Qvicm

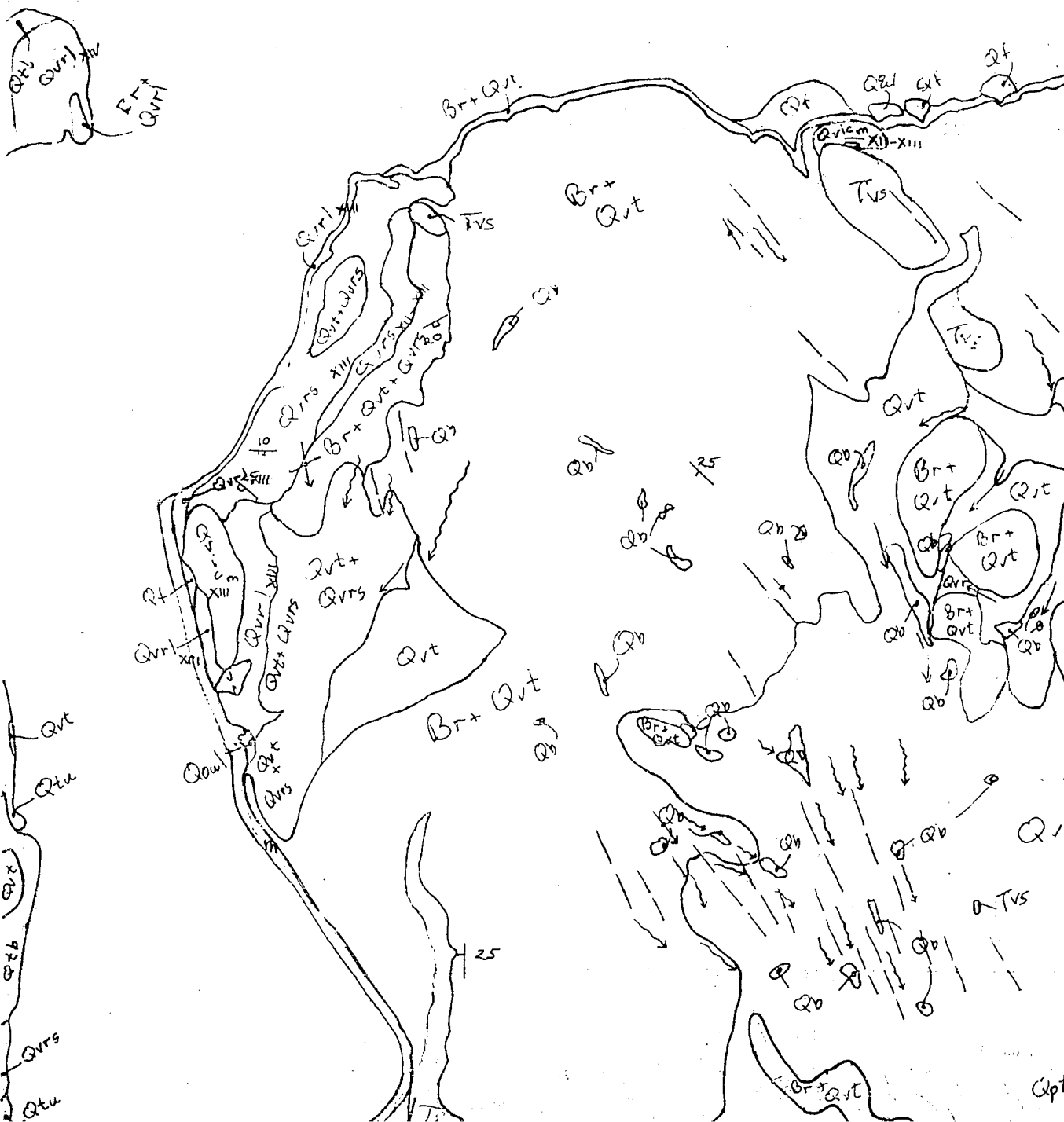
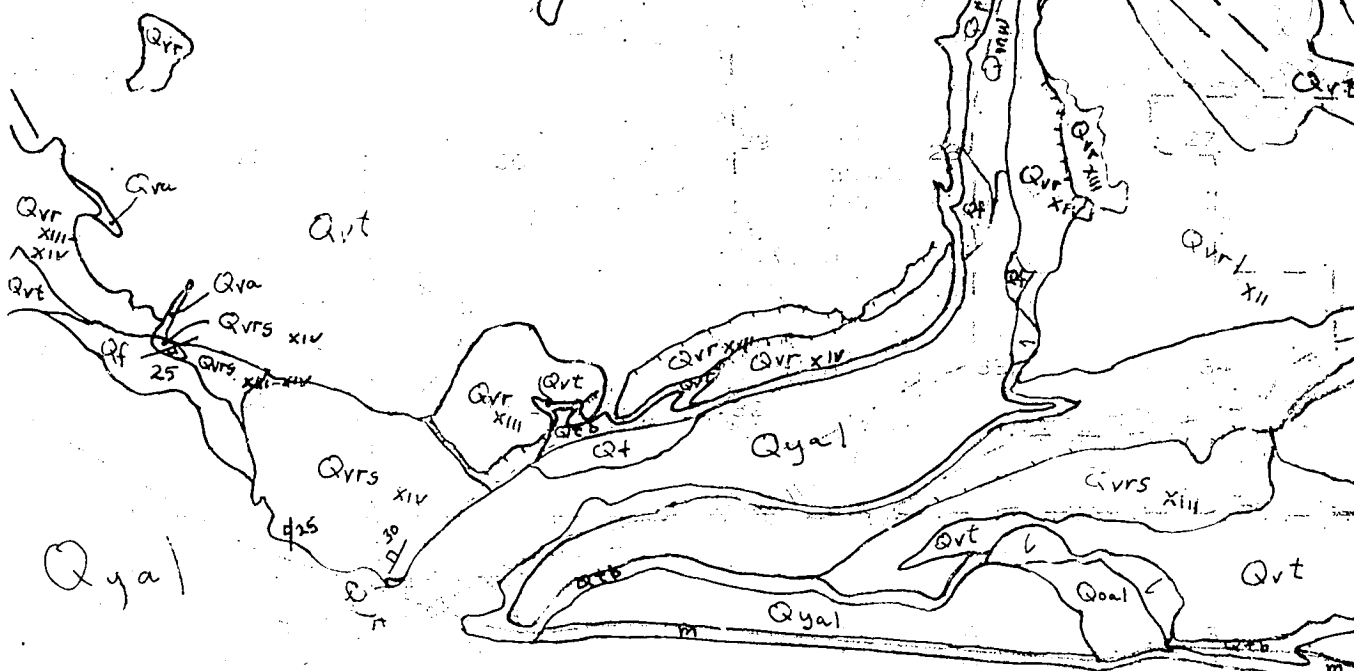
Mm



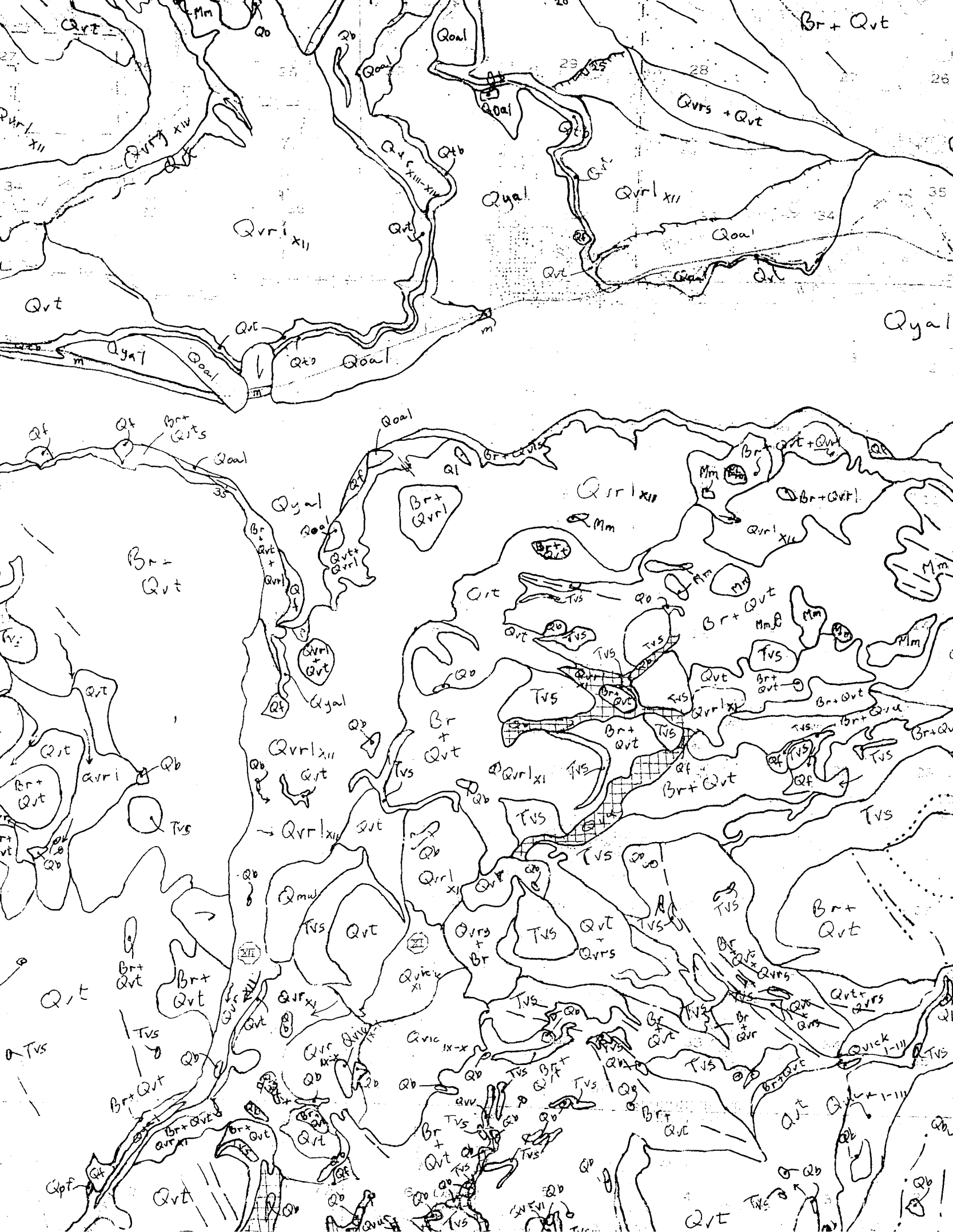




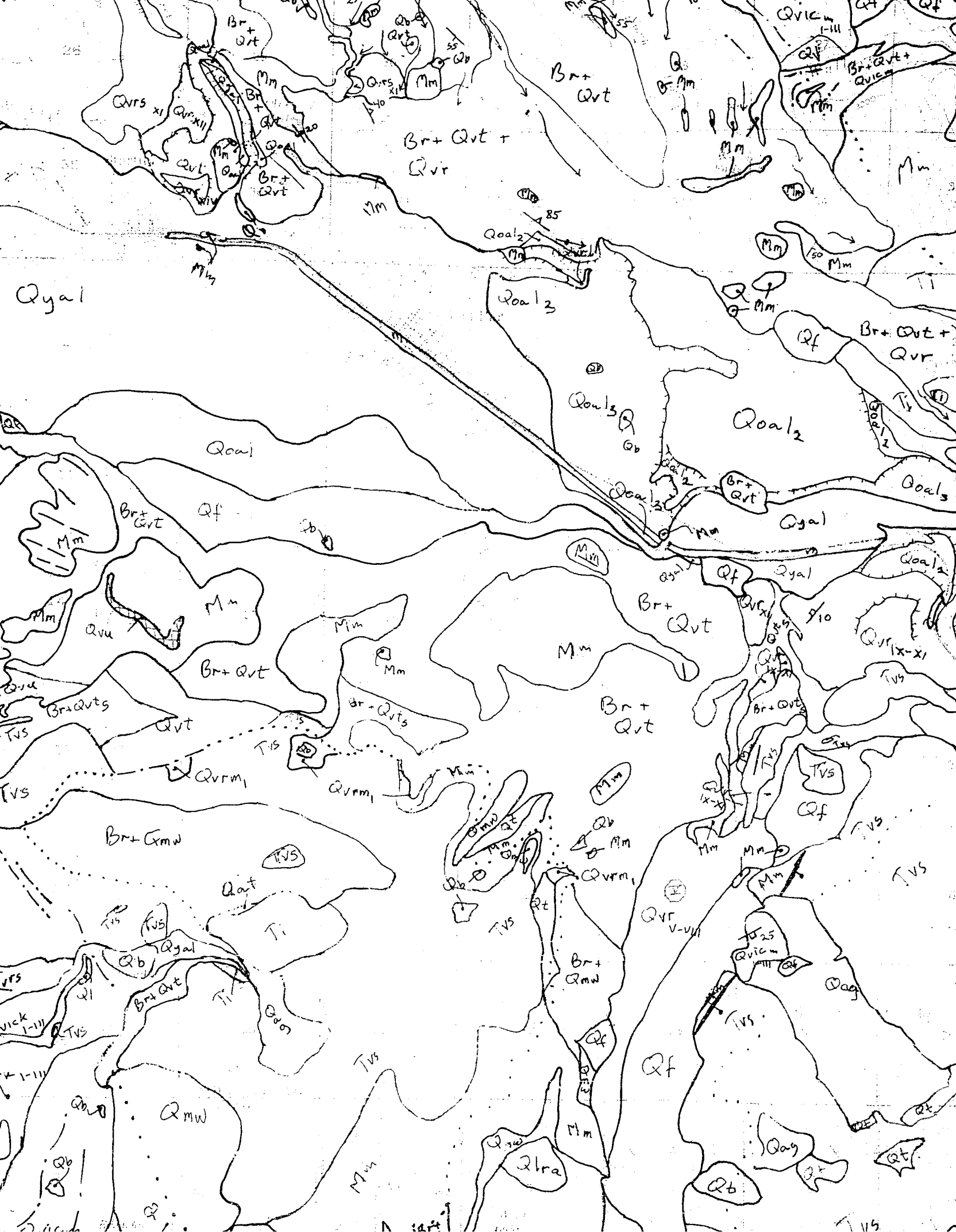






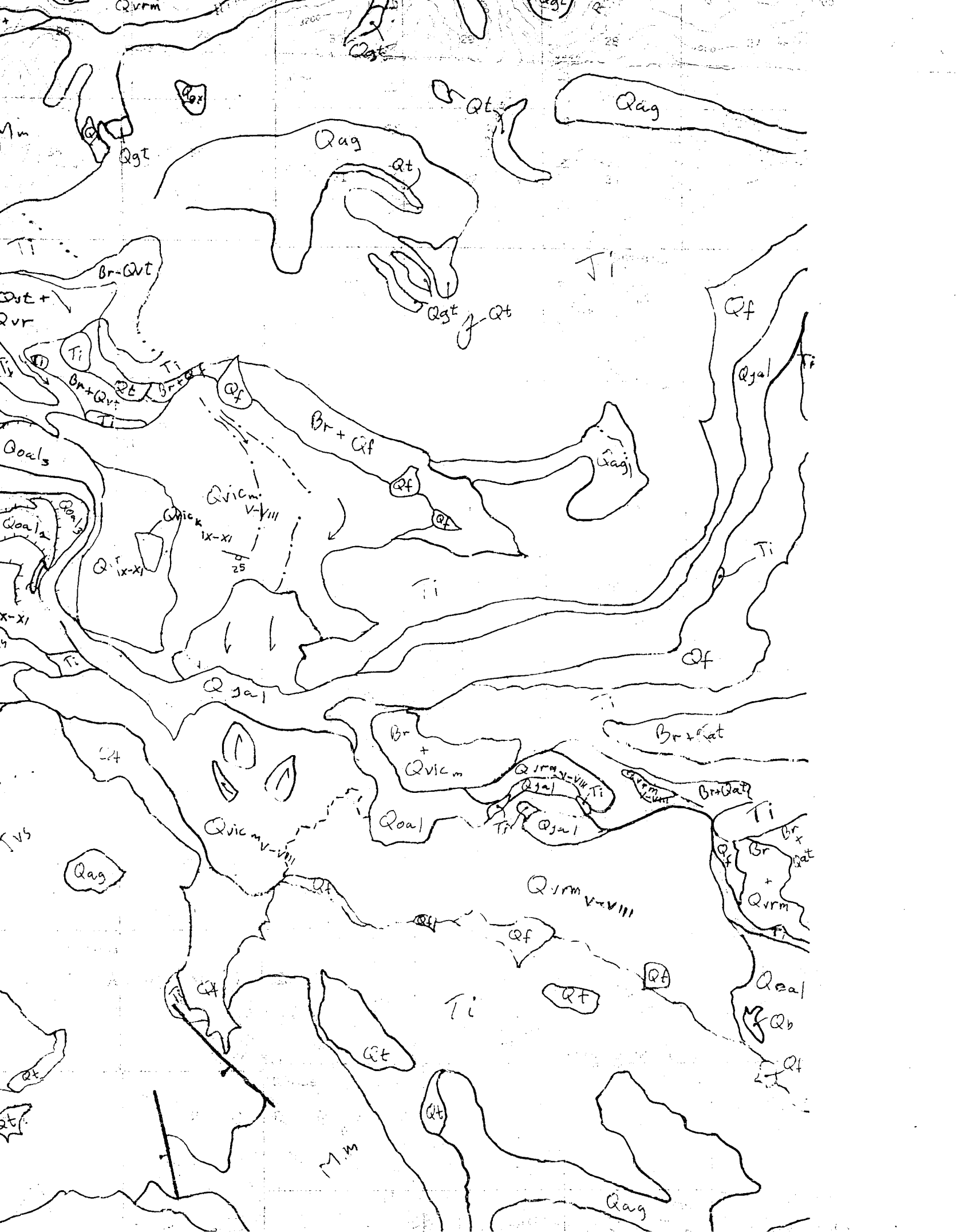


















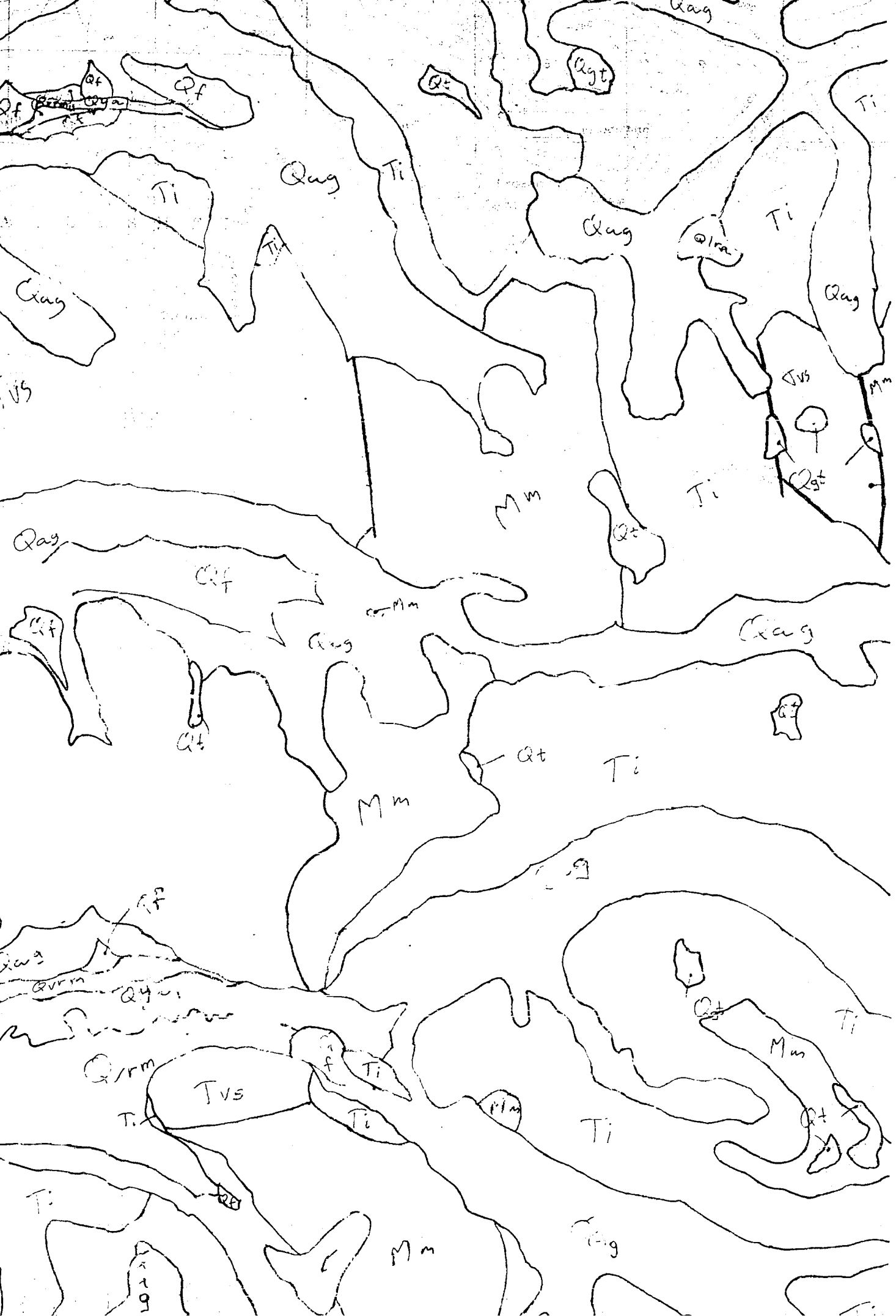






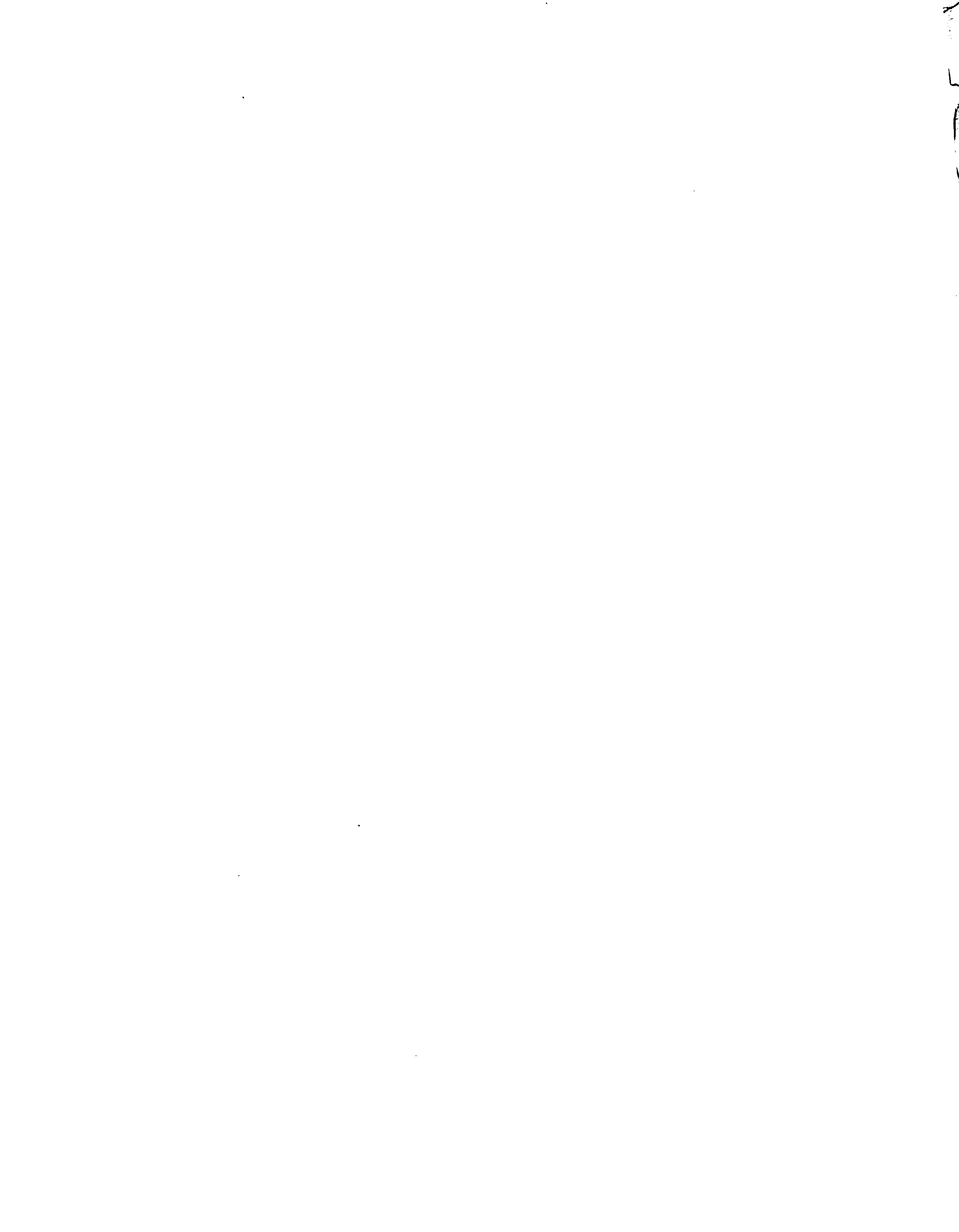


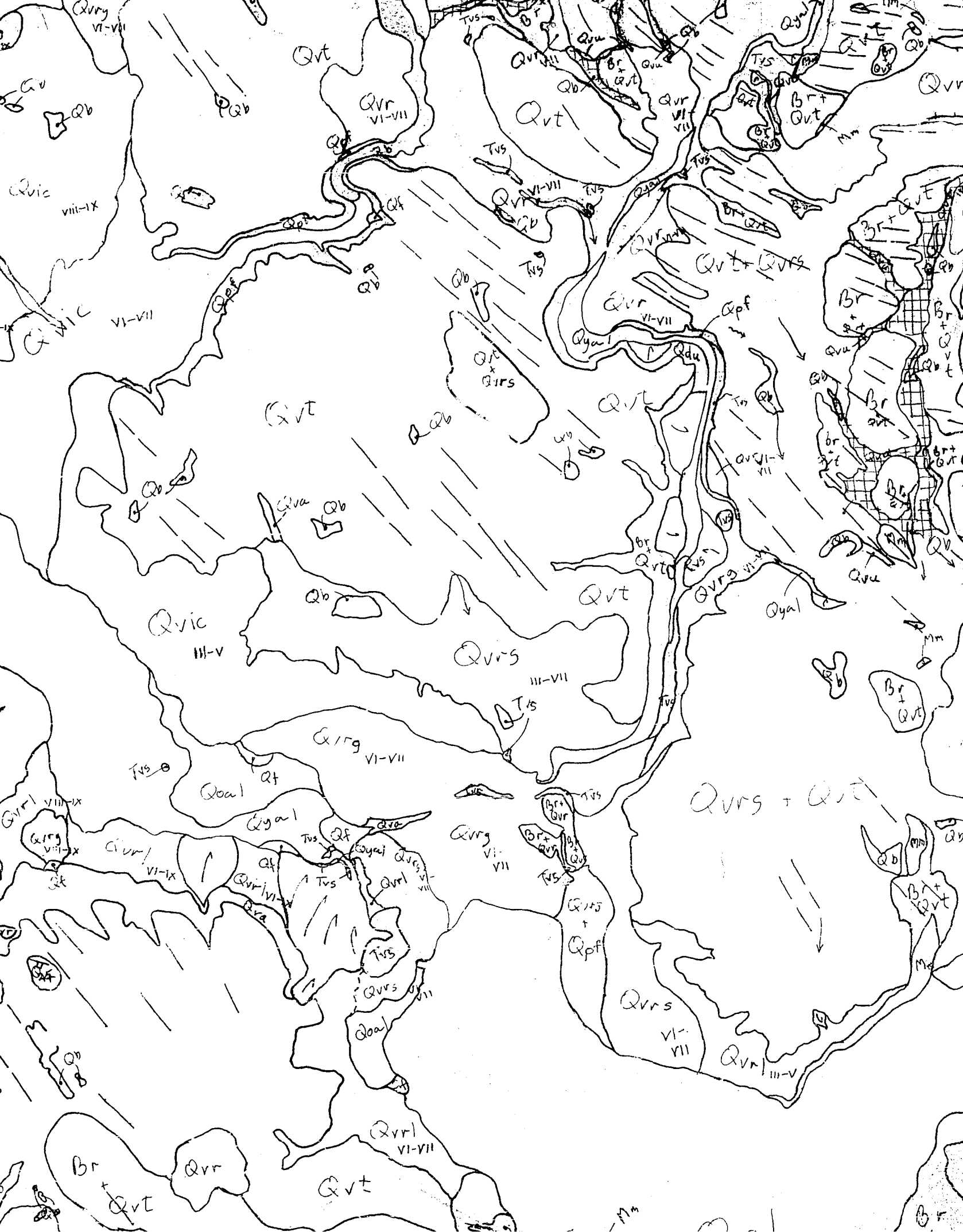




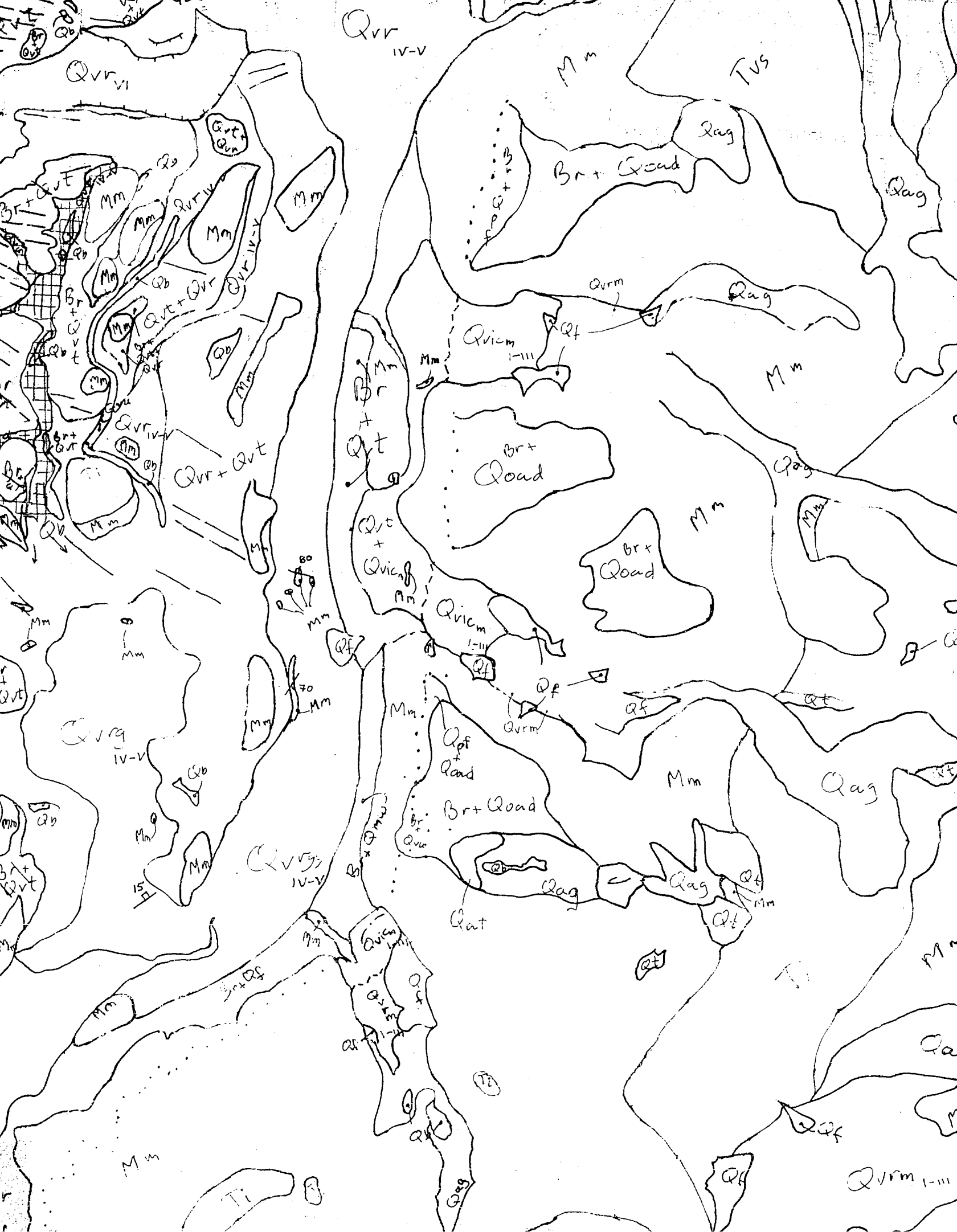






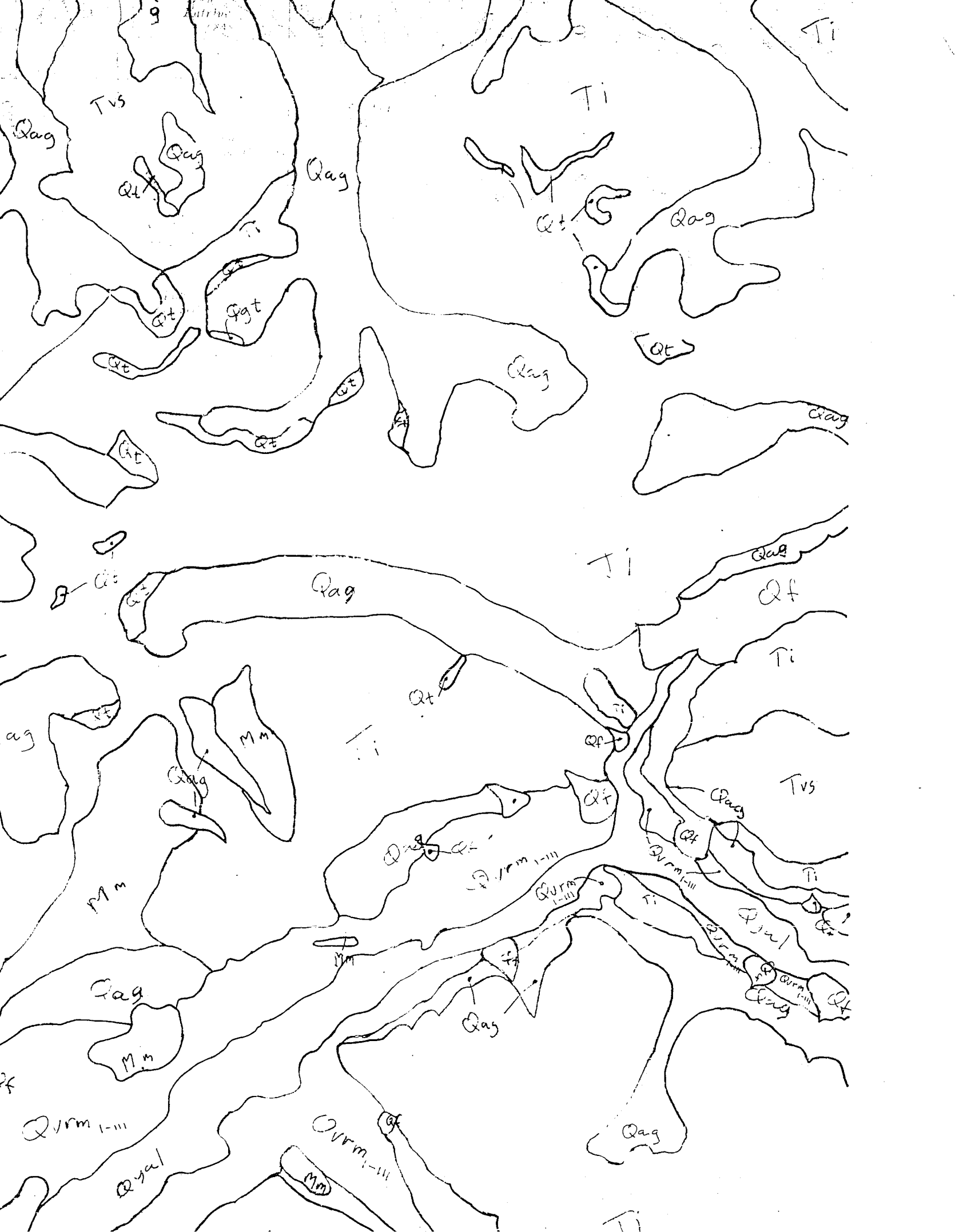




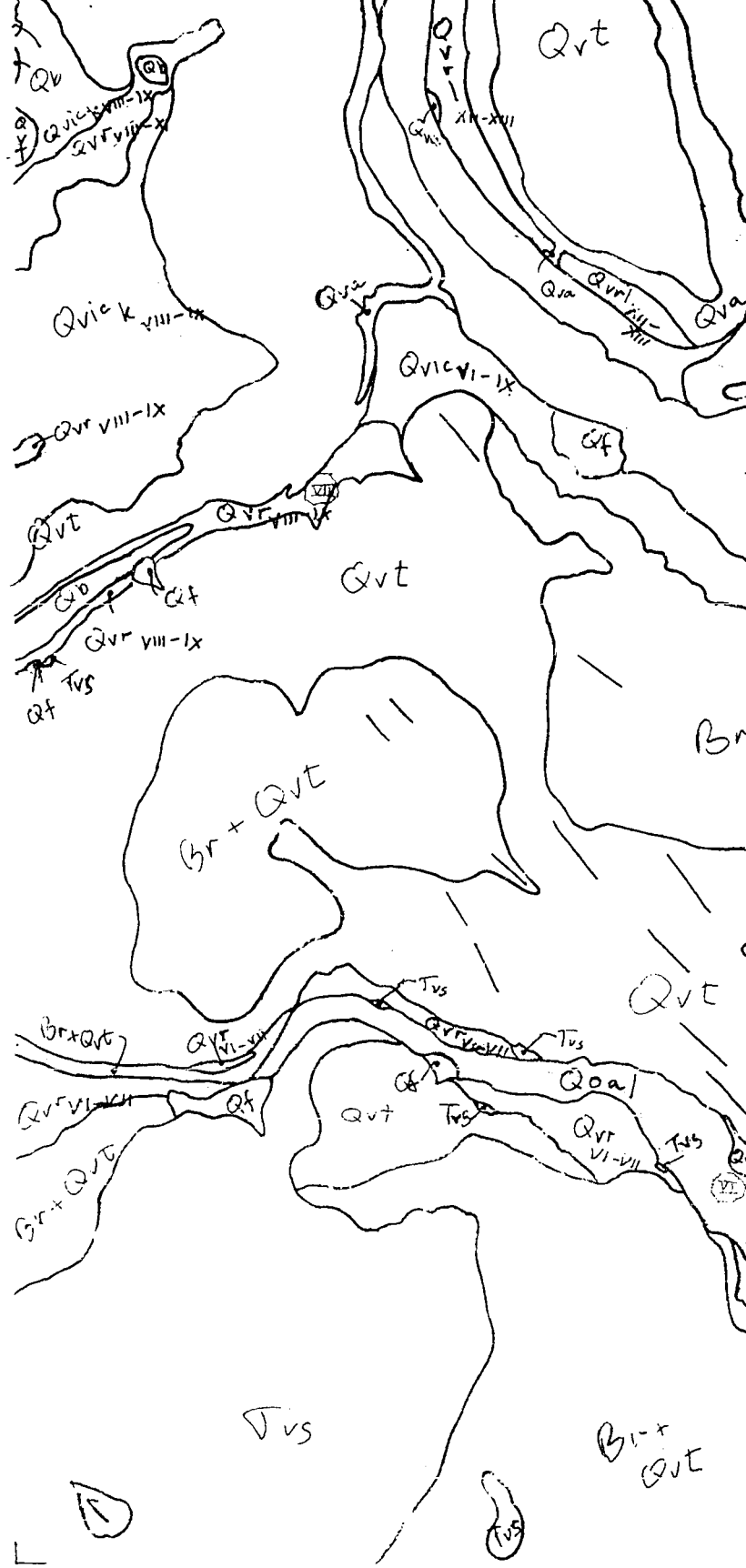




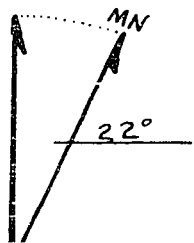




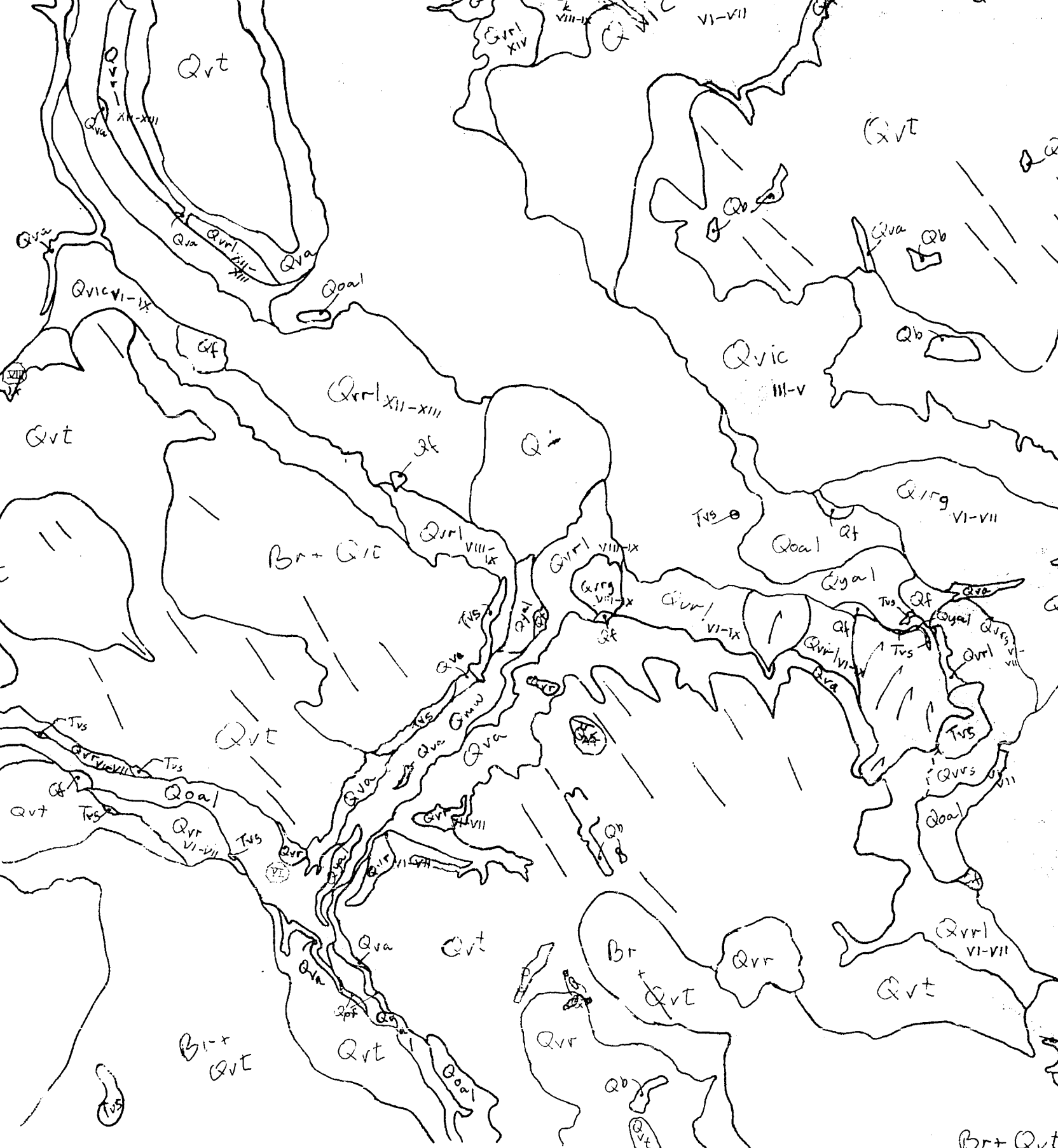




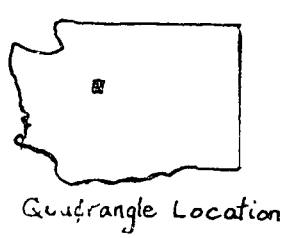
Base from U.S. Geological Survey  
 topographic maps: 15' series - Monroe,  
 Index, Mt. Si; 7.5' series - Fall City,  
 Carnation, Lake Joy



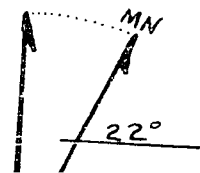




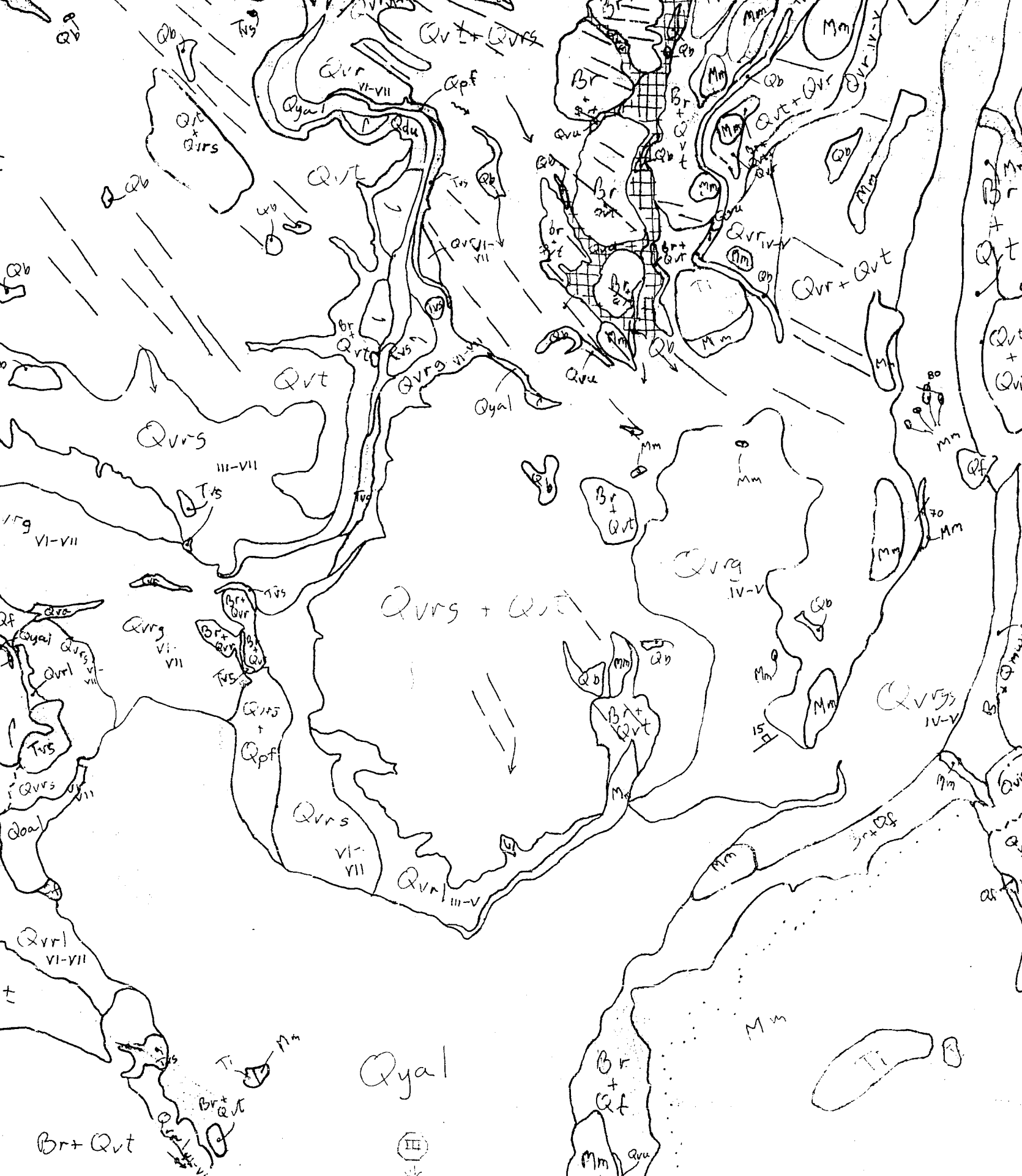
Geological Survey  
 15' series - Monroe,  
 7.5' series - Fall City,  
 Joy



SURFICIAL GEOLOGY  
 SKYKOMISH RIVER  
 SNOHOMISH AND KINGS COUNTIES







GEOLOGY OF THE WEST HALF OF THE  
 WASH RIVER QUADRANGLE  
 WASHINGTON











1:50,000

Mapped by D.B. Booth (1979-1982)  
 with assistance from S.A. Sandberg,  
 F. Moser, and F. Beall (1981).